

1987

ESTUARINE CHEMICAL REACTIVITY AT THE PARTICLE-WATER INTERFACE

GLEGG, GILLIAN A

<http://hdl.handle.net/10026.1/2374>

<http://dx.doi.org/10.24382/4394>

University of Plymouth

All content in PEARL is protected by copyright law. Author manuscripts are made available in accordance with publisher policies. Please cite only the published version using the details provided on the item record or document. In the absence of an open licence (e.g. Creative Commons), permissions for further reuse of content should be sought from the publisher or author.

This thesis is dedicated to my Mother and Father
with thanks.

"This book is your life blood -
Guard it and treat it as such"

G.E.M.

PLYMOUTH POLYTECHNIC LIBRARY	
Accr. No.	5500470-5
Class No	T 574 . 5832 9LE
Contl No.	X700618170

COPYRIGHT

Attention is drawn to the fact that the copyright of this thesis rests with the author, and that no quotation from the thesis and no information derived from it may be published without the prior written consent of the author.

This thesis may be made available for consultation within the Plymouth Polytechnic Library and may be photocopied or lent to other libraries for the purposes of consultation.

Signed *William Glegg*.....

ESTUARINE CHEMICAL REACTIVITY AT THE
PARTICLE-WATER INTERFACE

By

GILLIAN A GLEGG B.Sc.(HONS)

A thesis submitted to the Council for National
Academic Awards in partial fulfilment of the
requirements for admittance to the degree of:

DOCTOR OF PHILOSOPHY

Department of Marine Science
Institute of Marine Studies
Plymouth Polytechnic
Drake Circus
PLYMOUTH
Devon
Great Britain

In collaboration with:
Institute for Marine
Environmental Research
Prospect Place, The Hoe
PLYMOUTH
Devon
Great Britain

Submitted August 1987

DECLARATIONS

At no time during the registration for the degree of Doctor of Philosophy has the author been registered for any other C.N.A.A. or University award. This study was financed with the aid of a studentship from the Natural Environment Research Council and carried out in collaboration with the Institute for Marine Environmental Research.

A programme of advanced study was undertaken which included, within the Polytechnic, a lecture course in colloid chemistry given by Dr D.R. Glasson and several courses on the use of micro and mainframe computers. During the period of registration several scientific meetings were attended and papers published as listed below.

Paper Published or In Press

Millward, G.E., Glegg, G.A., Glasson, D.R., Morris, A.W. and Bale, A.J. (1985). The Microstructures of Estuarine Particles and Their Role in Heterogeneous Chemical Reactivity. American Chemical Society Symposium Series, Division of Environmental Chemistry. 25, 418-420.

Glegg, G.A., Titley, J.G., Glasson, D.R., Millward, G.E. and Morris, A.W. (1987). The Microstructures of Estuarine Particles. In "Particle Size Analysis-1985", (Ed. Lloyd, J.P.) 591-597. John Wiley, Chichester.

Titley, J.G., Glegg, G.A., Glasson, D.R. and Millward, G.E. (1987). Surface Area and Porosities of Particulate Matter in Turbid Estuaries. Continent. Shelf Res. In Press.

Conferences Attended

Marine Chemistry Discussion Group Meeting: "Oceanic and Continental Shelf Chemistry". Held at University College Swansea, 5-6th April 1984.

Physical Oceanography 84: A meeting held under the auspices of the Challenger Society. Held at University College of North Wales, Menai Bridge 16-21st September 1984. Paper presented by G.A. Glegg entitled "Surface Areas and Porosities of Estuarine Particles".

NERC Geocolloids Group Meeting: "Characterisation of Natural Particles". Held at University of Lancaster, 15-17th April 1985.

IAWPRC/NERC Meeting: "Estuarine and Coastal Pollution". Held at Plymouth Polytechnic, 16-19th July 1985.

American Chemical Society National Meeting: "Chemical Reactions at the Particle Water Interface". Held in Chicago, Illinois 8-13th September 1985. Paper presented entitled "The Microstructures of Estuarine Particles and Their Role in Heterogeneous Chemical Reactivity".

NERC Geocolloids Group Meeting: "Sorption Processes in Geocolloid Systems". Held at University of Lancaster, 1-3rd April 1986.

Council of Europe Intensive Course: "Evaluation of Criteria for the Management of Estuarine Systems". Held at The University, Southampton, 20-29th July 1986.

Estuarine and Brackish Waters Sciences Association Meeting: "Dynamics of Turbid Coastal Environments". Held at Plymouth Polytechnic, 1-5th September 1986. Paper presented entitled "Surface Areas and Porosities of Particulate Matter in Turbid Estuaries".

NERC Geocolloids Group Meeting: "Particle Aggregation Processes in the Natural Environment". Held at University of Lancaster, 21-23rd April 1987.

External Visits.

University of Miami, Florida, to see Dr F.J. Millero and visit the laboratories. September 1985.

British Geological Survey, Wallingford for discussion with Dr D.G. Kinniburgh on computerised analysis of gas adsorption data. April 1986.

Department of Oceanography, Southampton for discussions with Dr. P. Statham on clean handling of samples for trace metal analysis. April 1986.

ACKNOWLEDGEMENTS

I wish to thank all those who assisted in the completion of this work. In particular, I wish to thank Dr Geoff Millward for his indefatigable and wholehearted support throughout the entire project. I also wish to acknowledge the following:

Dr A.W. Morris for his help and supervision. Dr D.R. Glasson for his help in particular with the surface area and X-ray analyses. Dr A.J. Bale for his guidance and assistance with many aspects of practical work.

Dr A. Nelson for instruction in the use of anodic stripping voltammetry. Mr P. Davies for help with X-ray analyses. Dr D. Plummer for supplying results of surface area by dye adsorption.

Dr R. Uncles for provision of and assistance in the operation of a hydrodynamic computer model of the Tamar Estuary. Dr D.G. Kinniburgh for providing a computer programme for calculation of surface areas. Dr C. Ricketts for assistance with analysis of sorption kinetic results.

The staff of IMER for support on many field surveys. The technical staff of the Institute of Marine Studies and Faculty of Science for help both with field and laboratory work. Mr J.G. Titley for assistance on field surveys and early access to unpublished data.

The Natural Environment Research Council for the provision of a three year Research Studentship grant. Plymouth Polytechnic for the use of all facilities and for providing part time teaching and short term Local Education Authority Research Assistantship. IMER for supplying equipment and bench space for many experiments.

All members of the coffee club past and present for provision of essential light entertainment.

Finally, I am indebted to C.A.T.S. for typing this thesis.

ESTUARINE CHEMICAL REACTIVITY AT
THE PARTICLE WATER INTERFACE

Gillian A Glegg

ABSTRACT

A systematic study of the microstructures of particulate material from the Tamar Estuary using a BET nitrogen adsorption technique has been carried out. The results showed that suspended material had a higher BET surface area (approximately $20\text{m}^2/\text{g}$) than the associated sediments (approximately $13\text{m}^2/\text{g}$). Also the BET surface areas ($8\text{-}20\text{m}^2/\text{g}$) of suspended material collected during axial transects ($S = 0\text{-}30\text{‰}$) of the Tamar Estuary indicated relatively higher BET surface areas in the turbidity maximum zone as compared to material from up or down estuary. The BET surface areas were inversely related to the carbon content of the particles and although the role of Fe and Mn coatings was examined no definitive relationship to BET surface area was evident. Analysis of nitrogen adsorption-desorption hysteresis loops indicated the pores to be of the parallel plate or slit type in the size range $<2\text{-}50\text{ nm}$. The shape and dimensions of these pores would accommodate the penetration of metal ions, like Zn and Cu, into the pore spaces in the particle matrix.

A method was designed to enable the analysis of natural Zn and Cu concentrations in small volumes extracted from a reactor on a timescale suitable for kinetic analysis. Dissolved Cu and Zn adsorption-desorption experiments were carried out under controlled conditions using Tamar suspended solids as the adsorbents. The uptake and release profiles were interpreted in terms of a two stage reaction mechanism which involved both surface adsorption and solid state diffusion into the pores. Rate constants were derived from a kinetic analysis to enable evaluation of the chemical timescales of the sorption reactions. When compared to field data of Zn distributions in the Tamar Estuary the time constants allowed a reasoned explanation of the observations. They also pointed to a strong coupling between the physical and chemical timescales within estuaries.

This work has indicated an association between trace metal sorption reaction rates and estuarine particle microstructure. These rate constants are of value in the refinement of hydrodynamic models and this study has implications for the availability of trace metals for biological or chemical remobilisation.

CONTENTS

Page No.

Title	(i)
Declarations	(ii)
Acknowledgements	(v)
Abstract	(vi)
Contents	(vii)
 CHAPTER ONE: INTRODUCTION	 1
 1.1. Preamble	 1
1.1.1. The Importance of Estuaries	1
1.1.2. Physical Characteristics of Estuaries ...	4
 1.2. Trace Metals in Estuaries	 10
1.2.1. The Geochemical Significance of Estuaries	10
1.2.2. The Speciation of Cu and Zu in Estuarine Waters	12
1.2.3. Trace Metal Distributions in Estuaries	16
 1.3. Particles in Estuaries	 20
1.3.1. The Composition of Estuarine Particles	20
1.3.2. Flocculation in Estuaries	23
1.3.3. The Morphology of Estuarine Particulate Material	25
 1.4. Heterogeneous Chemical Reactivity	 28
1.4.1. Trace Metal Sorption Studies	28
1.4.2. The Surface Area of Particles	34
1.4.3. The Porosity of Particles	37
 1.5. Aims of Present Work	 43

CHAPTER TWO: EXPERIMENTAL TECHNIQUES AND METHOD DEVELOPMENT	45
2.1. Particle Characterisation Techniques	46
2.1.1. Particle Microstructural Analyses	46
2.1.2. X-ray Analysis	57
2.1.3. Carbon, Hydrogen and Nitrogen Analysis ..	58
2.1.4. Particle Size Analysis	59
2.2. Particle Collection and Preparation	63
2.2.1. Collection of Suspended and Sediment Particles	63
2.2.2. Drying of Natural Particulate Samples ...	66
2.2.3. Removal of Particulate Organic Coatings	71
2.2.4. Removal of Particulate Ferromanganese Coatings	72
2.3. Sorption Modelling Techniques	74
2.3.1. Methods of Sample Collection and Preparation	74
2.3.2. Development of Modelling Technique ...	75
2.3.2a. Adsorption Experiments	76
2.3.2b. Desorption Experiments	80
2.3.3. Development of the Micro-Chelex System ..	80
2.3.4. Analysis of Solutions by ASV	85
2.3.5. Analysis of Solutions by AAS	91
CHAPTER THREE: THE MICROSTRUCTURES OF ESTUARINE PARTICLES - RESULTS AND DISCUSSION	94
3.1. The Morphology of Estuarine Particles	95
3.1.1. General Considerations	95
3.1.2. The Relationship Between Suspended and Sediment Materials	100
3.1.3. The Surface Areas of Suspended Solids from the Tamar Estuary	113

3.2.	An Examination of the Effect of Chemical Composition on the Characteristics of Particles	123
3.2.1.	Identification of Crystalline Components	123
3.2.2.	The Influence of Organic Material on Surface Morphology	126
3.2.3.	The Influence of Fe and Mn Oxyhydroxide Surface Coatings on the Characteristics of Particles	139
3.3.	Conclusions from the Particle Characterisation Study	148
CHAPTER FOUR: THE SORPTION BEHAVIOUR OF Zn AND Cu IN ESTUARINE MEDIA		155
4.1.	Sorption of Metals in Tamar Estuary Waters ...	157
4.2.	Mixing Experiments Using Tamar Waters	162
4.2.1.	Zn Behaviour	163
4.2.2.	Cu Behaviour	172
4.3.	Mixing Experiments Using Carnon Water	182
4.3.1.	Zn Behaviour	182
4.3.2.	Cu Behaviour	187
4.4.	Release from Carnon Sediment	196
4.5.	A Qualitative Summary	199
CHAPTER FIVE: KINETIC ANALYSIS OF THE SORPTION DATA		201
5.1.	Results from the Tamar Experiments	202
5.1.1.	Kinetic Analysis of the Tamar Adsorption Data	202
5.1.2.	Desorption of Metals from Tamar Particles	207
5.1.3.	Comparison of Rate Constants with Tamar Estuary Field Observations	210

	<u>Page No.</u>
5.2. Kinetic Analysis of the Carnon Data	213
5.2.1. Method of Analysis of Zn Desorption Profiles	213
5.2.2. Analysis of Cu Desorption	222
5.2.3. Analysis of Carnon Adsorption Data ...	227
 CHAPTER SIX: CONCLUSIONS	 230
 6.1. The Relationship Between Particle Microstructure and Trace Metal Sorption Processes	 230
 6.2. The Refinement of Hydrodynamic Models of Estuarine Systems	 238
 6.3. Recommendations for Future Work	 243
 REFERENCES	 245
 APPENDIX I - Published Work	 A1

CHAPTER ONE

INTRODUCTION

1.1. Preamble.

1.1.1. The Importance of Estuaries.

Estuaries have, for centuries, been used by man for purposes of transport, fishing, industry and waste disposal. More recently, they have also been exploited for recreational pursuits and it is inevitable that due to the variety of stresses involved these uses eventually come into conflict. It is all too easy to see the environment as a flexible system which can be manipulated by man for his individual requirements. However, man is dependent on the entire environment and must manage it carefully if he wishes it to function naturally in the long term and thus continue to meet his ever growing needs (SCEP, 1970; Turekian, 1971).

Well publicized disasters (Gerlach, 1981; Clark, 1986) include cases of human fatalities due to severe mercury poisoning in Minamata Bay, Japan. There, mercury dumped in the bay sediments by factory workings, was released to the overlying water and accumulated in fish which were later consumed by the victims (So, 1978). The building of the Aswan dam while providing water for irrigation in the upper reaches of the Nile, lowered the quantity of nutrients reaching the delta and destroyed a once productive fishery (Lockwood, 1986). These alarming incidents, readily noticeable due to their close affinity to the wellbeing of man are probably the tip of an iceberg with regard to the welfare of the ecosystem as a whole.

Catastrophies of this type are often due to a lack of planning and investigation and, as a consequence, many governments now require Environmental Impact Assessments or similar studies to be carried out before new developments take place (Spellerberg, 1986). These assessments examine the projected effect of a particular action, be it building a new dam, the discharge of industrial effluent or other environmental perturbations. Estuaries, by their situation and their multifarious uses both to man and as an ecosystem, require particularly intensive study to develop measures to protect them from excessive exploitation and the eventual destruction of their natural capacity (Olausson and Cato, 1980). It has been shown, for example in the Clyde Estuary, that it is possible to some extent, to repair damage caused by pollution (McKay, 1986), but this often requires expensive longterm projects. It is apparent that a more sensible strategy is to attempt to develop predictive modelling techniques (Clark, 1983), to enable the effects of human intervention to be investigated prior to any change, and thus, avoid environmental damage. A prerequisite for these modelling techniques is a sound data base with which the models may be developed and validated.

Heavy metals, which are being increasingly mobilised into the environment by the action of man, are particularly injurious to the environment. Their infinite persistence and ability to change speciation, often to a more toxic form, makes them especially threatening. In addition, many forms of marine life will accumulate heavy metals, often to the detriment of their health, which will be further concentrated in the food chain ending, in some cases as in Minamata Bay, in fatalities in man (So, 1978).

The prevention of overuse of the estuarine capacity requires the investment of large sums of money on both controlling pollution now and researching for future requirements. Although the sums of money involved appear vast, it was concluded by the Royal Commission on Environmental Pollution (1972; 1984) that in comparison to other aspects of industrial costs, the costs of pollution abatement within estuaries would be very small indeed. This report also emphasised the importance of developing mathematical models as a scientific basis for future action on pollution control and of further investigation of persistent materials including heavy metals and organochlorine compounds.

This work concentrates on the estuarine behaviour of the elements Zn and Cu. They are both essential trace elements for the correct metabolism of animals but are toxic in large amounts (Rainbow, 1985) and have been classified as relatively accessible toxic metals by Forstner (1980). Table 1.1 gives the global geochemical and industrial mobilisation data for Zn and Cu. This shows that the elements have relatively short oceanic residence times. In addition man's utilisation of the elements appears to dwarf the natural weathering processes, although how much of the mined metal reaches the oceans is unclear. However, both these metals have been reported to be present in elevated concentrations in the sedimentary material of contaminated estuaries (Aston and Chester, 1976; De Groot et al., 1976; Forstner, 1980; Bland et al., 1982) and thus it is essential that their pathways within estuaries are studied to develop an understanding which will enable predictive modelling of this behaviour. This study investigates the reactivity of the trace metals

in the presence of well-characterised particles. Of importance here are the time-dependent sorption processes and the question of what proportion of particulate trace metals is available to biota. The study was undertaken using materials from the River Tamar which has been well characterised physically (Uncles et al., 1983a) and chemically (Morris et al., 1982a).

	<u>Cu</u>	<u>Zn</u>
Earth crust concentration (mg/kg)	45	40
Seawater concentration (µg/L)	2	3
Dissolved input by erosion (kt/y)	325	1,100
Ocean residence time (y)	20,000	20,000
Input by fossil fuel, cement manufacture (kt/y)	2.1	3.7
Mine production (kt/y)	7,500	5,000

Table 1.1. Geochemical and industrial data for Cu and Zn (GESAMP, 1976).

1.1.2. Physical Characteristics of Estuaries.

The definition of an estuary varies depending on the physical or biogeochemical aspects under investigation (Ketchum, 1951; Pritchard, 1967; Fairbridge, 1980). In this study the most appropriate definition appears to be:-

"an estuary is an inlet of the sea reaching into a river valley as far as the upper limit of tidal rise, normally being divisible into three sectors (a) a marine or lower estuary, in free connection with the open sea; (b) a middle estuary subject to strong salt and fresh water mixing and (c) an upper or fluvial estuary, characterised by fresh water but subject to daily tidal action".
(Fairbridge, 1980).

This definition is selected here since it closely describes the Tamar Estuary. The estuary is approximately 20-30km in length depending on the tidal state and river flow but it is constrained to a maximum of 32km due to a weir (See Figure 2.6). The Tamar Estuary is of the drowned river valley type (Pritchard, 1967) and while the upper 10km is canalised, in the lower reaches there are large expanses of mud flats exposed at low tide. The tidal range at Devonport is between 5.5 and 1.5m and typical monthly averages of river flow are from a maximum of $38\text{m}^3/\text{s}$ in January to $5\text{m}^3/\text{s}$ in June. In spate conditions, however, the river flow can exceed $100\text{m}^3/\text{s}$ (Bale, 1987).

Estuaries may also be categorised on the basis of their circulation, stratification (Hansen and Rattray, 1966) and mixing processes (Aarons and Stommel, 1951). Essentially these considerations give rise to four main categories (Dyer, 1973; Bowden, 1980). The salt wedge type, which is found in estuaries with low tidal energy and high river flow, has a strong vertical salinity stratification caused by less dense freshwater flowing out over the

top of the more dense seawater. Some entrainment between the two bodies will occur but there will be steep density gradient between the fresh and saline water; examples are the Rhone and Zaire estuaries (Martin and Letolle, 1979). An exaggerated form of this type of circulation is found in fjords mediated by their topography. The other extreme case is a fully mixed estuary in which a large tidal range has sufficient energy to break down the salinity stratification and give a vertically homogeneous salinity profile; an example is the Severn (Morris, 1983). The partially mixed estuary has some degree of variable salinity stratification; examples are the Gironde, Loire and Godavari estuaries (Martin and Letolle, 1979). In this type of estuary the turbulence between the two bodies of water as the tides rise and fall causes, with entrainment, weakening of the vertical salinity stratification. The Tamar Estuary is generally a partially mixed estuary although under appropriate river flow and tidal conditions the riverine end may become salt wedge or the saline end may be fully mixed (Morris, 1983; Uncles et al., 1985).

Within many estuaries a turbidity maximum is observed in the low salinity region of the estuary in which the turbidity is far in excess of that seen in either the sea or river water sources (Festa and Hansen, 1978). In estuaries with a small tidal variation, this increase is due to a gravitational density circulation which at the null point of the estuary holds particles in suspension (Festa and Hansen, 1978; Officer, 1980). In addition to this circulation in a macro- or meso-tidal estuary there will be tidal pumping of sediments upstream by the strong fast currents which will scour the estuary bed and suspend sediment material (Allen et al., 1980; Uncles et al.,

1985). In the Tamar Estuary a strong turbidity maximum (100- >1000mg/L) is formed due to this combination of tidal processes and gravitational circulation (Bale et al., 1985; Uncles et al., 1985). This maximum will move up estuary in low river runoff conditions when it will be very well developed and down estuary during high river runoff when it will be weaker due to the larger cross-sectional area.

Mixing processes in estuaries give rise to a physical timescale called the residence or flushing time (Dyer, 1973; Bowden, 1980) which may be estimated from:

$$T = Q / R$$

where Q is the volume of fresh water accumulated in the whole or a section of the river and R is the river flow (Dyer, 1973). In its simplest terms this represents the time taken for the existing freshwater in an estuary or a segment of an estuary to be replaced at a rate equal to the river flow. Thus the freshwater is acting as a tracer and the idea can be used to determine the flushing times of conservative pollutants in estuaries.

The Tamar Estuary has a flushing time for the whole length of 7-10 days (Harris et al., 1983/4; Uncles et al., 1983b). However, if the estuary is divided into small segments of equal length these will have individual flushing times varying from seconds to weeks as is shown diagrammatically in Figure 1.1. This demonstrates that for different portions of an estuary there will be a wide range of flushing times which will depend on the hydrodynamic regime of the estuary. The physical timescales of this mixing will be extremely

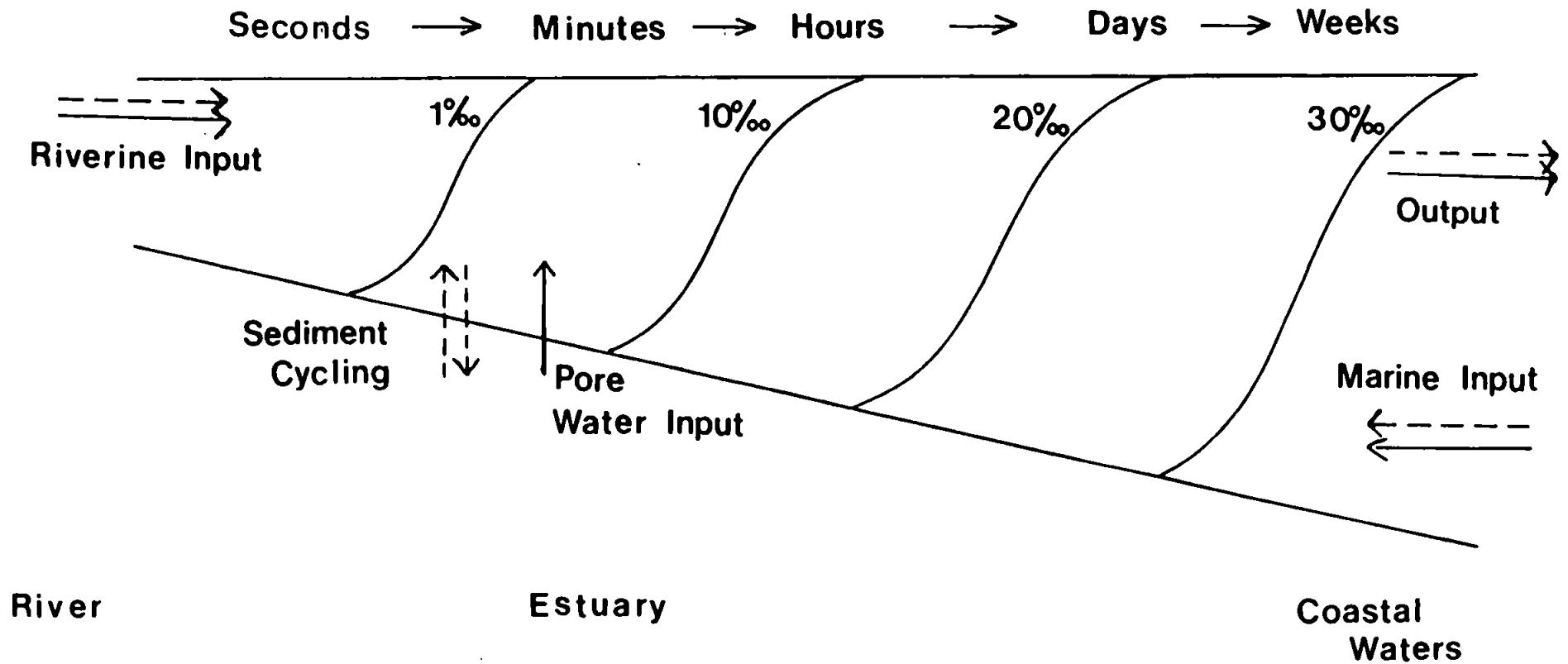


Figure 1.1. Approximate timescales of physical processes within the estuarine region.
 ----- Particulate ————— Dissolved

important in regulating chemical reactions within the water. With regard to dissolved/solid phase reactions it is likely that within the low salinity region of the estuary these reactions will be constrained by the timescales such that equilibrium will not be reached for kinetically slow reactions. It is more likely that equilibrium conditions will be a feature in the lower estuary and coastal waters, but of course, in these environments the reaction conditions are radically different. It is precisely this interplay between the physical and chemical timescales that needs evaluation. This is of utmost importance in attempting to predict the behaviour of non-conservative pollutants, like the reactive trace metals (Ackroyd et al., 1986) in estuaries.

1.2. Trace Metals in Estuaries.

1.2.1. The Geochemical Significance of Estuaries.

It has been estimated that 1.8×10^{10} tons per year of mainly fine grained sediment is supplied to the worlds' oceans and the majority of this is input via estuaries (Martin and Whitfield, 1983). Particles suspended within river water will originate from erosion and weathering within the catchment area (Martin and Meybeck, 1979) and thus the type and the quantity is dependent on the nature of this area (Turekian, 1969). Input to the oceans may not occur by direct transport through estuaries as a large fraction can be trapped within the estuarine zone for an extensive period (Aston and Chester, 1976; Fairbridge, 1980; Olausson and Cato, 1980). It has been estimated that more than 90% of the supplied riverine particulate material will settle at the river-ocean interface (Martin and Whitfield, 1983). Partially mixed estuaries, like the Tamar (see Section 1.1.3), are generally regions of net sediment accretion although river floods may transport to the coastal ocean large quantities of sediment sporadically (Dyer, 1979). Bale et al. (1985) have identified that while some particles may be transported through the Tamar Estuary quite rapidly others will have a residence time considerably in excess of 1.4 years.

Approximately 0.4×10^{10} tons per year of dissolved material is supplied to the oceans by river transport and the composition of this is very different compared to that seen in the open ocean (Burton, 1976; Martin and Whitfield, 1983). In order to calculate a geochemical mass balance it must either be assumed that the mixing of river and seawater is a simple dilution process or it is

necessary to identify the time-dependent bio-geochemical processes occurring within estuaries (Boyle et al., 1974).

In the case of Cu and Zn the total global river fluxes are 1.9Mt/y and 6.5Mt/y, respectively (Martin and Meybeck, 1979), as shown in Table 1.2. The Dissolved Transport Index (DTI = ratio of dissolved transport to total transport) is such that 80% of the riverine transport of both metals is in the particulate phase, although this is somewhat smaller than that for an element like Fe. However, Zn is in excess in river suspended solids compared to deep sea clays whereas Cu is enriched in deep sea clays rather than river suspended solids. There are various reasons why this should be so including anthropogenic inputs but the role that estuarine chemical processes play in conditioning the composition of marine particulate_matter, is not fully understood.

<u>Trace Metal Fluxes (Mt/y)</u>	<u>Fe</u>	<u>Cu</u>	<u>Zn</u>
River particulate load	733	1.55	5.4
River dissolved load	1.5	0.37	1.1
Total river load	734	1.9	6.5
Theoretical load	754	0.67	2.6
Discrepancy	---	+1.2	+3.9
World mining production	---	7.5	5.0
Dissolved Transport Index	0.2	19	15

Table 1.2. Annual trace metal fluxes to the oceans and the Dissolved Transport Index (DTI) (Martin and Meybeck, 1979).

In many estuaries it has been observed that the sediments may act as a sink for originally dissolved or particulate trace metals on either a permanent or temporary basis (Forstner, 1980). Much recent work has concentrated on the ability of organisms to mobilise trace metals in sediments and on the effects this mobilisation may have within the ecosystem (So, 1978). Numerous studies indicate bioaccumulation of trace metals to occur within some species of biological organisms (e.g. Sunila and Lindstrom, 1985; Rainbow, 1985; Vranken and Heip, 1986).

Thus it is essential with regard to both immediate effects on the estuarine ecosystem and long term effects on the global biosphere that the transport processes through an estuary are fully understood. Only by these means can the effects of pollution be projected and long term damage to the environment avoided.

1.2.2. The Speciation of Cu and Zn in Estuarine Waters.

The observed speciation of an element will be the result of a balance between free ions, ion pairs, organic complexes and surface adsorbed species. The determination of speciation of dissolved trace metals in natural waters is problematical due to the complexity of multicomponent systems and this difficulty is exacerbated in estuaries where rapid changes in pH, pE and salinity occur (Morris et al., 1982a; Morris, 1983). Nevertheless, equilibrium models of species in natural waters, including estuaries, have been developed (Mantoura et al., 1978; Turner et al., 1981; Bourg, 1983; Mouvet and Bourg, 1983). Turner et al. (1981) systematised the stability constants for major inorganic complexes of 58 trace elements in order that the

distributions of the various species, in sea and fresh waters, could be calculated. They also developed this further to include the complexation of some trace elements with humic material using data from Mantoura et al. (1978). However, probably the most advanced model now available is that of Bourg (1983) since it incorporates adsorption to the solid phase as well as inorganic and organic ligands.

	<u>Cu, % species</u>		<u>Zn, % species</u>	
	<u>0°/‰</u>	<u>30°/‰</u>	<u>0°/‰</u>	<u>30°/‰</u>
M ²⁺	0.3	3	36	45
M-HA ^a	65	22	1	--
M(OH) ₂	18	57	--	--
MCO ₃	2	9	3.2	1.5
MHCO ₃ ⁺	--	--	1.2	1.0
MSO ₄	--	1	0.5	11
MC1 ⁺	--	--	--	17
M _{ads} ^b	15	4	57	25
(M-HA) _{ads}	--	2	--	--

Table 1.3. Equilibrium speciation of Cu and Zn in model solutions of salinity 0°/‰ and 30°/‰ with a pH of 8.0 and a particle concentration of 30mg/L (Bourg, 1983). The particles have the surface properties of silica. ^a M-HA = Metal-humic acid species. ^b M_{ads} = Adsorbed metal.

The calculations by Bourg (1983) have shown the distribution of Cu and Zn in freshwater and seawater at pH = 8, in the

presence of 30mg/L of silica particles and some results of this are given in Table 1.3. Dissolved Cu in freshwater is dominated by the metal-humic acid complexes and the hydroxy-complex, $\text{Cu}(\text{OH})_2$. Only 15% of the metal is associated with the particulate phase. In seawater the major dissolved species is $\text{Cu}(\text{OH})_2$ with the metal humic acid complexes decreasing to about 20% of the total. In addition less Cu is adsorbed to the particles in seawater presumably because of competition for active sites by major cations in seawater. For Zn in freshwater the major dissolved phase component is the free ion, with the bulk of the remainder attached to the particulate phase. In seawater only 25% of the metal is associated with the solid phase while the dissolved metal is divided between Zn^{2+} , ZnCl^+ and ZnSO_4 . This difference in speciation is mirrored in the amount of dissolved metal recovered from natural waters by Chelex-100, a chelating resin. Florence (1977) found only 36.5% of Cu and 100% of Zn was extracted from a filtered river water. The residual Cu was found to be bound in organic complexes probably in the form of colloidal organic material.

Table 1.4 compares the speciation of Cu and Zn on silica and River Meuse sediment particles (Bourg, 1983; Mouvet and Bourg, 1983). For both metals the Meuse sediments show enhanced uptake compared to the model silica particles. This suggests that natural materials have considerably greater activity which is not evident on the silica particles.

	<u>Cu, % species</u>		<u>Zn, % species</u>	
	<u>Silica^a</u>	<u>Sediments^b</u>	<u>Silica^a</u>	<u>Sediments^b</u>
M ²⁺	0.3	0.3	36	11.7
M-HA	65	--	1	0.8
M(OH) ₂	18	6.4	--	--
MCO ₃ ⁺	2	4.4	3.2	2.7
MHCO ₃	--	0.1	1.2	1.2
MSO ₄	--	--	0.5	0.6
M _{ads}	15	87	57	79
(M-HA) _{ads}	--	1.5	--	3.5

Table 1.4. Equilibrium speciation of Zn and Cu in model solutions with silica particles and River Meuse sediments (Bourg, 1983; Mouvet and Bourg, 1983). ^a pH = 8; particle concentration 30mg/L. ^b pH = 7.8; particle concentration 60mg/L.

The true importance of these findings lies in the fact that the speciation of trace metals greatly influences their bio-availability (Nelson and Donkin, 1985). This is illustrated by a study of Cd toxicity which showed that the mortality of salmon was more closely related to a chelating resin labile fraction of Cd concentration than to the total Cd concentration (Buckley et al., 1985). It is also possible that trace metal speciation may control the rate of their heterogeneous chemical reactions.

1.2.3. Trace Metal Distributions in Estuaries.

The estuarine distributions of Mn and Fe are probably the most fully understood. For Mn the estuarine distributions (Holliday and Liss, 1976; Morris et al., 1978; Moore et al., 1979; Ackroyd et al., 1986; Keeney-Kennicutt and Presley, 1986), speciation (Krom and Sholkovitz, 1978; Mantoura et al., 1978), adsorption and flocculation behaviour (Sholkovitz, 1976; Morris and Bale, 1979; Sholkovitz and Copland, 1981; Millward and Moore, 1982) and diagenetic properties (Duinker et al., 1974; Elderfield and Hepworth, 1975; Knox et al., 1981) have all been extensively studied. This type of thorough research has enabled a definitive understanding of the observed non-conservative behaviour of Mn within the Tamar (Knox et al., 1981; Morris et al., 1981), St Lawrence (Sundby et al., 1981) and Rhine estuaries (Duinker et al., 1979). The knowledge of the controls on the behaviour of dissolved Mn gained in previous work also enabled an explanation (Morris et al., 1981) of the conservative behaviour of Mn seen in the Beaulieu Estuary (Holliday and Liss, 1976; Moore et al., 1979) and the Delaware Creek (Eastman and Church, 1984). A similar investigation of the behaviour of Fe has shown Fe to be non-conservative in almost all estuaries due to the flocculation of colloidal Fe oxyhydroxides (Boyle et al., 1974; Liss, 1976; Duinker, 1980).

Examples of the types of distributions observed for Zn and Cu in many estuaries are shown in Table 1.5. These disparate behaviour patterns of dissolved Zn and Cu in estuaries underline the importance of developing a complete understanding of the controls on the estuarine trace metal concentrations. In addition, the observation of

Concentration (µg/L)			
	<u>Zn</u>	<u>Cu</u>	
Tamar	1 - 14 (NC)	0.7 - 12 (NC)	Morris <u>et al.</u> (1978) Ackroyd <u>et al.</u> (1986)
Conwy	5 - 55 (C)	--	Elderfield <u>et al.</u> (1979)
Beaulieu	7 - 45 (C)	--	Holliday and Liss (1976)
Fraser	2 - 19 (NC)	0.1 - 5 (NC)	Thomas and Grill (1977)
Varde Å	2 - 4.5 (NC)	1 - 2.5 (NC)	Duinker <u>et al.</u> (1980)
Elbe	2 - 27 (NC)	0.8 - 1.3 (NC)	Duinker <u>et al.</u> (1982a)
Weser	2 - 15 (NC)	0.8 - 6 (NC)	Duinker <u>et al.</u> (1982b)
Gota	0.6 - 7 (C)	0.4 - 1.6 (UR)	Danielsson <u>et al.</u> (1983)
Amazon	--	0.1 - 1.7 (UR)	Boyle <u>et al.</u> (1982)
Brazos	--	0.4 - 2.7 (NC)	Keeney-Kennicutt and Presley (1986)
Rhine	5 - 20 (C + NC)	1 - 7 (C + NC)	Duinker and Nolting (1976; 1977; 1978)

Table 1.5. A comparison of the concentration of dissolved Zn and Cu found in estuaries around the world. The behaviour of the metal throughout the estuary is indicated in brackets; viz C - conservative; NC - Non conservative; C + NC - Both; UR - Unresolved.

both conservative and non-conservative behaviour in the Rhine and unresolved behaviour in other estuaries, indicates the need for accurate repetitive surveying of individual estuaries and for collection of data on the physico-chemical conditions prevalent in the estuary at the time of surveying (Bourg, 1983; Ackroyd et al., 1986).

In the Tamar Estuary repetitive surveying of the axial distribution of dissolved Mn, Zn and Cu has been carried out by Ackroyd et al. (1986) in conjunction with measurements of salinity, turbidity, dissolved oxygen and pH. These surveys show predominantly that these metals are non-conservative in the Tamar Estuary. Attempts to observe these sorption processes within the Tamar Estuary, by monitoring the composition of the particulate suspended and sediment material, were made by Morris et al. (1986). These were unsuccessful as the particle composition was substantially controlled by physical processes acting on the large reservoir of particulate material which made it impossible to observe small scale chemical variations (Morris et al., 1986). The dissolved Zn distribution in the Tamar Estuary, which closely follows the pattern of dissolved Mn, has a rapid loss from solution in the low salinity, high turbidity region of the estuary and a concentration maxima in the salinity range 3-20‰. This has been explained in terms of rapid adsorption of Zn onto the suspended particles in the low salinity region and by pore water infusions in the lower estuary coupled with desorption from the tidally resuspended sediments (Ackroyd et al., 1986). Dissolved Cu is reported to show a greater affinity for adsorption onto particles and has a generally more effective removal in the low salinity region (Morris, 1986). The mid-estuarine maxima for Cu occur between 1‰

and 8‰ and is also attributed to pore water infusions and desorption from tidally resuspended sediments (Ackroyd et al., 1986). Information of this type may be of great use in validating models developed, with chemical and physical estuarine parameters, to predict the behaviour of trace metals in estuaries.

1.3. Particles in Estuaries.

1.3.1. The Composition of Estuarine Particles.

Suspended particles within estuaries may originate from four major sources:

- (1) Riverine suspended material
- (2) Oceanic suspended material
- (3) Resuspended sediment material
- (4) Material formed in situ.

The geographical variation of the major elemental composition of riverine material can be ascribed to the nature of the catchment area (Martin and Meybeck, 1979). The marine suspended material will be mainly riverine derived material or eroded coastal sediment. Within estuaries large temporal and spatial fluctuations may be seen in the major elemental composition of suspended particles (D'Anglejan and Smith, 1973; Loring et al., 1983; Freely et al., 1986). These variations in an estuary may be regulated by sedimentological and hydrological features as observed in the Tay Estuary (Sholkovitz, 1979) or by biological activity as has been observed in the Amazon Estuary (Sholkovitz and Price, 1980). In addition they may be due to chemical interactions between the dissolved and particulate phases although attempts by Morris et al. (1986) to observe these changes for trace metals were unsuccessful due to the much larger changes in composition mediated by the physical processes. The actual concentration of suspended particulate material within the low salinity region of the estuary is in general far greater than that seen in the riverine or oceanic sources due to the formation of a turbidity maximum. This consists of material from all sources and will

contain a sub-population of permanently suspended particles (Duinker et al., 1980; Morris et al., 1982b).

As river water enters an estuary there is an increase in the ionic strength on mixing with seawater. This will alter the stability of colloidal and particulate material by compressing the electrical double layer around the particles, reducing the inherent repulsion and allowing the Van der Waals forces to dominate and cause flocculation (Shaw, 1970; Gibbs, 1986). Work by Sholkovitz (1976) has shown that addition of very small amounts of salt will initiate flocculation of colloidal material from river waters. He showed that this flocculation process is a very important mechanism for the removal from solution of trace metals (Sholkovitz and Copland, 1981). There is also evidence to suggest that the increasing particle concentration in the low salinity turbidity maximum zone encourages flocculation (Aston and Chester, 1973) and it has been suggested that this is the primary factor controlling flocculation in estuaries (Kranck, 1981).

With respect to trace metals it is most important that the distribution of the metal between the various phases of the particles is known, as opposed to the total metal concentration, in order that the bioavailability and physico-chemical reactivity may be investigated (Loring, 1981; Luoma and Bryan, 1981). Metals bound within the crystalline detrital fraction of the particles will be virtually unavailable to nature and thus of less importance when considering biological uptake (Gibbs, 1973).

To gain some idea of trace metal availability many sequential extraction schemes have been designed which use chemical methods to separate portions of the particulate material (e.g. organic material

or Fe hydroxides) and measure the trace metals associated with that portion (Chester and Hughes, 1967; Gibbs, 1973; Guy et al., 1978; Tessier et al., 1980; Luoma and Bryan, 1981; Tessier et al., 1985; Rosental et al., 1986). Many of these techniques lack specificity and different schemes have been used by different workers which leads to a lack of comparability (Tessier et al., 1980; Luoma and Bryan, 1981). However, these techniques have shown that while the residual detrital material contains a substantial proportion of the trace metals the ferro-manganese oxides and organic materials are also important carriers of Zn and Cu (Gibbs, 1973; Luoma and Bryan, 1981; Tessier et al., 1985).

In the Tamar Estuary Loring et al. (1983) found the composition of the suspended particle population to be entirely controlled by the riverine input under high river flow conditions. Under normal river flow conditions, when a turbidity maximum of 15 times the particle concentration in the river water was set up, the detrital composition averaged over the whole estuary was quite uniform and similar to that seen under high river flow conditions. However, within the turbidity maximum under normal river flow conditions there was an enhancement of Si and a depression of the nondetrital Fe, Zn and Cu (Loring et al., 1983). The non-detrital portion of Zn and Cu has been seen in the Tamar to vary between 67-91% and 71-95% respectively (Loring et al., 1983). This emphasises the importance of knowledge about the partitioning of toxic trace metals on particulate material. It would be of great assistance to studies of this nature if a general extraction scheme could be agreed to enable easy interlaboratory comparison for individual estuaries.

1.3.2. Flocculation in Estuaries.

As previously mentioned particles and colloidal material will flocculate or coagulate on entering the low salinity region of an estuary. Colloidal material consists of small particles (approximately between 1nm and 0.4 μ m in at least one dimension) of clay minerals, hydrous metal oxides (particularly Fe) and organic material (Shaw, 1970; Sigleo and Helz, 1981).

The flocculation of colloidal Fe oxyhydroxides has been most fully studied and it is this removal which causes the substantially non-conservative behaviour of dissolved Fe in estuaries (Boyle et al., 1977; Moore et al., 1979; Bale and Morris, 1981; Mayer, 1982; Eastman and Church, 1984). Aston and Chester (1973) have shown that increasing salinity and turbidity both increase the rate and extent of Fe precipitation. Flocculation begins while the salinity is <0.1‰ but the full extent of removal is not reached until between 15‰ and 30‰ (Bale and Morris, 1981; Mayer, 1982). The kinetics of this reaction have been found by Fox and Wofsy (1983) to be second order with a rate coefficient which is proportional to the square of the salinity. Mayer (1982) found it to be a two step salinity dependent removal in which the first step was very fast and the second a slower pseudo-second order reaction dependent on temperature.

About 80% of dissolved humic material has been observed to be removed in the Amazon Estuary and the major part of this occurred between 0‰ and 5‰ salinity (Boyle et al., 1982). Dissolved humic acid is only a small percentage of the total dissolved organic carbon in estuaries but its flocculation has been shown to have a major effect on the coagulation of some trace metals (Mantoura et al.,

1978; Sholkovitz and Copland, 1981; Sigleo and Helz, 1981). Particles suspended in natural waters have been widely reported to have a negative surface charge regardless of the charge observed in synthetic organic free solutions with a similar ionic composition (Neihof and Leob, 1972; Hunter and Liss, 1979; Hunter, 1980; Tipping and Cooke, 1982). This uniform negative charge in natural waters has been attributed to surface adsorption of organic materials and Fe oxides (Hunter and Liss, 1979). Within estuaries some intra- and inter-estuarine variability in the magnitude of the electrophoretic mobility has been observed but for all particles it is negative (Hunter and Liss, 1982).

Within the Patuxent River there is a significant proportion of sub-micron clay mineral particles which are removed from the colloidal fraction of the suspended matter in estuarine water of $<10\text{‰}$ salinity (Sigleo and Helz, 1981). Differential flocculation of clays has been seen in laboratory studies and leads to various types of clays sedimenting at different rates depending on the salinity (Dyer, 1973). However while this is a possibility there is much evidence to suggest that in natural waters a simultaneous flocculation process is more probable (Sholkovitz, 1976; Sigleo and Helz, 1981; Mayer, 1982). The uniform surface charge has been used to account for the lack of evidence for differential flocculation in natural estuarine environments (Hunter and Liss, 1982). Flocculation will also involve removal onto the surfaces of suspended particles as has been shown for Fe (Aston and Chester, 1973) and by electrophoretic mobility studies for the organics (Hunter and Liss, 1979; Tipping and Cooke, 1982). The possible particles resulting from this type of

formation processes are discussed in the following section.

1.3.3 The Morphology of Estuarine Particulate Material.

Within estuarine particulate material there are clay, quartz, hydrous metal oxide and biogenic materials which will form composite particles by interaction in the river and estuarine regions. Although flocculation of particles in the estuarine zone has long been recognised little work has been carried out to determine the effect of this on the surface of natural estuarine material except with respect to the electrophoretic mobility (Hunter and Liss, 1982). The surface shape and type must be of importance to site availability and thus to natural sorption reactions. However this has been considered in only very few studies directly applicable to the estuarine situation (Lion et al., 1982; Davies-Colley et al., 1984) although more often in soil experiments (Cabrera et al., 1981; Madrid and De Arambarri, 1985).

Investigations into the rheological properties of clay suspensions have shown that in single component systems on flocculation kaolinite platelets will form a cardhouse structure via platelet face-edge interactions with interior pore spaces of about 0.5 μ m (Williams and James, 1978). In a kaolinite/quartz suspension the combined flocs are composed with the quartz as a central support to which the kaolinite platelets attach with strong quartz-kaolinite edge interactions. This gives a more open pin-cushion structure with pore spaces of again approximately 0.5 μ m (Williams and James, 1978). In the formation of soil flocs, while these loosely held open structures may form on initial flocculation, organic material and metal oxides may be considered to act as stabilising agents holding

the clay particles together (Quirk, 1978). It has also been suggested that polyvalent metals may form bridges between clay and organic materials (Quirk, 1978). In soils several clay lamellae may also be held together by face-face interactions in domains which may in turn be bound to other clay and quartz particles (Rimmer, 1987). It may be that formation of bound domain type structures will be of significance in the consolidation of the estuarine sediment bed. Particles within the sediment bed may be resuspended if the shear stress of the currents is great enough to overcome the shear strength of the bed (Dyer, 1972). As the open structures are deposited and resuspended during many tidal cycles they will gradually consolidate on the sediment bed, lose water and the shear strength will increase possibly preventing erosion during a subsequent tidal cycle (Dyer, 1972). This suggests the resuspended sediment material in the estuarine zone will be mainly composed of the more open loosely held structures.

Electrophoretic mobility measurements on suspensions of kaolinite with Fe and Al precipitated onto the surface have shown that Fe is present not in a continuous coating but in discrete dispersed particles adsorbed to the surface (Torres-Sanchez et al., 1985). The characteristics of Fe oxide materials are discussed in more detail in Section 1.4.3. Organic material coating the surface of particles has been seen to homogenise the electrical characteristics of particles and it has been suggested that in soils it may occlude areas of the particle surface by blocking pore entrances (Burford et al., 1964).

These structural shapes could be considered to give an idea of the gross morphology of estuarine particles; clay platelets, domains and quartz particles in composite particles with hydrous metal

oxides and organic material. Information on the structures of natural particles of this type cannot be found using particle size measurements or through electron microscopy studies. The aggregates formed in estuaries are often very fragile and easily broken during handling (Eisma et al, 1983; Bale et al., 1984). However it is possible that these fragile assemblages will enclose sorption sites and make it necessary for diffusion into a floc structure to occur before the adsorption reaction. It will also be important for studies of trace metal ions, with diameters of approximately 1nm, to know about the internal particle structure on a nanometer size scale. This may be examined using gas adsorption onto the dried solid which will give a measure of surface area and an idea of internal porosity. This is discussed in Sections 1.4.2 and 1.4.3. All aspects of the structure will be very important in determining the rates and extents of sorption reactions as in some cases active sites will be partially enclosed and thus require longer reaction times if diffusion to the site has to take place.

1.4. Heterogeneous Chemical Reactivity.

1.4.1. Trace Metal Sorption Studies.

It is well documented that, in polluted estuaries, sediments may accumulate very high concentrations of trace metals to the detriment of the marine life (Aston and Chester, 1976; Forstner, 1980). For this reason the interaction of trace metals with suspended particulate material has attracted considerable research and relevant examples of such studies, designed to elucidate the controls on these complex reactions, are shown in Table 1.6. In view of the contrasts in the methodology adopted in these studies it is difficult to see how definitive comparisons can be made. Furthermore, although these studies attempt to mimic natural heterogeneous chemical processes, it is not clear how close to reality the models are. Some of the problems in experimental design are given below.

The majority of the studies listed use pH as the fundamental variable against which dissolved metal concentration in solution is followed. While this may be of use with regard to mine streams and other discreet pollutant outputs it is not of immediate relevance to many estuarine mixing regimes in which the pH will vary only between 7 and 8.2 (Dryssen and Wedborg, 1980; Mantoura and Morris, 1983). A further problem is with the composition and nature of the reactants. The particulate phases are often synthetic materials such as Fe or Al oxyhydroxides or pure clay minerals. The composition of the dissolved phase of many experiments is also very variable. For example, some studies (e.g. Kinniburgh et al., 1976; Millward and Moore, 1982) omit dissolved organic material, which has been shown to be of importance to adsorption by other workers (Davis, 1984; Davies-Colley et al.,

<u>Metal</u>	<u>Reactants</u>		<u>Variables</u>	<u>Reference</u>
	<u>Solution</u>	<u>Solid</u>		
Cu, Pb	Various electrolyte including synthetic seawater	Am-FeOOH	pH, [metal], [solid] electrolyte, solid age	Swallow <u>et al.</u> (1980)
Cd, Cu, Pb, Zn	Various electrolyte including synthetic seawater	Goethite	pH, [metal], electrolyte	Balistieri and Murray (1982)
Cu, Mn, Zn	Model estuarine water	Am-FeOOH	pH, salinity	Millward and Moore (1982)
Cd, Cu	Various electrolyte and lake water	Al ₂ O ₃ and natural organics	pH, [organics], [metal], [solid], electrolyte	Davis (1984)
Cd, Cu	Synthetic estuarine water	Model sedimentary phases	pH, [metal], salinity, solid type	Davies-Colley <u>et al.</u> (1984)
Cd, Cu, Zn	0.01 M NaNO ₃	Treated sediments	pH	Mouvet and Bourg (1983)
⁶⁵ Zn and others	Seawater	Marine sediments	[metal], [solid], salinity	Aston and Duursma (1973)
⁶⁵ Zn and others	River and seawater mix	Suspended river particles	salinity, time	Li <u>et al.</u> (1984a)
⁶⁵ Zn and others	Seawater	Marine sediments	time, solid type	Nyffeler <u>et al.</u> (1984)
⁶⁵ Zn and others	River and seawater mix	Suspended estuarine particles	pH, salinity, time	Bale (1987)

Table 1.6. Relevant examples of trace metal sorption studies which attempt to simulate natural conditions.

1984). Also adsorbates can sometimes be added to the reaction mixture in an inorganic form. These will not necessarily be in equilibrium with the dissolved organic material which will associate with the added metal to a much lesser extent than the already present metals (Millward and Burton, 1975). This is a problem which also exists with studies using spikes of radio-nuclides. These suffer from the additional disadvantage that an unknown percentage of the observed uptake may be due to the equilibration of the isotope with the existing metal on the particle surface (Nyffeler et al., 1984; Bale, 1987). However, the advantage of the use of radio-nuclides is that they can be used in low concentrations pertinent to the natural environment, unlike the high metal concentrations which have been used in some studies (Haas and Horowitz, 1986). It has been shown that the uptake behaviour at high concentrations may not be extrapolated to a low concentration situation (Kinniburgh and Jackson, 1982; Garcia-Miragaya et al., 1986). The approach to more realistic solution conditions is fraught with difficulty due mainly to the problems encountered while analysing trace metals at low concentrations in complex solutions. However in this work a serious attempt was made to reproduce natural adsorption behaviour in the laboratory by using natural solutions and particles.

Finally another important consideration is the timescale of the uptake and the approach to equilibrium. In many studies reactants are mixed for a predetermined equilibrium or arbitrary time (Aston and Duursma, 1973; Reid and McDuffie, 1981; Balistrieri and Murray, 1982). This time may not be of direct relevance to estuarine studies because as was discussed in Section 1.1.2 the system has continually

fluctuating properties which will prevent an equilibrium being attained for kinetically slow reactions. Equilibrium conditions are often expressed in terms of partition coefficients, K_d s, and under equilibrium conditions these are large for many trace elements and show a variation with salinity (Nyffeler et al., 1984; Morris, 1986; Bale, 1987). Very few attempts have been made to observe the kinetics of the approach to equilibrium although detailed studies of the kinetics of Fe (Mayer, 1982; Fox and Wofsy, 1983) and Mn (Morris and Bale, 1979; Morris et al., 1981) behaviour have been carried out. More recently Nyffeler et al. (1984) have shown that the kinetics of trace metal adsorption is governed by a two stage reaction of the form shown in Figure 1.2. The first stage is a fast surface adsorption which is followed by a migration of surface adsorbed species into the matrix of the particle. Figure 1.3 compiled from data abstracted from Ackroyd (1983) shows that in model solutions estuarine particles take up 70-80% of some added dissolved trace metals. If the doped particles are then resuspended in metal-free water only about 10% of the particulate metal is returned to solution, thus the metals show a strong preference for the particulate phase. This kind of irreversible adsorption has been observed for phosphate in contact with Fe oxyhydroxides which show different pH-induced hysteresis for 1 and 24h old particles (Lijklema, 1980). Crosby et al. (1983) have suggested this hysteresis is due to the pore size and shape in the Fe oxyhydroxide particles. In addition, the soil science literature contains evidence that this type of two step adsorption occurs when phosphate is adsorbed onto soil particles (Barrow, 1983). Madrid and De Arambarri (1985) and Cabrera et al. (1981) have both gone as far as

Amount Adsorbed

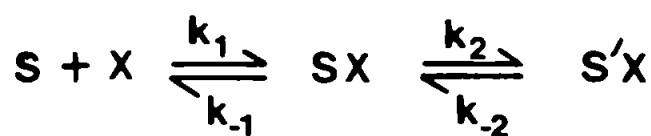
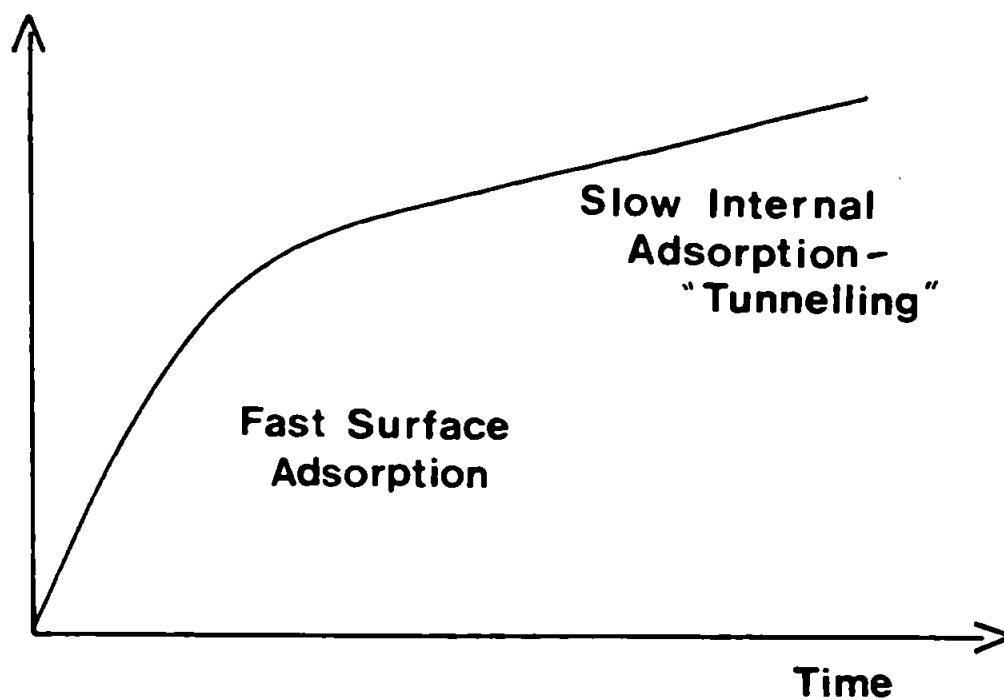


Figure 1.2. A typical adsorption profile for a two stage reaction of the type shown. S adsorption site; X adsorption species; SX surface adsorbed species, S'X matrix adsorbed species.

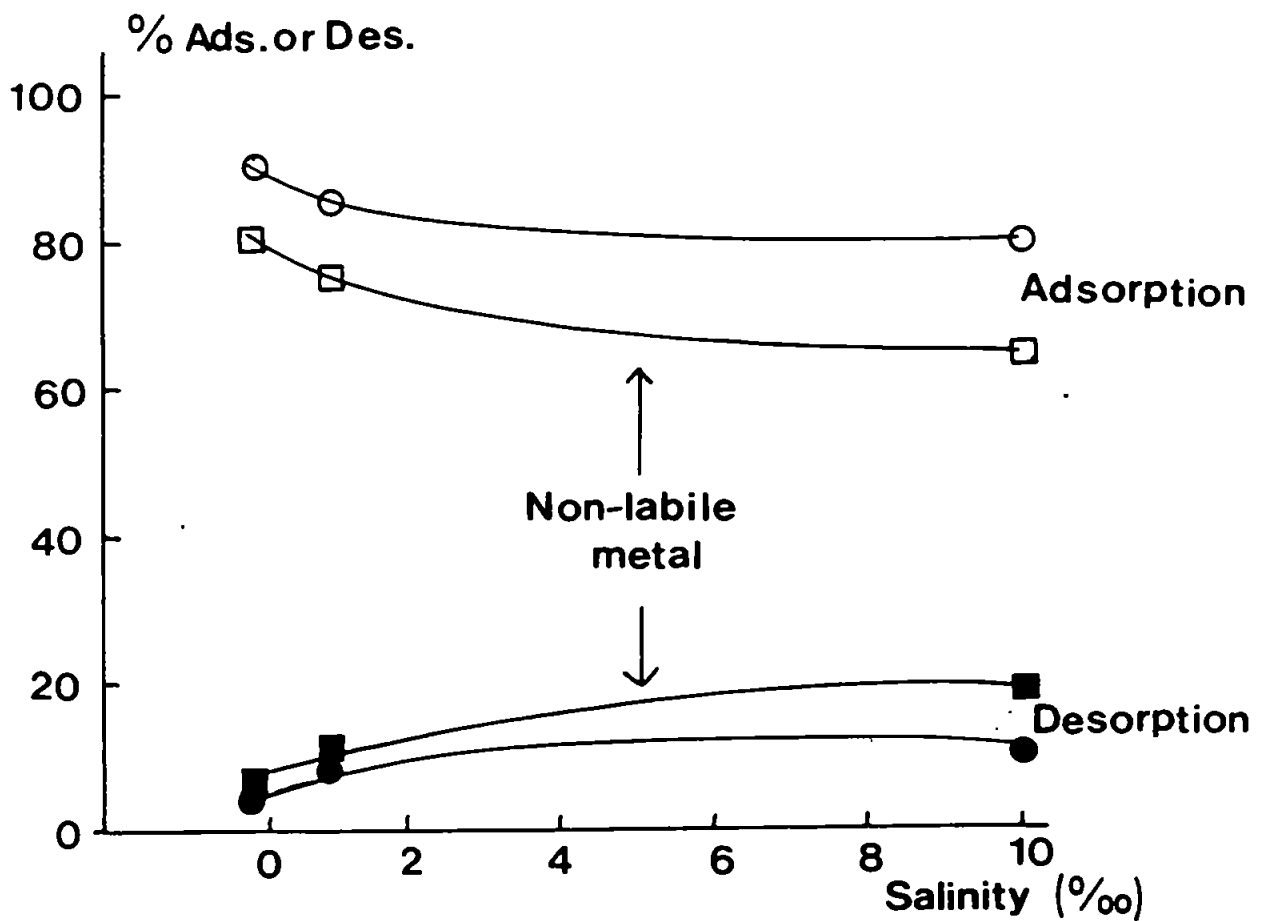


Figure 1.3. The percentage metal adsorbed by natural estuarine particles and the subsequent percentage of this metal desorbed on resuspension in metal free media with varying salinities. The turbidity of the suspensions was 500mg/L, the temperature 10°C, the pH 7.5 and the initial concentration of both Cu and Zn 100µg/L.
 Zn □ Cu ○

to relate the particle porosity to phosphate adsorption on Fe oxyhydroxides.

It is clear from the above discussion of previous work in this area that adsorption behaviour of particles is controlled to some extent by particle morphology. However this area has been under-researched especially with respect to trace metal interactions and so in this work an attempt is made to study the kinetics of sorption on realistic timescales and to relate this to the morphology of natural particles.

1.4.2. The Surface Area of Particles.

The specific surface area of a solid phase is one of the first parameters that must be determined if there is to be a detailed understanding of adsorption processes. There are many texts which detail the plethora of literature on the determination of surface areas of synthetic and industrial solids (e.g. Adamson, 1982; Gregg and Sing, 1982). The main problem with surface area determination is that the surface area observed is highly dependent on the analytical method used, as Adamson (1982) has described. Essentially, there is no such thing as absolute surface area (Adamson, 1982) but if a consistent methodology is adopted then the values of surface area, obtained by a specific technique, can be used in a comparative way. This is exemplified in a study of the surface area of AgI using different analytical techniques as shown in Table 1.7a (Van den Hul and Lyklema, 1968). This data shows that the specific surface areas determined by BET nitrogen adsorption (onto the dried solid) are a factor of three smaller than those determined on the wetted solid using negative adsorption but there is a consistent trend for the

<u>BET N₂</u> <u>gas</u>	<u>Negative</u> <u>adsorption</u>	<u>Particle</u> <u>size</u>	<u>Dye</u> <u>adsorption</u>	<u>Ratio of</u> <u>neg. ads./BET</u>
0.45	1.5	0.25	0.87	3.2
0.38	1.3	0.18	0.61	3.8
0.52	1.6	0.32	0.98	3.1
0.30	0.9	0.22	0.65	3.2
0.97	3.3	0.45	2.18	3.6
1.99	5.5	--	2.14	2.8

Table 1.7a. Surface areas (m²/g) of AgI samples determined by a variety of methods (Van den Hul and Lyklema, 1968).

<u>Method</u>	<u>Specific surface</u> <u>area (m²/g)</u>	<u>Reference</u>
Calculated from particle size	840	Davis and Leckie (1978a)
Negative adsorption PO ₄ ³⁻	720	Anderson and Malotky (1979)
Mg ²⁺	700	Avotins (1975)
Na ⁺	270-335	Davis and Leckie (1978b)
BET Ar adsorption	215-265	Van der Geissen (1966)
BET N ₂ adsorption	150-350	Borggaard (1983) Crosby <u>et al.</u> (1983) Marsh <u>et al.</u> (1984)

Table 1.7b. Comparison of surface areas (m²/g) of Am-FeOOH determined by a variety of methods.

surface areas determined by all four methods. Similar differences have been observed in experiments involving amorphous Fe oxyhydroxides as shown in Table 1.7b.

In the case of natural solids it would obviously be preferable to determine the specific surface area in situ to avoid adulterating the particle surface. However there are conceptual difficulties with the interpretation of adsorption data in the wet state (Van den Hul and Lyklema, 1968; Crosby et al., 1983). The problems of this lack of comprehension and theoretical development of aspects of liquid-solid adsorption have been highlighted by Professor Everett (1982) who has suggested that attempts to unify the theories of liquid-solid and gas-solid adsorption should be made. This understanding is a long way off but in the interim estuarine chemistry urgently requires information on particle morphology to further develop models on the fate of trace constituents. Therefore, in the absence of in situ methods it is necessary to use the BET nitrogen adsorption method on the dried solid with the least possible disruption to the particle surface. The use of the dried solid in conjunction with nitrogen adsorption can be used to give consistent information especially since this technique has already been used effectively in this laboratory to study Fe oxyhydroxides (Crosby et al., 1983; Marsh et al., 1984). An additional advantage of this technique is the ability to study both the adsorption and desorption of nitrogen from the particles. There is a well established theory which can be used with this data to give information on the internal porosity of the solid (See Section 1.4.3.) which is not available from the wet methods of analysis.

Finally, with this nitrogen adsorption technique it is also possible, with a consistent preparative methodology, to examine the effects of surface coatings of Fe oxyhydroxides and organic matter on the particle microstructures as has been shown for estuarine particles (Millward et al., 1985; Glegg et al., 1987; Martin et al., 1986). In view of the fact that no in situ method currently offers these advantages the BET nitrogen adsorption method has been used almost exclusively in this study. Thus, the words "surface area" quoted subsequently in this thesis refer specifically to this technique unless otherwise stated.

1.4.3. The Porosity of Particles.

Of particular relevance to this study was the ability, through gas adsorption and desorption experiments using a vacuum microbalance, to determine information on the shape, size and volume of internal pore structures within the particles (Gregg and Sing, 1982). Several different ways of analysing gas sorption data to obtain the pore size distributions have been described (e.g. Cranston and Inkley, 1957; Lippens et al., 1964; De Boer et al., 1966) and in this work the shape of the hysteresis isotherm has been used in conjunction with the Kelvin equation (Gregg and Sing, 1982). These methods have been used to examine the nature of soils (Burford et al., 1964; Greenland and Quirk, 1962; Quirk, 1978; Madrid and De Arambarri, 1985) but very little work has been carried out on other natural materials. Therefore, for the purpose of this review and in an attempt to understand something of the controls on particle microstructure the role of the individual components of natural

materials will be examined.

Natural silica minerals are usually non-porous materials which have a low BET surface area of approximately $<5\text{m}^2/\text{g}$ which is comparable to the geometric surface area calculated from the particle size (Barby, 1976; Martin et al., 1986). The specific surface area of clays varies considerably depending on their type and source (Dutta and Gupta, 1974; Van Olphen, 1976). A comparison between the water vapour adsorption properties of montmorillonite (an expanding clay) and illite (a non-expanding clay) has shown the penetration of water within the former to confer a larger surface area than seen for illite (Mikhail et al., 1979). This is because water cannot diffuse into the inter-lamellar space in non-expanding clays due to the strong Van der Waals and hydrogen bonding forces between crystalline sheets. The expanding clays will hold water within the structure as there is an interlayer space in which ions will have relatively easy access to internal sites. The non-expanding clays will have reactive sites available on the edges of sheets and in defects but not to the same extent within the lattice (Van Olphen, 1976). It has been observed by X-ray diffraction methods that Fe and Mn hydroxides adsorbed on expanding clay minerals can prevent swelling of the lattice (Eisma et al., 1978). This would presumably tend to give them a surface area and porosity similar to that seen in non-expanding clays.

The characteristics of particulate hydrous metal oxides have been shown to be greatly affected by the initial conditions in which precipitation and flocculation occurs and by the age of the sample (Kolthoff and Bowers, 1954; Bye and Sing, 1972; Crosby et al., 1983; Marsh et al., 1984). To demonstrate the variability and range of both

surface area and pore size of iron oxides four isotherms, selected from the work by Crosby (1982), are shown in Figures 1.4 a-d. The surface area and pore size range of these materials are shown in Table 1.8.

The hysteresis loops of Figures 1.4 a and b are indicative of so-called ink-bottle pores which have a narrow neck and wide body. The ink-bottle pores appear to be present in both synthetic (Figure 1.4a) and natural (Figure 1.4b) Fe(III) derived oxyhydroxides. In addition these isotherms indicate by the low pressure hysteresis ($P/P_0 < 0.38$) the presence of micropores within the solid (Sing, 1982). These have been shown by Crosby et al. (1983) to be absent in a similar synthetic sample aged for 48h. Figure 1.4c shows a hysteresis loop of a synthetic Fe(II) derived oxyhydroxide (i.e. a poorly crystallised lepidocrocite (Sung and Morgan, 1980; Crosby et al., 1983)) which has characteristic pores of parallel plates or slits. The isotherm in Figure 1.4d is indicative of a non-porous solid, which with such a large surface area of $164\text{m}^2/\text{g}$ and no porosity is a very finely divided solid.

Comparing the pore shapes and sizes of the natural and synthetic particles shows that there are similarities and also differences caused by the varying circumstances under which they were prepared. It has been suggested for example that organic material coating the surface of precipitated Fe oxyhydroxides will have caused a reduction in the surface area of some Fe oxyhydroxide samples (Crosby, 1982). Schwertmann and Fischer (1973) have also shown that ageing of amorphous Fe oxyhydroxides in natural solutions is severely retarded by organic material and other compounds retained within the

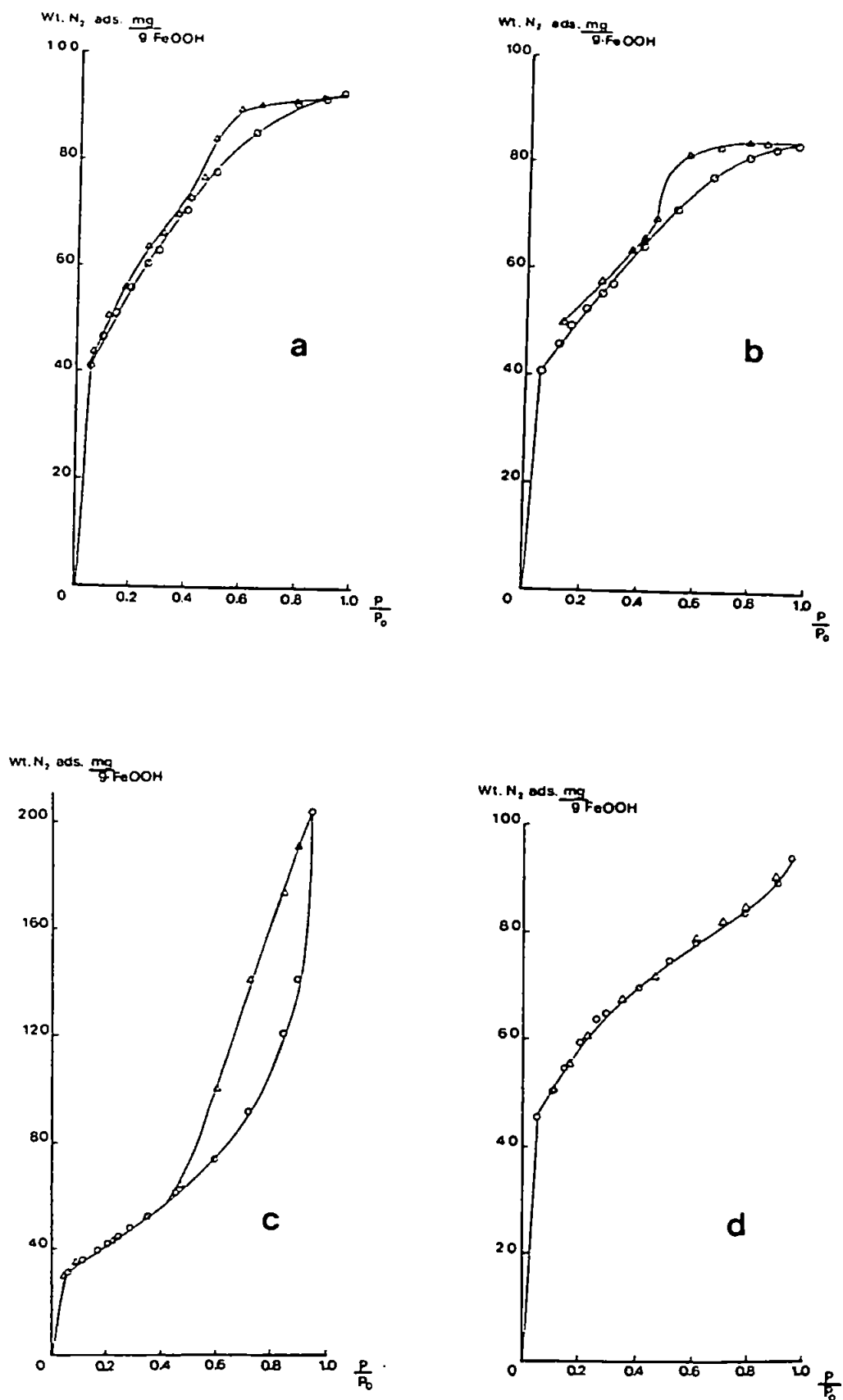


Figure 1.4. Nitrogen adsorption hysteresis isotherms for synthetic (a,c) and natural (b,d) iron oxyhydroxide materials (Crosby et al., 1983). The surface characteristics for these solids are shown in Table 1.8.

<u>Isotherm</u>	<u>Type of material</u>	<u>Surface area</u> <u>(m²/g)</u>	<u>Pore shape and</u> <u>size range (nm)</u>
a	Synthetic Fe(III) derived Am-FeOOH	159	Ink-bottle type, <2-50
b	Natural stream ppt. Am-FeOOH	141	Ink-bottle type, <2-200
c	Synthetic Fe(II) derived lepidocrocite	120	Parallel plates or slits, 20-200
d	Natural mine stream sediment	164	Non-porous

Table 1.8. The surface areas, pore shapes and range of pore sizes for the isotherms shown in Figure 1.4 a-d (Crosby et al., 1983).

oxide. Hydrous Fe-Mn oxide compounds have been indicated to be major carriers of trace metals in sequential extraction (Gibbs, 1973; Tessier et al., 1980; Luoma and Bryan, 1981; Loring, 1982) and adsorption and flocculation studies (Sholkovitz and Copland, 1981; Lion et al., 1982; Millward and Moore, 1982; Tessier et al., 1985). Changes in particle microstructure induced by surface coatings must have some effect on the ability of these particles to remove trace metals from solution.

This section has given an outline of the complexity of the micro-structural controls that could influence sorption processes at natural particle surfaces. Examining the individual phases (such as Fe oxyhydroxides and clay minerals) does not give conclusive

information on the surface micro-structure of natural materials as the way the materials interact will be of importance. For example, clay minerals may be weathered into individual platelets, thus generating a larger specific surface area; on the other hand expandable clays may be prevented from swelling by the presence of hydrous metal oxides (Eisma et al., 1978). Organic material may block the internal pore structures of natural particles (Burford et al., 1964) and in addition organics may cover over specific adsorption sites (Davis, 1982). It has also been shown that the age and initial conditions for precipitation may affect the surface characteristics of Fe oxyhydroxides. These contrasting influences which will control the surface area to which the solution phase has access cannot be easily identified in natural samples individually. It is for this reason that BET surface areas and porosities are used in this work to give information which is indicative of the nature of the whole estuarine particle population.

Work by Martin et al. (1986) has shown the BET (argon adsorption) surface area of natural suspended estuarine particulates to vary throughout the salinity regime in the Loire and Gironde estuaries ($5\text{--}30\text{m}^2/\text{g}$). They also observed an increase in BET surface area on removing organic material ($30\text{--}40\text{m}^2/\text{g}$) and a decrease on removing hydrous metal oxides ($5\text{--}10\text{m}^2/\text{g}$) from the same samples. However, no work has been carried out in other estuaries nor have the internal pore characteristics of estuarine material been examined and as was indicated in Section 1.4.2 this may be of fundamental importance when considering the controls on sorption of trace metals.

1.5. Aims of Present Work.

The overall aim of this work is to investigate the behaviour of dissolved trace metals with respect to studies of surface morphology of estuarine particulate materials in natural estuarine media. The individual steps necessary for such a study are enumerated below.

(1) To collect, prepare and determine the microstructure of natural suspended and sediment material from the Tamar Estuary and Restronguet Creek.

(2) To determine the carbon and non-detrital (leachable) Fe and Mn contents of estuarine particulate material and examine the effects of their removal on the surface morphology of the particles.

(3) To develop a method suitable for the preparation and analysis of dissolved trace metals at natural concentrations in small volume water samples which are to be collected on a timescale suitable for kinetic analysis during estuarine modelling studies.

(4) To investigate the behaviour of the reactive trace metals, Zn and Cu, on the addition of suspended estuarine particles to a natural estuarine media in which the salinity, turbidity and initial metal concentrations are varied.

(5) To determine relevant kinetic parameters from the sorption data on timescales appropriate to estuarine mixing.

(6) To relate the kinetic parameters determined in the modelling studies to the morphology of natural particle surfaces and discuss the information which may be derived from the synthesis of these observations with respect to estuarine mixing processes.

CHAPTER TWO

EXPERIMENTAL TECHNIQUES AND METHOD DEVELOPMENT

This chapter gives details of all experimental techniques required for this work and includes discussion of the development and refinement of the methods used. It is divided into three sections dealing with techniques used to characterise particles, the preparation of particulate samples and the development and implementation of the approach used to model particle-water interactions.

The first two sections deal with the methods used to prepare and characterise natural estuarine particles in a consistent manner. The particles comprise a complex mixture of materials including quartz grains, aluminosilicate clays, organic matter and hydrous ferromanganese oxides. Thus, drying particles for characterisation studies presents some obvious problems with respect to particle integrity and the homogeneity of samples.

The last portion of this chapter discusses the development of a method suitable for the preparation of small volume natural water samples and the analysis of dissolved trace metals contained in them. It outlines the problems highlighted during attempts to analyse for these metals by Anodic Stripping Voltammetry (ASV) and gives the reasoning for eventually favouring Atomic Absorption Spectrometry (AAS) as the analytical method.

2.1. Particle Characterisation Techniques.

2.1.1. Particle Microstructural Analyses.

Nitrogen adsorption has been used throughout this work as the principal means of examining the surface area and porosity of the particles. It is important to remember that surface area is a method dependent quantity and while values are internally consistent they may not be compared directly with those determined using a different gas or other means (e.g. Greenland and Quirk, 1962; Van den Hul and Lyklema, 1968; Giles et al., 1979; Rouqu  rol et al., 1979). Other methods which could have been used for surface area determination include for example, negative adsorption from solution (Van den Hul and Lyklema, 1968), dye adsorption from solution (Giles et al., 1979) or geometric calculation from electron microscopy (Gregg and Sing, 1982). However none of these methods would give quantitative information on the internal porosity of the particles and this information is thought to be extremely important with regard to sorption processes in solution (Barrow, 1983; Nyffeler et al., 1984; Madrid and De Arambarri, 1985; Martin et al., 1986). Gas adsorption is the only method available which may be easily used to determine the porosity characteristics of the particles as well as the surface area.

A gravimetric Brunauer, Emmet and Teller (BET) nitrogen adsorption technique was used to determine the nature of the surface of the natural particle samples (Brunauer et al., 1938). A sample is initially weighed under vacuum conditions and then changes in its weight are monitored as nitrogen gas is introduced into the apparatus and subsequently adsorbed onto the sample. These weight changes are used to calculate the surface area of the sample and full adsorption-

desorption hysteresis loops are used for a porosity analysis.

The apparatus used is that described by Carter (1983) and shown in Figure 2.1. Approximately 0.2g aliquots of dried sample were placed in the aluminium weighing bucket of a C.I. Microforce MK11 balance. In the range of partial pressures used to calculate the surface area, 1mg or more nitrogen gas was adsorbed. If less sample was available, due to problems encountered for example when removing samples from filter papers, aluminium counterweights were added to the bucket to increase the weight to the 0.2g required for analysis. The apparatus was evacuated and the sample retained under vacuum until constant weight was achieved (between 0.5 and 5h) when the sample was cooled to 77°K with liquid nitrogen (Glasson and Linstead-Smith, 1973). For the BET surface area determination (up to relative pressure, $P/P_0 = 0.3$) the nitrogen gas (>99.9% pure, Air Products) was allowed into the balance in doses of about 40mm Hg with up to 0.5h being necessary between doses for equilibration. Above $P/P_0 = 0.3$ the pressure was increased in doses of 100mm Hg, with similar equilibration times as the BET range, until $P/P_0 = 1$. The desorption was then carried out in steps of 100mm Hg with equilibration times of up to 2h. A typical adsorption-desorption isotherm for an estuarine suspended sample is shown in Figure 2.2.

The BET equation (Brunauer et al., 1938) states

$$\frac{P}{X(P_0 - P)} = \frac{1}{X_m C} + \left[\frac{(C-1)}{X_m C} \times \frac{P}{P_0} \right] \quad (2.1)$$

where P_0 is the saturated vapour pressure of nitrogen, X_m is the weight of nitrogen molecules adsorbed at monolayer coverage, and X is

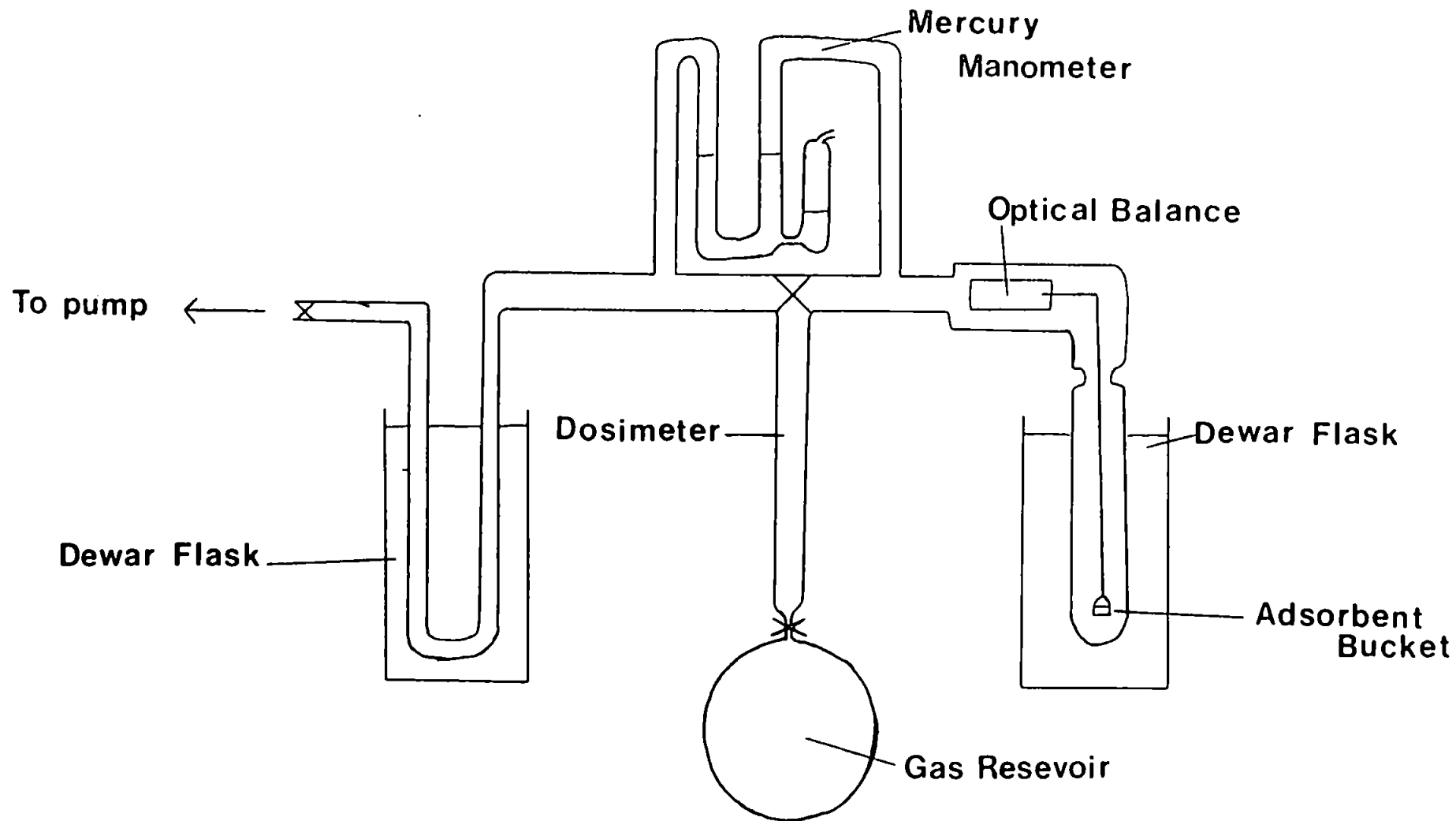


Figure 2.1. A schematic outline of the vacuum microbalance apparatus.

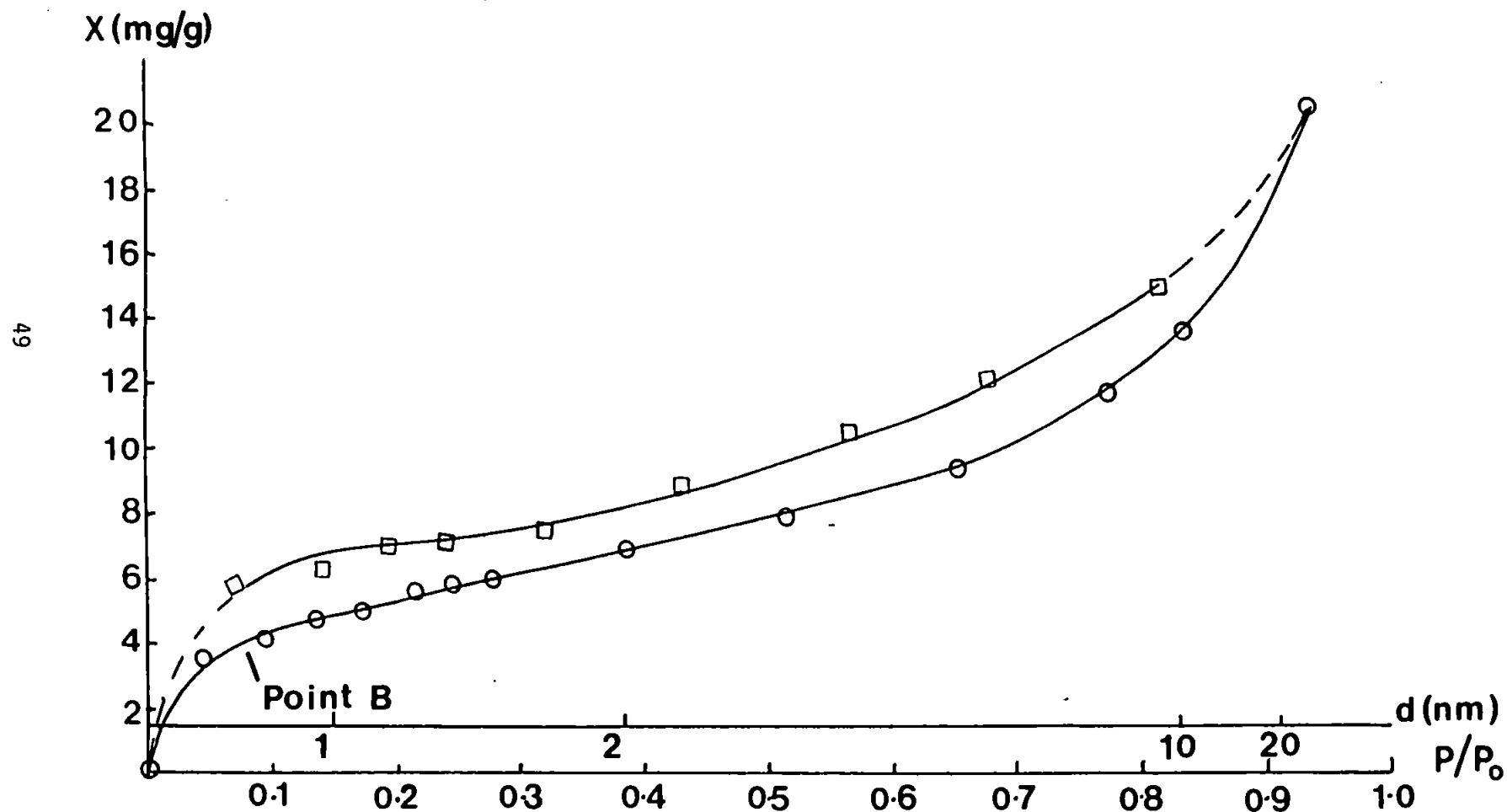


Figure 2.2. A complete adsorption-desorption isotherm for a natural sample with a surface area of $16.1 \text{ m}^2/\text{g}$. The region of the B-point which may be used for surface area determination is indicated. A scale of pore diameters calculated using the Kelvin equation as discussed in Section 2.1.1 is also shown. ○ Adsorption □ Desorption

the weight of nitrogen adsorbed at pressure P , the pressure inside the apparatus. C is quantitatively related to the heat of adsorption of the first layer of gas but no precise mathematical description is available (Sing, 1982).

Plotting $P/X(P_0 - P)$ versus P/P_0 for the range $0.05 < P/P_0 < 0.3$ will give a straight line as shown in Figure 2.3 which is derived from the results in Figure 2.2. From this graph the slope, $(C-1)/X_m C$, and intercept $1/X_m C$ may be read and these may be used to determine the monolayer capacity as shown in Equation 2.2.

$$\frac{C-1}{X_m C} + \frac{1}{X_m C} = \frac{1}{X_m} \quad (2.2)$$

The surface area of the particles can then be calculated from

$$\text{Surface area} = X_m \times L \times A_N \quad (2.3)$$

where L is the number of gas molecules in one mg and A_N is the area of the adsorbed molecule. The recognised area for a nitrogen molecule of $A_N = 0.162 \text{ nm}^2$, calculated from the liquid density of nitrogen at 77°K , has been used in this work (Adamson, 1982; Sing, 1982).

Linear regression of $P/X(P_0 - P)$ versus P/P_0 was carried out using the Minitab statistical package on a Prime 950 mainframe computer. For the natural samples this gave a straight line (correlation coefficient >0.99) for the partial pressure range $0.05 - 0.3$. The methods were checked using standard reference materials.

Standard reference graphitised carbon samples (M11-01 and M11-02) were supplied by NPL in the dried state. Analyses on these, as

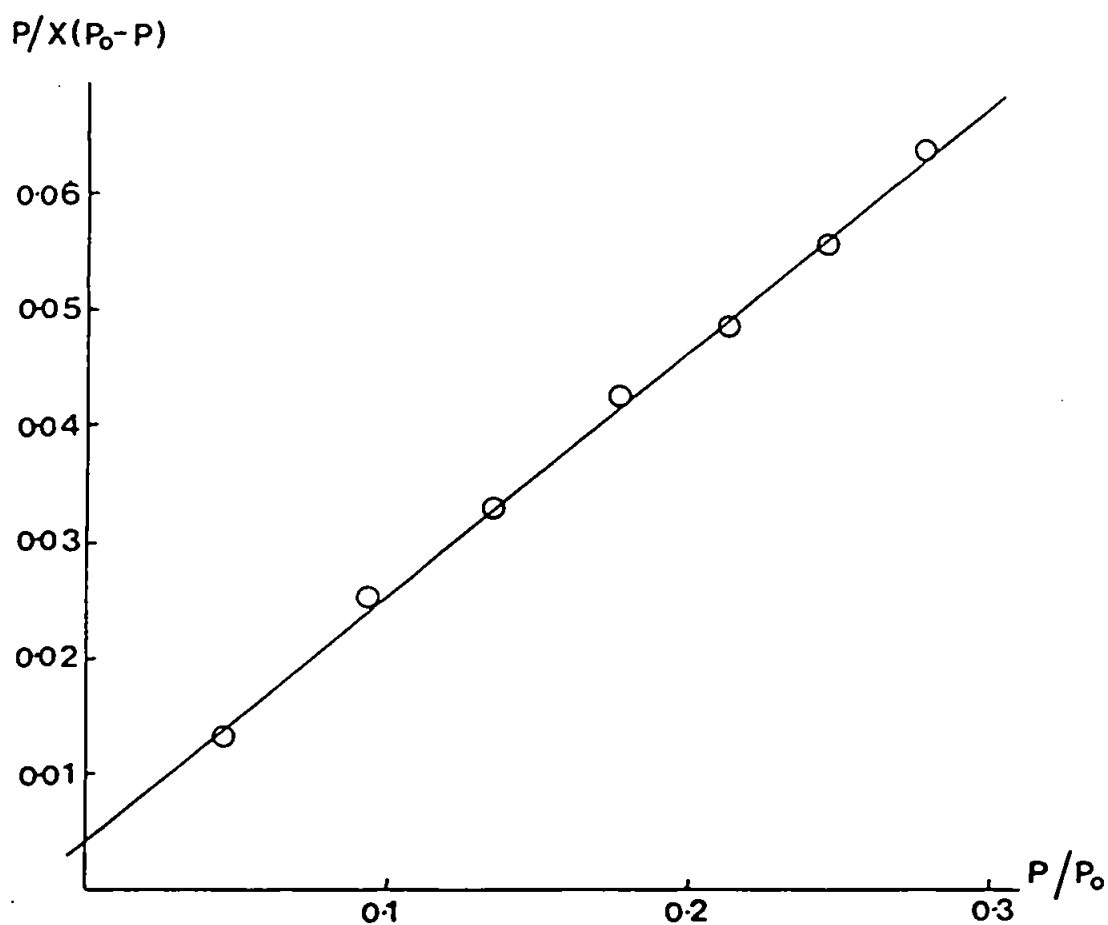


Figure 2.3. A BET plot of $P/X_m(P-P_0)$ versus partial pressure for a natural sample with a surface area of $16.1 \text{ m}^2/\text{g}$. The correlation coefficient for this line is 0.998.

would be expected for carbon black samples (Sing 1982), did not give a straight line for the complete range 0.05 - 0.3 and so higher points on these plots were excluded and the resulting straight line used. A comparison of measured surface areas of these standards with those specified by the suppliers and also with areas determined by Mr J.G. Titley is shown in Table 2.1.

<u>Sample</u>	<u>Reference</u>	<u>Surface areas (m²/g)</u>	
		<u>This work</u>	<u>Titleys' work</u>
M11-01	11.1±0.8	9.2	9.9
		9.7	10.6
		9.3	12.9
		9.7	11.8
		9.4	12.9
Mean of replicates	--	9.5 ± 0.2	11.6 ± 1.3
M11-02	71.3 ± 2.7	66.2	67.9

Table 2.1. Replicate surface area analyses for two previously dried reference carbon black samples (NPL) carried out for this work and by Mr J.G. Titley. These values were calculated using the linear regression model.

A second method of computerised calculation was employed to see if this would give a better comparison with the NPL standards or generally improved reproducibility. This method used a non-linear regression model, developed by Dr D.G. Kinniburgh, to identify the so-

called point B, the region of which is shown in Figure 2.2 (Roebens, 1980; Kinniburgh, 1985). Use of the B-point for some types of isotherm can avoid laborious calculations as at this point, the knee of the isotherm, monolayer coverage should be complete and the surface area may be calculated from this X_m value using Equation 2.3. This method gave results very much in agreement with those from the linear regression model for the natural samples as shown in Table 2.2.

<u>Sample</u>	<u>Surface areas (m²/g)</u>		
	<u>Reference</u>	<u>Linear</u>	<u>Non-linear</u>
Suspended	--	8.4	8.6
Suspended	--	26.8	27.0
Sediment	--	14.6	14.7
M11-01	11.1 ± 0.8	9.2	11.1
	--	9.7	12.1
	--	9.3	11.7
	--	9.4	10.6
M11-03	152.4 ± 2.1	138.3	138.6
M11-04	263.3 ± 0.5	231.1	228.8

Table 2.2. Typical surface areas for natural samples and reference materials (NPL) calculated using linear and non-linear regression models. The M11-01 standard is a graphitised carbon and M11-03 and M11-04 are porous silica materials.

The results calculated with the non-linear regression model for the two porous silica standards (NPL; M11-03 and M11-04) were also in agreement with values calculated using the linear regression model but those for the graphitised carbon black (NPL; M11-01) were noticeably different. Those calculated using the non-linear regression model were nearer to the supplied reference values probably because point B is more easily identified for these samples, as shown by the high C values as defined in Equation 2.1. Since this calculation method offered no advantage for the natural samples all future data was analysed using a BET plot as this allowed visual inspection of the plotted data (as in Figure 2.3) to help avoid errors.

A comparison was carried out on some suspended particulate samples, taken from the Tamar Estuary, with Dr D. Plummer to see if the surface area calculated from the nitrogen adsorption data was comparable to that taken in the wet state by adsorption of Cetyl Piridinium Chloride (CPC). The results of this, given in Table 2.3, illustrate that the dye adsorption gives a surface area 6-9 times greater than that measured by nitrogen adsorption for natural suspended Tamar particles. Although these values are higher they are by no means any more correct. They are different method dependent values which follow the same trend seen using the nitrogen adsorption technique. Studies by Greenland and Quirk (1962) and Burford et al. (1964), also show comparisons of surface areas measured using Cetyl Piridinium Bromide and nitrogen adsorption techniques and their results indicate a wide range of comparisons depending on the character of the material on which the surface areas are being determined.

<u>Surface area (m²/g)</u>	
<u>Nitrogen adsorption</u>	<u>CPC adsorption</u>
23.1	146
16.5	127
14.6	133
11.5	106

Table 2.3. A comparison of surface areas of suspended estuarine particles measured by nitrogen and dye adsorption methods. Dye adsorption data courtesy of Dr D. Plummer.

Other comparative studies have also been carried out between this and another laboratory involving the drying and subsequent nitrogen adsorption analysis of the surface areas of estuarine suspended material. These show a good correlation and are detailed in Millward and Titley (1985).

Data from the complete adsorption-desorption isotherms can be plotted in the form shown in Figure 2.2 and this may be used for quantitative assessment of pore size, shape and volume. The difference between the adsorption and desorption branches of an isotherm is due to condensation of nitrogen within the pores of the sample. This condensation is described by the Kelvin equation which may be written for cylindrical pores in the form,

$$\ln\left(\frac{P}{P_0}\right) = -\frac{2Vj}{rRT} \quad (2.4)$$

where V is the molar volume of nitrogen, j is the surface tension and r is the pore radius (Gregg and Sing, 1982). R is the universal

gas constant (8.314 J/Kmol) and T is the temperature in °K. Using Equation 2.4 and taking $V = 34.68 \text{ cm}^3/\text{mol}$ and $j = 8.72 \times 10^{-7} \text{ J/cm}^2$, a scale of pore radii appropriate for nitrogen at 77°K has been calculated and plotted onto Figure 2.2 to show how hysteresis may be related to pore sizes as the position at which the hysteresis loops open and close is indicative of the pore size (Ponec et al., 1974). These pore sizes are generally split into three ranges, micropores (diameter < 2nm), mesopores (diameter 2-50nm) and macropores (diameter > 50nm) (Sing, 1982).

Hysteresis in the low pressure region of the isotherm is indicative of the presence of micropores and some samples did not regain their original weight after complete desorption at 77°K. This is because nitrogen molecules may become irreversibly adsorbed in narrow slits, possibly deformed by the gas adsorption, or in entrances to micropores which have dimensions similar to the gas molecules (Sing, 1982). At high pressures, due to operational problems it was impossible to reach $P/P_0 = 1$. Therefore, the form of the hysteresis loop between the highest adsorption point and first desorption point may be inaccurate as a result of this although the presence or absence of macropores may be determined. The portions of the isotherm which, as a consequence of these problems, are not well defined are drawn with a dotted line.

Pore shape may be estimated by examining the isotherm hysteresis as the particular shape of the desorption branch may be related to specific pore shapes for industrial particles (Roebens, 1980; Sing, 1982) and natural particles (Crosby et al., 1983; Marsh et al., 1984). The pore volume may be estimated for a particular pore

size classification by considering the amount of nitrogen adsorbed over the appropriate partial pressure range. The pore volumes used in this text are unless otherwise stated minimum mesopore volumes calculated from the weight of nitrogen adsorbed over the partial pressure range 0.38-0.96 (the diameter range 2-50nm) as shown in Equation 2.5.

$$V_o = X \times \frac{V}{M} \quad (2.5)$$

V_o is the pore volume in cm^3/g , X and V are, as before, the weight of the gas adsorbed (g/g solid) and the molar volume of nitrogen (cm^3) respectively and M is the weight of one mole of nitrogen.

Thus, nitrogen adsorption can give a great deal of information on the surface morphology of dried particles which may be very useful when related to the solution sorption processes of estuarine particles.

2.1.2. X-ray Analysis.

X-ray analyses were carried out using a Philips P1710 X-ray diffractometer with a copper K (α) source lamp. The samples were prepared by being ground up in an agate pestle and mortar and then <0.1g was carefully placed onto a glass coverslip and put into the instrument. Analysis of the traces was carried out with the aid of an A.S.T.M. cardfile. These analyses were carried out on key samples before and after removal of surface coatings (see Section 2.2.4).

2.1.3. Carbon, Hydrogen and Nitrogen Analysis.

Carbon, hydrogen and nitrogen (CHN) analyses were also carried out on samples before and after oxidative digestion of organic material in the samples (see Section 2.2.3) with a Carlo Erba Elemental Analyser model 1106 (Morris *et al.*, 1982b). This technique involves the combustion of the samples, followed by a chromatographic separation which elutes first the nitrogen then carbon dioxide then water. This method does not differentiate between organic and inorganic carbon but a comparative estimate was gained for some samples by determining the % carbon before and after oxidative digestion.

Approximately 2-10mg samples were weighed into small tin buckets on a Cahn automatic electro-balance and put into the carousel from which samples were added to the furnace tube. For each run approximately 5 blanks and 10 acetanilide standards, with 71.09% carbon, 6.71% hydrogen and 10.36% nitrogen (Elemental Micro Analysis Ltd), were included. Smaller weights of the standard material were used so that both the standards and samples had similar signals. The results from the standards were linearly regressed, using the Minitab statistical package, to give a calibration graph from which the results were calculated. The precision of the instrument is $\pm 0.2\%$ for carbon (Carlo-Erba) and for freeze dried sediment samples the coefficient of variation for ten samples was found to be $\pm 2.7\%$ (see Table 2.4). The difference between these two numbers is thought to be due to the inhomogeneous nature of the samples. The samples are composed of quartz grains, aluminosilicates, Fe and Mn oxyhydroxides, organic detritus and biogenic materials and therefore extracting a few

mg samples can be subjective. To minimise the variation due to this inhomogeneity analyses were usually replicated at least four times and the values quoted are averages of these analyses.

<u>Weight of sample (mg)</u>	<u>% Carbon</u>
2.960	4.38
1.186	4.43
1.454	4.56
1.847	4.68
1.663	4.63
1.905	4.58
1.874	4.41
0.772	4.73
0.949	4.53
1.358	4.40
Mean \pm S.D.	4.53 \pm 0.12

Table 2.4. The % carbon determined in ten aliquots of the same sediment sample. This shows the coefficient of variation to be 2.7% for samples with weights varying from 0.5-3mg.

2.1.4. Particle Size Analysis.

Particle size analysis was carried out within 48h of sample collection using a Malvern Instruments 2200 particle sizer system. This system uses a laser to produce a Fraunhofer diffraction pattern which is then analysed to estimate the distribution of the particles in suspension in a cell (Bale et al., 1984).

The laser was initially aligned with distilled water in the sample cell by maximising the light passing directly through to the detector. Small aliquots of suspended solids or resuspended sediments, previously ultrasonicated, were put into the cell and kept in suspension by a small stirrer. Some samples had to be diluted to reduce the obscuration. Each sample was scanned one hundred times, and the results of this were transferred to a mini-computer. The model independent algorithm supplied with the instrument by Malvern was then used to calculate the particle size distribution in the range 1.9-188 μ m, which was displayed in a fifteen element histogram. Standard beads of 5 μ m diameter (Duke Scientific glass microspheres) with a standard deviation of 7.8% were used to check the calibration of the instrument some results of which are shown in both numerical and graphical form in Figure 2.4. Mean particle sizes and standard deviations were calculated from the data using grain size statistics (Folk, 1966). Examples of this for the standard beads and for a suspended estuarine sample are shown in Figure 2.5.

SIZE BAND		CUMULATIVE WT BELOW	WEIGHT IN BAND	CUMULATIVE WT ABOVE	LIGHT ENERGY	
UPPER	LOWER				COMPUTED	MEASURED
198.0	87.2	100.0	0.0	0.0	17	0
87.2	53.5	100.0	0.0	0.0	30	0
53.5	37.6	100.0	0.0	0.0	51	29
37.6	28.1	100.0	0.0	0.0	83	72
28.1	21.5	100.0	0.0	0.0	133	129
21.5	16.7	100.0	0.0	0.0	229	241
16.7	13.0	98.6	1.4	0.0	382	396
13.0	10.1	98.6	0.0	1.4	615	629
10.1	7.9	98.6	0.0	1.4	946	946
7.9	6.2	72.9	25.7	1.4	1372	1364
6.2	4.8	36.2	36.7	27.1	1790	1773
4.8	3.8	7.0	29.2	63.8	2047	2047
3.8	3.0	5.1	1.9	93.0	1909	1942
3.0	2.4	3.7	1.5	94.9	1392	1328
2.4	1.9	3.7	0.0	96.3	865	834

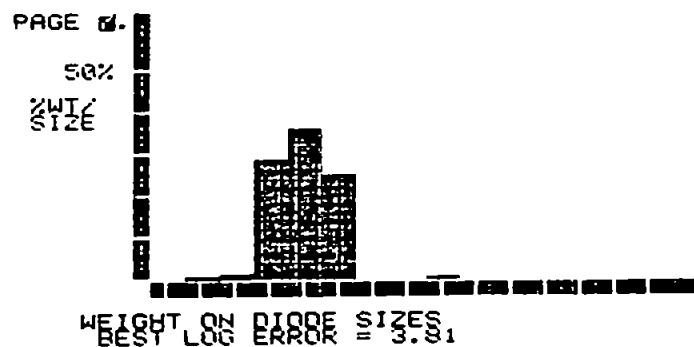


Figure 2.4. Data as presented by Malvern Instruments 2200 particle sizer, in graphical and numerical form for standard 5 μ m beads (Duke Scientific; standard deviation = 7.8%).

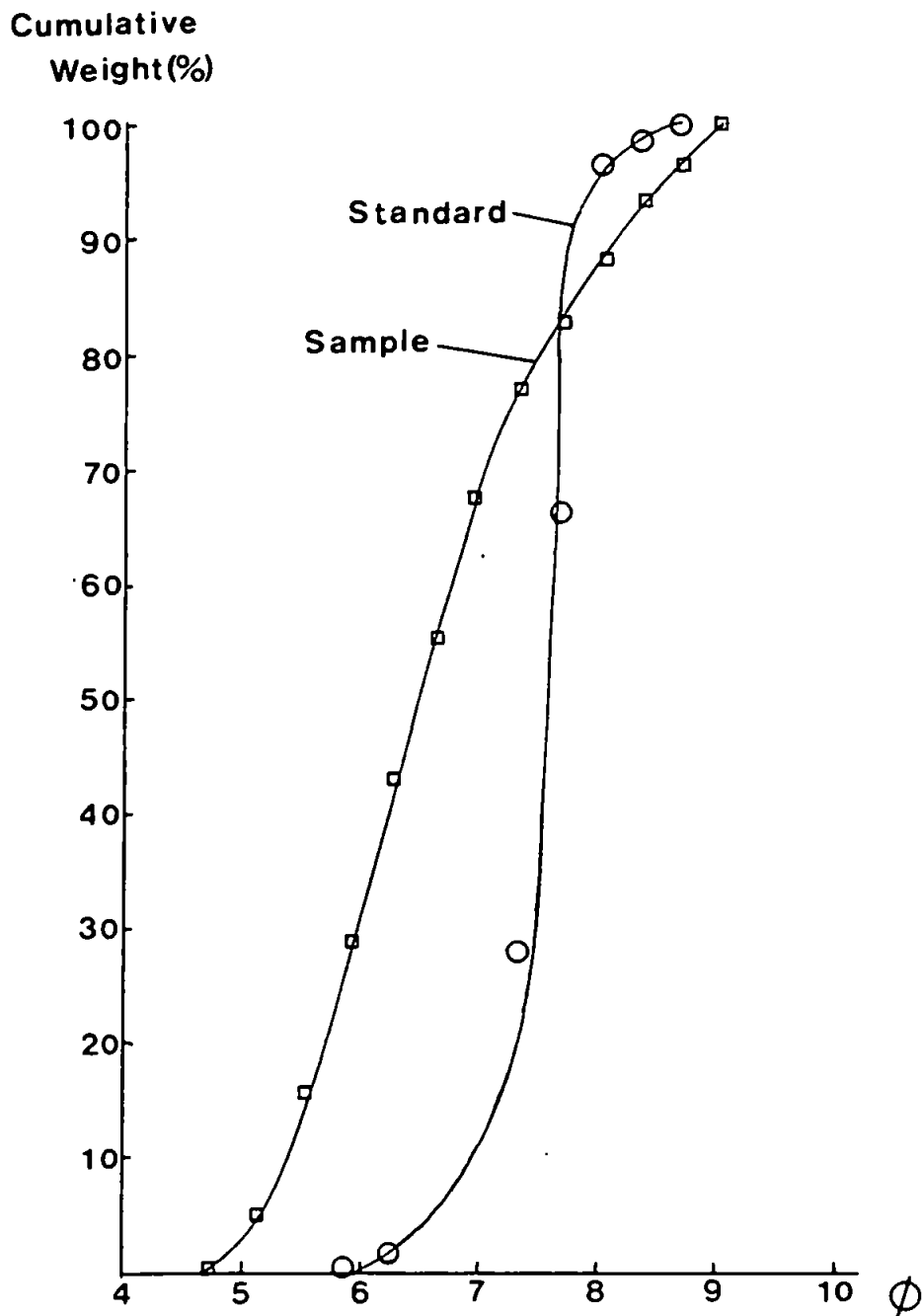


Figure 2.5. A plot of cumulative weight versus the phi scale for standard 5 μm beads and a Tamar suspended sample. The mean particle sizes calculated from these plots are 5.75 μm and 9.8 μm for the standard beads and natural sample respectively.

2.2. Particle Collection and Preparation.

2.2.1. Collection of Suspended and Sediment Particles.

The samples for investigation were collected from the Tamar Estuary and Restronguet Creek, seen in Figure 2.6 and 2.7, during twenty surveys, half of which utilised the Institute for Marine Environmental Research (I.M.E.R.) Seatruck vessel 'Tamaris', which has a continuous monitoring system for salinity, temperature, pH, oxygen and turbidity (Morris et al., 1982a). Other samples were taken while using a shallow draughted vessel or on foot. In general, suspended samples were taken as part of an estuarine axial traverse usually covering the salinity range 0-30‰. The intention was to compare particle characteristics from different parts of the estuary and to examine discrete suspended solids samples with associated sediment samples collected synchronously from immediately below the boat.

Suspended solids were collected in a plastic bucket from the side of the boat. Usually about 1-2g of material was required for analyses, therefore between 5 and 25 litres, depending on the turbidity, were collected for filtration. A sub-sample of the main suspension (about 200ml) was retained in a dark glass bottle, to inhibit biological activity, for particle size analysis. The large volume sample was filtered on site or immediately on return to the laboratory to minimise ageing effects. The filtration system was based on pressure and could accommodate large water volumes (up to 8 litres). Samples were filtered through Sartorius or Millipore 0.45µm membrane filters and then washed with <20ml distilled deionised water (Nanopure, Barnstead).

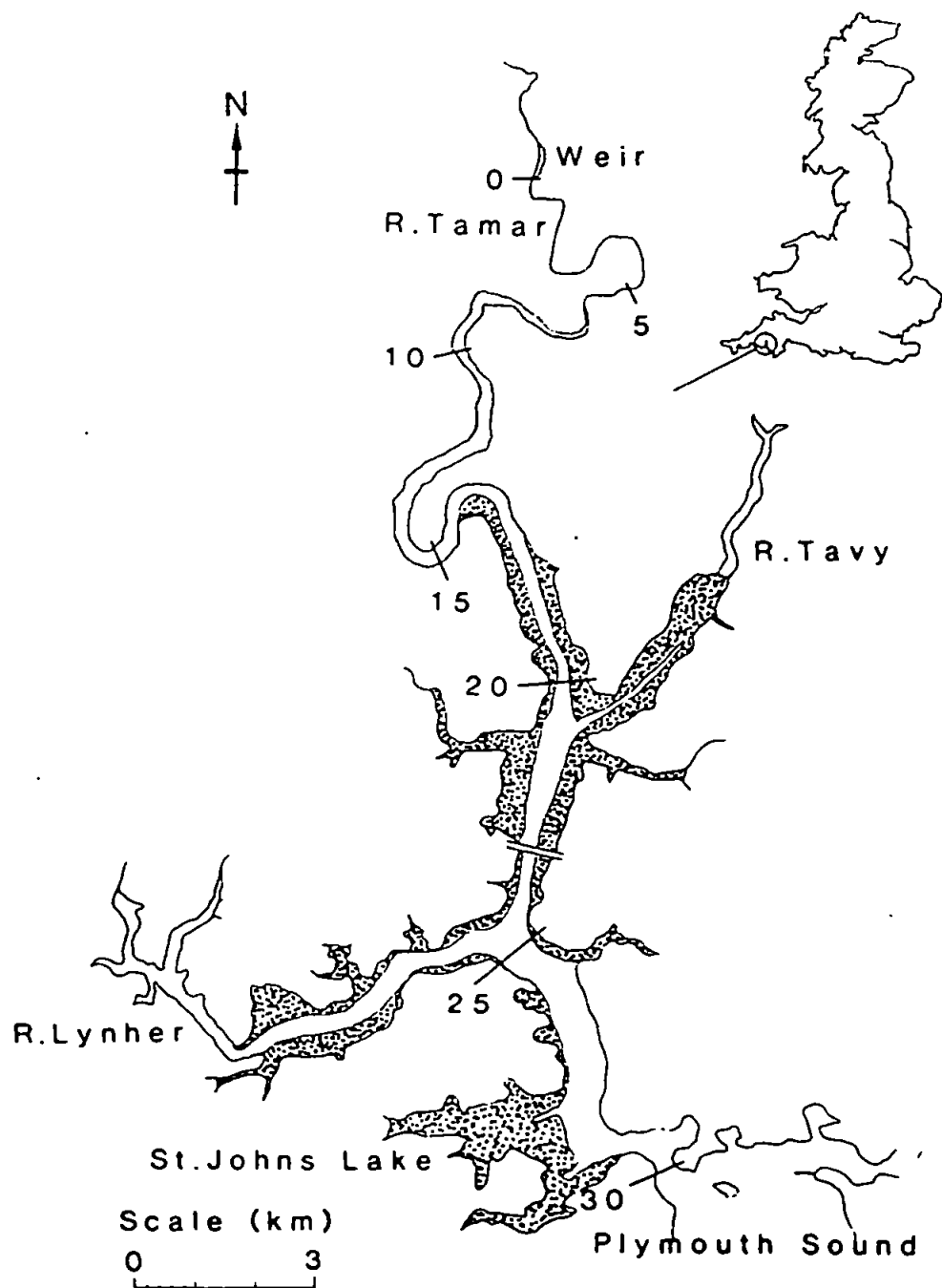


Figure 2.6. A map showing the geographical location of the Tamar Estuary. The dotted region indicates mudflats uncovered at low tide.

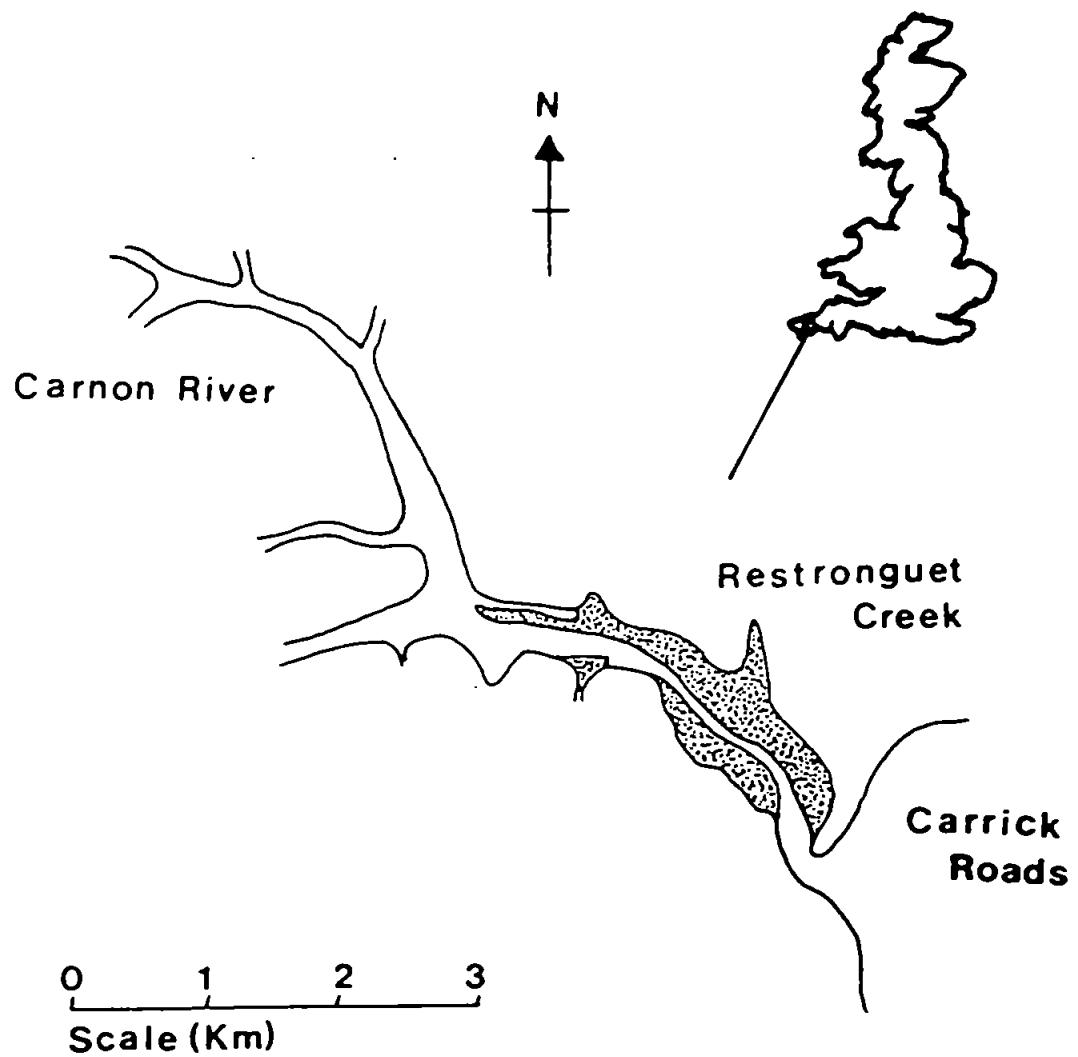


Figure 2.7. A map showing the geographical location of the Restronguet Creek. The dotted region indicates mudflats uncovered at low tide.

Sediments were sampled using a small gravity corer fitted with a plastic sheath, in which the surface sediment could be resuspended by shaking. Alternatively, larger sediment samples to compare preparation techniques were obtained by scraping the surface when the sediments were uncovered at low tide. These samples were also filtered and washed with <20ml of Nanopure water.

2.2.2. Drying of Natural Particulate Samples.

It is important to study the surface characteristics of the particles in as natural a state as possible. Drying is essential with the BET technique and although this presents some problems the advantages offered outweigh any difficulties encountered. The main difficulty is to retain the reticular structure of the solids during the evasion of water. Once particles are dried it is also necessary to arrest the ageing process induced by contact with humid air. One further consideration is that the method must be consistent from sample to sample.

Ageing has been seen, particularly in iron oxides, to cause a loss of surface area, due to continuing surface chemical reactions. This has been arrested by washing in acetone, or other organic solvents, and thus removing the gel water before drying (Bye and Sing, 1972; Crosby et al., 1983; Marsh et al., 1984). However, for natural organically coated particles although the rapid drying using organic solvents could be of benefit, the acetone or alcohol could cause considerable modification of the particle coating by removing the soluble surface organic matter. Studies have been carried out on critical point drying of natural particles from a water-ethanol

mixture by Millward and Titley (1985) and this has also shown the lighter fraction of the surface organic material to be extracted into the organic solvent. Therefore, in these experiments particles were washed in distilled water only.

Air drying at 50°C was then selected as a drying method. Drying at a high temperature (>100°C) has been shown to cause a decrease in surface area (Egashira and Aomine, 1974) and this could in addition, cause loss of low molecular weight compounds. However, after filtration and air drying the particles formed a solid mass from which it was difficult to obtain a representative sample unless it was ground to a powder, possibly destroying the natural structure of the particles. Ten duplicate surface area analyses carried out on an air dried sample gave a coefficient of variation of $9.9\text{m}^2/\text{g} \pm 14.5\%$. To assess whether the reproducibility of the method could be improved additional procedures were examined including freeze drying using a vacuum freeze-dryer (Edwards High Vacuum Ltd) after freezing at -18°C. The product of freeze drying was a powder from which it was easier to extract a more representative sample. The coefficient of variation for ten replicate analyses of a separate aliquot of the sample analysed above but in this case freeze dried, was $12.6\text{m}^2/\text{g} \pm 10\%$. Other techniques examined were grinding with a pestle and mortar and fast freezing in liquid nitrogen, to prevent settling, rather than at -18°C. These methods proved to be unnecessary because the freeze drying gave a powdery product from which a sub-sample could easily be extracted.

Surface tension forces at the air-water interface have been seen, during air drying of particulate samples to cause partial

collapse of the pore structure and hence loss of internal surface area (Egashira and Aomine, 1974). By freeze drying the samples these surface tension forces and the resulting loss of surface area may be avoided (Cohen, 1974). The freeze/freezing drying technique gave the highest surface area for the same samples and was shown to give consistent results with a good coefficient of variation. Thus freeze drying was adopted as the best method although some early analyses were carried out on air dried material because of logistical problems. A comparison between aliquots of two samples which have been air dried and freeze dried is shown in Table 2.5. This shows that although there are small differences between the surface areas determined on air and freeze dried material the trend remains the same, in this case the suspended material having a higher surface area than the corresponding sediment material.

	<u>Surface area (m²/g)</u>	
	<u>Air dried</u>	<u>Freeze dried</u>
Suspended (1)	11.6	13.6
Sediment (1)	6.9	8.6
Suspended (2)	15.2	16.2
Sediment (2)	8.1	13.0

Table 2.5. A comparison of the surface areas of freeze dried and air dried suspended and sediment particulate samples.

Two additional problems regarding ageing were addressed. The first is concerned with the ageing of the particles while still in suspension in their storage vessels. This is probably related to aggregation of the particles on standing and continuing chemical reactions at the particle surface (Mayer, 1982; Crosby et al., 1983; Marsh et al., 1984). In one experiment one sample was filtered, dried and the surface area determined immediately after collection while a duplicate sample was treated in the same way 48 hours later. The results of this, shown in Table 2.6, indicate a loss of surface area after ageing in the storage vessels. All filtration was therefore carried out immediately on collection.

<u>Sample</u>	<u>Surface area (m²/g)</u>	
	<u>Filtered immediately</u>	<u>Filtered after 48 hours</u>
(1)	22.1	19.2
(2)	27.6	22.1

Table 2.6. A comparison of the surface areas measured on two suspended samples one filtered immediately, one 48 hours later.

The second problem with regard to ageing is that if the particles are stored in the presence of water vapour, it will adsorb onto the particle surface. Surface tension forces at the particle-water interface can cause collapse of the pore structure and a loss of internal surface area (Egashira and Aomine, 1974). The changes observed in particle characteristics over a period of several months

are shown in Table 2.7 and indicate a decrease in surface area although why such a large change in carbon content should occur is unknown. In all the analyses here surface characteristics were determined within one month of drying and samples were stored in a vacuum dessicator.

	<u>Analysed within</u> <u>1 month</u>		<u>Analysed after</u> <u>6 months</u>	
	<u>Susp.</u>	<u>Sed.</u>	<u>Susp.</u>	<u>Sed.</u>
Surface area (m ² /g)	20.4	12.4	17.0	8.9
% Carbon	2.6	4.6	5.0	4.7
% Nitrogen	0.9	0.6	0.6	0.4

Table 2.7. Surface area, % carbon and % nitrogen for air dried suspended and sediment material when fresh and after having aged in the air dry state for six months.

In summary, the majority of the samples for surface area analysis were filtered within 5h of collection, washed with Nanopure water to remove any salt, then frozen, freeze dried and kept in a vacuum dessicator until required for analysis. The individual components of this preparative and analytical procedure are all well documented (eg. Cohen, 1974; Gibbs, 1974; Sing, 1982) and it is considered reasonable to assume that combined in this form they will give a clear idea of the actual characteristics of natural particles.

2.2.3. Removal of Particulate Organic Coatings.

Oxidative digestion of particles was carried out to investigate the role of particulate organic carbon and to ascertain the effects it may have on the surface characteristics of the particles. Work by Bale (Personal Communication, 1985) has shown disaggregation of particles after digestion and this with the suggestion from some data that surface area could be related to carbon content (for example see Table 2.7) lead to this line of research.

Initially 0.5g samples of suspended solids or sediment material were placed in test-tubes to which 10ml of 30% v/v hydrogen peroxide was added (Jackson, 1958). These were digested for 2h at a constant temperature of 30°C to ensure the frothing did not cause any loss of material. They were then washed with distilled water and air dried (as Section 2.2.2). Carbon analysis of the products of these digests showed the digestion to be incomplete as there was still up to 1% carbon left in the samples as shown in Table 2.8.

	<u>% Carbon</u>	
	<u>Before digestion</u>	<u>After digestion</u>
Suspended	4.0	0.5
Sediment	6.2	1.0

Table 2.8. A comparison of % carbon before and after oxidative digestion with 30% hydrogen peroxide.

Subsequent experiments to try to improve the efficiency of the digest involved a 6% w/v hydrogen peroxide solution in which the samples were gently heated to prevent vigorous effervescence, for times varying up to 24h when gas evolution had stopped. The samples were then washed and freeze-dried (as Section 2.2.2). The results of this experiment showed that the digestion removed progressively more carbon with time but even after 24h heating some carbonaceous material, presumably inorganic, resistant to wet oxidation remained as shown in Table 2.9.

<u>Digestion time (h)</u>	<u>% Carbon</u>
Untreated	4.53
0.5	4.00
2.5	2.46
4.5	1.21
24	0.71

Table 2.9. The % carbon left in a natural sample after various lengths of digestion time.

2.2.4 Removal of Particulate Ferromanganese Coatings.

Iron and manganese were leached from the particles to identify effects they have on the surface characteristics of natural particles. The presence and age of Fe oxyhydroxides has been shown to have a distinct relationship with the porosity and surface areas of precipitated material (Crosby et al., 1983; Marsh et al., 1984). Two types of leaching solution were used to try to identify a relationship

between a particular type of Fe and the surface area.

An acetic acid/hydroxylamine hydrochloride leach at pH = 3 was prepared by dissolving 1.737g of hydroxylamine hydrochloride in Nanopure water, adding 125ml of glacial acetic acid and making this solution up to 500ml with Nanopure water (Tessier et al., 1980). About 20ml of this solution were mixed with a weighed amount (approximately 0.5g) of the particulate matter. These were left for 16h at room temperature before they were filtered. The particles collected by filtration were resuspended in Nanopure water and frozen to be dried as in Section 2.2.2.

For the second leaching experiment approximately 0.5g sample was mixed with 80ml of 0.1M EDTA (Analar). The samples were shaken at 25°C for 24h before collecting the particles and filtrate as before. The pH for this leach was 7 ± 0.2 , and so it was hoped this would only remove loosely bound amorphous Fe oxyhydroxides (Aggett and Roberts, 1986). The particles from these leaches were also collected for surface area analysis.

The filtrate from both these leaches was analysed for Fe and Mn by AAS using an Instrumentation Laboratories 151 spectrophotometer. Acidified standard solutions were prepared from 1000mg/l Spectrosol solutions (BDH) and used to draw a calibration graph over the linear range from which sample concentrations were calculated.

2.3. Sorption Modelling Techniques.

2.3.1. Methods of Sample Collection and Preparation.

The sorption experiments were carried out by mixing, under controlled conditions, particles from either the Tamar Estuary or the Carnon River with water of various compositions. The Tamar particles were collected from the turbidity maximum zone of the Tamar Estuary at a salinity of $<0.5\text{‰}$. Taking particles from this region meant the salinity could be easily manipulated by addition of a synthetic saline solution to give a range of ionic strength in the sorption media. The turbidity maximum was located by recording the turbidity on an axial traverse of the river on a rising spring tide. On returning to the identified maximum (approximately 1000mg/l), 50-100 litres of turbid river water were collected from which the particles were then filtered, resuspended in a small volume of filtrate and stored at low temperature. Mobile sediment from the Carnon River (see Figure 2.7) was collected by scraping up sediment under the surface of the water. These particles were then stored in the same way as the Tamar material. All particles were equilibrated prior to the experiment in a constant temperature room for 24h.

The Tamar river water, to which the particles were added, was collected in the fresh water above the weir (see Figure 2.6), filtered within 12h, and used within 48h. River water was also collected from the Carnon River at the position shown in Figure 2.7. This water was filtered just before beginning an experiment as discussed in Chapter 4. About 10 litres of water was required for each experiment as 5-8 litres were removed in 200ml aliquots for analysis.

The salinity and pH of the river waters was for some experiments manipulated to enable a range of sorption experiments to be carried out. An artificial seawater solution of triple strength was prepared using the recipe of Lyman and Fleming (1940) with Analar grade salts. The high concentration of the salts made it possible to mimic estuarine conditions without greatly altering the original concentration of the dissolved metals of interest or the volume of the sample. Analysis of the artificial seawater showed the trace metal concentrations to be 0.02mg/l for Zn and <0.01 mg/l for Cu. This would increase the trace metal concentrations in the Tamar water by approximately 10% and 1% for solutions of 10‰ and 1‰ salinity, respectively. Any alteration in pH required was carried out by addition of 2M Aristar HNO_3 or NaOH.

Desorption experiments were carried out by resuspending particles in Nanopure water or buffered water at approximately the same particle concentration as would be used for the adsorption experiment. A solution of buffered water for desorption experiments was prepared by dissolving 1.8g NaHCO_3 in 10 litres of Nanopure water. Air was bubbled through this overnight and the pH then altered as appropriate using either 2M Aristar HNO_3 or NaOH (Crosby, 1982).

2.3.2. Development of the Modelling Technique.

The highest priorities in this experimental approach were reproducible results at low concentrations and the avoidance of contamination. Considerable effort was put into developing a clean method for the filtration, concentration and analysis of small volumes of suspension abstracted from the reaction mixtures. What is detailed

below is the development of a method specifically designed to overcome the difficulties encountered in an approach of this type. The procedure for cleaning all glass and plasticware, except the 10 litre carboys, before an experiment was:

- (1) Soaking for at least 24h in Decon90
- (2) Thoroughly rinsing in tap water
- (3) Soaking for 48h in 2M Analar HNO_3 acid
- (4) Rinsing thoroughly in Nanopure water
- (5) Soaking for 48h in Nanopure water
- (6) Rinsing again in Nanopure water and securely capping or wrapping in plastic bags.

The 10 litre carboys which were used as the reaction vessels were rinsed with 2M Analar HNO_3 and kept filled with tap water until required.

2.3.2a. Adsorption Experiments.

The river water was contained in a continually stirred 10 litre carboy from which the samples could be extracted via a tap at the bottom. The temperature of the river water was equilibrated to 10°C in a constant temperature room in which the experiments were carried out. Any salinity or pH changes required were implemented before extracting two or three 250ml samples from the carboy. These were filtered to establish a reliable starting concentration for dissolved metals in the water sample.

At time t_0 the particles were added to the river water and samples of the suspension rapidly extracted and filtered. The pH was

measured at intervals throughout the experimental run and samples were taken to measure turbidity gravimetrically on Whatman filters. For most of the mixing experiments a duplicate was run at the same time to be used as a control. These were treated in a similar way except that instead of adding particles, filtrate from the particle sample was added at time t_0 . If the control and sample experiments were started simultaneously, there were too many sub-samples to be taken at one time and so the control run was started 2-4h later. This facilitated more consistent sampling and it was felt that this time disparity would cause no appreciable effect after 24h equilibration. The dissolved metal concentrations for the filtrate from the particle samples of the Tamar and Carnon rivers are shown in Table 2.10 and it was calculated from the volume added that this was <2% of the typical dissolved metal concentration in the river water.

	<u>Concentration ($\mu\text{g/L}$)</u>	
	<u>Zn</u>	<u>Cu</u>
Tamar River	9.7	12.6
Carnon River	3200	1200

Table 2.10. The dissolved metal concentrations determined by AAS in the filtrate from the particle samples used in the mixing experiments.

Several different filtration systems were examined before the method discussed below was implemented. These utilised different types of glass and plastic filtration apparatus but filtration through

a Hartley sintered glass funnel directly into the sample bottle seemed to give rise to the cleanest sampling as it had the least number of sample handling steps. Experiments were carried out to test various ways of washing the filters which were 90mm membrane Sartorius or Millipore ($<0.45\mu\text{m}$) filters. These involved filtering aliquots of one sample through filters which had been washed with various volumes of water, 2M Analar HNO_3 and sample followed by in all cases a further 50ml of sample. As shown in Table 2.11 the results of this suggested that washing with 200ml of 2M HNO_3 gave the most accurate (compared to the untreated values) and consistent values when considering Zn, Cd and Cu.

Washing acid could become contaminated if used repeatedly during an experiment and it would be difficult to be certain that all acid was removed from a sintered filter funnel. Thus since it would be uneconomic to use fresh acid for each filter they were soaked in 2M Aristar HNO_3 for 96h and repeatedly rinsed and soaked in Nanopure water before use. The filter was then used directly from soaking and was rinsed with 50ml of sample which was also used to rinse the sample bottle. About 200ml (measured) of suspension was filtered and then 5ml of ammonium acetate buffer was added to the filtrate which was capped and saved for extraction. Between samples the funnel was rinsed with Nanopure water only. The ammonium acetate buffer was used both to improve the storage properties of the filtered estuarine samples before analysis and as a media for the ASV analyses. The buffer was prepared using Aristar grade chemicals (BDH) by mixing 57ml of acetic acid and 76ml of NH_4OH and making this up to a litre. The pH was then adjusted to 5 ± 0.1 with concentrated Aristar HNO_3 and

Volume (ml)	<u>Concentration (µg/L)</u>								
	<u>Zn</u>			<u>Cd</u>			<u>Cu</u>		
	<u>Water</u>	<u>Acid</u>	<u>Sample</u>	<u>Water</u>	<u>Acid</u>	<u>Sample</u>	<u>Water</u>	<u>Acid</u>	<u>Sample</u>
50	14.9	13.7	13.5	0.36	0.35	0.39	8.0	8.2	7.2
	20.1	14.9	14.2	0.36	0.34	0.39	8.0	10.6	9.1
200	13.0+0.7 ^a	13.1+1.5 ^a	15.6	0.42+0.18 ^a	0.40+0.07 ^a	0.41	8.5+0.3 ^a	9.2+0.3 ^a	9.5
			14.2			0.47			10.2
500	14.6	11.6	13.7	0.35	0.43	0.33	8.0	8.8	8.8
	19.2	14.5	12.4	0.45	0.43	0.35	8.8	9.7	8.2
Untreated	14.3+0.3 ^b			0.35+0.05 ^b			9.3+0.3 ^b		

Table 2.11. A comparison of the analysed concentrations of Zn, Cd and Cu in aliquots of the same filtered sample which had been refiltered through filters washed with various volumes of water, acid and sample followed by 50 ml of sample.

^a Average of 4 analyses. ^b Average of 3 analyses.

the resulting solution was cleaned prior to use through a 15ml column of Chelex 100 resin (Bio-Rad, 100-200 mesh).

2.3.2b. Desorption Experiments.

Several timed series desorption experiments were run using particles from the turbidity maximum zone of the Tamar Estuary and Carnon River sediments. For two experiments Tamar particles were "doped" with trace metals before desorption by suspending in Carnon River water with a high metal concentration for different lengths of time. These experiments were carried out in either Nanopure or buffered water (see Section 2.3.1). Actual sampling and filtration techniques and also methods used to control the temperature, salinity and pH were the same as discussed in Section 2.3.2a for the adsorption experiments.

Another type of desorption experiment was carried out by suspending washed Carnon River sediment in Nanopure water in which the pH had been reduced with 2M Aristar HNO_3 (Tipping et al., 1986). After a timed period (3 days or 3 weeks) at 10°C the particles were filtered out and the metal concentrations in the filtrate determined by AAS (see Section 2.3.5).

2.3.3. Development of the Micro-Chelex System.

In previous work in these laboratories the ion-exchange resin Chelex-100 has been used to preconcentrate trace metals from large volume (up to 10 litres) estuarine samples (Morris et al., 1978; Ackroyd et al., 1986). These studies used a resin column consisting of 10ml of Chelex-100 which gave a high flow rate (approximately

250ml/h) consistent with the requirement for processing a large volume. However, the objectives here were to further develop this preconcentration technique so that it was suitable for a large number of small volume samples (200ml) for kinetic studies and could provide a significant improvement in the trace metal signal during subsequent determination by either ASV or AAS.

A preliminary investigation was carried out on samples in which 5-8 litres of water was preconcentrated by Chelex-100 into 25ml of 2M HNO_3 (Morris et al., 1978; Ackroyd et al., 1986). These samples were analysed by ASV and AAS to determine whether the ASV technique was suitable for this type of sample. Analysis by ASV using the conditions discussed in Section 2.3.4 was most successful as there was a good correlation between ASV and AAS for Zn and Cu as shown in Figures 2.8 and 2.9. This encouraged further work into the development of the micro-Chelex system for the rapid analysis of small volume samples.

The Chelex-100 was obtained in the sodium form (Bio-Rad, 100-200 mesh) and converted to the ammonium form before use. The process for converting and subsequent cleaning after use was:

- (1) Wash with Nanopure water until pH > 6
- (2) Rinse with 2M Aristar HNO_3
- (3) Wash with Nanopure water until pH > 6
- (4) Rinse with 2M Aristar NH_4OH (200ml)
- (5) Wash with Nanopure water until pH < 8
- (6) Rinse with 2M Aristar NH_4OH (200ml)
- (7) Wash with Nanopure water until pH < 8

The Chelex was treated in batches and where possible one batch

ZINC

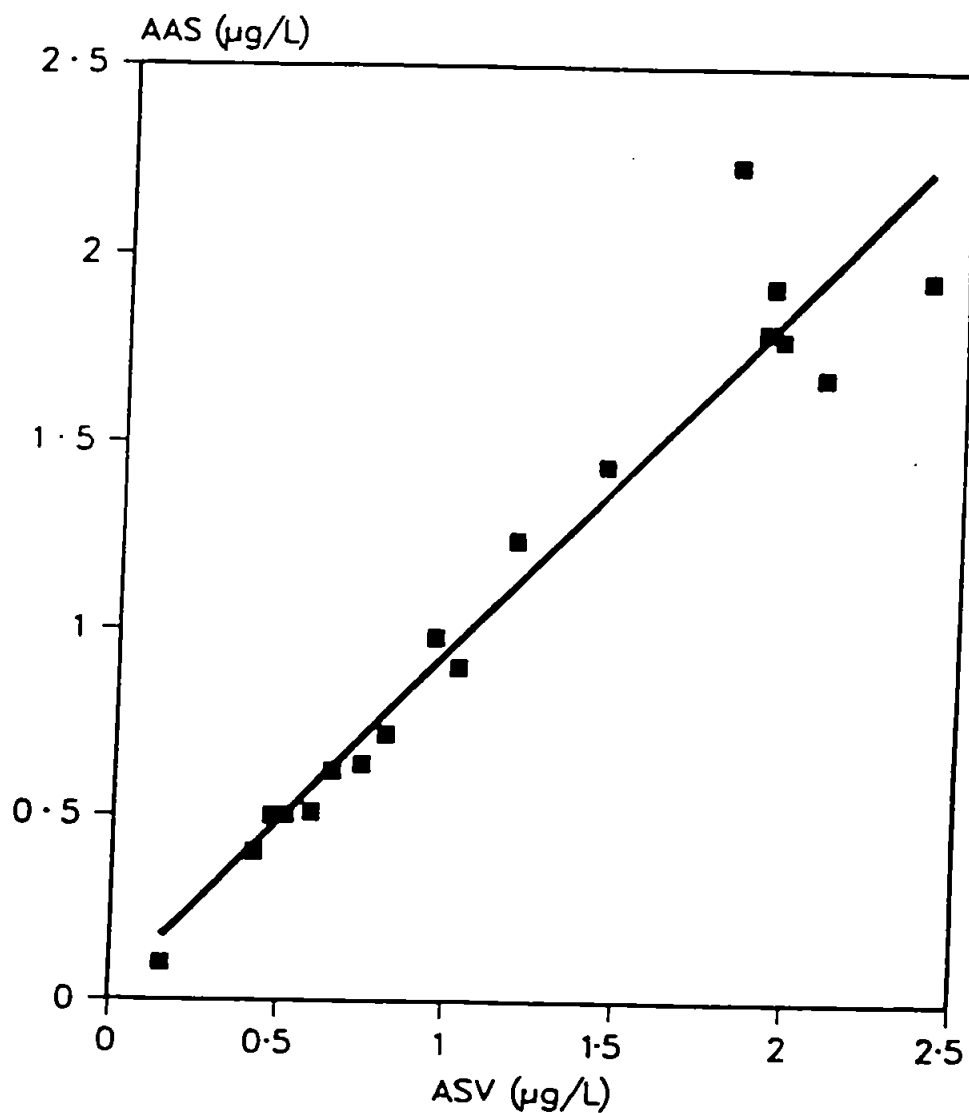


Figure 2.8. A comparison of Zn concentrations determined by ASV and AAS in bulk Chelex treated samples (8 litres sample into 25ml HNO_3) from an estuarine survey.

COPPER

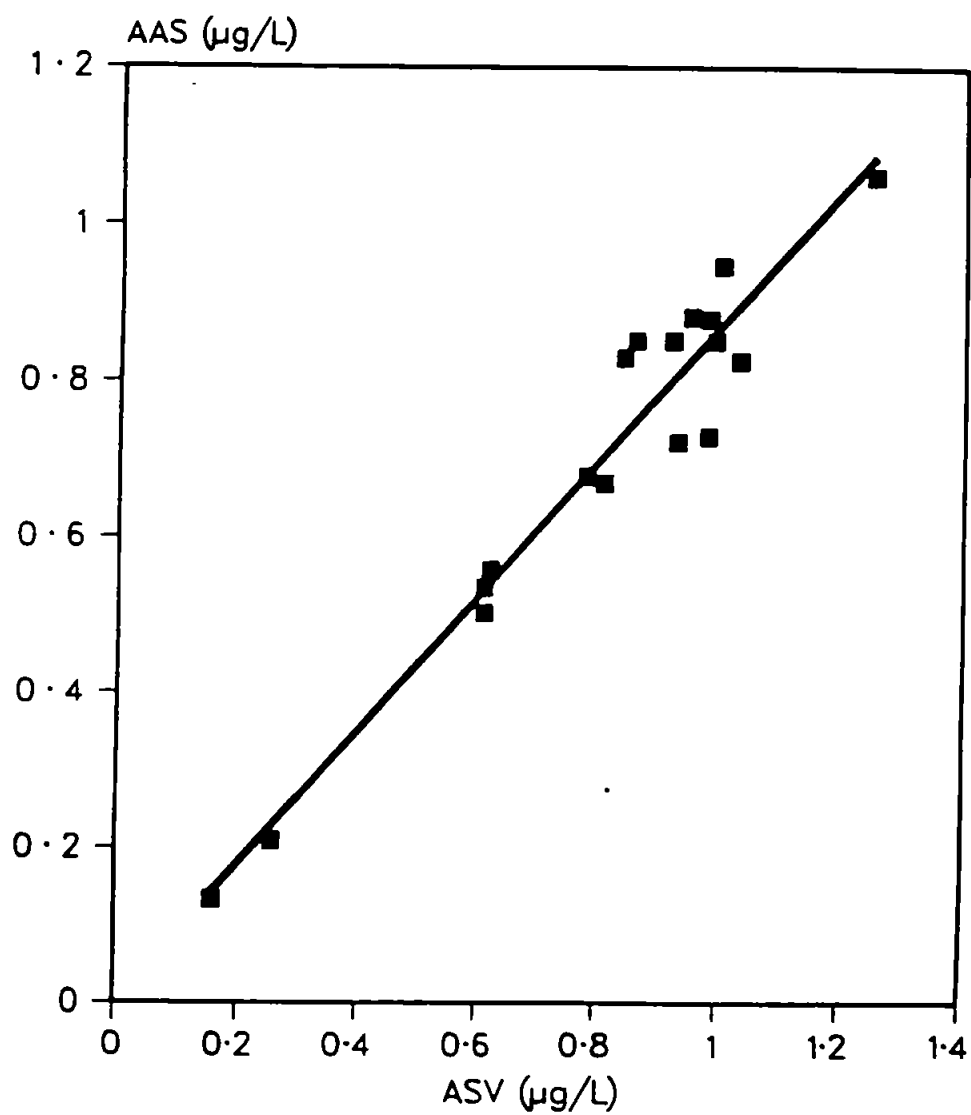


Figure 2.9. A comparison of Cu concentrations determined by ASV and AAS in bulk Chelex treated samples (8 litres sample into 25ml HNO_3) from an estuarine survey.

was used for all the samples from one experiment.

The preconcentration technique was developed as a 12-channel micro-Chelex system. Samples were run through resin columns, containing 3ml of Chelex-100 in the ammonium form, via a peristaltic pump at the rate of about 5ml/min. Then 10ml of Nanopure water was put through the columns before 5ml of 2M Aristar HNO_3 was used to elute the metals from the columns into a volumetric flask. The efficiency of the stripping was checked by collecting a second 5ml of acid from the Chelex column and analysing this for the metals. Blanks were run by feeding the effluent from one column through another Chelex column and then eluting this in the same way as the other samples. The results of these analyses are shown in Table 2.12. The sample blanks read consistently between 10 and 100 $\mu\text{g/L}$ for Zn and Cu regardless of the sample concentration. Studies on Chelex-100 have shown 80%-100% efficiency depending on the salinity of the media (Ackroyd, 1983; Morris et al., 1978). Since the salinity of the solution for one experiment was always the same it was not felt this would present any problems.

	<u>Concentration ($\mu\text{g/l}$)</u>	
	<u>Zn</u>	<u>Cu</u>
Blank	10-100	10-70
Second eluant	<30	<20

Table 2.12. The concentrations of dissolved metals analysed in the sample blanks and eluant from a second aliquot of acid passed through a Chelex column. These results are for the acidic 5ml concentrate and must be divided by 40 to enable comparison with samples.

The samples were extracted in batches of twelve within four days of filtration. Between samples the glass columns were emptied, thoroughly rinsed with 2M HNO_3 followed by Nanopure water before refilling with Chelex-100. The pump tubing was rinsed with Nanopure water.

A smaller Chelex system was attempted after the success with the 5ml acid system. This involved passing 50ml of sample through a cleaned 25mm ($<0.45\mu\text{m}$, Millipore) syringe filter system (Swinnex, Millipore) and directly through a 1ml column of Chelex in a 5ml auto-pipette tip. A few ml of Nanopure was then passed over the column followed by approximately 4ml (measured) of 2M Aristar HNO_3 which was collected. This was analysed by ASV but no reproducibility was found for the samples or for a "spike" of dissolved metals, which was added to some samples, at either of two rates which were used to pass the sample over the Chelex. Therefore, future work utilised the system which concentrated 200ml of sample into 5ml of acid and the reproducibility of this can be seen in Tables 2.13 and 2.14 as discussed in the subsequent sections.

2.3.4. Analysis of Solutions by ASV.

Anodic Stripping Voltammetry has been developed to analyse simultaneously for dissolved Zn, Cd, Pb and Cu in estuarine samples (Chau and Lum-Shue-Chan, 1974; Gardiner and Stiff, 1975). This analytical technique has also been used successfully to study the speciation of Cu and its interaction with organic compounds in estuarine media (Nelson and Mantoura, 1984a; Nelson and Mantoura, 1984b). The original aim was to find a simple, rapid and sensitive

method of analysing the large numbers of solutions of varying compositions associated with particle-metal interaction studies. However, problems encountered during this study were those of contamination, lack of sensitivity and irreproducibility due to variation in sample composition particularly with respect to dissolved organic material (Brezonik et al., 1976; Florence, 1977).

A Princeton Applied Research model 174A polarographic analyser was used with a hanging mercury drop working electrode, a silver/silver-chloride reference electrode and a platinum counter electrode. All glassware and electrodes had to be washed once in 2M Analar HNO_3 and twice in Nanopure water before every sample analysis (Gardiner and Stiff, 1975). Initial analyses were attempted on 25ml of untreated estuarine water but many difficulties were found with this. The variation in salinity meant some samples did not have a suitable conductivity for analysis and differing amounts of dissolved organic carbon lead to poor reproducibility. An addition of 0.5ml of 25M acetate buffer was made to improve the conductivity and 25 μL of pure gelatin was added as a surfactant, to counteract interference from dissolved organic carbon (Nelson and Mantoura, 1984b). However, neither of these additions gave readily reproducible traces, although the coefficient of variation for standard additions to a solution of potassium chloride or buffer was $<10\%$. Ammonium citrate buffer was tried as a sample media but although this gave a very smooth baseline the reagent had a high metal content. Cleaning the buffer using a 15ml Chelex-100 column was attempted but this appeared to have little effect, the baseline still having a high dissolved Zn and Cu content, probably due to the low pH of the citrate buffer (pH = 3). A second

problem which arose while using citrate buffer was that the baseline changed position dramatically when the sample was added due to the change in volume and pH in the sample cell.

It was, therefore, decided that a Chelex resin would be used, as described in Section 2.3.3, to strip the metals from the estuarine water. This preconcentrates the dissolved metals, reducing the effect organic materials will have and seemed to remove some of the variation in composition and reduce interference from dissolved organic carbon. As discussed in Section 2.3.3 a bulk Chelex system was used in the initial developmental stages to ascertain whether or not the ASV was a useful analytical technique for this type of sample. Typical concentrations in the Tamar Estuary for Zn and Cu are about 0.5 - 30 $\mu\text{g/l}$ and 0.5 - 10 $\mu\text{g/l}$ respectively while concentrations of Cd and Pb are usually lower with generally $<2 \mu\text{g/L}$ and $<5 \mu\text{g/L}$ respectively (Ackroyd, 1983). The bulk samples would be approximately 10 times more concentrated than the micro-Chelex and this higher concentration in conjunction with a relatively lower organics concentration made analysis easier and more reproducible.

The conditions found most suitable for ASV analysis used 24ml of a 2M ammonium acetate buffer as the cell media which was prepared as in Section 2.3.2a. Some difficulty was found initially in cleaning this buffer (pH = 5). It was found that the maximum capacity of a 15ml column of Chelex-100 was approximately 1 litre of buffer with respect to Pb. This would appear very low considering Aristar chemicals were used but could be due to the pH or affinity of the buffer for dissolved metals. A 0.5ml addition of 2M Aristar HNO_3 prior to analysis suppressed the baseline change encountered if the pH

of the media was altered. The baseline was analysed and then a 0.5ml aliquot of the eluted solution was added to the cell for analysis. Since the concentrations of the four dissolved metals are considerably different and Zn and Cu have a higher sensitivity to ASV than Cd and Pb two different current ranges had to be used to give the appropriate responses. A typical trace of an analysis is shown in Figure 2.10.

The sample concentrations were calculated from standard addition of appropriate standards, diluted from Aristar 1000mg/l metal nitrate solutions. Aliquots of 25 μ L of a mixed metal standard were put into the cell for each addition this being the smallest reproducible volume. For 10 weighed standard additions the coefficient of variation was 10%. The deposition time was chosen to be 2 min as the longer this time the more likely is interference from dissolved organic material which although partially excluded from the sample has still to be carefully avoided. The deposition voltage was -1.3V and the scan through +1.5V.

Several experimental runs were analysed using ASV after the sub-sampling and preconcentration steps had been fully developed. The results of duplicate measurements of one sample are shown in Table 2.13. This sample was split into two portions one of which was further subdivided into four 200ml aliquots which were filtered and Chelexed. The other portion was filtered and then divided into three 200ml aliquots for separate Chelexing. These results show that a considerable variation, in particular for Pb and Cd, is introduced during the filtration step but also suggest that there are problems with the analyses of the samples. The blank concentrations of Pb and Cd were often up to 5 μ g/l and 1 μ g/l respectively which was very high

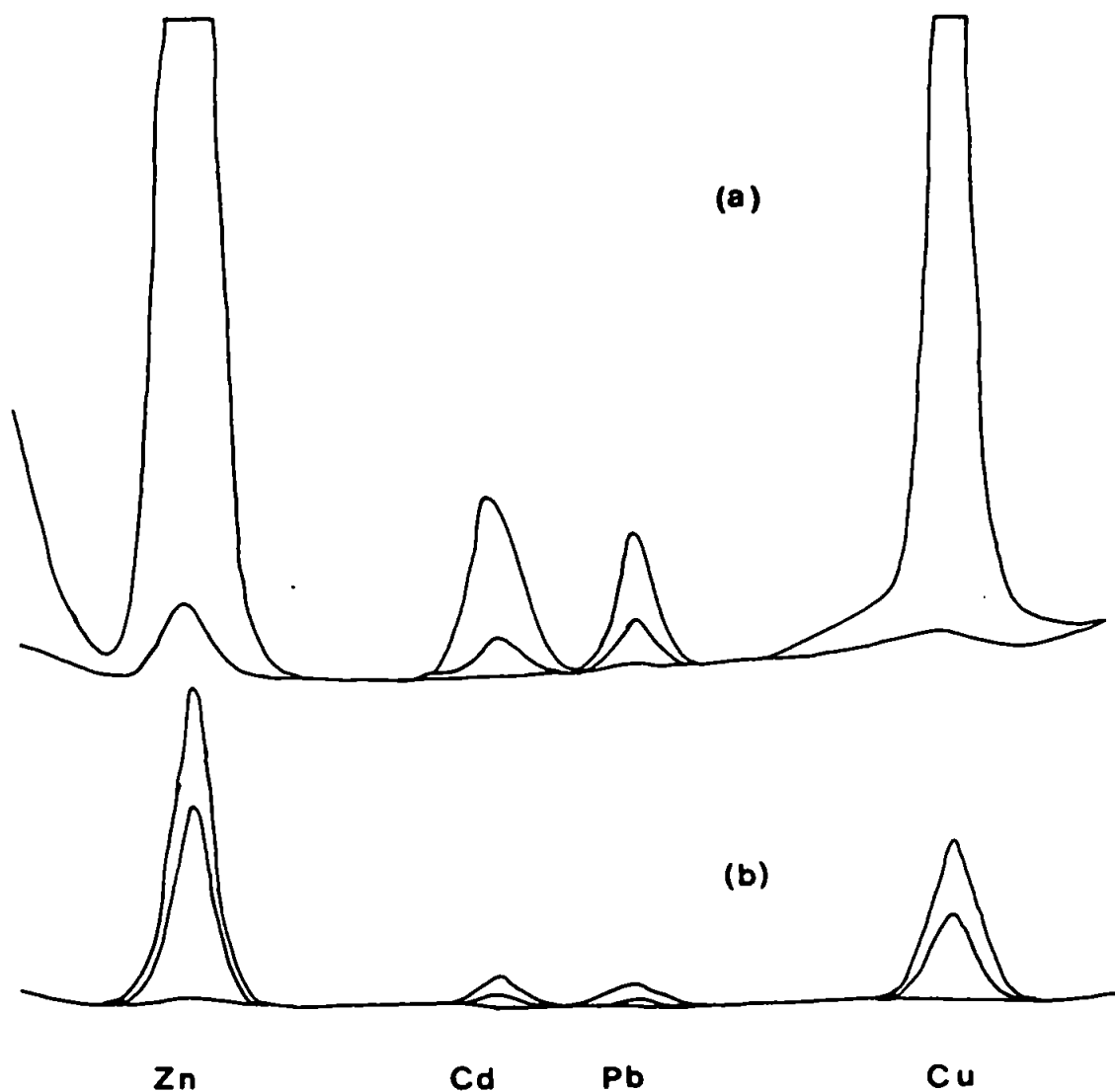


Figure 2.10. A typical trace for an analysis by ASV showing the baseline, the sample and the standard addition peaks. The sensitivity in (a) is used to analyse for Cd and Pb while trace (b) would be used for Zn and Cu. These two traces would normally be superimposed on each other.

compared to typical concentrations shown in Table 2.13.

	<u>Concentration ($\mu\text{g/l}$)</u>			
	<u>Zn</u>	<u>Cd</u>	<u>Pb</u>	<u>Cu</u>
Separately treated				
(1)	15.1	0.39	0.97	9.4
(2)	16.0	0.71	1.14	10.6
(3)	11.0	0.67	1.68	10.1
(4)	14.6	0.43	0.97	9.4
Mean \pm S.D.	14.4 \pm 2.3	0.55 \pm 0.16	1.19 \pm 0.34	9.9 \pm 0.6
Chelexed separately				
(5)	13.8	0.86	1.07	8.8
(6)	12.7	0.84	1.04	8.3
(7)	11.2	0.77	0.81	7.8
Mean \pm S.D.	12.6 \pm 1.3	0.82 \pm 0.05	0.97 \pm 0.14	8.3 \pm 0.4

Table 2.13. The results of analyses carried out on one sample after separate portions had been treated in different ways. Samples 1-4 were filtered, Chelexed and analysed completely separately. Samples 5-7 were filtered as one sample and subsequently split into three portions for Chelexing and analysis.

Comparing the profiles of the Pb and Cd with those of Zn and Cu it was apparent that there was little consistency for the analysis of these metals. Thus determinations of Pb and Cd were abandoned in favour of Cu and Zn. This did not actually speed up the work but the

analytical precision improved and fewer repetitive analyses were necessary. However, considering all factors, it was realised that an analysis of this nature for two metals, particularly Cu and Zn, offered few advantages over conventional AAS.

2.3.5 Analysis of Solutions by AAS

Atomic Absorption Spectrometry (AAS) analyses were carried out on an Instrumental Laboratories 151 spectrophotometer using an air/acetylene flame and the appropriate hollow cathode lamps for Zn and Cu and sometimes Fe and Mn. Analysis was either direct on samples from the volumetric flasks or after dilution in 25ml plastic beakers. Blanks were determined on Nanopure water and four mixed metal standards, prepared from 1000mg/l solutions (BDH), were used to give a calibration graph over the linear range (approximately 0.1-1.2mg/l) for Cu and Zn. Background correction was used where appropriate.

Comparison of this technique of analysis with the ASV on samples which had been treated by the micro-Chelex method showed that AAS gave a far smoother curve for concentration versus time. An example of this for the Zn control for one experiment is shown in Figure 2.11. Plotting the results from ASV versus those from AAS, as described in Section 2.3.4, had shown a very similar analytical reproducibility can be achieved but this is only at the high metal concentrations generated by concentrating 8 litres into 25ml. Therefore, for analysis of further samples AAS was used to examine the behaviour of Cu and Zn only. Table 2.14 gives the results of the analyses of five replicate samples from an experimental run. This shows the coefficient of variation to be $\pm 15\%$ for both Zn and Cu after

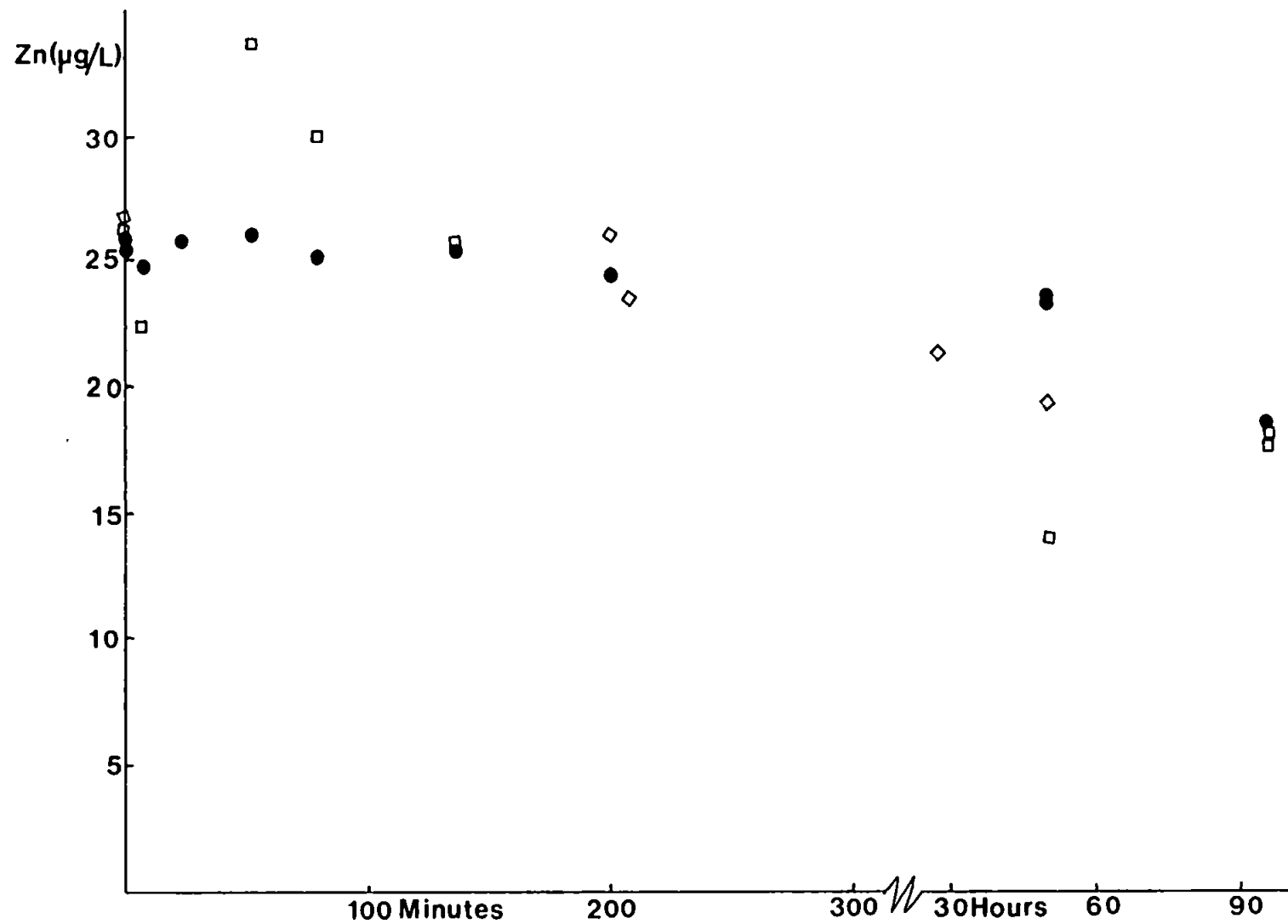


Figure 2.11. An example of Zn concentrations, plotted versus time, determined by both ASV (□) and AAS (●). This sample was a control run concurrently with an adsorption experiment.

the preparative and analytical procedures.

	<u>Concentration</u>	
	<u>Zn (mg/l)</u>	<u>Cu (µg/l)</u>
Replicate		
samples	12.2	7.6
	14.4	7.8
	13.8	7.1
	17.7	7.8
	12.6	5.4
Mean ± S.D.	14.1 ± 2.2	7.1 ± 1.0

Table 2.14. Results from analyses by AAS of five replicate samples and their mean and standard deviation.

CHAPTER THREE

THE MICROSTRUCTURES OF ESTUARINE PARTICLES-

RESULTS AND DISCUSSION

This study of the microstructures of estuarine particles was undertaken because little is known about the morphologies of natural particle surfaces and their relationship to sorption processes. This is the first attempt to determine the surface area and porosity of natural estuarine particles and to examine the role surface coatings (ferromanganese oxyhydroxides and organic matter) have in controlling these characteristics. Many such studies have been carried out on the surfaces of synthetic and natural substances (eg. Parfitt and Sing, 1976) but these concentrate on single component materials with industrial applications. It is essential that the surfaces of multi-component estuarine materials are correctly perceived before the heterogeneous chemical reactivity in estuaries can be fully interpreted.

This chapter is divided into three sections dealing first with some physical characteristics of the particles, then with the chemical components, followed by the conclusions from this aspect of the study. Throughout this chapter it is worth recalling that "surface area" refers to values obtained specifically by the BET method in m^2/g unless otherwise stated.

3.1. The Morphology of Estuarine Particles.

3.1.1. General Considerations.

It has been identified in this work and by others (Adamson, 1982; Sing, 1982) that surface areas are not directly comparable when determined using different preparation techniques or analytical methods (see Section 2.1.1). However, if one assumes that dried estuarine material, prepared by a consistent method, is representative of the natural particles, it is possible to deduce important information about particle surface characteristics by comparing relative differences in surface areas and porosities.

Preliminary studies deriving the BET surface areas of particles revealed a wide range of areas for both natural and synthetic materials. Table 3.1 shows that natural sediment particles from the mid-estuarine region of the Plym River have a very low surface area ($2.9\text{--}4.3\text{m}^2/\text{g}$) while the areas for sediments from the Carnon River are an order of magnitude greater ($63.8\text{m}^2/\text{g}$). The surface areas of sediments and suspended particles from the Tamar Estuary lie between those of the Carnon and Plym materials. Furthermore, it is apparent that the surface area of the Tamar Estuary suspended material is about 80% greater than that obtained for associated sediment material. The fact that this intra- and inter-estuarine variability can be identified, indicates that this well established nitrogen probe technique can be applied to natural samples, removed from their normal environment, to compare and contrast their surface morphology. The wide range of surface areas found in these samples also suggests that there may be a variety of

<u>Sample</u>	<u>Surface area (m²/g)</u>
Plym Estuary - sediments	4.3
Plym Estuary - sediments	2.9
Tamar Estuary - suspended solids	19.0
Tamar Estuary - sediments	10.8
Tamar River - suspended solids	10.3
Carnon River - suspended solids	56.0
Carnon River - sediments	63.8

Table 3.1. Examples of surface areas determined by BET nitrogen adsorption for natural samples from three different localities in S.W. England

<u>Sample</u>	<u>Surface area</u> <u>(m²/g)</u>	<u>Reference</u>
Humic acid (Aldrich-Technical)	0.7	This work
Crystalline SiO ₂	3.3	Martin <u>et al.</u> (1986)
Pure Kaolinite	12.9	This work
Haematite	44	Madrid and De Arambarri (1985)
Illite	93-132	Greenland and Quirk (1962)
Goethite	9-153	Schwertmann <u>et al.</u> (1985)
Lepidocrocite	97-121	Crosby <u>et al.</u> (1983)
Amorphous FeOOH (natural)	141-211	Marsh <u>et al.</u> (1984)
Amorphous FeOOH (synthetic)	159-234	Crosby <u>et al.</u> (1983)
Amorphous MnO ₂	470	This work

Table 3.2. Surface areas determined for various constituents of natural samples, during this work and by others, using the BET nitrogen adsorption technique.

chemical components which control the surface areas of natural materials.

Table 3.2 shows the surface areas of some environmentally relevant materials determined during this work and by others. These show a range of surface areas ($0.5\text{--}470\text{m}^2/\text{g}$) for various constituents which are known to be present in natural estuarine particles (quartz, aluminosilicate clays, amorphous Fe and Mn hydroxides and organic material). The surface areas of the constituent materials vary considerably, as seen by the values given in Table 3.2, which depend on the source, weathering regime and the potential for ageing, especially for freshly formed precipitates.

Studies on the major elemental composition of estuarine particle populations would suggest that the differences observed are due to variation in the particle sources (D'Anglejan and Smith, 1973, Martin and Meybeck, 1979). However, around the fresh water brackish water interface flocculation of organic material and hydrous iron oxides has been widely reported (Aston and Chester, 1973; Sholkovitz, 1976, Sholkovitz et al., 1978). These materials which coat the underlying lithogenous material have a significant effect on the charge properties of the particles (Hunter and Liss, 1982) and may modify the surface area and porosity of the particles (Eisma et al., 1978; Saleh and Jones, 1984). For example, if the lithogenous component of a sample was kaolinite ($12.9\text{m}^2/\text{g}$) and this was coated with freshly precipitated amorphous Fe oxyhydroxides ($141\text{--}211\text{m}^2/\text{g}$) one anticipates the surface area would increase. On the other hand, if these same particles were coated by flocculated organic material, a decrease in surface area may be expected as the measured surface area

for humic acid is apparently very low ($0.7\text{m}^2/\text{g}$). Thus, knowledge of the way in which coatings control the observed surface area of natural estuarine particles is essential if any understanding of surface sorption processes is to be realised (Martin et al., 1986).

The additional advantage of this study is that, for the first time, the internal porosity of natural estuarine particles was examined. BET nitrogen adsorption hysteresis loops give information on the pore size, volume and shape so that details of the morphology of the particle surface can be gained and comparisons made. Examples of the hysteresis loops for the Plym and Tamar estuarine sediment samples drawn in Figure 3.1 show the mesopore volume of the Tamar material ($6.7 \times 10^{-3} \text{ cm}^3/\text{g}$) to be 3 times that of the Plym ($2.5 \times 10^{-3} \text{ cm}^3/\text{g}$). The shapes of the hysteresis loops indicate for both samples that micro- and meso-pores ($<2\text{-}50\text{nm}$) are present. Information on the size of pores is of value when assessing whether or not surface adsorbed ions can penetrate the particle matrix. This penetration, or tunneling, will involve a kinetically slow diffusion into the matrix of the particles after which adsorption may or may not occur. There have been few attempts to try to specify the relationship between particle porosity and surface sorption reactions (Cabrera et al., 1981; Madrid and De Arambarri, 1985) although several studies have indicated tunneling to be of importance for kinetically slow sorption reactions (Barrow, 1983; Nyffeler et al., 1984). It is the intention of this study that, through a rigorous examination of the morphology of natural particle surfaces, some of the complex physico-chemical controls on surface sorption processes can be elucidated.

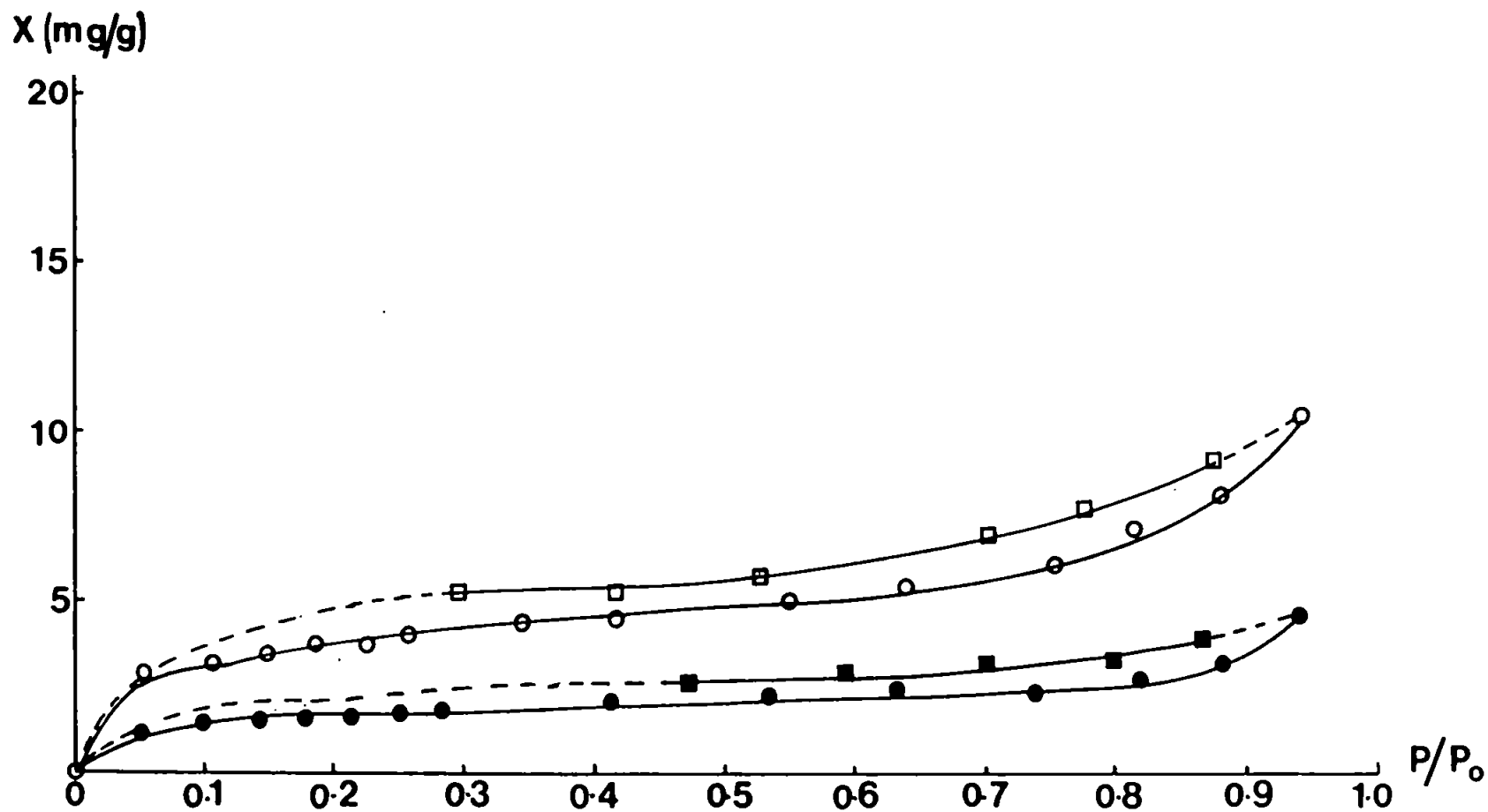


Figure 3.1. Nitrogen adsorption-desorption isotherms for a Tamar sediment sample of surface area of 10.8m²/g (open symbols) and a Plym sediment sample of surface area 4.3m²/g (closed symbols). ○ Adsorption □ Desorption

3.1.2. The Relationship Between Suspended and Sediment Materials.

To investigate the variation in surface areas of estuarine material, samples of Tamar suspended solids from the vicinity of the turbidity maximum zone, and the associated sediment particles were collected in the summer of 1984 and their surface areas determined after air drying. The values for these samples in Table 3.3 show that suspended material has significantly more surface area than the corresponding sediment particles (Millward et al., 1985).

As discussed in Section 2.2.2 problems were encountered in the analysis of air dried material because it was difficult to extract a representative sample. Therefore, to ascertain that the differences seen between suspended and sediment were real, a t-test was carried out on 5 replicate analyses of corresponding suspended and sediment samples as shown in Table 3.4. This confirms that to 99% confidence the two samples have different surface areas as is the case for all samples. The two possible reasons advanced to explain the data in Table 3.3 are (1) the selective resuspension (or retention in suspension) of a particular fraction of the sediment within the turbidity maximum zone and (2) the formation of fresh flocculants in the low salinity region of the estuary.

Firstly, particles of a particular size or settling velocity may be suspended within the turbidity maximum zone depending on the prevailing turbulence in the estuary (Festa and Hanson, 1978; Bale et al., 1984; Eisma, 1986). Disaggregation of resuspended particles may occur and can be regulated by the fluctuations in salinity (Festa and Hanson, 1978). Particles may also be disaggregated by the shear stress on the sediment during tidal stirring since interparticle

<u>Turbidity (mg/L)</u>	<u>Salinity (‰)</u>	<u>Surface area (m²/g)</u>	
		<u>Suspended</u>	<u>Sediment</u>
65	2.3	19.4	13.1
190	0.4	22.1	16.2
260	0.1	20.4	12.4
270	0.3	22.5	14.8
690	0.7	22.7	9.1

Table 3.3. Surface areas of air dried Tamar Estuary suspended solids and associated sediment samples collected in the summer of 1984.

	<u>Surface area (m²/g)</u>	
	<u>Suspended</u>	<u>Sediment</u>
	17.4	10.3
	17.7	8.4
	19.2	8.2
	15.1	8.0
	15.6	8.1
Mean ± s.d.	17.0 ± 1.7	8.6 ± 0.9
t-test limits		
Upper	20.4	10.5
Lower	13.5	6.7

Table 3.4. A t-test analysis on five replicate determinations of the surface area of suspended and sediment material which shows to 99% confidence that the two materials have different surface areas.

forces are extremely weak and aggregates can be broken into smaller units or their primary particles (James, 1987). Particle size distributions were measured as described in Section 2.1.4 for samples of Tamar resuspendable sediment and suspended particles. An example of the results for corresponding sediment and suspended material is shown in Figure 3.2. The data show the modal particle size for the suspended particles to be smaller than that for the sediment particles.

Folk-Ward statistics were used to calculate mean particle sizes assuming spherical non-porous particles (Folk, 1966). The results are shown in Table 3.5 with other comparative samples, some of which had a higher modal size for the suspended particles than the sediment particles. The calculated mean values, although in general agreement with the histograms, do not indicate any consistent trend between all suspended and sediment samples. Geometric surface areas which have been calculated from these mean particle sizes (see Table 3.5), range from $0.14\text{m}^2/\text{g}$ to $0.34\text{m}^2/\text{g}$ and these are two orders of magnitude smaller than those measured by nitrogen adsorption ($13.1\text{--}22.5\text{m}^2/\text{g}$). Also shown in Table 3.5 are the standard deviations, for the mean particle sizes, in phi units, which can be used as an index of particle sorting (Folk, 1966). All these natural particle populations would fall into the poorly sorted category as the standard deviations are between 1 and 2 while the example for kaolinite would be moderately sorted.

In this work $>0.45\mu\text{m}$ was used as the operational definition of particulate material but the lowest measurable particle size by laser diffraction was $1.9\mu\text{m}$. This cut-off presents a problem since

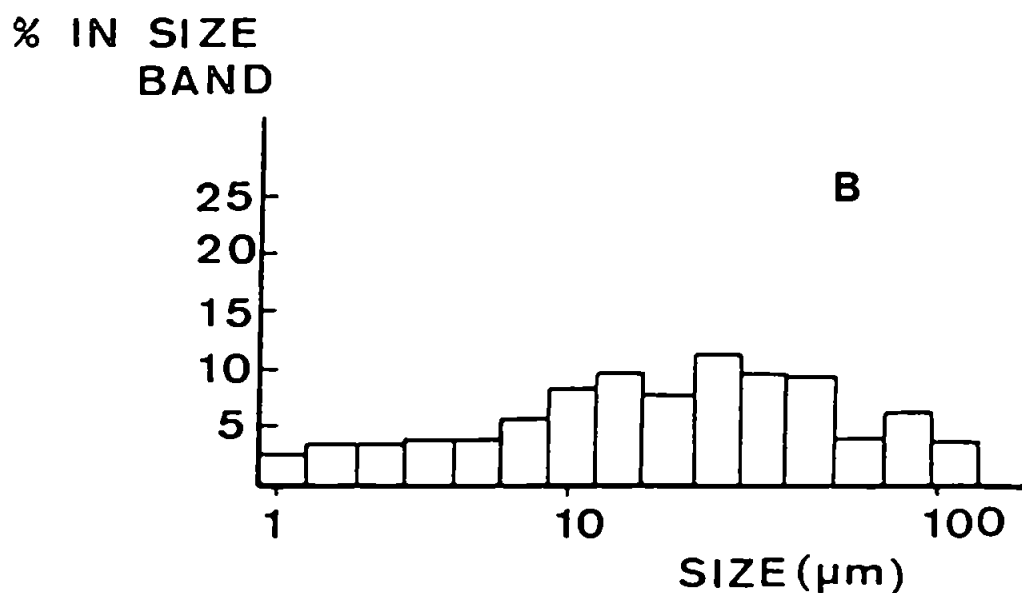
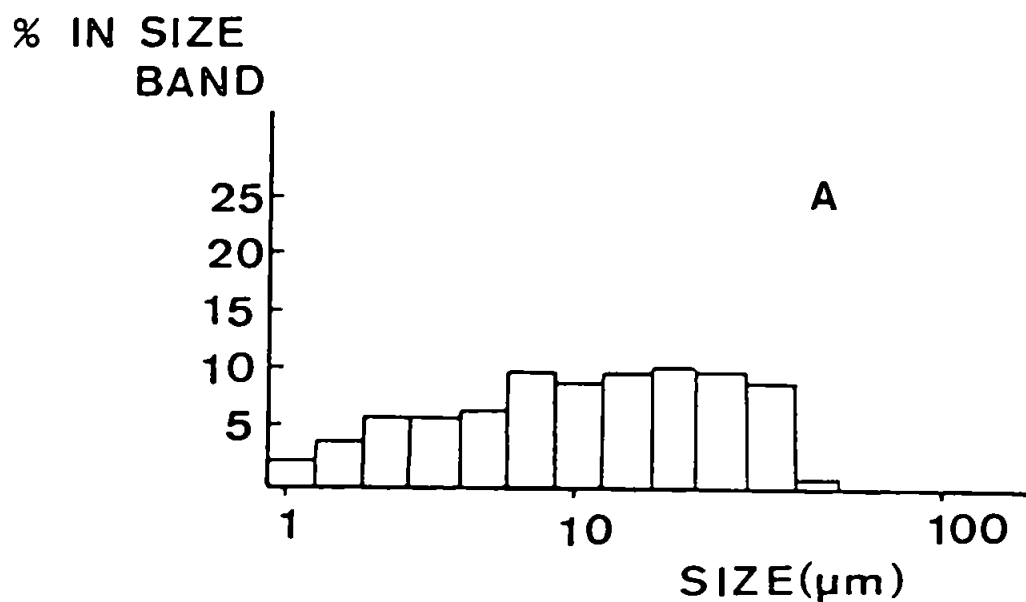


Figure 3.2. Examples of the particle size distribution determined by laser particle sizing. (A) The distribution for a Tamar suspended particle population with a mean particle size of 8.7μm. (B) The distribution for a resuspended sediment sample with a particle size of 13.5μm.

<u>Turbidity</u> <u>(mg/L)</u>	<u>SUSPENDED</u>				<u>SEDIMENT</u>			
	<u>BET</u> <u>surface area</u> <u>(m²/g)</u>	<u>Mean</u> <u>particle</u> <u>size(μm)</u>	<u>S.D.</u>	<u>Geometric</u> <u>surface area</u> <u>(m²/g)</u>	<u>BET</u> <u>surface area</u> <u>(m²/g)</u>	<u>Mean</u> <u>particle</u> <u>size(μm)</u>	<u>S.D.</u>	<u>Geometric</u> <u>surface area</u> <u>(m²/g)</u>
65	19.4	8.7	1.07	0.24	13.1	13.6	1.45	0.15
190	22.1	12.5	1.16	0.16	16.2	8.4	1.24	0.24
270	22.5	10.1	1.11	0.20	14.8	8.6	1.09	0.23
Kaolinite	12.9	5.2	0.84	0.38	-	-	-	-

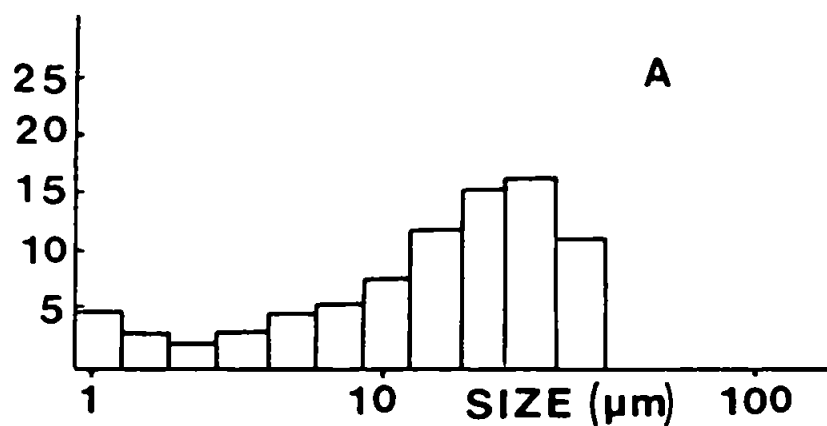
Table 3.5. The mean particle size and calculated geometric surface areas for selected Tamar suspended and associated sediment samples and for a kaolinite sample. Also included is the standard deviation (S.D.) of the particle size using the ϕ scale.

there is a region in the size distribution where there is no information about particle size. This problem is similar to many other analytical methods (Riley, 1975). As an example of this uncertainty Figure 3.3 shows the results of determining the range of particle sizes of a natural suspended sample before and after digestion with hydrogen peroxide to remove organic matter. These show a decrease in particle size after digestion, the calculated mean particle size decreasing from $10.7\mu\text{m}$ before treatment to $5.7\mu\text{m}$ after oxidation. However this method does not quantify the region between $0.45\mu\text{m}$ and $1.9\mu\text{m}$ which for the untreated particles contains 4.6% of the cumulative weight while for the digested particles contains 17.8%.

This source of error in the calculation of the mean particle sizes is not sufficient to increase the small geometric surface areas relative to those measured by BET nitrogen adsorption. The particles would need to have an average diameter of $0.1\mu\text{m}$ in order to give a calculated surface area of $20\text{m}^2/\text{g}$. Since all particulate samples were filtered through $0.45\mu\text{m}$ filters and even taking into account filter clogging effects (Gibbs, 1974; Riley, 1975; Faisst, 1980), it is highly improbable that a large proportion of these very small particles would be retained within the sample for surface area analysis.

Therefore, it is deduced that the majority of the surface area seen using gas adsorption techniques must be as a result of irregular particle shape and internal pore structure and there is little evidence to suggest that there is a connection between particle size and measured surface area for estuarine particles. The pore space may be in cylindrical or ink-bottle shaped pores, slits in clay

**% IN SIZE
BAND**



**% IN SIZE
BAND**

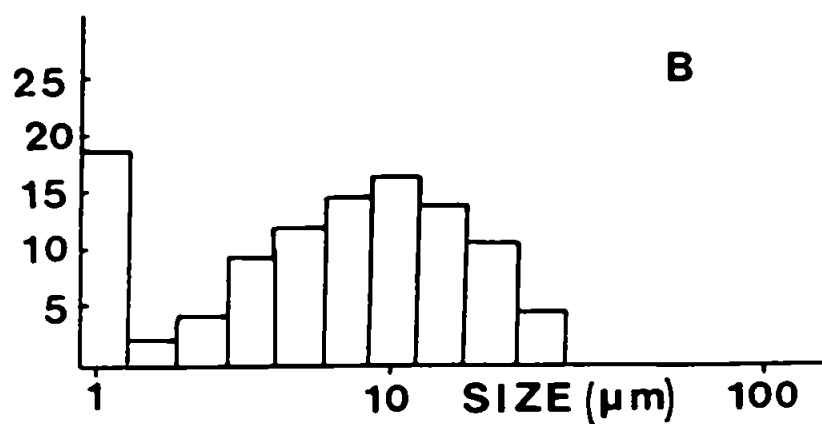


Figure 3.3. The particle size distribution for a Tamar suspended sample (A) before digestion with hydrogen peroxide and (B) after digestion. Data courtesy of Mr A.J. Bale.

minerals or in spaces between particles joined together as aggregates. In reality it is probably a combination of all these spaces.

The second possible reason for observing a higher surface area in the suspended material than in the sediment material could be the formation of fresh flocculants. In the low salinity region of the turbidity maximum, the dissolved and colloidal, organic and inorganic material present in the river water can flocculate on meeting the brackish water (Boyle et al., 1974; Sholkovitz, 1976; Sholkovitz et al., 1978; Fox and Wofsy, 1983). Constituents which flocculate onto the surfaces of the suspended particles will alter the surface characteristics of the particles (Gibbs, 1973; Hunter and Liss, 1982). Suspended particles have been seen to age and lose surface area while left for 48h in the sample bottles during this project (see Section 2.2.2), and a similar ageing process has been seen for precipitated Fe oxyhydroxides left in suspension for 2h or longer (Crosby et al., 1983). Thus newly flocculated material will be present in the suspended matter of the estuary and the suspended material may have a higher surface area than comparable sediment material because of the presence of fresh surface coatings of Fe oxyhydroxides.

Comparing the hysteresis curves for suspended and sediment material (see Figures 3.4 and 3.5) shows similar characteristics for pore size and shape but a lower pore volume for the sediment ($9.9 \times 10^{-3} \text{ cm}^3/\text{g}$) than for the suspended sample ($1.6 \times 10^{-2} \text{ cm}^3/\text{g}$). The isotherms are of the type B using the De Boer classification (Sing, 1976) which is indicative of slit shaped pores or parallel plates in the mesopore range (2-50nm) and they also show low pressure hysteresis. This low pressure hysteresis, superimposed on the

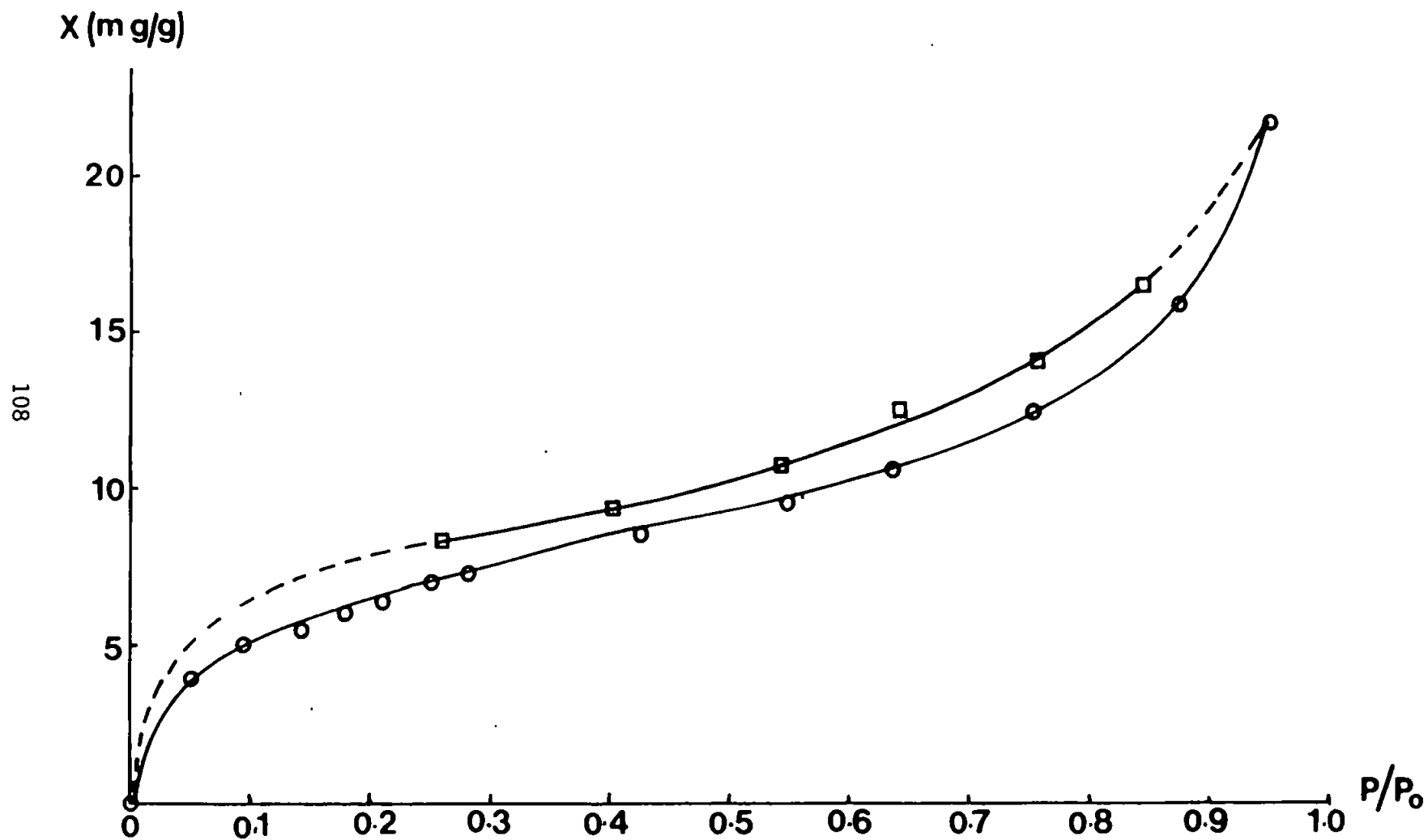


Figure 3.4. A nitrogen adsorption-desorption isotherm for a Tamar suspended sample of surface area $19.4\text{m}^2/\text{g}$ associated with the sediment sample for which the hysteresis loop is shown in Figure 3.5. \circ Adsorption \square Desorption

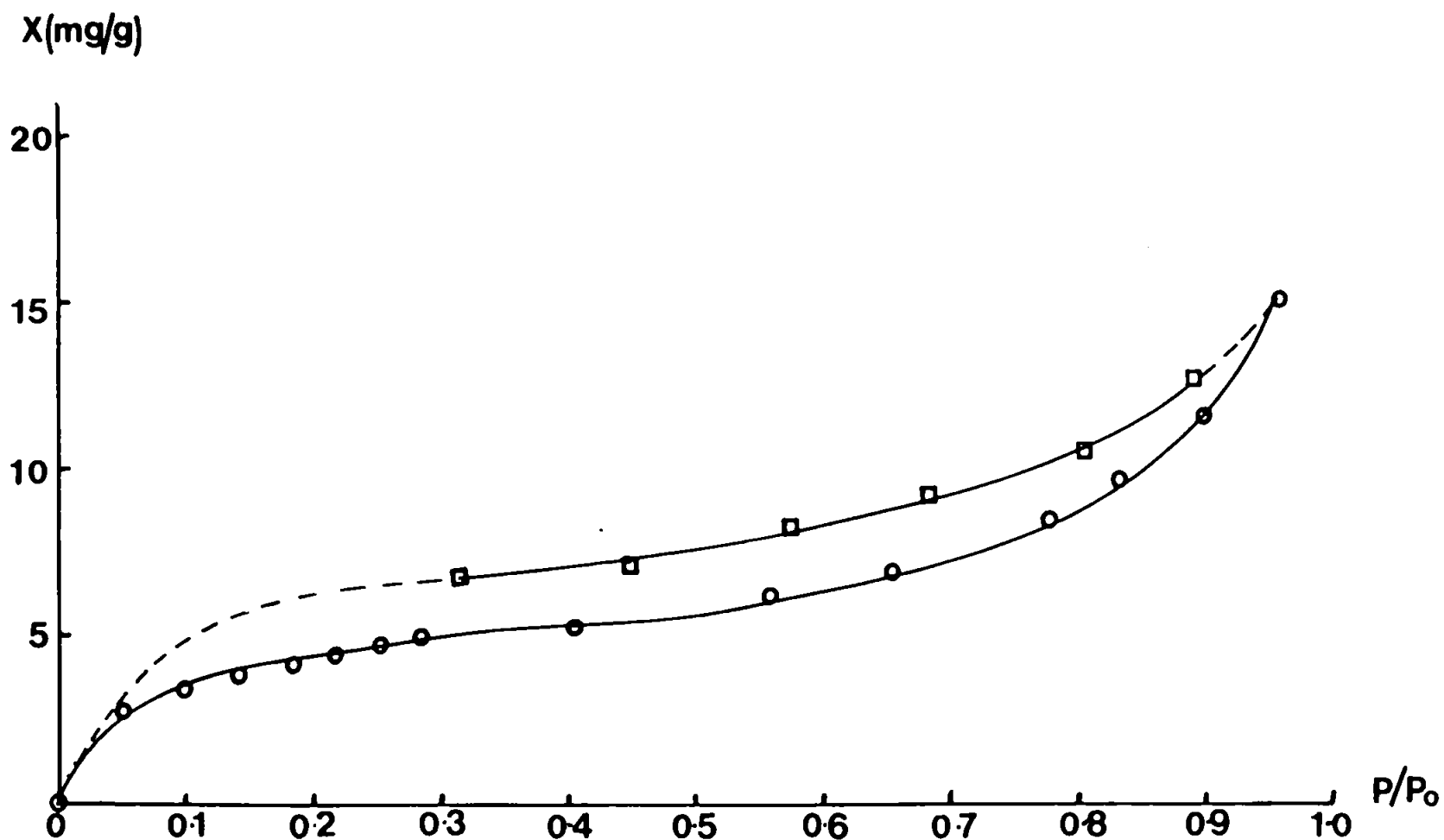


Figure 3.5. A nitrogen adsorption-desorption isotherm for the sediment sample of surface area $13.1\text{m}^2/\text{g}$ associated with the suspended sample for which the hysteresis loop is shown in Figure 3.4. \circ Adsorption \square Desorption

isotherm, is thought to be due to irreversible intercalation of the nitrogen molecules in narrow slits ($<2\text{nm}$) or across the neck of other types of pores.

An analogous decrease in pore volume while the other pore characteristics are retained has been seen for Fe(II) derived Fe oxyhydroxides aged for two hours and one week by Crosby et al. (1983). As shown in Table 3.6 the pore volume decreased from $1.8 \times 10^{-1} \text{cm}^3/\text{g}$ for two hour old material (surface area = $121 \text{m}^2/\text{g}$) to $6.3 \times 10^{-2} \text{cm}^3/\text{g}$ for week old material (surface area = $97 \text{m}^2/\text{g}$). This suggests that it is feasible for the higher surface area of the suspended material to be due to the freshness of certain components of the particles. This is discussed in more detail in subsequent sections.

A comparison of the surface area of Restronguet Creek suspended solids and sediment material was also carried out. This gave a surface area for the sediments of $35.5 \text{m}^2/\text{g}$ and for the suspended material of $125.5 \text{m}^2/\text{g}$ as is shown in Table 3.6 with values for other selected materials. This indicates that each estuarine system is individual although trends within different estuaries are the same. Examination of the hysteresis curve seen in Figure 3.6 for the suspended material from the Restronguet Creek shows in particular large mesopores and macropores to be present. There is no evidence of micropores in this solid, possibly because there is very little aluminosilicate clay in the Restronguet Creek. The pore volume for the Restronguet Creek suspended material is of a magnitude intermediate between the natural Fe oxides precipitated by Crosby et al. (1983) and the Tamar material. The very high Fe concentrations

<u>Sample</u>	<u>Surface area</u> (m^2/g)	<u>Pore volume</u> (cm^3/g)
Tamar suspended	19.4	1.6×10^{-2}
Tamar sediment	13.1	9.9×10^{-3}
Restranguet suspended	125.5	3.7×10^{-2}
Restranguet sediment	35.5	--
Amorphous FeOOH^{a}		
2 hour old	121	1.8×10^{-1}
1 week old	97	6.2×10^{-2}
Ca-Willalooka illite ^b	164	1.9×10^{-1}

Table 3.6. A comparison of surface areas and pore volumes of natural and precipitated materials.

^a Values from Crosby et al. (1983) ^b Value from Quirk (1978).

(up to 5mg/l) found in the Carnon River which flows into the Restranguet Creek will greatly influence the surface area of this material (Marsh et al., 1984; Johnson, 1986). In the low salinity region of the estuary amorphous Fe oxides would precipitate and a large quantity of fresh Fe oxyhydroxides would increase the surface area and porosity of the suspended material. The fact that the pore volume and surface area are not directly related is also worth consideration. It is most important to determine the porosity of particles before attempting to relate sorption reactions to particle morphology (Cabrera et al., 1981; Madrid and De Arambarri, 1985).

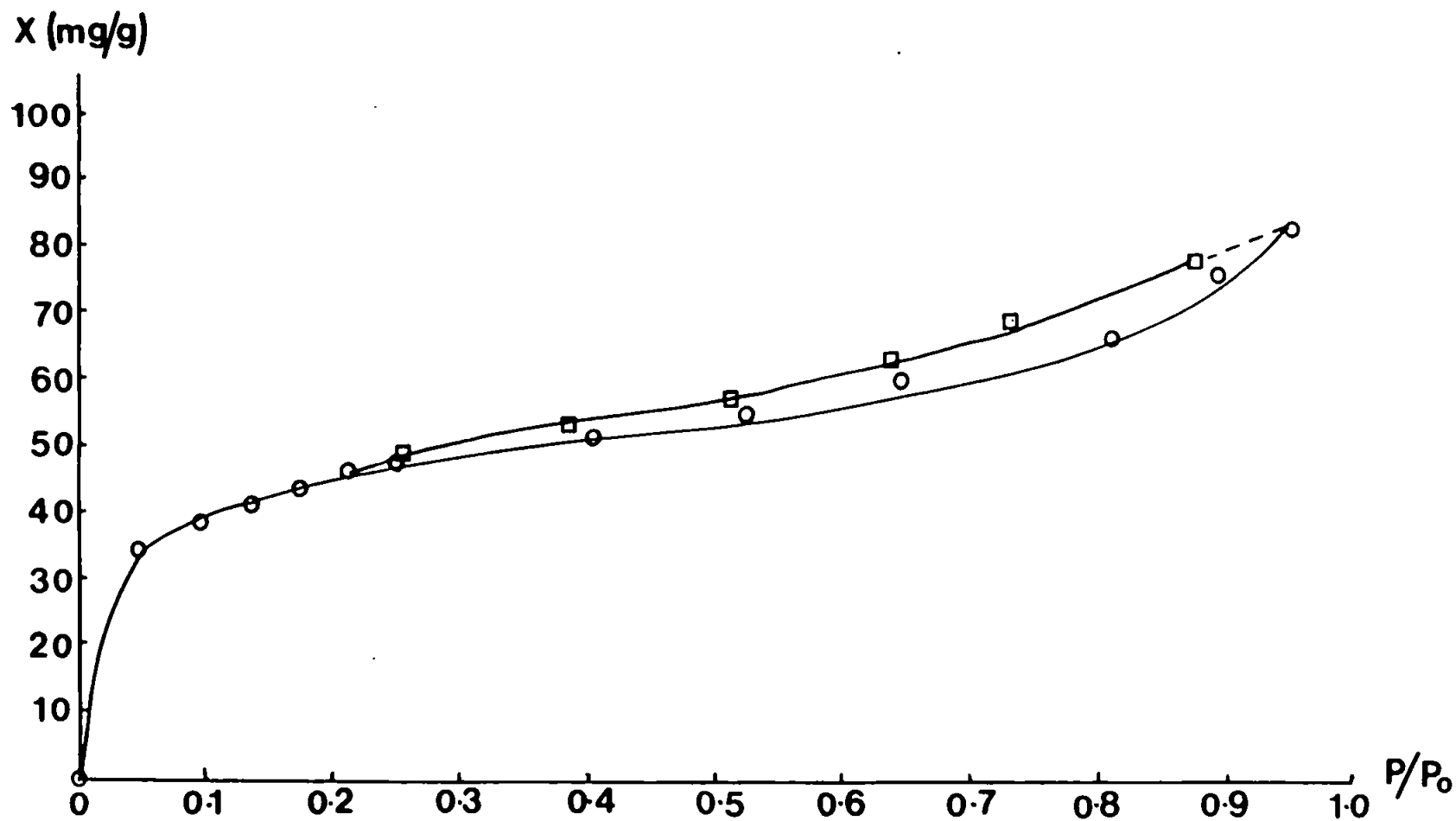


Figure 3.6. A nitrogen adsorption-desorption isotherm for suspended material, from Restronguet Creek, of surface area of 125.5 m²/g. ○ Adsorption □ Desorption

3.1.3. The Surface Areas of Suspended Solids from the Tamar Estuary.

Two axial traverses of the Tamar Estuary (29-10-85 and 18-9-86) were carried out to collect discrete samples of suspended particulate material through the whole hydrodynamic regime of the estuary. Table 3.7 shows the range of conditions during the surveys and Tables 3.8a and 3.8b show the salinity, turbidity and surface area for each sample. The data exhibit a clear link, for both surveys, between surface area and salinity, the highest surface area being found for material from the low salinity region of the estuary (Titley *et al.*, 1987). The data from 29-10-85, plotted in Figure 3.7 affirm this trend when surface area and salinity are plotted versus distance down estuary. This also shows a correlation between surface area and turbidity.

To test if this was a reproducible phenomenon other results from the Tamar were plotted versus log (salinity) together with the data from the two axial surveys as shown in Figure 3.8. This gives a curve which indicates the non-conservative behaviour of surface area particularly in the low salinity region of the estuary. A similar trend has recently been seen in the Gironde and Loire estuaries by Martin *et al.* (1986) which suggests observations like these are applicable to many estuaries. It is also interesting to note that the surface areas of suspended material from these French estuaries, determined by BET argon adsorption (approximately $8-40\text{m}^2/\text{g}$), are very similar in magnitude to those measured in the Tamar Estuary.

A similar plot of surface area versus turbidity was constructed as shown in Figure 3.9 but this gives only a moderate correlation (significant at the 95% level). This could be because

Survey date	29-10-85	18-9-86
Rainfall (mm) in previous 2 weeks	0	6.4
Tidal Range (m)	4.4	4.7
River Flow (m ³ /s)	5.7	8.7
Range of turbidity (mg/L)	80-530	70-580
pH range	7.7-7.9	7.4-7.8
Temperature range (°C)	10.7-8.0	13.2-11.4

Table 3.7. An outline of the conditions observed during two axial surveys of the Tamar Estuary. The ranges quoted are for the salinity range of 19‰ to <0.5‰ to enable an intersurvey comparison to be made. The rainfall data is from the Plymouth Polytechnic meteorological station and therefore relevant to Plymouth.

<u>Salinity</u>	<u>Turbidity</u>	<u>Surface area</u>
<u>(‰)</u>	<u>(mg/L)</u>	<u>(m²/g)</u>
28.5	60	8.4
22.5	190	10.7
9.7	115	14.0
5.0	130	17.2
3.1	470	18.0
2.2	480	19.8
0.15	530	17.8
0.09	140	14.6
0.06	215	13.9

Table 3.8a. Salinity, turbidity and BET nitrogen adsorption surface area data for the 29-10-86 survey of the Tamar Estuary.

<u>Salinity</u>	<u>Turbidity</u>	<u>Surface area</u>
<u>(‰)</u>	<u>(mg/L)</u>	<u>(m²/g)</u>
19.0	70	14.2
13.5	210	12.0
8.2	150	13.3
4.7	235	15.1
2.6	500	16.7
0.9	580	15.8
<0.5	410	15.2

Table 3.8b. Salinity, turbidity and BET nitrogen adsorption surface area data for the 18-9-86 survey of the Tamar Estuary.

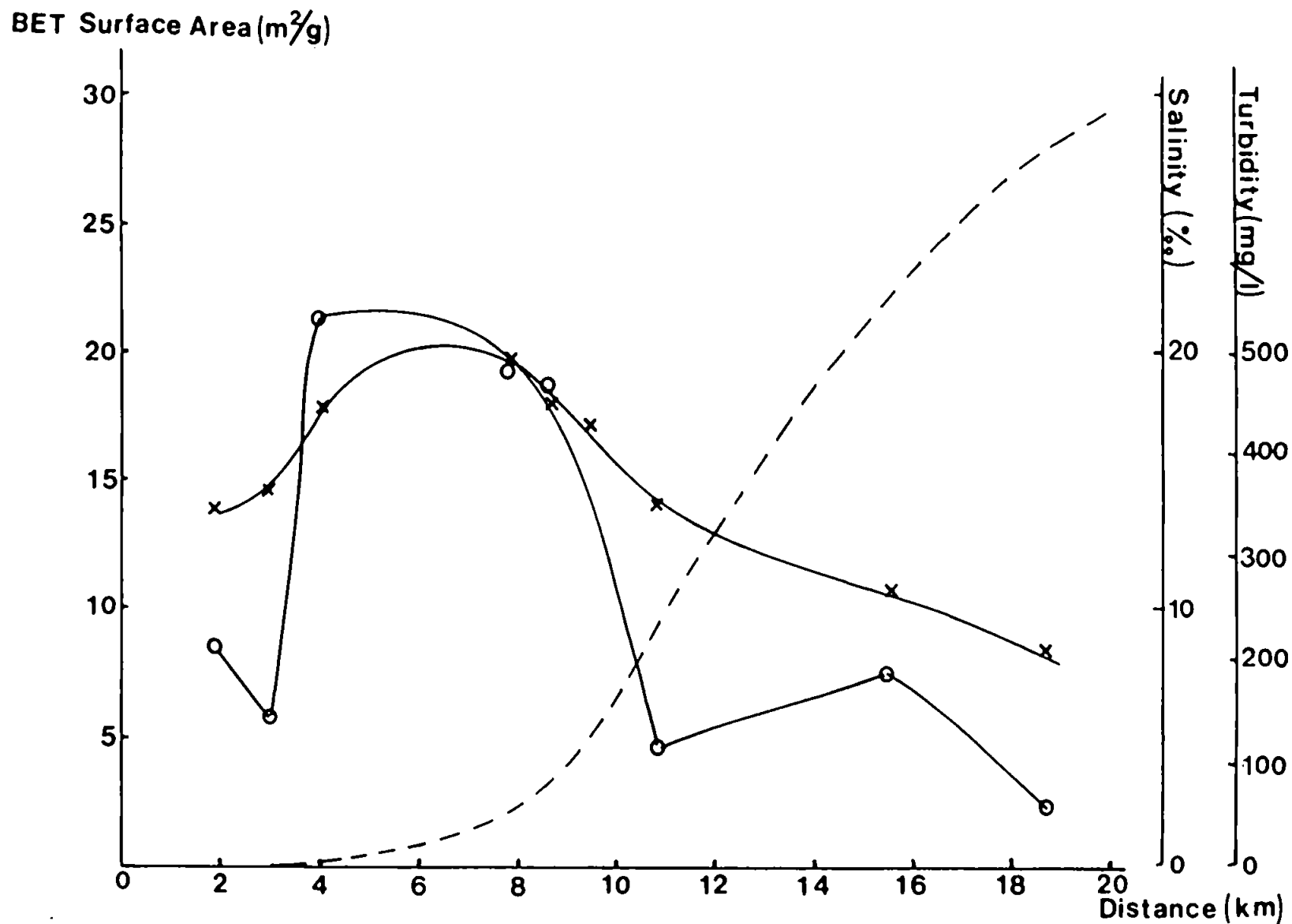


Figure 3.7. A plot of surface area (X), turbidity (O) and salinity (hashed line) versus distance down estuary for the 29-10-85 survey.

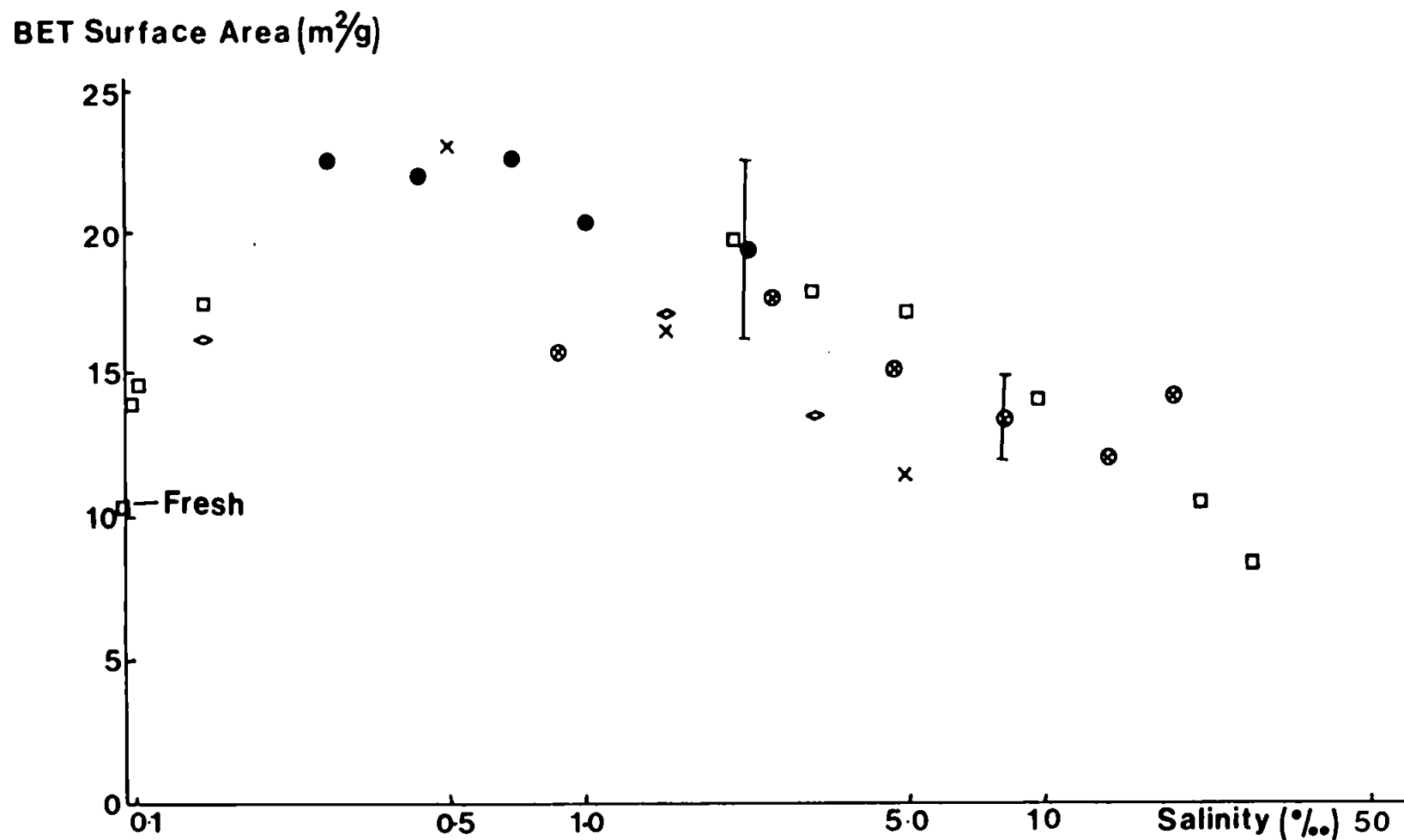


Figure 3.8. A plot of BET surface area versus log (salinity) for samples collected from the Tamar Estuary. Error bars are shown for two examples, the larger for air dried material and the smaller for freeze dried material. The area shown at 0‰ salinity is for a freshwater sample. ◊ See Table 2.5. ● See Table 3.3. □ See Table 3.8a. ⊗ See Table 3.8b. X See Figures 4.1-4.4.

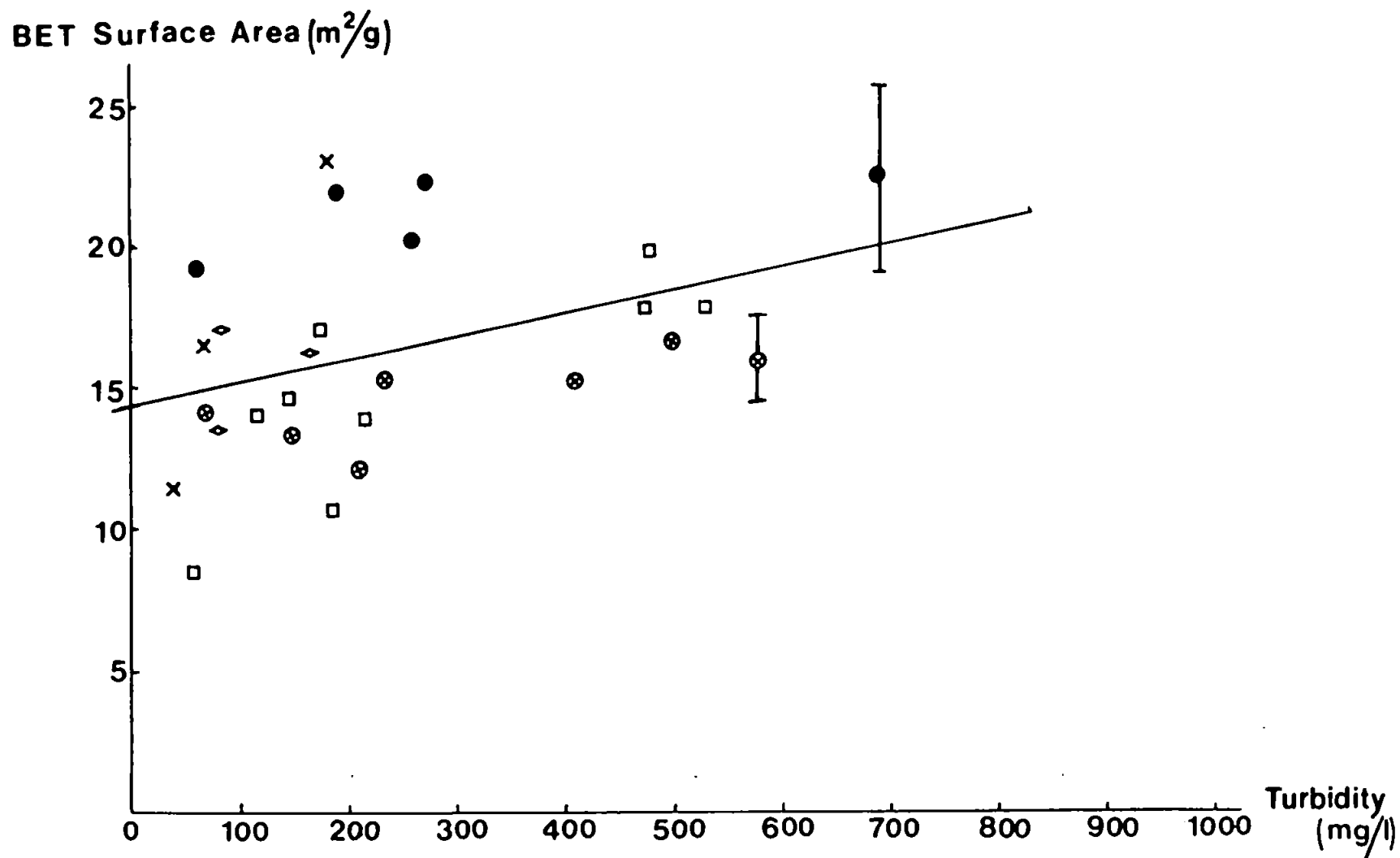


Figure 3.9. A plot of BET surface area versus turbidity for samples collected from the Tamar Estuary. Error bars are shown on two points, the larger relating to air dried samples and the smaller to freeze dried samples. The correlation for the regression line is significant at the 95% level.

◇ See Table 2.5. ● See Table 3.3. □ See Table 3.8a. ⊗ See Table 3.8b. × See Figures 4.1-4.4.

turbidity is dependent on many factors including river flow, tidal range and topography (Allen et al., 1980; D'Anglejan and Ingram, 1984). Also, in some parts of the Tamar Estuary there are very obvious localised areas of sediment resuspension due to friction of water on the banks of meanders and in areas exposed to strong winds which give rise to pools of very high turbidity.

During the two axial estuarine surveys the size distributions of the suspended particles were measured and in Tables 3.9a and 3.9b calculated geometric surface areas and measured nitrogen adsorption areas are represented (Titley et al., 1987). Again the standard deviations suggest these samples are poorly sorted and no correlation between the geometric and measured surface areas can be seen.

Studies by Rhodes (1985) in the Tamar Estuary found that for nine axial estuarine surveys, during the neap to spring cycles, the modal particle size within the turbidity maximum was reasonably constant. An increase in particle size was indicated within the turbidity maximum for only one survey and for six of these surveys an increase was observed in the freshwater and at high salinities ($>15\text{‰}$). In addition Bale et al. (1984) used the laboratory-based laser particle sizer for samples collected in the turbidity maximum of the Tamar Estuary. This showed that the lowest mean sizes, 20-25 μm , were observed in the turbidity maximum while the lower estuary had sizes in the range 40-60 μm . The data in the two surveys reported here show similar features. For example at the turbidity maximum (530mg/L) on the 29-10-85 the mean particle size is 13.7 μm while on 18-9-86 (580mg/L) the mean particle size is 9.8 μm .

<u>Salinity</u> <u>(‰)</u>	<u>Surface area</u> <u>(m²/g)</u>	<u>Mean particle</u> <u>diameter (μm)</u>	<u>Geometric surface</u> <u>area (m²/g)</u>
28.5	8.4	26.6	0.07
22.5	10.7	17.1	0.12
9.7	14.0	15.2	0.13
5.0	17.2	12.3	0.16
3.1	18.0	26.1	0.07
2.2	19.8	20.1	0.09
0.15	17.8	13.7	0.15
0.09	14.6	16.0	0.12
0.06	13.9	23.9	0.08

Table 3.9a. The mean particle diameters of Tamar suspended material collected 29-10-85 and the calculated geometric surface areas for comparison with the measured BET surface areas.

<u>Salinity</u> <u>(‰)</u>	<u>Surface area</u> <u>(m²/g)</u>	<u>Mean particle</u> <u>diameter (μm)</u>	<u>Geometric surface</u> <u>area (m²/g)</u>
19.0	14.2	11.0	0.18
13.5	12.0	12.7	0.16
8.2	13.3	10.7	0.19
4.7	15.1	11.6	0.17
2.6	16.7	10.9	0.18
0.9	15.8	9.8	0.20
<0.5	15.2	7.7	0.26

Table 3.9b. The mean particle diameters of Tamar suspended material collected 18-09-86 and the calculated geometric surface areas for comparison with the measured BET surface areas.

The laser particle size analyses reported above and the earlier studies of Bale et al. (1984) and Rhodes (1985) were carried out on particulate samples returned to the laboratory for analysis. Collecting natural suspensions for particle size analysis has been reported to modify the integrity of large aggregate particles (Eisma et al., 1983). More recent work by Bale (1987) in which the laser particle sizer has been used in situ has apparently confirmed that particle sizes do decrease in the region of the turbidity maximum. However, it has to be recognised that the deployment of a large instrument in the turbulent regime of the turbidity maximum may introduce sufficient shear stress for fragile aggregates to disintegrate into their constituent particles. Thus, to some extent the question of the particle size distribution in the turbidity maximum remains an open question. Nevertheless it would appear that as far as the variation in the BET surface areas in the low salinity region is concerned, the particle size plays a minor role because it gives rise to very small geometric surface areas.

It is possible from these observations of the coincidence of low salinity and high surface area that the cause may be the newly flocculated riverine material. Colloidal riverine material will enter the estuary and flocculate onto particle surfaces on meeting the saline water. These particles will have a half life in the estuary of at least 1.4 years (Bale et al., 1985) being continually resuspended and deposited. During that time the material may age and its surface area decrease. If the circulation patterns within the estuary were to be the cause of particle selection a better correlation could be expected for surface area and turbidity although this is not

conclusive. This hypothesis is discussed in greater detail in the following section on the chemical components of natural estuarine particles.

3.2. An Examination of the Effect of Chemical Composition on the Characteristics of Particles.

3.2.1. Identification of the Crystalline Components.

X-ray diffraction analyses were carried out to identify the crystalline components of the underlying lithogenous matrix. Materials from the Plym, Tamar and Restronguet estuaries were examined before and after chemical treatments but few variations in the crystalline matrix were seen after treatment.

An analysis of Plym sediment (surface area = $4.3\text{m}^2/\text{g}$) revealed that it contained quartz, kaolinite and muscovite only, no other crystalline component being present in an identifiable quantity (approximately >5%). Natural silicas tend to have surface areas very similar to their geometric surface areas and kaolinite was measured to have a surface area of $12.9\text{m}^2/\text{g}$ in this work although this can vary considerably depending on source, as is common with all clays (Greenland and Quirk, 1962; Dutta and Gupta, 1974; Barby, 1976; Van Olphen, 1976). The muscovite was actually a muscovite-illite intermediate which had been considerably weathered as can be seen from peak broadening on X-ray diffraction patterns. The surface areas of illites may also vary widely and values from $70\text{--}132\text{m}^2/\text{g}$ have been quoted depending on their origin (Greenland and Quirk, 1962; Martin et al., 1986). Muscovite has been found by water adsorption to have a surface area of $10\text{--}46\text{m}^2/\text{g}$ (Mikhail et al., 1979).

Suspended and sediment particulate material from the Tamar Estuary also contained quartz, kaolinite and weathered muscovite but in addition most samples contained chlorite and traces of Fe. These samples indicated the presence of small amounts of crystalline Fe

oxides in the form of lepidocrocite, magnetite and goethite although the low peak heights and complexity of the diffractograms prevented specific identification. An example of a typical trace for a Tamar suspended solids sample is shown in Figure 3.10 with some key peaks identified. The amorphous Fe oxyhydroxide "ferrihydrite" could not be identified as all recognised X-ray diffraction lines were obscured by kaolinite, quartz and muscovite in these samples (Schwertmann and Fischer, 1973; Murray, 1979). The diffractogram for the freshwater suspended particles from the Tamar River indicated the presence of quartz, kaolinite and weathered muscovite only.

The analysis for the Restronguet Creek suspended material showed weathered muscovite and small traces of quartz but no other crystalline material was present. The corresponding sediment material indicated the presence of quartz, muscovite and also goethite. Hydrrous Fe oxides, as previously discussed (see Table 3.2), tend to have high surface areas but synthetic goethite has been reported to have surface areas ranging from 9-153 m²/g depending on the temperature of formation (Schwertmann et al., 1985).

These analyses show that natural estuarine samples are a complex mixture with clays, quartz and possibly Fe and Mn oxyhydroxides as major components. Each of these components have different surface areas which may vary widely depending on the source and age of the material. Quantitative information was not available from these analyses and thus it was impossible to compare relative amounts of materials using these data. Having established the nature of the lithogenous components of the particles the purpose of the following sections is to try to determine which of these components

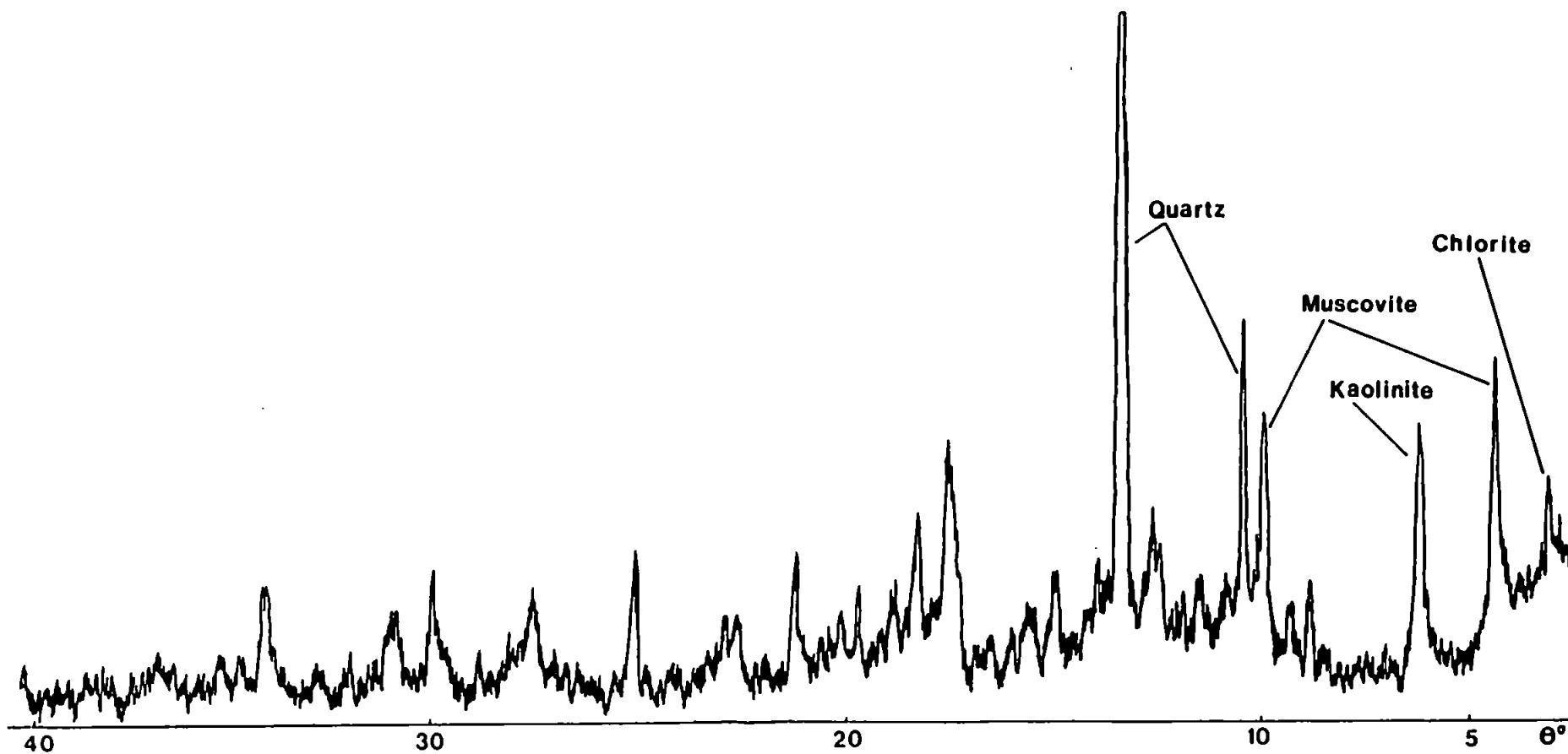


Figure 3.10. An example of a typical X-ray diffractogram of a suspended Tamar sample. Some key peaks are identified.

are instrumental in determining the surface area and porosity of natural particles.

3.2.2. The Influence of Organic Material on Surface Morphology.

There is evidence from studies of electrophoretic mobility that estuarine and seawater particles are coated with organic materials which confer a uniformly negative surface charge on the particles (Neihof and Loeb, 1972; Hunter and Liss, 1979; Hunter and Liss, 1982). It has been suggested that this uniform surface coating may mask the properties of the underlying lithogenous material and present a different type of surface to adsorbing species (Lion et al., 1982; Davis, 1984). There is also evidence for Fe and Mn oxyhydroxides having a significant role in coating the surfaces of particles and this will be discussed in Section 3.2.3. Examining the effects of organic matter (and the effects of Fe and Mn oxyhydroxides) on the surface area and porosity of estuarine particles is therefore important if a detailed picture of natural surface sorption reactions is to be built up.

During the surveys discussed in Section 3.1, sub-samples of the dried particles used for surface area determination were analysed for their carbon content. Table 3.10 shows results of this for compatible suspended and sediment samples from the Tamar Estuary and Restronguet Creek (Millward et al., 1985). For the Tamar samples there was a correlation (>95%) between increasing carbon content and decreasing surface area. This correlation was not seen for the Restronguet Creek samples but the intertidal zone of this estuary has sediments contaminated by a high Fe and trace metal content (Johnson,

1986; Millward and Marsh, 1986) and thus very little biological activity.

<u>Turbidity</u> <u>(mg/L)</u>	<u>Suspended</u>		<u>Sediment</u>	
	<u>Surface area</u> <u>(m²/g)</u>	<u>% Carbon</u>	<u>Surface area</u> <u>(m²/g)</u>	<u>% Carbon</u>
65 ^a	19.4	4.0	13.1	6.2
190 ^a	22.1	3.6	16.2	4.0
260 ^a	20.4	2.6	12.4	4.6
270 ^a	22.5	3.2	14.8	3.8
690 ^a	22.7	3.8	9.1	4.7
150 ^b	125.5	2.7	35.5	1.7

Table 3.10. BET nitrogen adsorption surface areas and carbon contents determined on air dried suspended and associated sediment samples. ^aTamar Estuary; ^bRestrouguet Creek.

To continue this line of attack, one pair of the Tamar samples and those from the Restrouguet were digested with hydrogen peroxide (see Section 2.2.3) and the surface area and carbon content of the products reanalysed. These results, shown in Table 3.11, indicate a large increase in surface area and a decrease in carbon content for samples from both estuaries (Millward et al., 1985). Regressing data for both the undigested and digested samples from the Tamar gave a good correlation (>95%) between surface area and carbon content and it is interesting to note that the Restrouguet material

which had a low carbon content before digestion has also lost carbon and gained surface area. A similar increase in BET nitrogen adsorption surface area on removal of organic material has been seen for a series of soil samples (Burford et al., 1964). This gain in surface area suggests that the organic material, which has a low surface area, may be blocking internal pores on the particles which then become available on the removal of organic carbon (Burford et al., 1964).

<u>Sample</u>	<u>Suspended</u>		<u>Sediment</u>	
	<u>Surface area</u> (<u>m²/g</u>)	<u>% Carbon</u>	<u>Surface area</u> (<u>m²/g</u>)	<u>% Carbon</u>
Tamar-				
Untreated	19.4	4.0	13.1	6.2
Tamar-				
Digested	31.5	0.5	15.4	1.0
Restronguet-				
Untreated	125.5	2.8	35.5	1.7
Restronguet-				
Digested	184.7	0.1	60.9	<0.1

Table 3.11. A comparison of the surface areas and carbon contents of digested and untreated, suspended and sediment material from the Tamar Estuary and Restronguet Creek.

To examine in more detail the relationship between carbon content and surface area and having observed that for all samples some

residual carbon was not removed by the digest a further experiment was carried out to follow the digestion process. Samples were digested for various lengths of time (up to 24h) and the surface area and carbon content of the digested particles measured. The plotted curve in Figure 3.11 of surface area against carbon content shows an increase in surface area as the carbon is removed from the surface of the particles although some resistant carbon remains on the particles (Glegg et al., 1987). Included in this figure are the surface areas for some pure materials listed in Table 3.2. These materials which may control the surface area of the natural particles show possible extreme surface area values. The residual carbon is presumably inorganic carbon in the form of carbonate which is resistant to mild oxidation (Morris et al., 1982b).

This gain in surface area could arise for three reasons. The first could be the unblocking of internal pores or cavities which have been covered in organic material. The second reason could be the disaggregation of the component particles to reveal the smaller primary particles as was discussed for a digested sample in Section 3.1.2. Experiments designed to elucidate this mechanism were carried out in this laboratory (Titley, Personal Communication, 1986) on a sample of china clay which initially had a surface area of $11.2\text{m}^2/\text{g}$ and contained little or no carbon ($<0.02\%$). After digestion this sample had a surface area of $13.7\text{m}^2/\text{g}$. The small increase in surface area of $2.5\text{m}^2/\text{g}$, presumably due to disaggregation, is much less than the increases in surface area observed on digestion of natural samples. The third explanation for the increase in surface area on digestion could be the loss of the mass of the low surface

BET Surface Area (m^2/g)

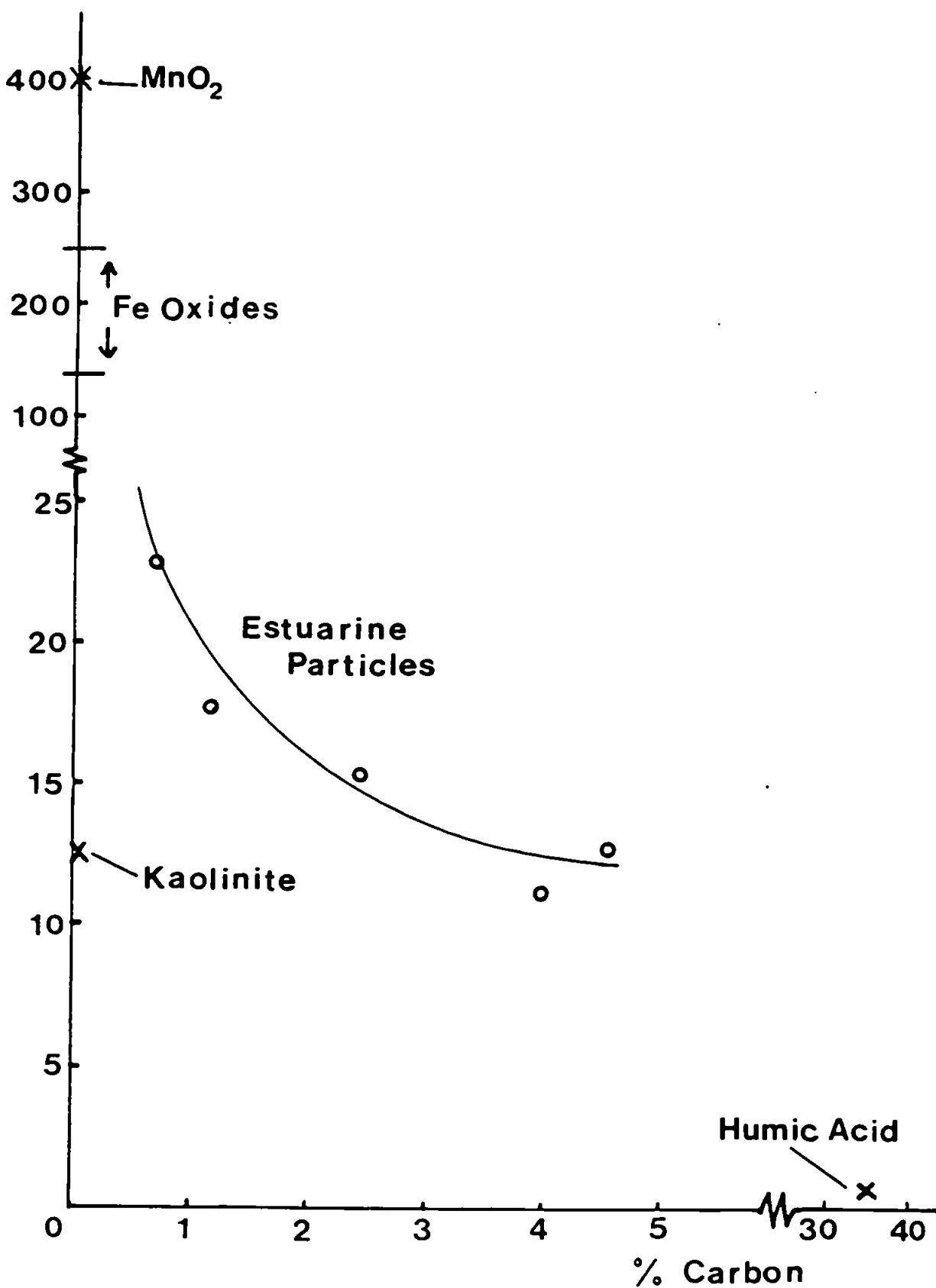


Figure 3.11. A plot of surface area versus carbon content for a series of digested Tamar estuarine particles (O). Also included are values for some samples listed in Table 3.2.

area component in the organic material ($<1\text{m}^2/\text{g}$). The expected surface area increase on the removal of organic material (due to the increased weight of the residual material which has a higher surface area) would be approximately 10% for Tamar material and less for Restronguet particles. This does not account for the sometimes very large increases in surface area observed. On this evidence it may be deduced that the higher surface areas seen for the digested natural samples are due to the unblocking of pores on removal of organic carbon.

Figure 3.12 shows the hysteresis loop for the digestion product of the suspended sample used previously for porosity analysis (see Figure 3.4). The calculated minimum mesopore volume for this digested sample is $2.3 \times 10^{-2}\text{cm}^3/\text{g}$ compared to $1.6 \times 10^{-2}\text{cm}^3/\text{g}$ for the undigested material. In conjunction with this increase in mesopore volume visual examination of the hysteresis curves suggests there is a change in the shape of the curve at near atmospheric pressures. This alteration in shape indicates the presence of macro- and large meso-pores which were not found in the natural sample. This same trend can be seen by comparing Figures 3.13 and 3.14 for a similarly treated sample of Tamar suspended particles. These changes must be interpreted with great care (Sing, 1982) but they do concur with the proposition that removal of organic material can uncover pores in which gas adsorption may subsequently take place.

The samples from the two complete axial surveys of the Tamar were also analysed for carbon and the results of this with the C/N ratio are shown in Tables 3.12a and 3.12b. No correlation can be seen

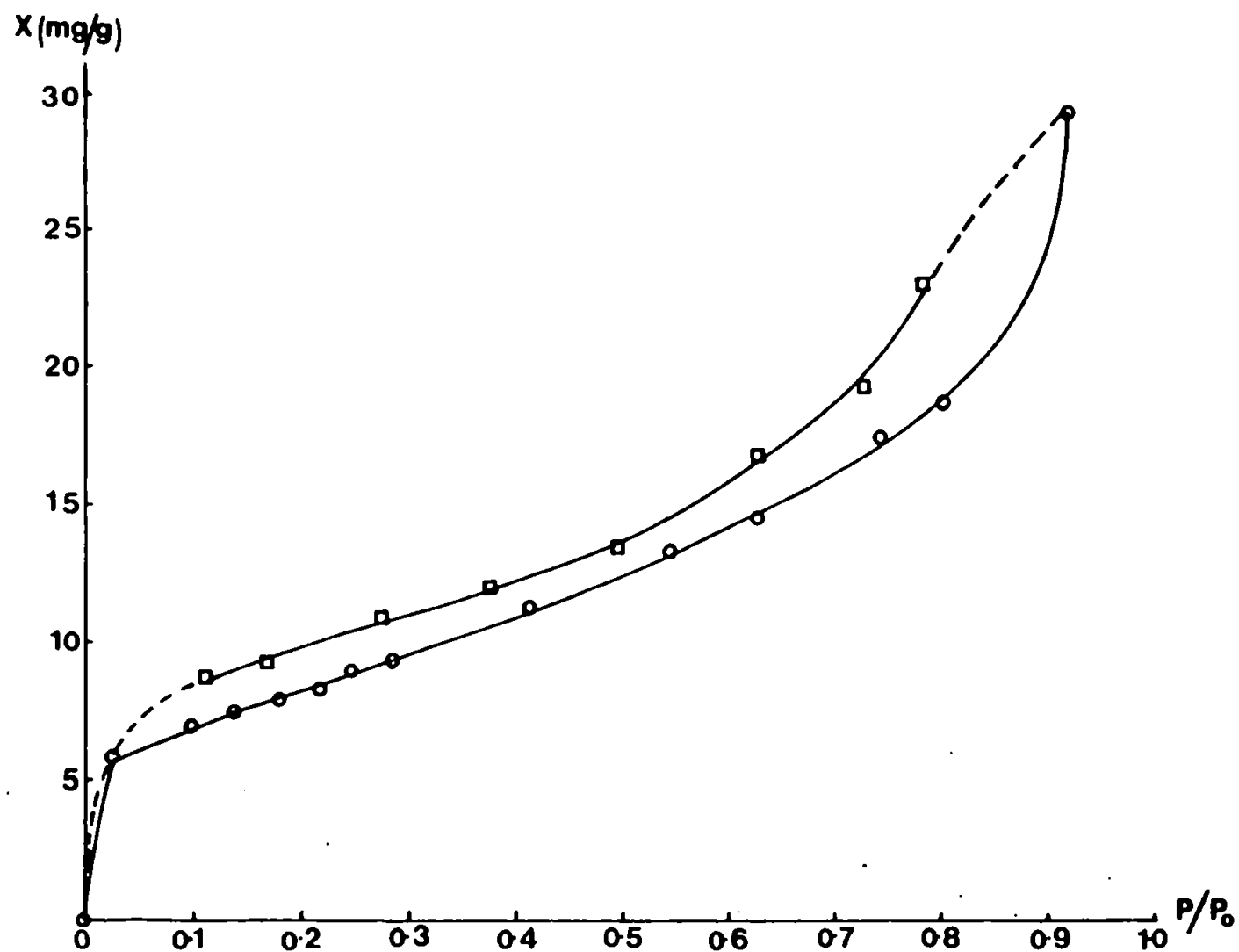


Figure 3.12. A nitrogen adsorption-desorption isotherm for a digested sample of Tamar suspended particles (cf. Figure 3.4). The surface area after digestion was $31.5\text{m}^2/\text{g}$. ○ Adsorption □ Desorption

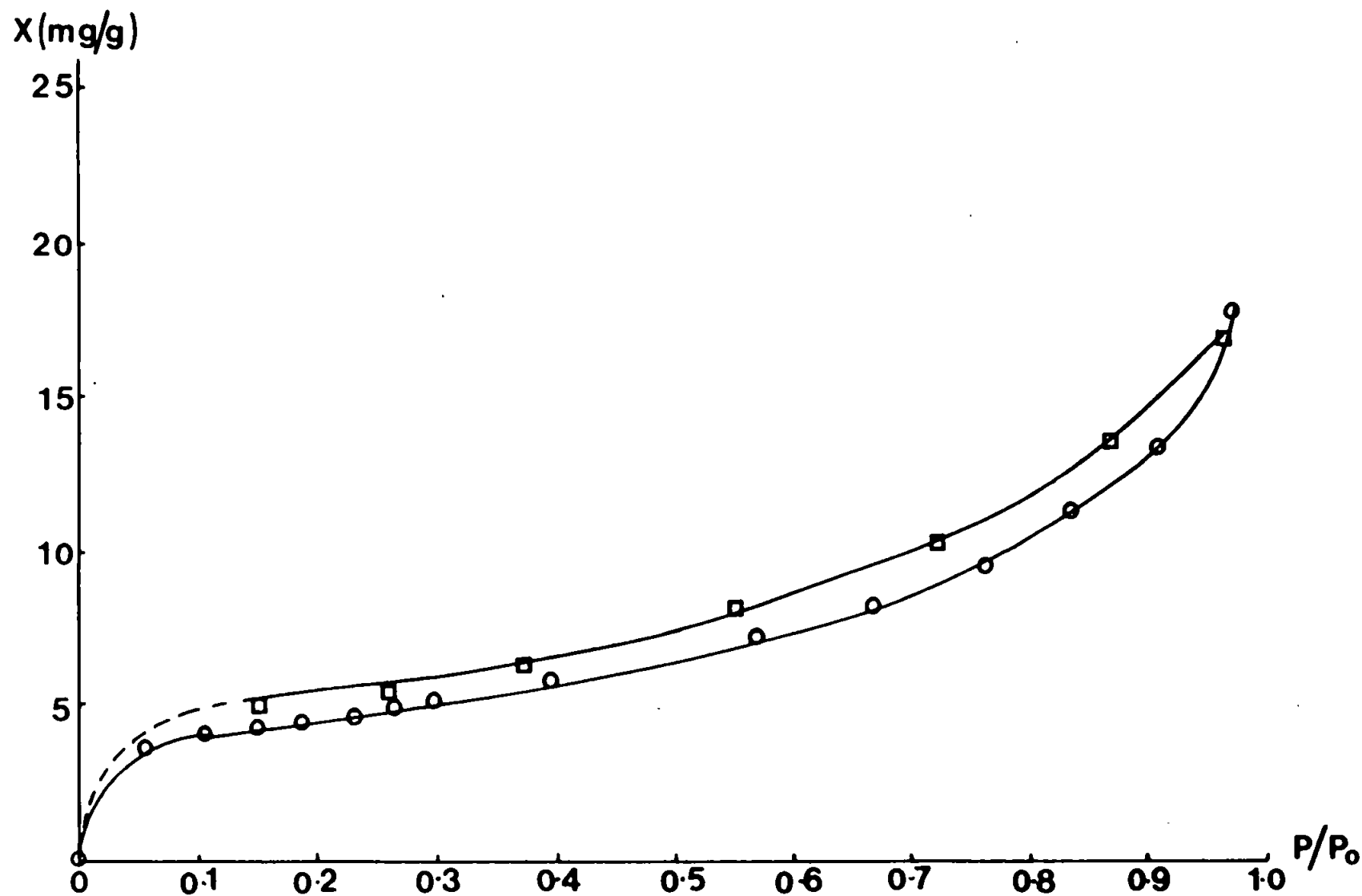


Figure 3.13. A nitrogen adsorption-desorption isotherm for an untreated suspended Tamar sample of surface area $14.0\text{m}^2/\text{g}$ (cf. Figures 3.14 and 3.17). \circ Adsorption \square Desorption

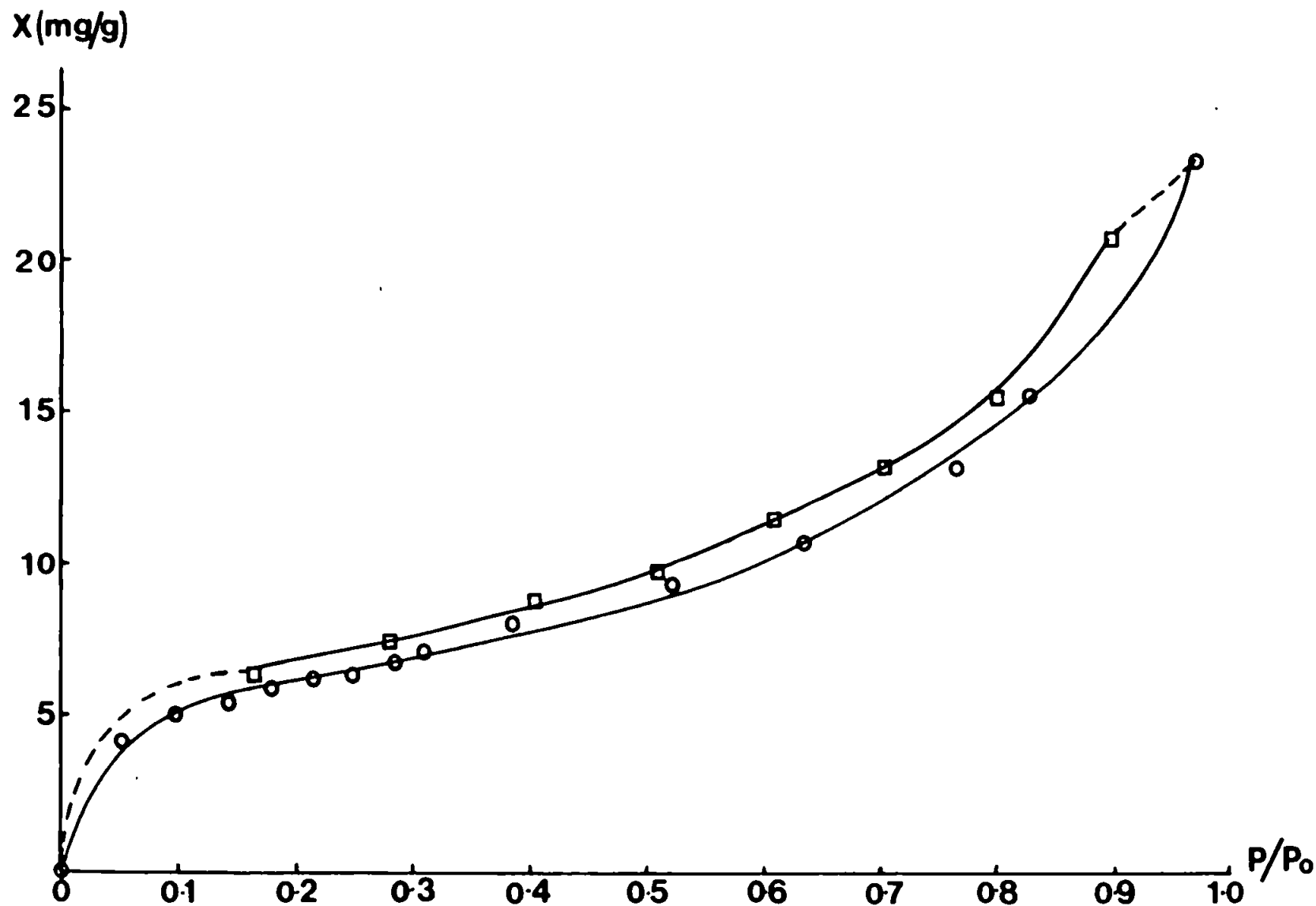


Figure 3.14. A nitrogen adsorption-desorption isotherm for a digested sample of Tamar suspended particles (cf. Figures 3.13 and 3.17). The surface area after digestion was $17.7\text{m}^2/\text{g}$. \circ Adsorption
 \square Desorption

<u>Salinity</u>	<u>Surface area</u>	<u>% Carbon</u>	<u>C/N</u>
(‰)	(m ² /g)		
28.5	8.4	6.7	12.1
22.5	10.7	6.4	13.2
9.7	14.0	6.6	12.3
5.0	17.2	6.4	13.3
3.1	18.0	6.4	12.3
2.2	19.8	6.9	13.1
0.15	17.8	6.0	11.9
0.09	14.6	6.6	12.2
0.06	13.9	7.1	12.1

Table 3.12a. Surface areas, carbon content and carbon/nitrogen ratio of the suspended samples collected on the 29-10-85 from the Tamar Estuary.

<u>Salinity</u>	<u>Surface area</u>	<u>% Carbon</u>	<u>C/N</u>
(‰)	(m ² /g)		
19.0	14.2	6.2	4.8
13.5	12.0	5.2	6.8
8.2	13.3	5.1	5.6
4.7	15.1	4.5	6.2
2.6	16.7	5.2	6.2
0.9	15.8	4.7	6.2
<0.5	15.2	4.9	6.6

Table 3.12b. Surface areas, carbon content and carbon/nitrogen ratio of the suspended samples collected on the 18-9-86 from the Tamar Estuary.

between the carbon content or C/N ratio and surface area for either survey. The trend between carbon content and turbidity in the present work is not in complete agreement with the results of Morris et al. (1982b) as shown in Figure 3.15. However, there may be seasonal variability in the organic content and more than one survey is required to show this temporal effect. The dissolved and colloidal organic matter within the estuary may change its composition according to season and this in turn may affect the composition of the organic material associated with the particles. For aquatic planktonic material the C/N ratio would be expected to be 6.63 (Stumm and Morgan, 1981). This is applicable to the 18-9-86 survey when presumably planktonic activity would be prevalent and contributing carbon to nitrogen in the ratio 6.63. In comparison, the 29-10-85 data has a C/N ratio of around 13 which would be more akin to terrestrial plant fragments with a low protein content and a high carbohydrate content (McLusky, 1981). Seasonal changes in carbon content have been shown in the colloidal material from the Patuxent Estuary and this is attributed to a high in situ biological activity in the summer (Sigleo and Helz, 1981). Organic material on the surface of particles has been shown to control the uptake of some trace metals and different types of organic materials may interact in different ways (Davis and Leckie, 1978b; Davis, 1984).

The samples from the 29-10-85 survey of the Tamar Estuary were digested and their surface areas remeasured. The surface areas for the digested material (shown in Figure 3.16) are higher than the undigested material and all the digested samples have the same surface areas within analytical reproducibility (mean surface area =

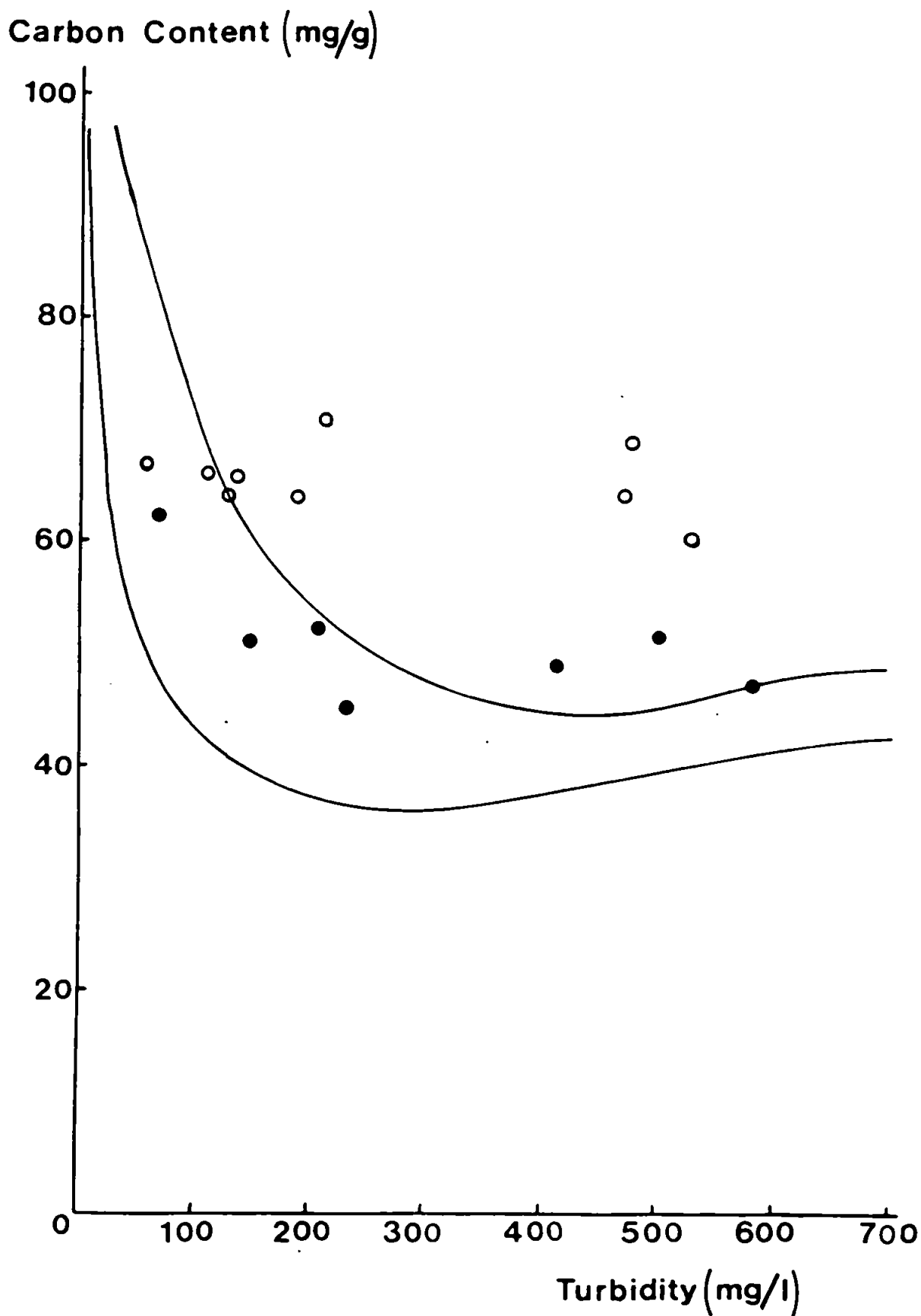


Figure 3.15. A plot of total carbon content versus turbidity for the 29-10-85 survey (open symbols) and for the 18-9-86 survey (closed symbols). Also included is the range of the data from a survey carried out by Morris *et al.* (1982b) on the 27/28-8-80. (==).

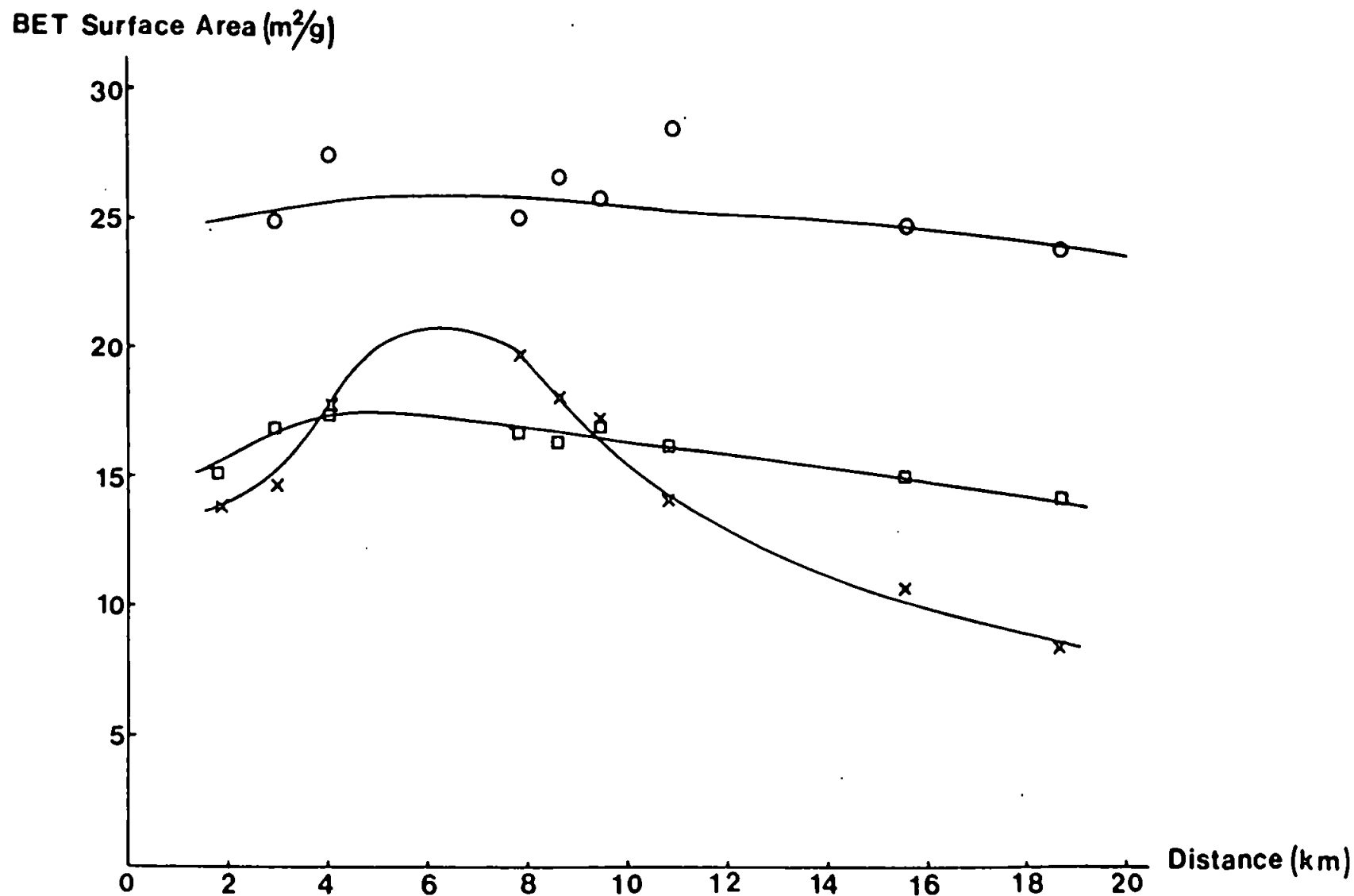


Figure 3.16. A plot of BET surface area for untreated, hydrogen peroxide digested and acetic acid/hydroxylamine hydrochloride leached suspended Tamar particles versus distance down estuary. \times Untreated \circ Digested \square Leached.

25.8m²/g ± 5.8%) irrespective of the initial surface area (Titley et al., 1987). This suggests as before that organic material is blocking the pores of the sample and its removal has revealed additional internal surface of the particles. An equivalent series of samples from the Gironde Estuary has shown a similar increase to a uniform surface area after hydrogen peroxide digestion (Martin et al., 1986).

The samples from the Tamar Estuary have an almost constant carbon content for each survey from the freshwater just beyond the turbidity maximum to a salinity >20‰. In the Gironde where sampling was carried out from the seawater to 100km upstream of the fresh water brackish water interface, a correlation between surface area and carbon content can be seen. This has also been interpreted as organic matter blocking some surface sites on the particles (Martin et al., 1986). It is possible that the macropores which are revealed on digestion of the particles are the internal structures of Fe and Mn oxyhydroxides and this is investigated in the following section.

3.2.3. The Influence of Fe and Mn Oxyhydroxide Surface Coatings on the Characteristics of Particles.

It has long been established that colloidal Fe oxyhydroxides flocculate during the mixing of river and sea waters (Boyle et al., 1977; Mayer, 1982; Fox and Wofsy, 1983; Li et al., 1984) and there is evidence that they may form coatings on natural estuarine particles (Aston and Chester, 1973; Gibbs, 1973; Anderson et al., 1984; Eastman and Church, 1984). Work by Crosby et al. (1983) and Marsh et al.

(1984) has shown that Fe oxyhydroxides flocculated from natural waters have very large surface areas and porosities but the effect that these oxyhydroxides may have on the physical surface characteristics of natural particles has been little examined. This effect may be instrumental in controlling the surface sorption processes within estuaries (Martin et al., 1986).

An acetic acid/hydroxylamine hydrochloride mix (Tessier et al., 1980) was used at pH = 3 to remove surface Fe and Mn oxyhydroxides from natural particles collected during the survey of 29-10-85 (see Section 2.2.4). The results in Table 3.13 show the amount of Fe and Mn leached and the surface areas before and after leaching. Neither the amount of Fe nor of Mn leached show any relationship to the surface areas found in the untreated samples. However it is interesting to note that the leached samples of particles all have the same surface area within analytical reproducibility (mean surface area = $16.3\text{m}^2/\text{g} \pm 8\%$), and that this surface area is lower than that determined before treatment for the majority of the samples (Titley et al., 1987). This surface area is also far lower than that seen for the hydrogen peroxide digested particles ($25.8\text{m}^2/\text{g}$) (see Section 3.2.2). The leached surface areas are shown for comparison in Figure 3.16 with the digested and untreated surface areas. It could be concluded that the surface area of the leached material is the surface area of the underlying lithogenous material.

Martin et al. (1986) found a relationship similar to this on removal of amorphous oxide coatings with NaOH and Na-dithionite as the surface area (BET argon adsorption) decreased to a uniform level of

<u>Salinity</u> (‰)	<u>Leached Fe</u> (mg/g)	<u>Leached Mn</u> (mg/g)	<u>Surface area</u> (m ² /g)	
			<u>Natural</u>	<u>Leached</u>
28.5	9.92	0.62	8.4	14.2
22.5	7.09	0.49	10.7	15.0
9.7	7.98	0.54	14.0	16.2
5.0	7.00	0.48	17.2	17.3
3.1	6.52	0.50	18.0	16.3
2.2	6.55	0.52	19.8	16.8
0.15	7.47	0.44	17.8	18.7
0.09	7.11	0.55	14.6	16.9
0.06	7.25	0.74	13.9	15.0

Table 3.13. The quantities of Fe and Mn leached by an acetic acid/hydroxylamine hydrochloride leach for the 29-10-85 samples. The mean surface area for the leached samples is $16.3 \pm 1.4 \text{ m}^2/\text{g}$.

about $10 \text{ m}^2/\text{g}$. They conclude from this and other experiments that there is a near uniform coating of amorphous oxides on the surface of the particles. Work by Torres Sanchez et al. (1985) indicates that Fe oxyhydroxides precipitated onto the surface of kaolinite form small evenly dispersed particles with a surface area of $>150 \text{ m}^2/\text{g}$. This idea is in good agreement with the present results which show that after acetic acid/hydroxylamine hydrochloride leaching the carbon content in the sample was only slightly decreased from an average of 6.6% to an average of 5.0%. This decrease may be due to flocs comprising Fe oxides and organic material being released into solution

by the leaching agents (Perdue et al., 1976) but indicates that the majority of the carbon is either still present on the surface of the particles thus blocking the pores or incorporated in the sample as pure organic particles.

The hysteresis curve for acetic acid/hydroxylamine hydrochloride leached particles shown in Figure 3.17 is very similar to that seen for the untreated particles (Figure 3.13) as there is no high pressure hysteresis and thus no macropores accessible to nitrogen gas. This affirms the idea that organic matter on the surface modifies the gas adsorption properties of the samples. If the residual organic matter in the sample after acetic acid/hydroxylamine hydrochloride leaching was due to purely organic particles, the surface organic matter all being removed, it would be expected that the hysteresis curve would be similar to that seen for the peroxide digested particles as humic material has a very low surface area ($<1\text{m}^2/\text{g}$) and porosity. However, since this is not the case it may be concluded that the surface area and porosity seen for the leached particles is that of the particles with part or all of the organic surface coatings but without the hydrous Fe and Mn oxides which were present in an easily leachable form.

An EDTA leach (pH = 7) (Aggett and Roberts, 1986) was used on the samples from 18-9-86 (see Section 2.2.4) to see if this would remove a different fraction of fresh and aged Fe and Mn hydroxides compared to the acetic acid/hydroxylamine hydrochloride leach. However as shown in Table 3.14 a very similar amount of Fe was leached when compared to the 29-10-85 dataset but there was consistently less Mn removed. This suggests that the leaches were not removing

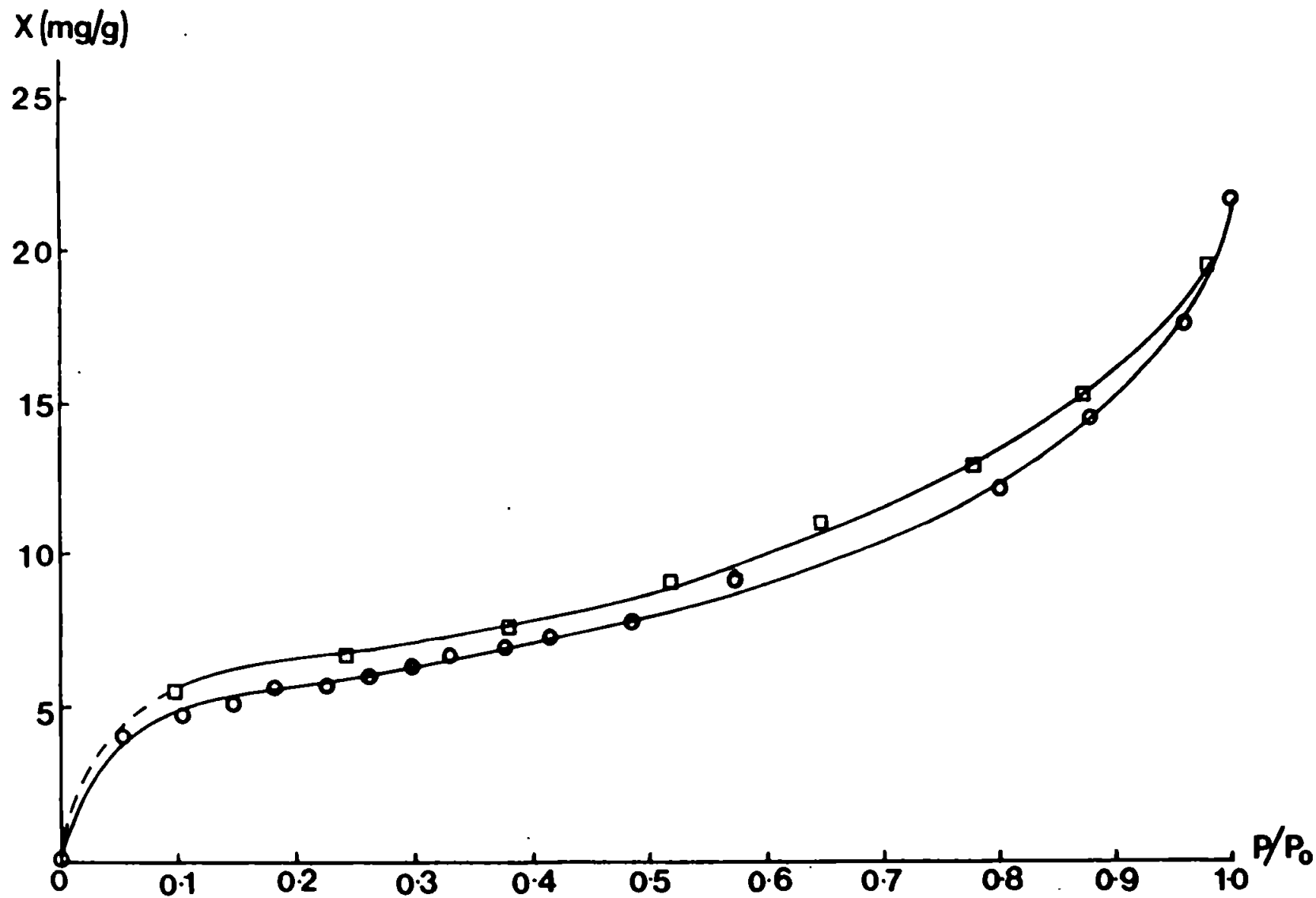


Figure 3.17. A nitrogen adsorption-desorption isotherm for an acetic acid/hydroxylamine hydrochloride leached sample of Tamar suspended particles for which the surface area is $16.7\text{m}^2/\text{g}$. (cf. Figures 3.13 and 3.14). \circ Adsorption \square Desorption

significantly different fractions of fresh and aged Fe oxides. The surface areas after leaching were again found to decrease to a constant level (mean surface area = $10.2\text{m}^2/\text{g} \pm 9.8\%$) which although lower than was seen for the 29-10-85 survey ($16.3\text{m}^2/\text{g}$) indicates the same trend.

The surface areas of the untreated particles from the 29-10-85 survey were more variable and in general higher than those seen

<u>Salinity</u> (‰)	<u>Turbidity</u> (mg/L)	<u>Leached Fe</u> (mg/g)	<u>Leached Mn</u> (mg/g)	<u>Surface area</u> (m^2/g)	
				<u>Natural</u>	<u>Leached</u>
19.0	70	9.85	0.31	14.2	10.5
13.5	210	5.96	0.37	12.0	9.1
8.2	150	7.16	0.32	13.3	9.9
4.7	235	6.42	0.29	15.1	10.7
2.6	500	6.35	0.37	16.7	10.7
0.9	580	6.45	0.33	15.8	11.7
<0.5	410	6.01	0.41	15.2	8.8

Table 3.14: The amounts of Fe and Mn removed by an EDTA leach on the samples from the 18-9-86 survey. Also shown are the surface areas measured before and after the leaching. The mean surface areas are for the natural samples $14.6 \pm 1.6\text{m}^2/\text{g}$ and for the leached samples $10.2 \pm 1.0\text{m}^2/\text{g}$.

for the 18-9-86 survey. The possibility that this was due to the increased amount of leachable Mn in the 29-10-85 survey was

investigated. Using the surface area value for amorphous MnO_2 determined in this work ($400\text{m}^2/\text{g}$) it can be calculated that 20mg Mn/g solid would be required to increase the surface area of the solid by $8\text{m}^2/\text{g}$. Approximately 0.5mg Mn/g solid was leached and this in conjunction with the observation that a similar amount of Mn was leached from all samples of the 29-10-85 survey (surface areas 8.4 - $19.8\text{m}^2/\text{g}$) leads to the conclusion that it is improbable that amorphous Mn oxides are the key factor determining surface area.

To try to elucidate the reasons for the different surface areas for the two surveys before leaching the conditions during the surveys in Table 3.7 were examined. Both surveys were run on a rising spring tide and for both surveys the rainfall in the two weeks previous to the survey was negligible. The turbidities for each survey were very similar. The only characteristics which have been identified as varying are the pH and temperature of the estuarine water and of these two characteristics the temperature is the most obviously different (3°C).

Work by Marsh et al. (1984) has shown that two synthetic materials precipitated in similar conditions but at different temperatures (2°C and 15°C) from Fe(II) have given very different surface areas. The one precipitated from a solution at 2°C had a surface area of $299\text{m}^2/\text{g}$ while that precipitated at 15°C had a surface area of $121\text{m}^2/\text{g}$. It is therefore possible that the difference in temperature may have influenced the surface areas of the particles from the two surveys. The high temperature for the 18-9-86 survey may have caused the samples to have a lower surface area while the low temperatures prevailing during the 29-10-85 survey would be

the reason for the samples having a generally higher surface area. This is a possible explanation of why although samples from the two surveys have different surface areas a similar amount of Fe was leached. It infers that the amorphous Fe and Mn oxides are present in the similar concentrations but in different states of crystallinity.

A second reason for the differences between the two surveys may be related to the C/N ratio. It may be that particular types of organic material will have a distinct effect on the BET surface area of the particles perhaps due to some type of specific site binding. However it has not been possible to investigate this any further.

It is more difficult to explain why the same amount of Fe is leached from samples of one survey although they all may have different surface areas. As previously discussed when Fe oxyhydroxides age they lose surface area (Bye and Sing, 1972; Crosby et al., 1983) and it is possible that this variation in surface area is due to the different age of the material. Using values from the work of Crosby et al. (1983) it would be necessary for approximately 50mg of new iron to be present in 1g of sample if the surface area was to be increased by $10\text{m}^2/\text{g}$. This is a far higher amount than was removed from any of the samples by either leaching agent. The conclusion which is drawn from this study is that during initial stages of ageing the amorphous Fe and Mn oxyhydroxides in the particles will age but remain only weakly associated (extractable) with the particles throughout the estuary. Therefore the same amount of flocculated Fe and Mn oxyhydroxide coating will be present and available for leaching from the suspended particles but the surface area will differ. If this is the case then surface area may be the

only method available to distinguish between the freshly precipitated and aged Fe and Mn oxyhydroxides present on estuarine particles which may be instrumental in controlling the surface sorption processes.

3.3 Conclusions from Particle Characterisation Study.

Natural particles from the Tamar Estuary have been shown to comprise a complex mixture of quartz, kaolinite, muscovite, illite and chlorite with surface coatings of organic matter and Fe and Mn hydrous oxides. These particles have BET nitrogen adsorption surface areas ranging from $8\text{-}25\text{m}^2/\text{g}$. The suspended material has a higher surface area than the associated sediment material and the highest surface area for suspended material is in the low salinity region of the estuary.

An examination of the particle size of samples has shown no correlation between mean particle size and the BET surface area. The sizes measured are, if anything, too small, due to disaggregation on handling (Eisma et al., 1983; Bale et al., 1984) but these give geometric surface areas at least two orders of magnitude smaller than the BET adsorption areas. Nitrogen adsorption-desorption experiments on the natural samples indicated micro- and meso-pores to be present and this could be in the form of cylindrical pores, slit shaped pores, spaces in between particles joined as aggregates or a combination of these with ink-bottle pores (Rohrbaugh, 1980; Sing, 1976).

All the particles from the Tamar contained approximately 6% carbon and removal of these surface coatings gave an increase in the surface areas. For one axial traverse all the suspended samples increased in surface area to $25.8 \pm 1.5\text{m}^2/\text{g}$ after oxidative digestion regardless of the initial value and hysteresis analysis showed macropores to be revealed on digestion. This has been interpreted as the opening of pores previously blocked by the coating of organic matter, which has a low surface area ($<1\text{m}^2/\text{g}$).

Fe and Mn oxyhydroxide coatings were removed from the particles by leaching. Approximately the same amount of Fe was removed from all samples even when using two types of leaching solution on samples of very different surface areas. No correlation between surface area and leached Fe or leached Mn could be found. After leaching the particles have a constant low surface area for each survey but this area was different for each of the two estuarine traverses carried out. This suggests that Fe oxyhydroxides increase the surface area of the underlying lithogenous material as would be expected considering the large surface areas found for precipitated hydrous Fe oxides from natural solutions (Crosby et al., 1983; Marsh et al., 1984). Temperature was the most easily identifiable difference between the two surveys and it is suggested that this may have altered the characteristics of the flocculated solid and thus explain the difference between the surface areas of the two surveys (29-10-85 and 18-9-86) although it is possible that the composition of the organic material also has an effect.

Organic material and hydrous Fe oxides have long been considered to be present on the surface of natural particles and this study has shown that they are instrumental in controlling the surface area available for nitrogen gas adsorption. The organic matter appears to block off pores (particularly macropores) in the surface of the particles which can only be revealed by oxidative digestion. The hydrous Fe and Mn oxides are dispersed over the particles and confer a larger surface area on the particle matrix. Since no correlation can be found with organic content or with leached Fe oxyhydroxides it is the conclusion of this study that surface area determination may be

the only way to identify a large, possibly active, surface area in natural particles.

A study of the effects these coatings have on the heterogeneous chemical reactivity of the particles with dissolved constituents is urgently required (Lion et al., 1982). Many studies have reported that adsorption involves a two stage reaction - an initial kinetically fast reaction followed by a slower diffusion controlled step during which the ions may tunnel into the pore spaces in the solid (Barrow, 1983; Nyffeler et al., 1984; Bolan et al., 1985; Theis and Kaul, 1985).

The adsorption of phosphate has been most widely examined. Crosby et al. (1984) reported contrasting behaviour with regard to uptake of phosphate onto precipitated Fe oxyhydroxides. They found that the short term (2h) uptake behaviour in simulated natural conditions varied depending on the oxidation state of the Fe before precipitation and on the age of the precipitate. The age and initial oxidation state of Fe have also been shown to have significant effects on the porosity and surface area of the precipitates (Crosby et al., 1983). Anderson et al. (1985) also report the bulk and surface properties of Al/Fe hydroxides to be related to their chemical history.

Hansmann et al. (1985) have shown that the uptake of phosphate onto colloidal goethite causes bridging between particles. This affects the reaction site availability and the rate of disaggregation shows hysteresis depending on the initial extent of phosphate adsorption. Lijklema (1980) has observed hysteresis when studying the pH dependence of phosphate adsorption onto different ages

of amorphous Fe and Al oxides. Other workers have reported the penetration or tunneling of phosphate into the interior of soils (Barrow, 1983) and Fe and Al hydroxides (Bolan et al., 1985). Cabrera et al. (1981) have found that for lepidocrocite and goethite the relative amounts desorbed can be related to the quantity of micropores within the particulate phase. The adsorption and desorption of phosphate from lepidocrocite and haematite has also been related to the porous nature of the solids by Madrid and De Arambarri (1985). They explained the differing rates of sorption reactions in terms of the shape of mesopores within the solid. These results show the importance of the nature of the adsorbent when discussing the adsorption of phosphate to oxide surfaces.

Little work has been carried out to attempt to relate the porosity of complex natural materials to the sorption behaviour of trace metal ions. Natural Tamar suspended solids have been shown in this study to have slit shaped pores in the size range $<2-50\text{nm}$. Pores of $<2\text{nm}$ are typically found in clay minerals between lattice layers. The clays found in the Tamar samples were of the non-expanding type which have a fixed inter-layer spacing of 0.72nm for kaolinite and approximately 1nm for illites. Kaolinite will not, in a perfect crystal, allow water between the layers but defects will be found within the structure giving areas into which diffusion may occur. Within illites, the weathering products of muscovite, there is no swelling of the clay but water does permeate the interlamellar spaces (Van Olphen, 1976). Therefore the small ($<2\text{nm}$) slit-like pores seen associated with the dried Tamar samples will in situ be filled with water and diffusion of trace metals may occur. The layer spaces of

illites are reported to be large enough to accommodate the diffusion of K ions into the lattice (Van Olphen, 1976). These K ions have a Pauling crystal diameter of 0.27nm, compared to 0.18nm for Zn and 0.20nm for Cu ions (Millero, 1969). Thus, the possibility exists that these trace metal ions could diffuse into the interlamellar spaces of the clay matrix.

Montmorillonite, an expanding clay has been reported as showing low pressure gas adsorption hysteresis due to intercalation of small polar molecules (Sing, 1976). It has also been shown to intercalate organic molecules within the interlamellar spaces and may be used for catalytic processes (Breen et al., 1985; Yasunaga and Ikeda, 1985). Therefore it may also be expected that the non-expanding clays which have water in the network due to defects or a large layer spacing may be able to adsorb and intercalate trace metal ions as shown diagrammatically in Figure 3.18a.

In soils weathered clay lamellae may aggregate with either face-face or edge-face interactions as shown in Figure 3.18b. Domains, built up with face-face interactions, from illitic clays have been shown to have pores mainly in the range 0.5-10nm with a dominant peak of pore size at about 3.5nm (Quirk, 1978). These are built up, overcoming electrostatic repulsion, during successive wetting and drying, freezing and thawing cycles within the soil (Rimmer, 1987) and it may be that these are carried into the estuarine zone. Edge-face interactions will result in structures of the "cardhouse" or "pin-cushion" types. These involve energetically favourable interactions of clay platelets and will give rise to a large internal volume (Williams and James, 1978).

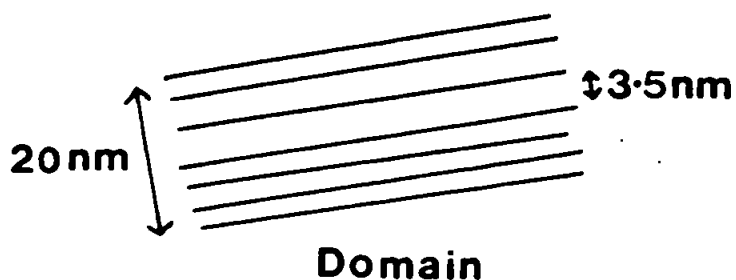
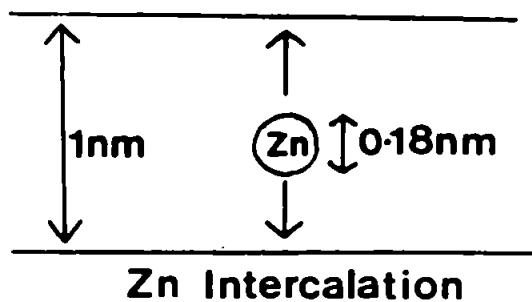


Figure 3.18a. An example of Zn intercalation between parallel plates within an aluminosilicate clay matrix and some likely dimensions of a domain formed from weathered clay platelets.

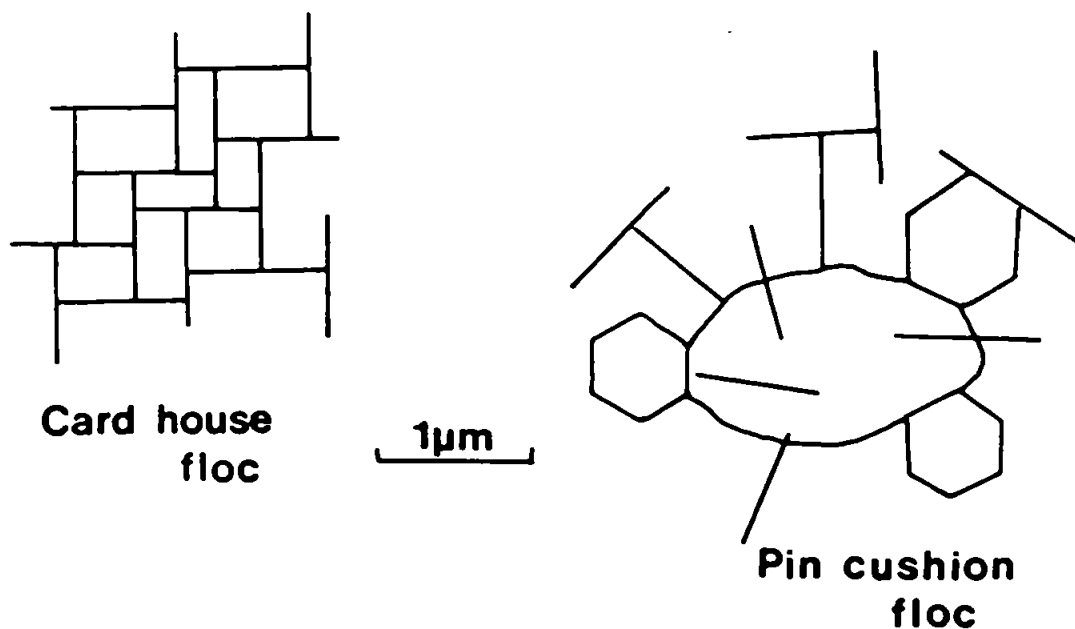


Figure 3.18b. A schematic representation of a cardhouse floc consisting of kaolinite edge-face interactions and of a pincushion floc consisting of a central quartz grain which interacts with the edge of the kaolinite platelets.

Diffusion into pore spaces such as these, before adsorption can take place, will be slow and this process may be the cause of the secondary slow reaction often observed in adsorption experiments (Li et al., 1984a). Once the ions have diffused into these pores their adsorption may be influenced by additional bonding to other nearby surfaces across narrow areas of the pores (see for example the "card-house" structure, Figure 18b). These intercalated ions will then be less likely to desorb as the solution conditions change. This behaviour may explain the observations of slow desorption of phosphate from soils (Barrow, 1983) and from Fe oxides (Cabrera et al., 1981; Madrid and De Arambarri, 1985) as the ions could be firmly held by these multiple bonds.

Therefore, it is possible that slow sorption reactions may be attributed to both penetration of the porous network (from which it is difficult to diffuse) and intercalation across narrow porous structures. However there is no information on these effects with regard to natural particles and solutions. In the following chapter it is shown that the sorption of trace metal ions on the surface and within the porous structures of natural estuarine particles can be examined and related to the information about the surface characteristics gained in this chapter. Information on the controls of surface sorption reactions is of great importance if an understanding of these heterogeneous processes is to be developed.

CHAPTER FOUR

THE SORPTION BEHAVIOUR OF Zn AND Cu IN ESTUARINE MEDIA.

The discussion of particle characteristics in Chapter 3 suggested that the porosities as well as surface areas could play a role in the sorption behaviour of trace metals. Thus, the central objectives of the sorption experiments carried out in this work were to examine the relationship between the particles and the removal of Zn and Cu from solution as well as providing quantitative information on the rates of these reactions. Essential kinetic data for estuarine systems is extremely sparse in the literature as it is restricted to studies of Mn (Morris and Bale, 1979; Morris et al., 1981). This study represents the first attempt to provide rate constants for sorption processes involving the uptake of Zn and Cu onto estuarine particles.

At the beginning of this work it was decided to undertake the experiments as close to natural conditions as possible. This meant that a method for the rapid analysis of many samples had to be developed, to enable a detailed study of the uptake process. Hence the multi-channel micro-Chelex method (see Chapter 2) was developed which, apart from the recent developments of Flow Injection Analysis-Atomic Absorption Spectrophotometry (Olsen et al., 1983), is the only procedure available for processing samples on a short enough timescale for kinetic studies. Developments of this type are important because one of the drawbacks of the sorption studies (involving added radio-tracers) carried out by Nyffeler et al. (1984) is that they attempt

kinetic analysis on only 4-6 data points covering up to 50 days. The small dataset produced by these workers has obvious limitations, especially when applying it to partially mixed estuaries like the Tamar with flushing times in the range 5-10 days (Uncles et al., 1983a). Clearly there is a need to examine the short- and long-term sorption behaviour on timescales comparable to those seen in estuaries (minutes-days).

In all experiments shown in the following sections the filtered river waters contained trace metals present as natural dissolved species at natural concentrations. The well characterised particles were from the turbidity maximum of the Tamar Estuary and they represent a particle population which river water would encounter in the high turbidity mixing zone. Furthermore, in order that some comparison could be made with field observations the experimental conditions selected were similar to those encountered in field work by Ackroyd et al. (1986). In keeping with this work the dissolved metal analyses were determined on the Chelex extractable fraction (Florence, 1977).

4.1. Sorption of Metals in Tamar Estuary Waters.

Firstly, control runs on filtered river water were carried out to ascertain the uptake onto the walls of the containers (see for example Figure 2.11). This showed, in all cases, that over a period of several days the loss to the walls for both Cu and Zn was <10% of the dissolved metal.

At the start of the particle/water mixing studies four preliminary experiments were carried out in order to determine the expected concentration ranges and to verify the preparative and analytical procedures. These involved following the concentrations of Zn and Cu in 10 litre samples of untreated estuarine water, collected from the turbidity maximum region of the Tamar Estuary. The samples were continuously mixed and aliquots of suspension withdrawn over a 40 hour period. The starting conditions of these experiments are shown in Table 4.1 and they show similar features to those described in this work and by Ackroyd et al. (1986). There was a weak turbidity maximum at very low salinity which contained suspended particles with the highest surface areas. The dissolved metal concentrations were highest in the freshwater samples and decreased as the salinity increased to 2‰. For both Zn and Cu there was an increase in the dissolved concentration at the highest salinity (5‰).

The time dependent behaviour of these samples is depicted in Figures 4.1 and 4.2. In general the results for Zn and Cu show the same trends. Results were also obtained for Pb and Cd which were in reasonable agreement with the Zn and Cu but as was discussed in Section 2.3.4 there was a large scatter on the data and so they are not reported here. In freshwater there was clear evidence of rapid

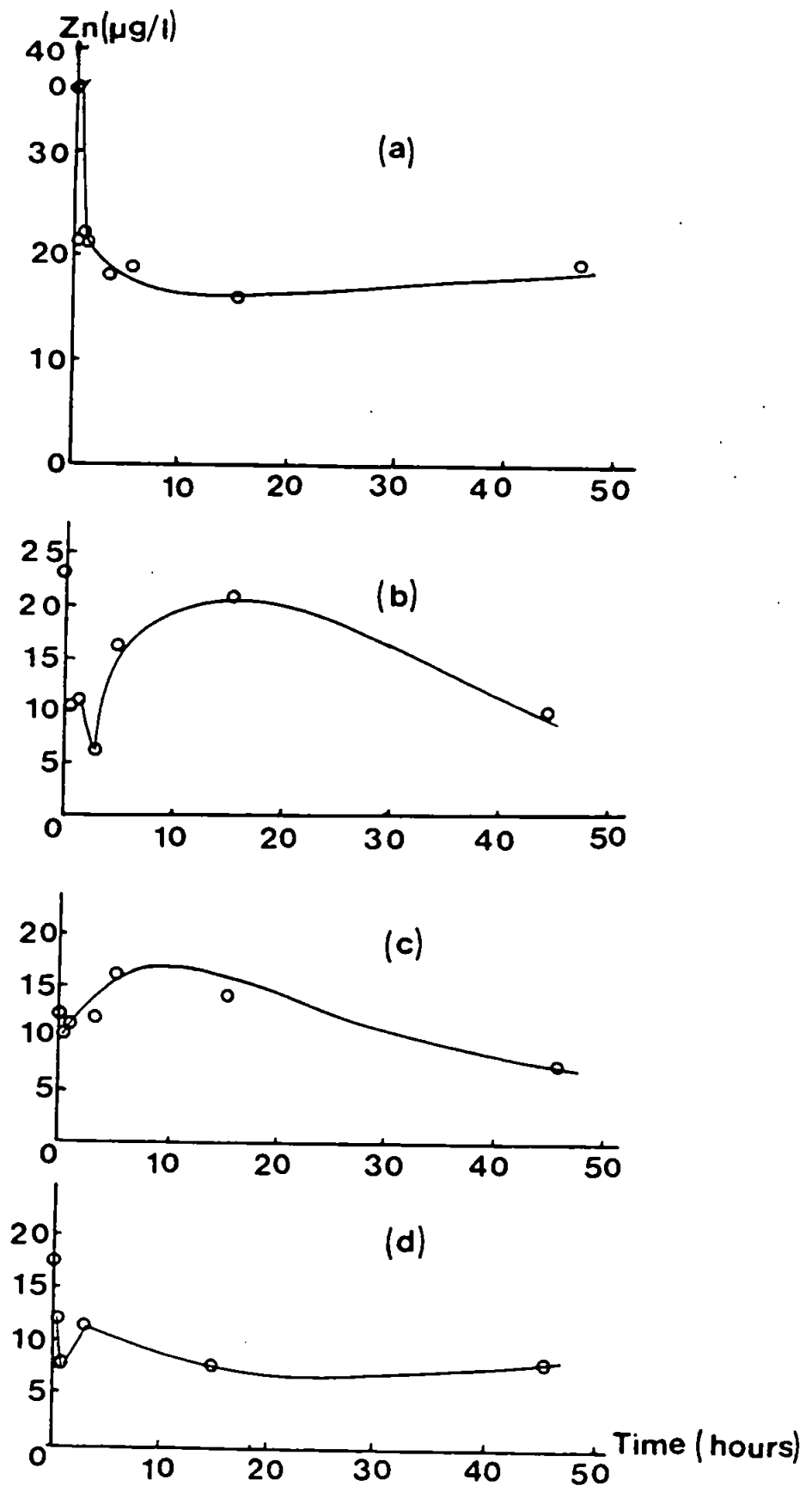


Figure 4.1. Time dependent behaviour of dissolved Zn in natural Tamar estuarine suspensions. (a) 0‰ (b) 0.5‰ (c) 2‰ (d) 5‰.

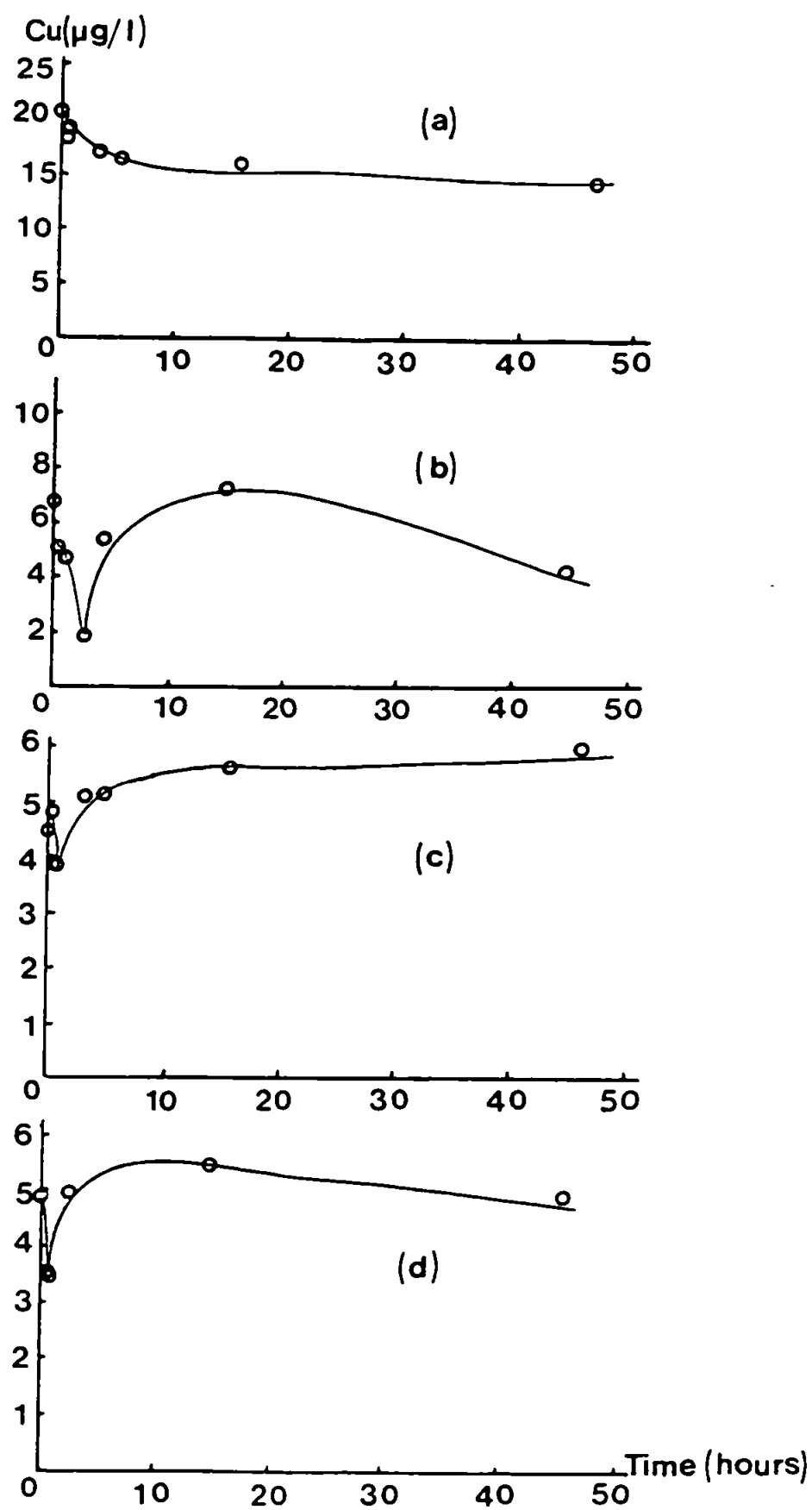


Figure 4.2. Time dependent behaviour of dissolved Cu in natural Tamar estuarine suspensions. (a) 0‰. (b) 0.5‰. (c) 2‰. (d) 5‰.

<u>Salinity</u> <u>(‰)</u>	<u>Turbidity</u> <u>(mg/L)</u>	<u>BET surface</u> <u>area (m²/g)</u>	<u>Initial metal</u> <u>concentrations (µg/L)</u>	
			<u>Zn</u>	<u>Cu</u>
0	50	10.3 ^a	36	21
0.5	180	23.0	23	7
2	70	16.5	12	4
5	40	11.5	17	5

Table 4.1. Characteristics of the samples from the Tamar Estuary used for the experiments shown in Figures 4.1 and 4.2.

^a Insufficient material for analysis; this value is representative of data obtained in other surveys.

uptake of the metals onto the particles over a period of 40h with about 50% of dissolved Zn and 30% of dissolved Cu being removed. At 0.5‰ uptake appeared to continue for the first 4h after which a desorption from the particles was evident. A similar trend was seen in the two higher salinity samples (2‰ and 5‰) but with greatly reduced magnitudes. The fact that some sorption behaviour was observed suggests that the particles were not at equilibrium with the dissolved phase when collected. This might be expected as in the upper estuary the physical timescales of mixing and advection are of the order of minutes or hours. Thus, these results are indicative of reactions which were continuing to equilibrium.

This time dependent behaviour also agrees with the results of Ackroyd et al. (1986) as they found that the highest metal removal was in the freshwater near the turbidity maximum and suggest that

desorption from the particles at higher salinities can explain the often observed mid-estuarine maxima in dissolved Zn and Cu.

Experiments by Campbell et al. (1985) with Mersey Estuary waters showed an increase in dissolved Cu, after storage for 25h, of 140% and 10% in low (<1‰) and high (22‰) salinity samples, respectively. While the desorption of Cu in the low salinity sample was far greater than was seen for this work, possibly due to large particulate pollutant inputs, it emphasises the high reactivity of low salinity estuarine samples. Laboratory mixing experiments (Van der Weijden et al., 1977; Li et al., 1984a) have confirmed that both Zn and Cu appear to desorb from particles when river and seawater are mixed. Field observations by Evans and Cutshall (1973) also reported that Zn desorbed from suspended solids in the Columbia River.

One further observation from these results is that the validity of some estuarine trace metal distributions could be in doubt when these are measured on filtered, preconcentrated bulk (>5L) samples. Generally up to 4hr may be required to filter the samples and these studies demonstrate that during this timescale there may be large changes occurring in the trace metal partitioning. Of particular interest to this study is the indication that both adsorption and desorption processes should be investigated in studies of heterogeneous chemical reactivity.

4.2. Mixing Experiments Using Tamar Water.

Several mixing experiments were carried out using portions of Tamar particles from the same bulk sample and different conditions of salinity and turbidity which were manipulated as discussed in Section 2.3. Data on the nature of the particle population are shown in Table 4.2. Using these particles for all the Tamar mixing experiments enabled the uptake behaviour of well-characterised particles to be examined under different conditions. The temperature was constant in all cases at 10°C.

	<u>Tamar Expts.</u>	<u>Carnon Expts.</u>
BET surface area (m ² /g)	14.0	13.1
Mean particle diameter (µm)	9.8	--
% Carbon	5.1	5.2
% Nitrogen	1.0	0.7
Leached by EDTA ^a		
Fe(µg/g)	6770	5690
Mn(µg/g)	390	380
Leached by Acetic mix ^a		
Fe(µg/g)	9100	7030
Mn(µg/g)	600	430
Zn(µg/g)	85	--
Cu(µg/g)	95	--

Table 4.2. The characteristics of suspended particles taken from the turbidity maximum of the Tamar Estuary for use in the mixing experiments with Tamar water (see Section 4.2) and Carnon water (see Section 4.3). The trace metal data is in agreement with previous surveys of the Tamar Estuary suspended particles by Morris et al. (1986). ^a Leached as discussed in Section 2.2.4.

4.2.1. Zn Behaviour.

The results of a freshwater and a brackish water adsorption experiment are shown in Figure 4.3. These were carried out using a turbidity of about 400mg/L. In the freshwater case there was a rapid uptake of 50% of dissolved Zn in the first 2h followed by a steady decrease in solution concentration with about 70% removal after 96h. The second set of results presented in Figure 4.3 are for salinity = 10‰ with a resultant increase in pH to 8.2. There was no discernible rapid initial uptake of Zn only a slow steady removal over the experiment duration (90h) of 30% of the dissolved Zn.

The conditions for the freshwater experiment in Figure 4.4 were basically the same as before except the turbidity was lower (200mg/L). This gave much the same kind of reaction curve with both the initial and final concentrations being similar. In the brackish water experiment where salinity = 1‰, again with a lower turbidity (200mg/L), the rate and extent of uptake was not as great. This run showed a relatively small (10%) uptake in the first hour and 50% uptake over the whole 90h period. This is 20% more uptake than was observed for the sample where the salinity was 10‰.

The results from the freshwater experiments were very similar and indicated that doubling the total available particle surface area had no noticeable effect on the adsorption of Zn. The results suggest that the particles and water were far removed from equilibrium when mixed but rapidly (<2h), via a kinetically fast reaction, reached a quasi-equilibrium state. True equilibrium was not apparently reached even by 90h, indicating a kinetically slow reaction. This slow approach to equilibrium was also observed by Li et al. (1984a) and

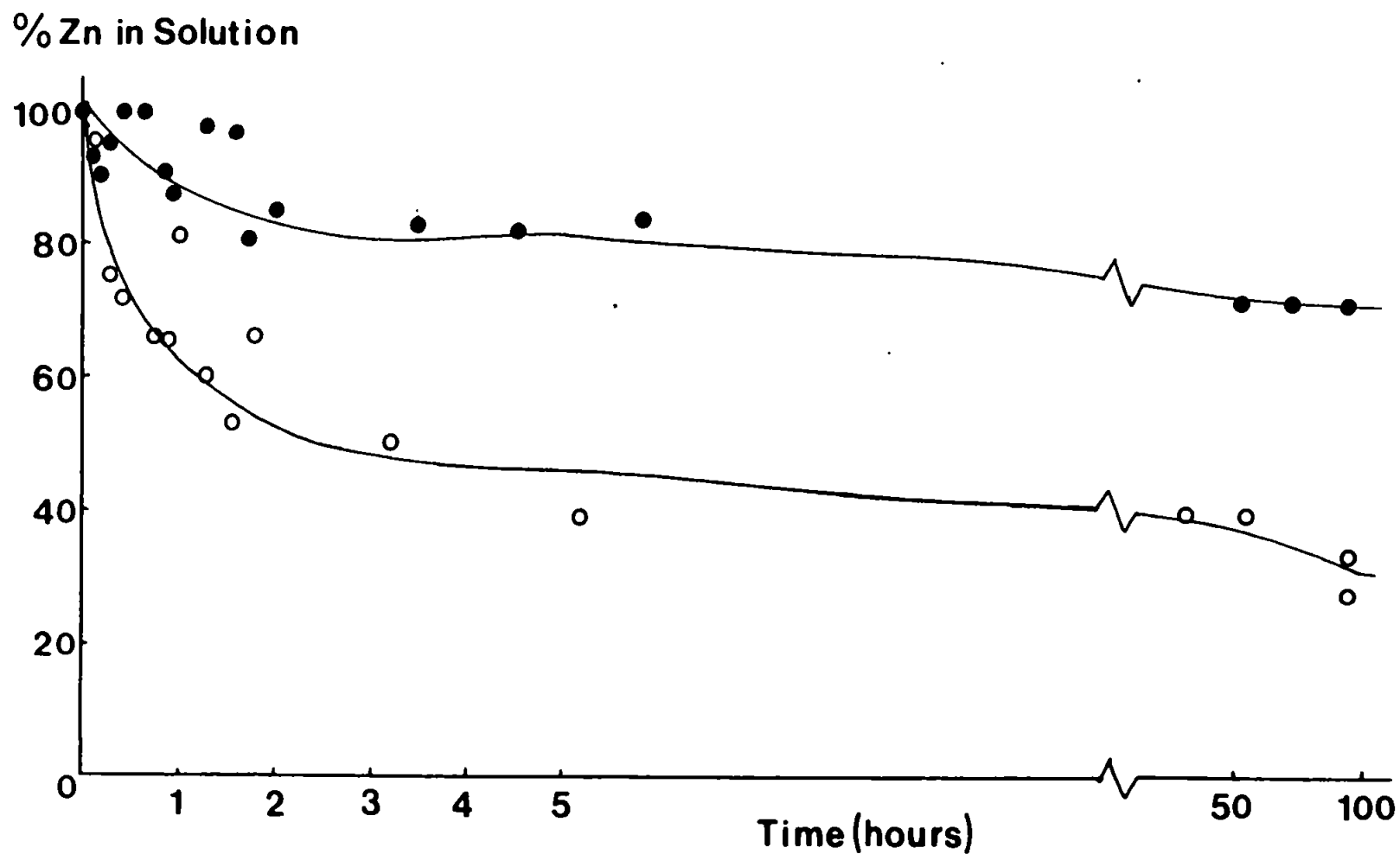


Figure 4.3. The percentage Zn remaining in solution versus time for two Tamar water suspensions with a turbidity of 400mg/L.

- Salinity = 0‰, pH = 7.5, 100% [Zn] = 14.5µg/L.
- Salinity = 10‰, pH = 8.2, 100% [Zn] = 15.0µg/L.

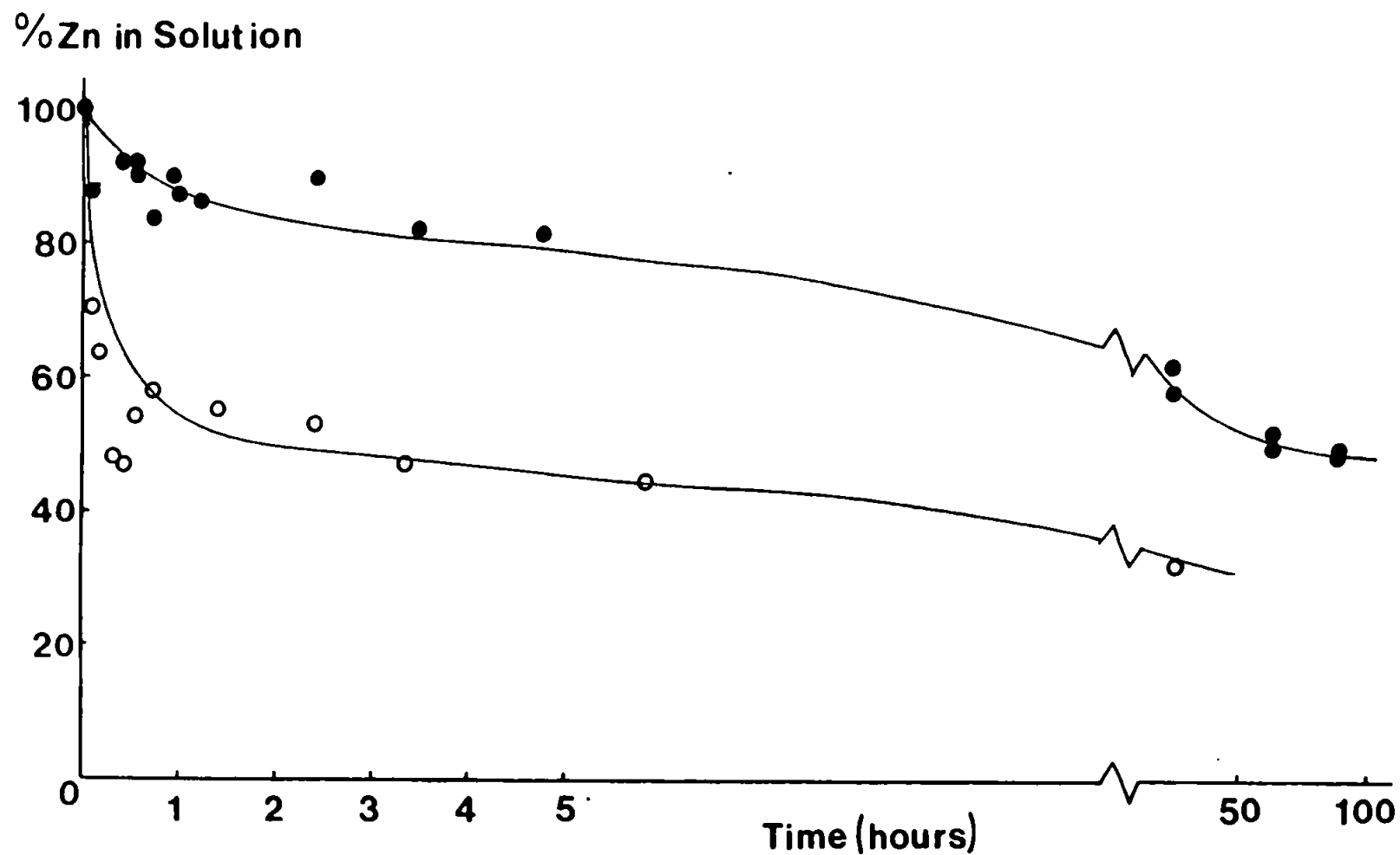


Figure 4.4. The percentage Zn remaining in solution versus time for two Tamar water suspensions with a turbidity of 200mg/L.

- Salinity = 0‰, pH = 7.5, 100% [Zn] = 13.7μg/L.
- Salinity = 1‰, pH = 8.2, 100% [Zn] = 16.0μg/L.

Nyffeler et al. (1984) who showed, by following the K_d values, rapid initial changes in the dissolved metal concentration followed by a slow approach to equilibrium over more than ten days. Using the quantity of leachable Zn, from Table 4.2, with the 90h adsorbed and dissolved concentrations for the freshwater experiments it is possible to calculate that 80-90% of the reactive Zn in the sample was in the adsorbed form. This is in good agreement with the results of Mouvet and Bourg (1983), determined using Meuse River samples, where 79% was found to be in the particulate phase.

In brackish water both the extent and the apparent rate of adsorption were reduced compared to the freshwater experiments. This difference is probably due to competition of major seawater cations (Ca and Mg) with Zn for active sites on the particles (Bourg, 1983; Schindler, 1981). These data contrast with those of Aston and Duursma (1973) who showed by radio-isotope studies no dependence of Zn adsorption on salinity. However, they are in good agreement with the work of Bale (1987) and Li et al. (1984a) who carried out sorption studies in natural solutions with the addition of radio-isotopes. Bale (1987) reported that in freshwater a rapid initial uptake (<1h) of 50% of the dissolved Zn was followed by a further 10% in the subsequent 15h. A proportion of this initial uptake in these experiments may have been due to simple equilibration of the particle surface with the radio-isotope. However, as the salinity was increased to 5‰ the extent of removal in 16h was reduced from approximately 60% to 40% and this is consistent with these results.

An additional experiment was carried out in which the desorption of Zn and Cu was followed as a function of time. (These

"metal-free" particles were then used in subsequent adsorption experiments and for the purposes of this work are called "cleaned" particles). The particles were "cleaned" by suspending them in Nanopure water for 6h. The desorption was monitored and as illustrated in Figure 4.5 there was a maximum desorption of $4\mu\text{g/L}$ (i.e. 10% of labile particulate Zn, see Table 4.2) of which $1.5\mu\text{g/L}$ was released immediately. The profile for the uptake onto these particles shows, in Figure 4.6, an immediate removal from solution of 40% of the dissolved Zn. As compared with the other freshwater profiles this is 10-20% more initial adsorption than was previously observed (see Figures 4.3 and 4.4). This rapid uptake can be envisaged for Zn as being equivalent to (1) the replacement of the metal desorbed from the particles and (2) the usual rapid adsorption observed in the freshwater experiments (see Figures 4.3 and 4.4). After initial adsorption there was a further 50% removal of dissolved Zn from solution in a manner consistent with the other freshwater isotherms. The equilibrium concentration in solution was about $5\mu\text{g/L}$ which is very similar to that seen in both the other Tamar freshwater adsorption runs.

The equilibrium data and solution conditions for all experiments are tabulated in Table 4.3. The only significant correlation is between the final concentrations of Zn in solution and salinity, as presented in Figure 4.7. These data indicate that the final Zn concentration in solution was similar for all experiments irrespective of turbidity ($200\text{--}500\text{mg/L}$), initial Zn concentration in solution ($14\text{--}25\mu\text{g/L}$) or amount taken up by the particles but dependent on salinity. Also in Table 4.3 values of metal concentration on the

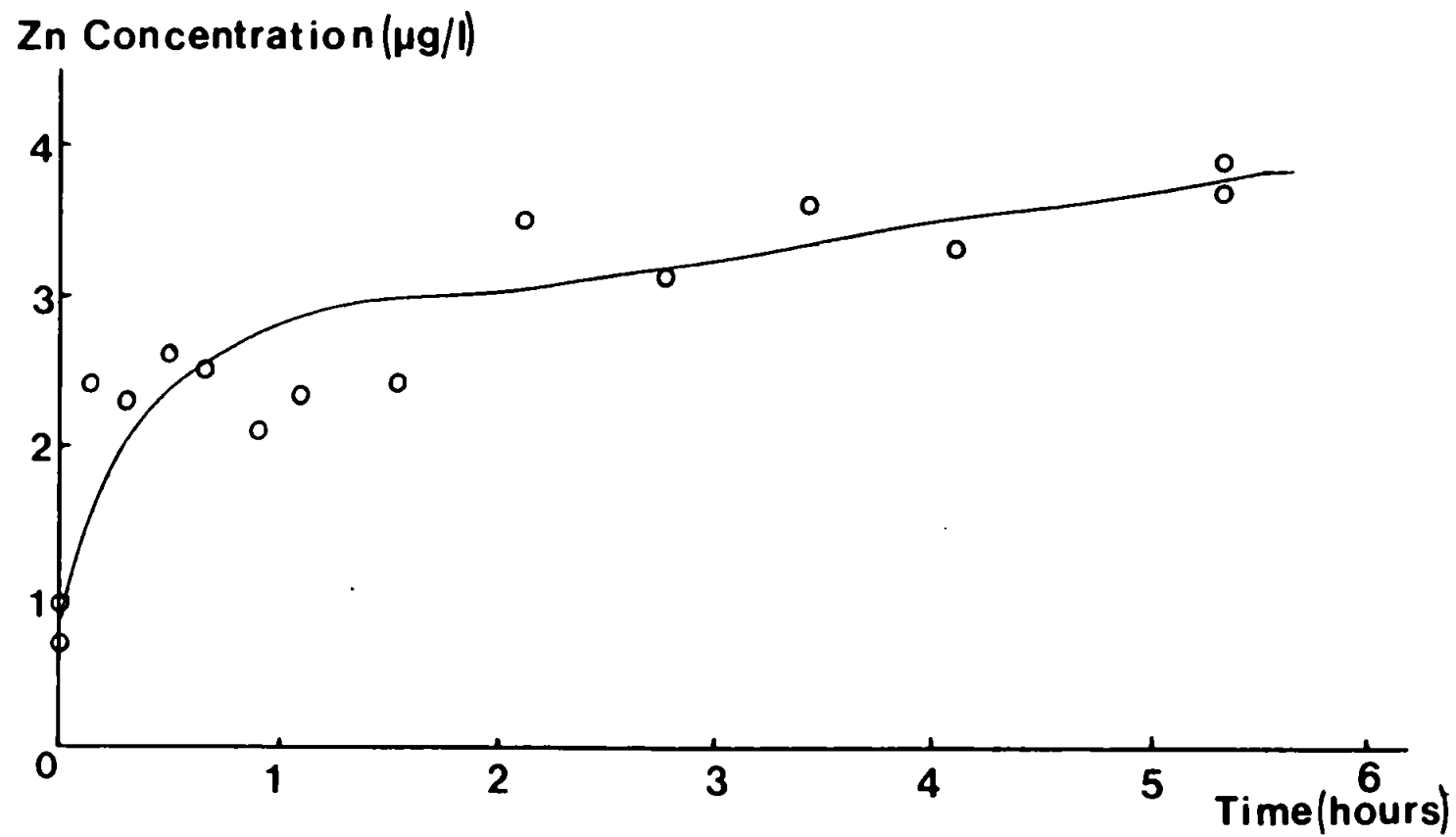


Figure 4.5. The concentration of Zn in solution versus time in a suspension of Tamar particles in Nanopure water at a turbidity of 500mg/L.

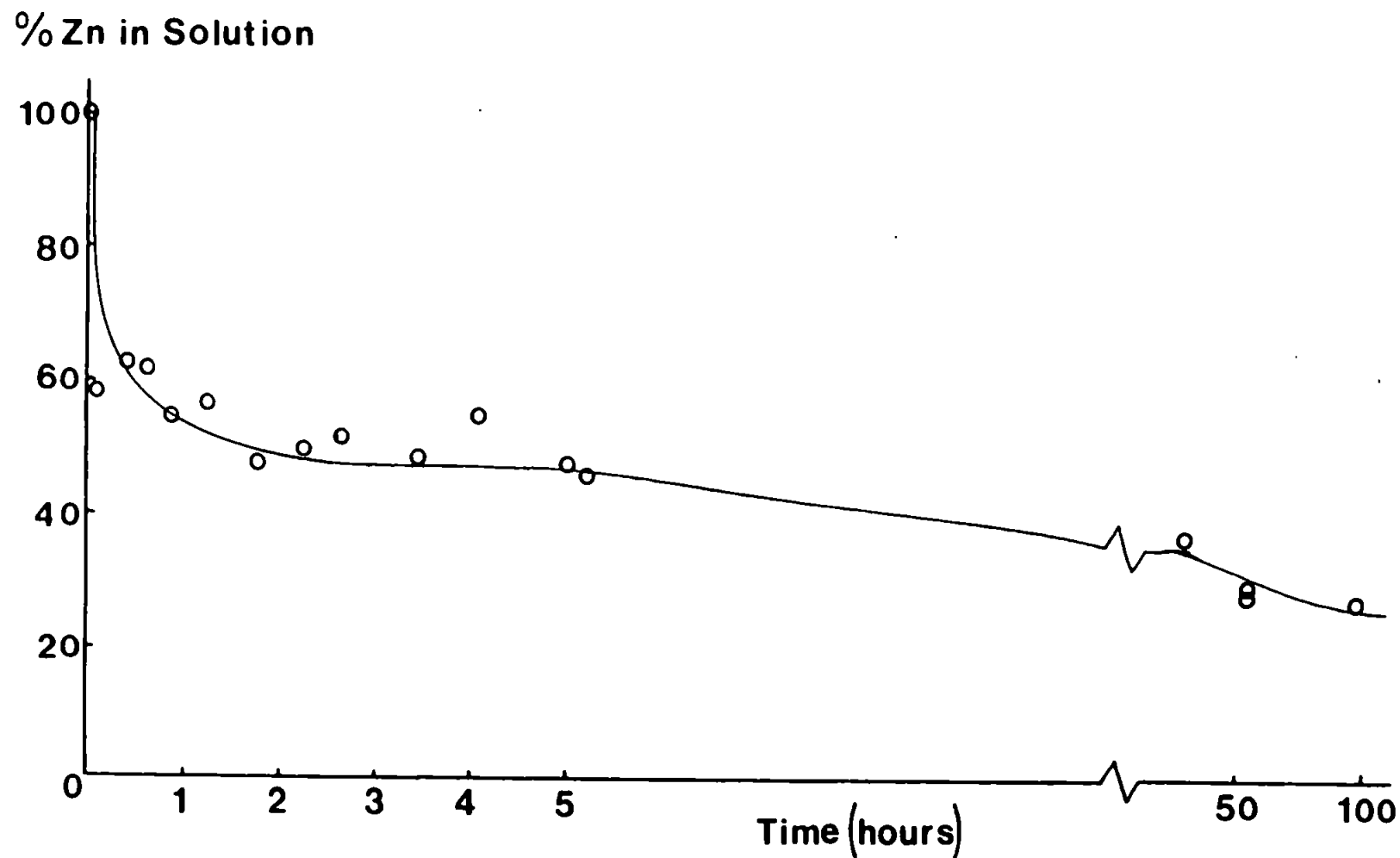


Figure 4.6. The percentage Zn remaining in solution versus time after the "cleaned" particles (see Figure 4.5) were suspended in Tamar River water with turbidity = 500mg/L, pH = 7.5 and 100% [Zn] = 26.4 μ g/L.

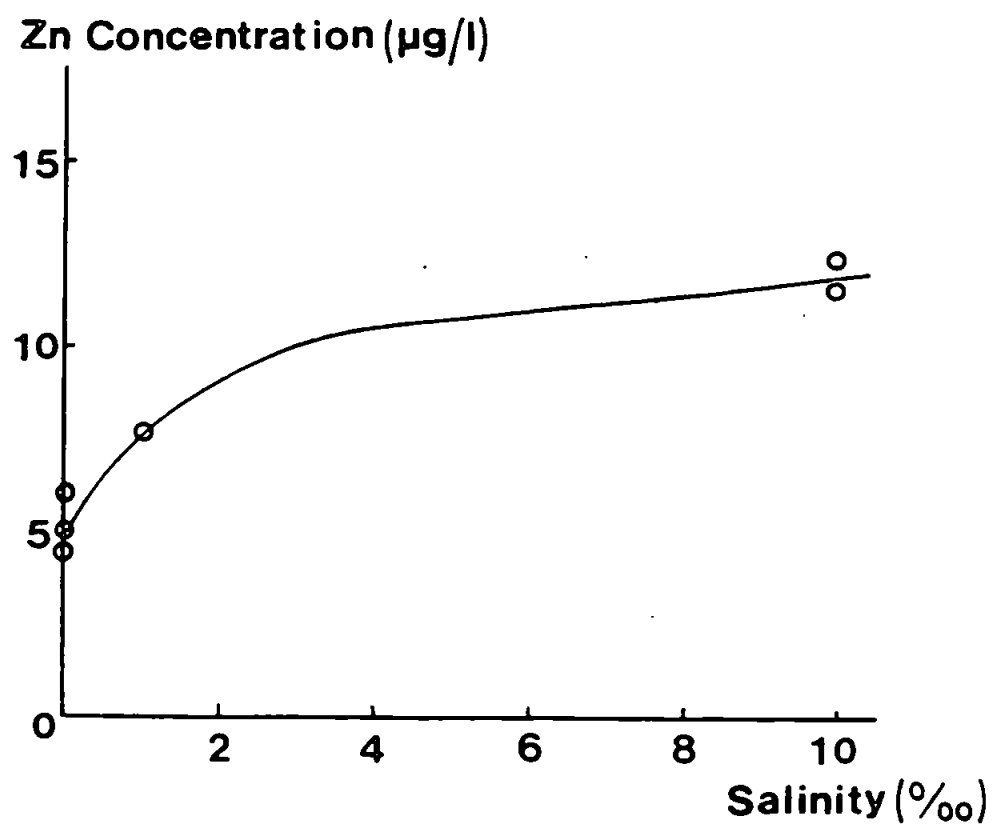


Figure 4.7. Final concentration of Zn determined after 90h in the Tamar mixing experiments versus salinity.

<u>Salinity</u> (‰)	<u>Equilibrium</u> <u>Conc. (µg/L)</u>	<u>Turbidity</u> (mg/L)	<u>Total uptake</u> (µg/L)	<u>Uptake by</u> <u>particles (µg/g)</u>	<u>Calculated^b</u> <u>Concentration</u> <u>on particles (µg/g)</u>
0	5	400	10	28	65
0	5	200	9	56	65
0 ^a	6	500	20	42	78
1	8	200	8	40	78
10	11	400	4	13	45

Table 4.3. A comparison of the characteristics of the Zn adsorption to particles suspended in Tamar Water.

^a Particles used in "cleaning" experiment.

^b Calculated using the K_d values from Bale (1987).

particles calculated using the K_d values of Bale (1987) are shown. These values are in reasonable agreement with the leachable Zn concentrations from this work (see Table 4.2) and with those quoted by Morris et al. (1986). Considering the adsorbed and leachable Zn in total the value calculated from the K_d is only half the possible labile surface Zn. This suggests that during the course of the experiment some metal becomes irreversibly bound to the particles.

4.2.2. Cu Behaviour.

The results of mixing experiments carried out at 0‰ and 10‰ salinity and with a turbidity of 400mg/L are depicted in Figure 4.8. In the freshwater run the Cu concentrations were low and the data were scattered but there was a slow adsorptive loss over 90h of about 20%. The brackish water experiment (where $S = 10‰$) had a slightly higher starting concentration of Cu and gave a smoother profile with a total loss of about 50%. As in the Zn case an additional set of experiments were carried out with the turbidity decreased to 200mg/L and the results for 0 and 1‰ salinity are shown in Figure 4.9. This illustrates that in the freshwater there was again a slow uptake of about 30% of the dissolved Cu over 24h. The profile for the brackish water sample showed up to 10% less removal than the freshwater sample over 24h but this removal continued to 40% after 90h.

These results show the uptake of Cu from freshwater to be slow and smaller in extent than in brackish water. Using the value for leachable Cu for these particles (95µg Cu/g particles) and the total in solution in freshwater it has been calculated that about 70-

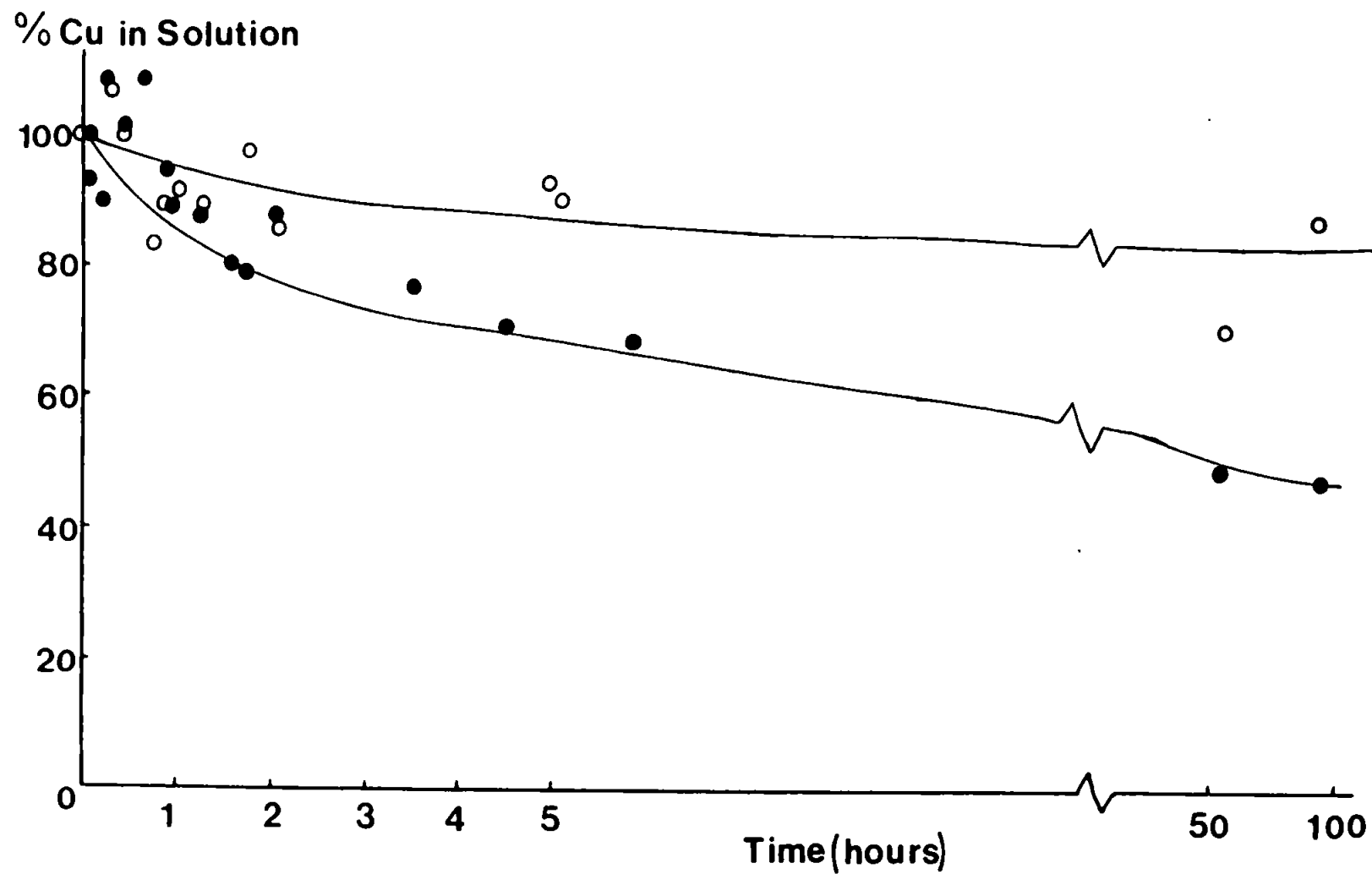


Figure 4.8. The percentage Cu remaining in solution versus time for two Tamar water suspensions with a turbidity of 400mg/L.

- Salinity = 0‰, pH = 7.5, 100% [Cu] = 9.0µg/L.
- Salinity = 10‰, pH = 8.2, 100% [Cu] = 10.5µg/L.

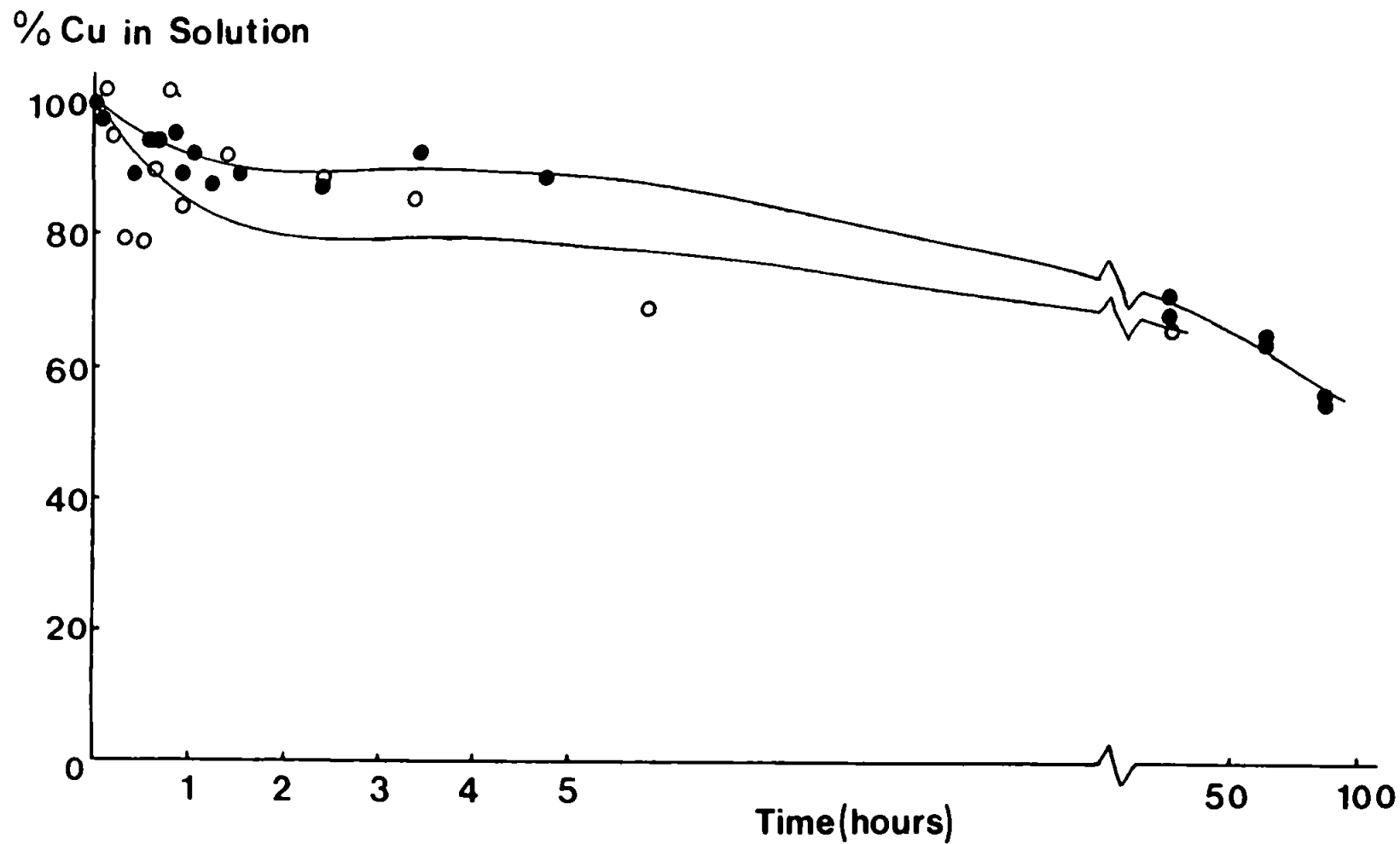


Figure 4.9. The percentage Cu remaining in solution versus time for two Tamar water suspensions with a turbidity of 200mg/L.
 ○ Salinity = 0‰, pH = 7.5, 100% [Cu] = 9.0μg/L.
 ● Salinity = 1‰, pH = 8.2, 100% [Cu] = 14.0μg/L.

80% was in the adsorbed form at equilibrium. This is lower than the 89% reported by Mouvet and Bourg (1983) who also saw a surprisingly small amount complexed by humics when compared to other work in freshwaters (Florence, 1977; Mantoura et al., 1978; Bourg, 1983) and in seawater (Van den Berg et al., 1987).

In saline water there was a larger uptake than in freshwater due to the flocculation of colloidal organic material in which Cu is complexed. Sholkovitz and Copland (1981) observed the coagulation of organic material in filtered river water samples to which major ions were added at seawater concentrations. Their work indicated a removal of 40% of dissolved Cu in 3h due to this coagulation of colloidal organic material, with complexed Cu, on encountering the more concentrated ionic media. Sholkovitz (1976) has also shown a removal of about 40% of Cu from filtered river water on the addition of filtered seawater. The observation by Millward and Moore (1982) that adsorption of Cu from an organic free model estuarine media was salinity independent corroborates the suggestion that the additional removal seen here was due to the flocculation of organic material in which Cu was complexed. The profile for Cu adsorption when the salinity = 1‰ shows no observable competition for active surface sites between Cu and major seawater ions. It also indicates that the small increase in salinity to 1‰ was sufficient to cause some flocculation of colloidal material.

These Cu adsorption results contrast starkly with those found for Zn. There was far less removal from freshwater of Cu than Zn but within brackish water they had similar adsorption profiles. This can be explained by examining their differing speciation within synthetic

estuarine waters in the presence of quartz particles (Bourg, 1983). Zn was present in freshwater primarily (57%) in the particulate form but as the water becomes more saline it is in competition with the major seawater ions for active sites and thus there is more in the Zn^{2+} free ion form (up to 45% in 30‰ seawater). In contrast, Cu is mainly present as humic complexes in freshwater (65%), some of which will be labile and observable after Chelex-100 extraction. A further 18% is in the $\text{Cu}(\text{OH})_2$ form and only 15% in the adsorbed form in freshwater. The percentage Cu in the complexed and adsorbed forms will decrease as the salinity of the water increases. Thus to account for the additional observed removal from the dissolved phase in brackish water ($S = 10\text{‰}$) it is surmised that Cu in organic complexes was destabilised, by the increased ionic strength, and flocculated, and thus a greater proportion of the dissolved Cu was removed (Gibbs, 1986).

A final experiment was carried out involving the "cleaning" of particles by desorption in Nanopure water. The desorption profile of Cu over 6h in deionised water is shown in Figure 4.10. This represents an immediate desorption of $1.5\mu\text{g/L}$ of Cu (i.e. about 3% of labile particulate Cu, see Table 4.2) which remains constant (within experimental error) throughout the 6h period. These "cleaned" particles were then used in an adsorption experiment depicted in Figure 4.11. This adsorption had a very marked initial uptake of about $5\mu\text{g/L}$ (30%) of Cu followed by a more gradual uptake until only 35% remained in solution.

This is in direct contrast with all other results for Cu adsorption from Tamar water. It is interpreted by considering surface

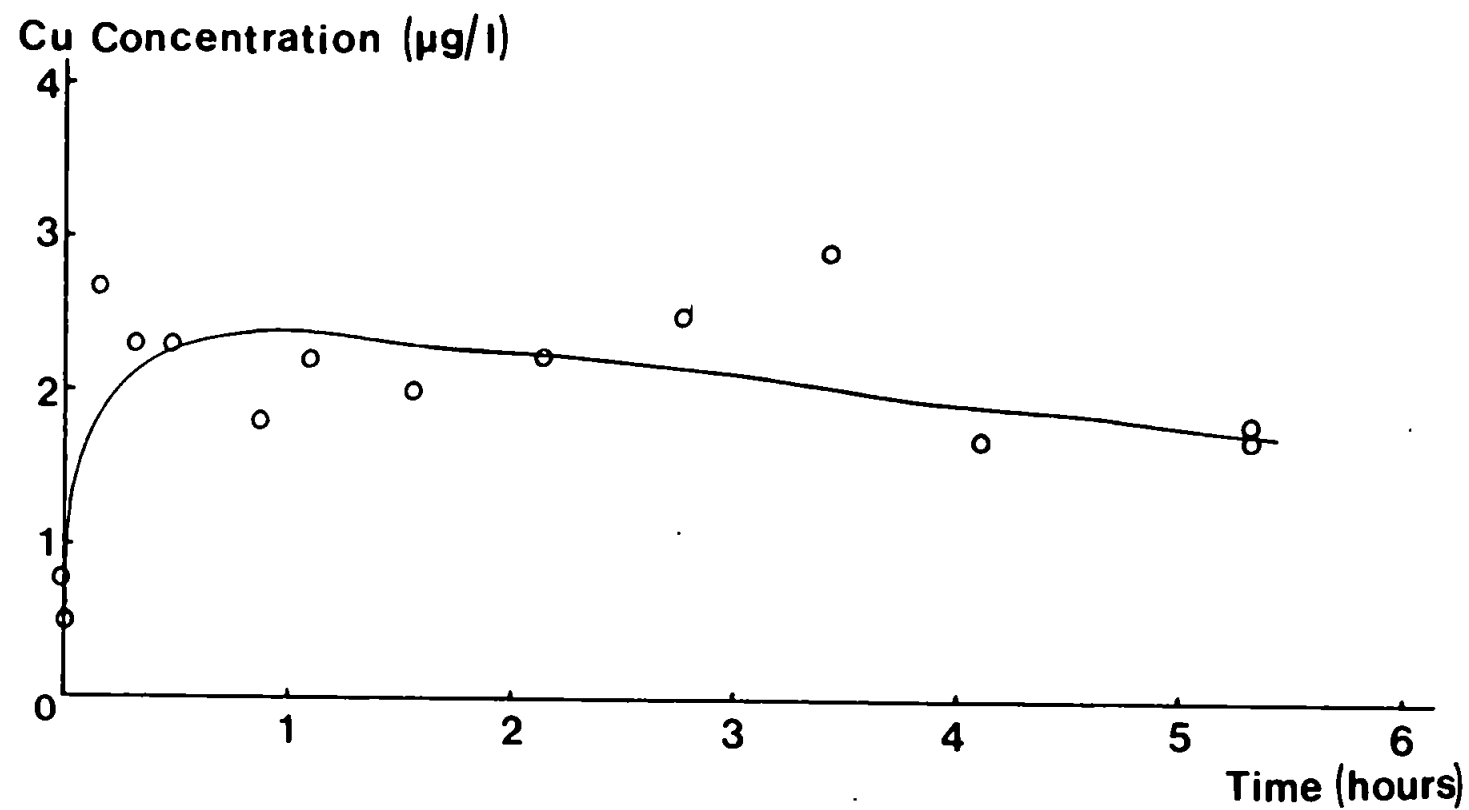


Figure 4.10. The concentration of Cu in solution versus time in a suspension of Tamar particles in Nanopure water at a turbidity of 500mg/L.

% Cu in Solution

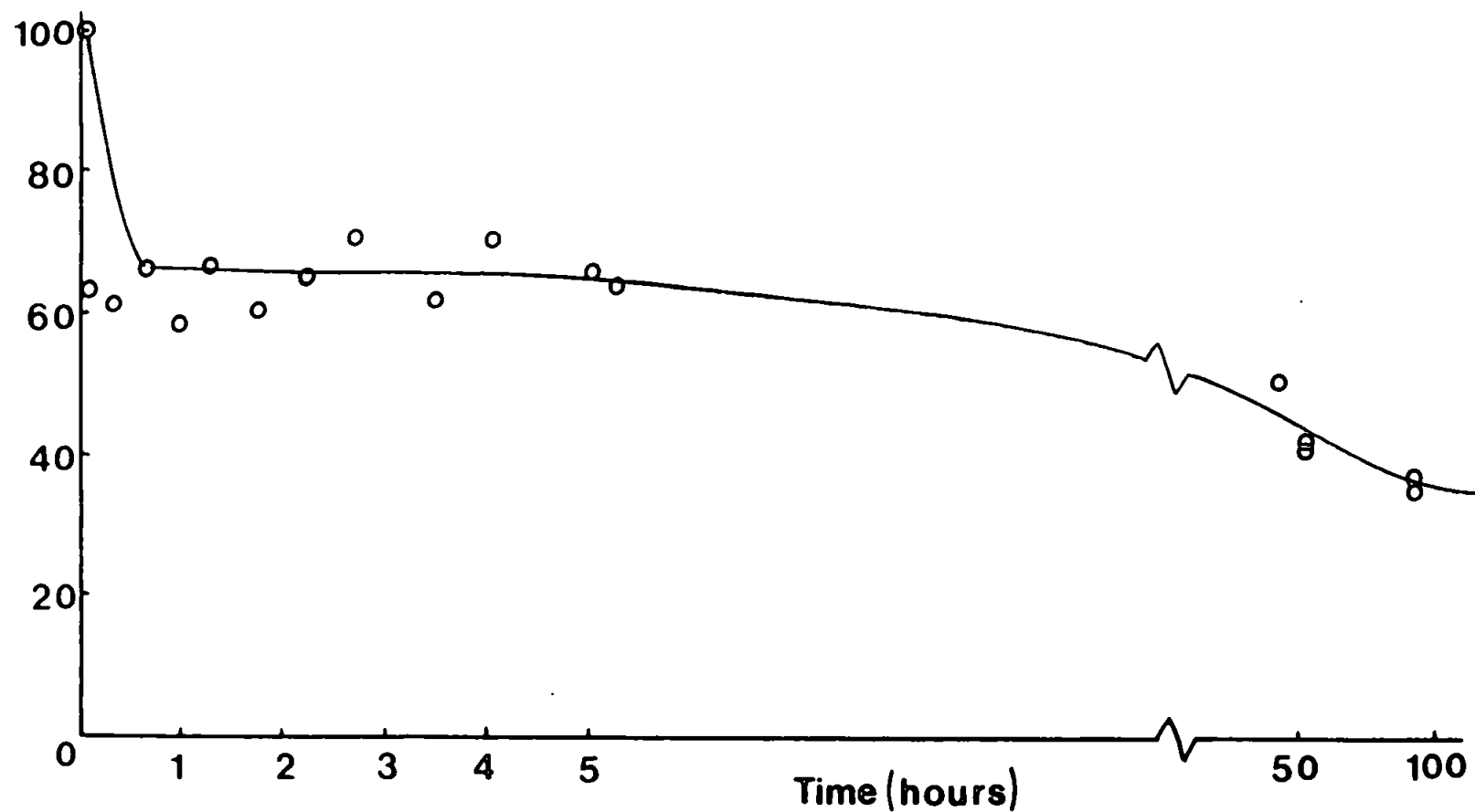


Figure 4.11. The percentage Cu remaining in solution versus time after the "cleaned" particles (see Figure 4.10) were suspended in Tamar River water with turbidity = 500mg/L, pH = 7.5 and 100% [Cu] = 14.0 μ g/L.

Cu active sites on the particles before "cleaning" to be occupied. Therefore on removal of the Cu by desorption many possible adsorption sites for Cu became vacant and were rapidly filled on resuspension. The additional initial uptake of $3.5\mu\text{g/L}$ may have been due to extra sites on the particles normally filled by other ions in freshwater also becoming vacant on desorption and enabling a larger uptake of Cu. Calculation shows that 90% of the total Cu after adsorption was present in the particulate phase which is in excellent agreement with the results of Mouvet and Bourg (1983). Why this comparability should improve after cleaning is unclear although it is likely to be because Mouvet and Bourg (1983) also "cleaned" their particles before experimental runs.

From these results it can be seen that in Tamar freshwater, with a Cu concentration of around $10\mu\text{g/L}$, the particles and solution were generally not far from equilibrium on mixing and thus there was a small slow uptake throughout the experiment. This initial quasi-equilibrium was disturbed by suspending the particle population in deionised water to remove the labile Cu after which there was a rapid re-establishment of the quasi-equilibrium on resuspension in river water.

The values for the final concentration in solution and the amount taken up by the particles are shown in Table 4.4. In contrast to the Zn results there is no pattern to the final concentration of Cu in solution but all samples have reached a similar concentration. There is no evidence of a correlation between either salinity or turbidity and the total metal adsorbed at equilibrium. The minimum distribution coefficient, K_d , was calculated from the dissolved and

adsorbed Cu and these are also given in Table 4.4. These values are reasonably consistent and show no variation with salinity. They are much higher than values determined by Gupta and Harrison (1982) for Cu in the presence of kaolin and humic acid.

<u>Salinity</u> (‰)	<u>Equilibrium</u> <u>Conc. (µg/L)</u>	<u>Turbidity</u> (mg/L)	<u>Total uptake</u> (µg/L)	<u>Uptake by</u> <u>particles (µg/g)</u>	<u>Minimum K_d (ml/g)</u>
0	7.5	400	1.5	4	5×10^5
0	5.5	200	3	15	2.7×10^6
0 ^a	5	500	9	18	3.6×10^6
1	8	200	6	30	3.7×10^6
10	5	400	5.5	14	2.8×10^6

Table 4.4. A comparison of the characteristics of the Cu adsorption to particles suspended in Tamar Water.

Values for the minimum K_d have also been calculated from the observed uptake.

^a Particles used in "cleaning" experiment.

4.3. Mixing Experiments Using Carnon Water.

Further adsorption experiments were carried out using water from the polluted Carnon River. This was to enable higher concentrations of metal to be examined without the need for addition of spikes of the metals which would not be in equilibrium with the river water. The Carnon water was taken from immediately below a minestream output and on collection the pH was <5 and the dissolved metal concentrations were high as reported in Table 4.5. The water was kept overnight in a constant temperature room, (10°C) in which the experiments were carried out, and filtered immediately before mixing when the pH was also altered. The presence of high Fe(II) concentrations which precipitated with time, reduced the metal concentrations to those which are given for the starting value for each experiment. The particles used were very similar to those used in the Tamar experiments and the details of their characteristics are given in Table 4.2.

<u>Metal</u>	<u>Cu</u>	<u>Fe</u>	<u>Mn</u>	<u>Zn</u>
Concentration (µg/L)	500	3000	1800	16000

Table 4.5. Typical trace metal concentrations in the Carnon River Water immediately on collection.

4.3.1. Zn behaviour.

Two freshwater adsorption experiments were run using Carnon River water with different turbidities and Zn concentrations. The

results for the 500mg/L sample presented in Figure 4.12 indicate an immediate uptake (<10 minutes) of 20% of dissolved Zn (from 2600µg/L to 2100µg/L) followed by a slower removal to a final concentration of 40% of the original dissolved Zn. The results from the sample with a turbidity of 1500mg/L are shown in Figure 4.13. This sample had a much higher Zn starting concentration (16400µg/L) but there was initially a similar amount of removal (2500µg/L) which translates to only 20% of the total dissolved Zn. After this initial uptake there was a slower removal which gave an overall loss of 30% of the dissolved Zn to the particulate phase. For these two experiments the removal at equilibrium was about 3000µg Zn/g particles whereas in the Tamar water it was around 40µg Zn/g particles. The coincidence of the maximum Zn adsorption for these two different Carnon experiments may indicate that 3000µg Zn/g particles saturates the particles although two samples are not conclusive. However, since essentially the same type of particles were used in all experiments this suggests that there are a substantial number of active sites available on Tamar particles and under normal conditions (Ackroyd et al., 1986) these will never be saturated with trace metals.

The freshwater K_d values from Bale (1987) were used to calculate the "theoretical" particulate Zn concentrations. The calculations gave a concentration of 14000 and 150000µg Zn/g particles for the samples of 500 and 1500mg/L turbidity, respectively. However as stated above the amount of metal actually removed from the Carnon water was only 3000µg Zn/g particles and this with the original labile Zn (<100µg Zn/g particles observed after leaching) falls far short of the predicted value. Suitable values of K_d were then calculated

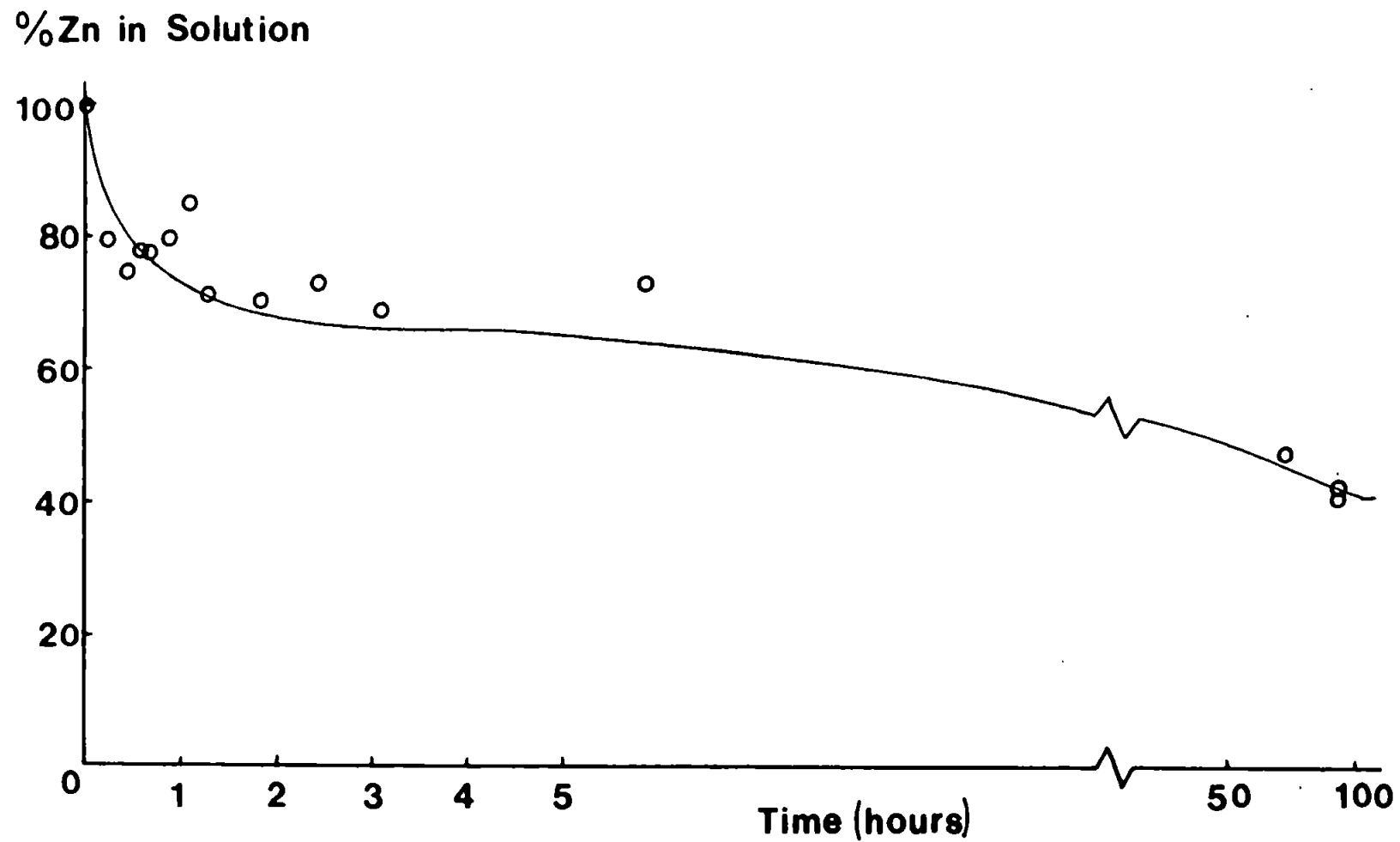


Figure 4.12. The percentage Zn remaining in solution versus time in a Carnon Water suspension with turbidity = 500mg/L, pH = 7.5 and 100% [Zn] = 2600 μ g/L.

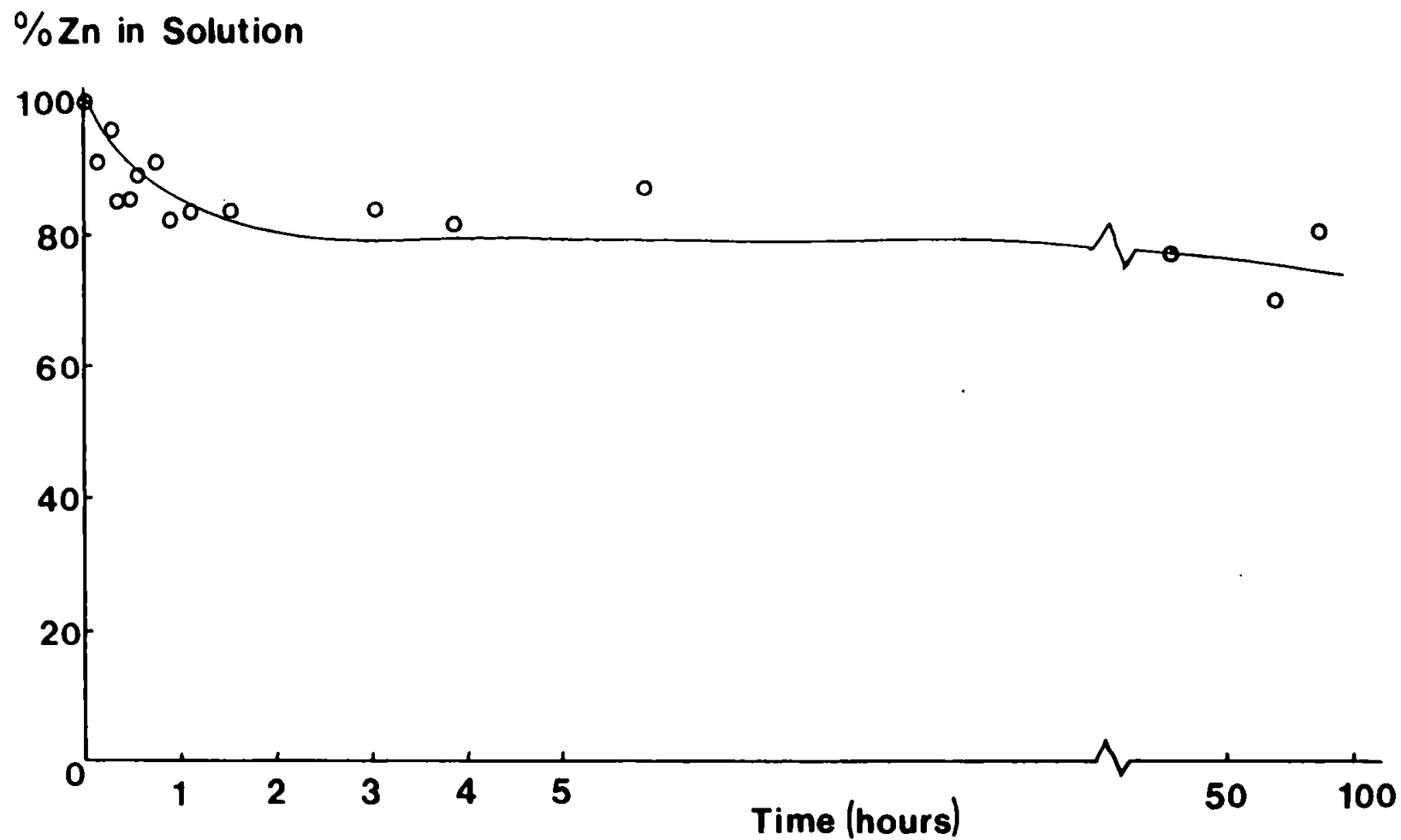


Figure 4.13. The percentage Zn remaining in solution versus time in a Carnon Water suspension with turbidity = 1500mg/L, salinity = 0‰, pH = 7.0 and 100% [Zn] = 1600µg/L.

from the observed dissolved and particulate Zn and these are shown in Table 4.6. These K_d values are approximately two orders of magnitude less than those quoted by Bale (1987) and show that each estuarine system has its own chemical as well as physical characteristics. Bale (1987) has previously described the dependence of K_d values on salinity, pH and temperature and this work indicates that they are also dependent on the dissolved metal concentration. While the complexity of the controls on K_d values implies that attempting to provide a unique set of values applicable to all estuaries is futile, the low K_d values observed in Table 4.6 must be very important with respect to mine streams entering estuaries similar to the Tamar. They suggest that if water with a very high Zn concentration enters an estuary even with a turbidity of up to 1500mg/L a large proportion of this metal will remain in solution. The rate of adsorption will then presumably be controlled by the timescale of physical mixing of the polluted water with fresh particles rather than the chemical adsorption reaction rates.

<u>Initial Zn</u> <u>concentration</u> <u>($\mu\text{g/L}$)</u>	<u>Turbidity</u> <u>(mg/L)</u>	<u>Uptake by</u> <u>particles</u> <u>($\mu\text{g Zn/g}$)</u>	<u>Observed</u> <u>K_d (ml/g)</u>
1100	500	3120	2.8×10^3
16400	1500	2930	1.8×10^2

Table 4.6. The concentration of Zn taken up by the particles at 90h in the Carnon mixing experiments. Calculated values of K_d for these experiments are also given.

Following on from these adsorption experiments two other 10 litre samples were initially treated in the same way as the high turbidity sample (see Figure 4.13), but in these cases the particle populations were completely filtered out after 1h and 24h. These filtered particles were then resuspended in buffered water and their desorption profiles observed over 90h. The profiles were nearly identical in shape and indicated desorption of up to 500µg/L after 2h followed by almost complete readsorption of the dissolved Zn by 90h. Figures 4.14 and 4.15 show a maximum desorption of 25% of the experimentally absorbed Zn in the case of the sample aged for 1h in Carnon water but only 20% of the particulate Zn by the sample aged for 24h. These desorption experiments disagree with those carried out by Bale (1987) which showed no readsorption of Zn between 4 and 40h. They are in agreement with the Th sorption results of Moore and Millward (1987) which showed desorption followed by readsorption of the radiosotope to marine particles suspended in seawater. They also reported a difference in the amount of desorption depending on the time for which the particles were aged in suspension but their discrepancy was considerably larger.

4.3.2. Cu Behaviour.

Two freshwater adsorption experiments with turbidities of 500mg/L and 1500mg/L were carried out, in which all other solution characteristics were similar. The results are presented in Figures 4.16 and 4.17. Both isotherms showed a rapid initial (<2h) removal of 60% of the dissolved Cu after which there was a slower adsorption of a further 25%. This supports the proposition that the surface of the

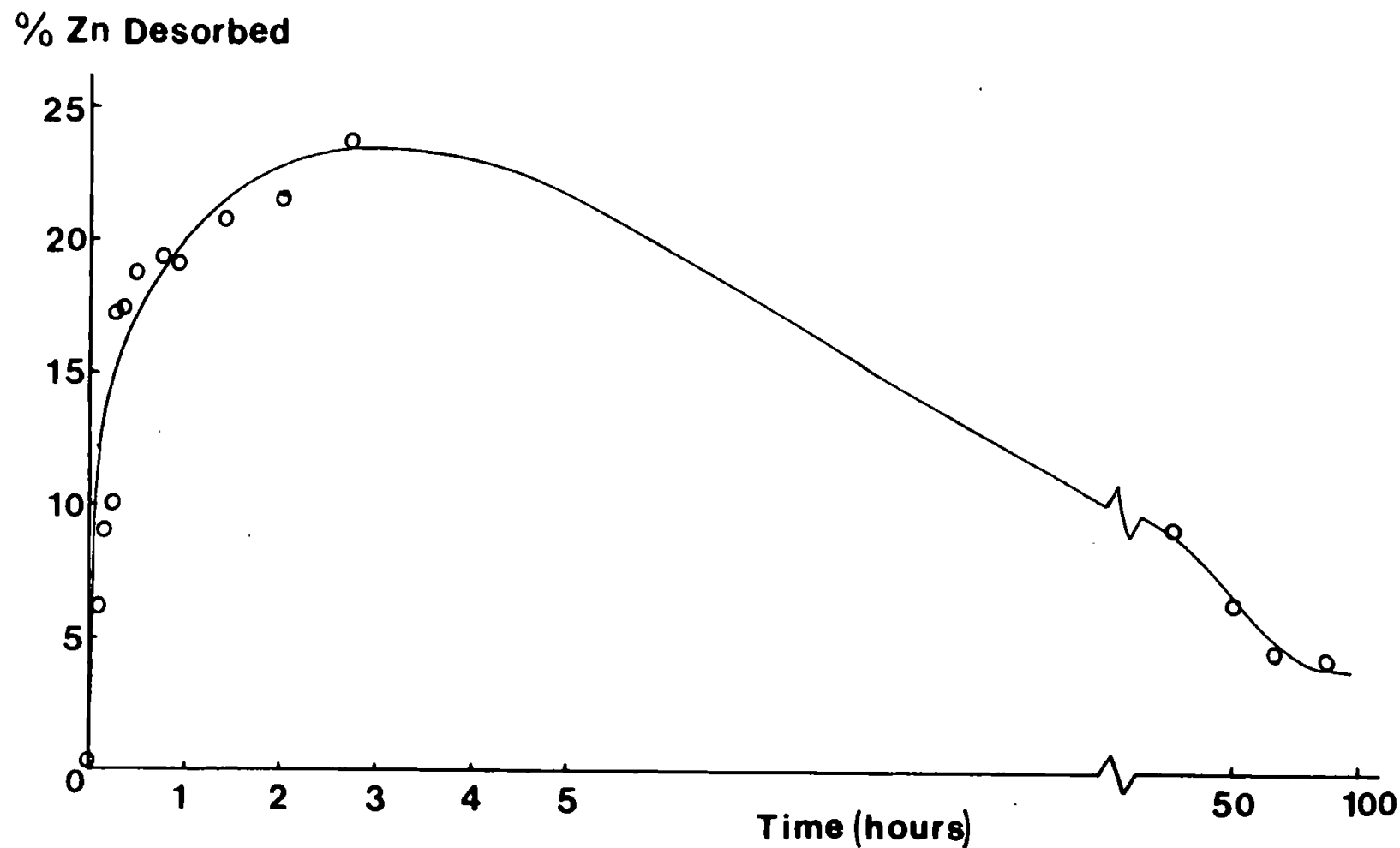


Figure 4.14. The percentage adsorbed Zn released to solution by particles aged for 1h in a suspension similar to that shown in Figure 4.13. The total Zn adsorbed during ageing was $2100\mu\text{g/L}$, the pH = 6.5 and the turbidity = 1500 mg/L.

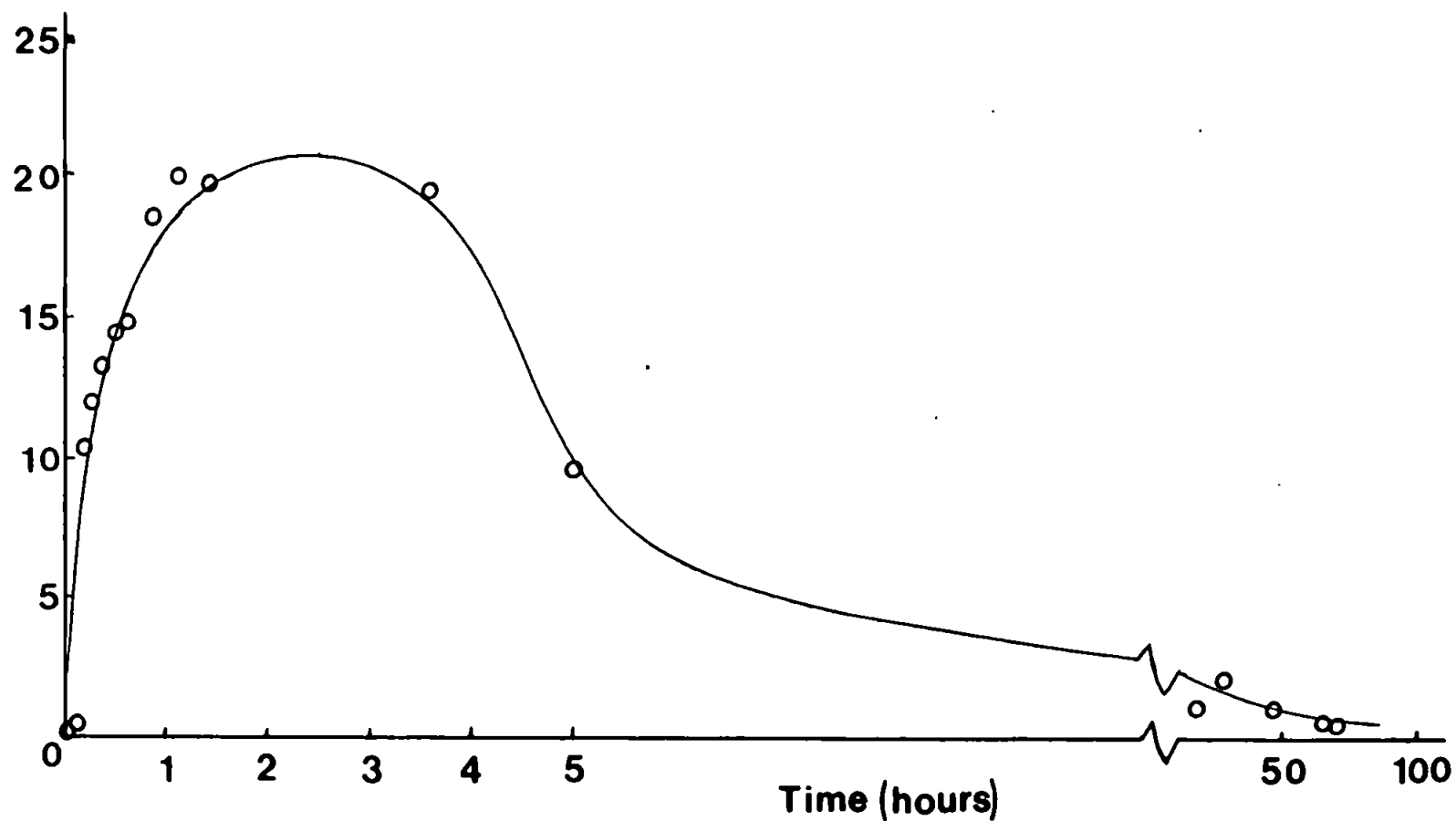
% Zn Desorbed

Figure 4.15. The percentage adsorbed Zn released to solution by particles aged for 24h in a suspension similar to that shown in Figure 4.13. The total Zn adsorbed during ageing was 2600 μ g/L, the pH = 6.5 and the turbidity = 1500 mg/L.

% Cu in Solution

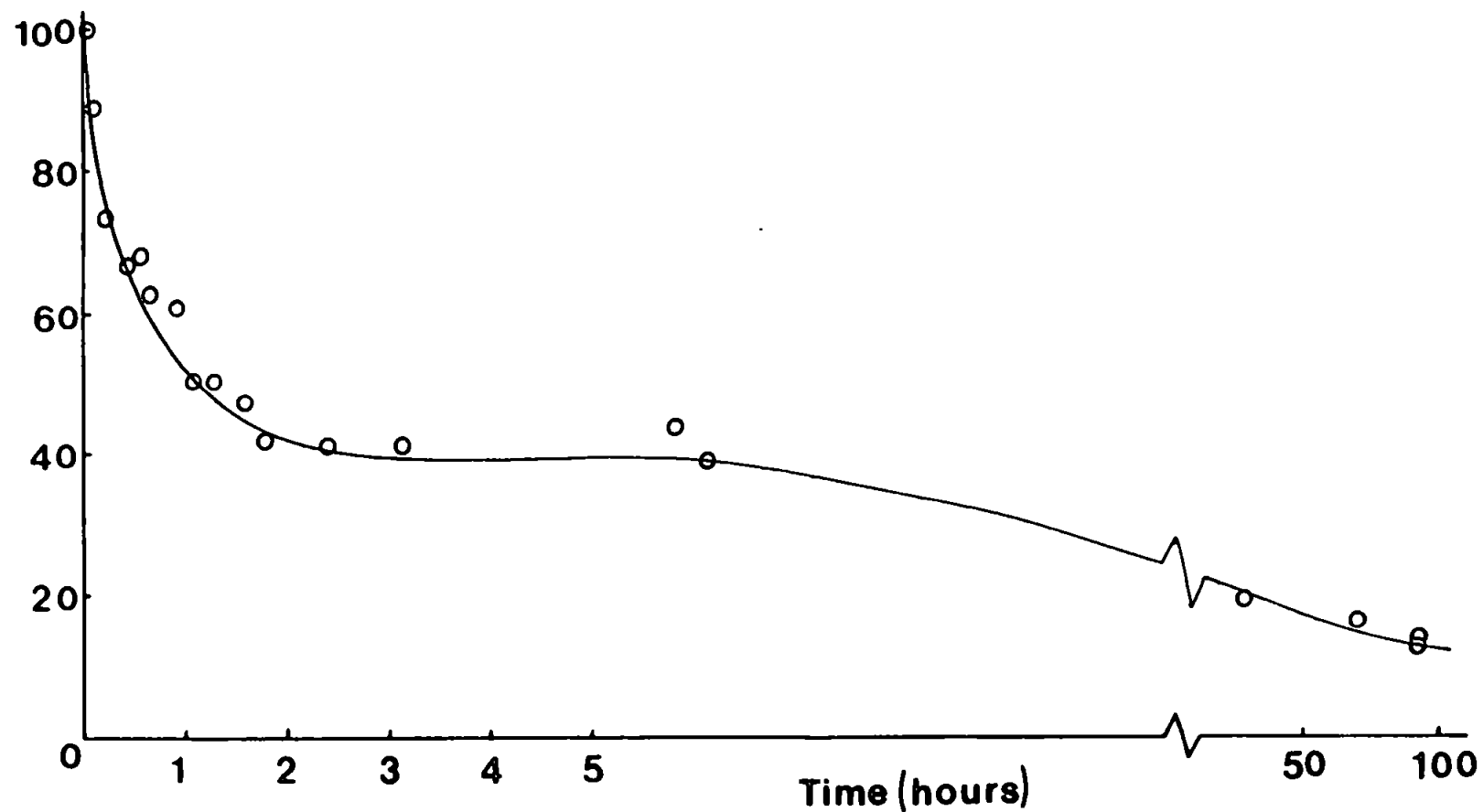


Figure 4.16. The percentage Cu remaining in solution versus time in a Carnon water suspension with turbidity = 500mg/L, salinity 0‰, pH = 7.0 and 100% [Cu] = 42μg/L.

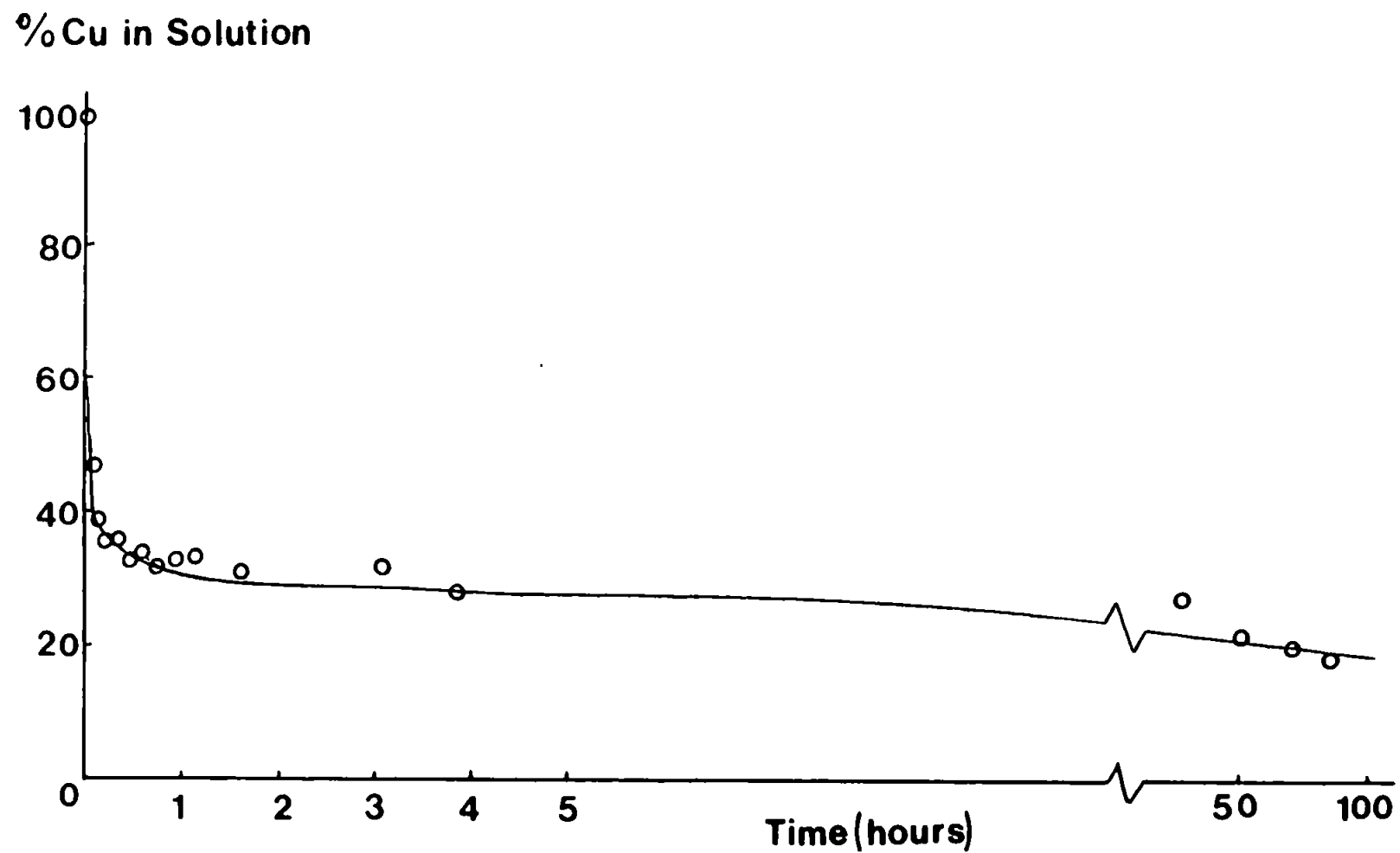


Figure 4.17. The percentage Cu remaining in solution versus time in a Carnon water suspension with turbidity = 1500mg/L, salinity 0‰, pH = 7.0 and 100% [Cu] = 38µg/L.

particles was already at quasi-equilibrium with Tamar freshwater in which the Cu concentration was approximately 10µg/L and shows they were far from equilibrium with the Carnon water. The particles had a capacity to adsorb at least twice as much Cu as was adsorbed in the Tamar freshwater as shown in Table 4.7. The percentage of the total metal which was taken up by the particles is higher than was seen by Mouvet and Bourg (1983) and the final concentration in solution was very similar to that found in the Tamar runs. The minimum values of K_d for these samples were calculated and as presented in Table 4.7 they are not dissimilar to those seen in the Tamar adsorption experiments. They are considerably higher than the values of 10^2 - 10^4 ml/g determined for Zn, in this work and by Bale (1987), and this affirms that the major portion of the Cu in these samples was present in the particulate form.

<u>Initial Cu</u> <u>concentration</u> (µg/L)	<u>Turbidity</u> (mg/L)	<u>Uptake by</u> <u>particles</u> (µg/g)	<u>Minimum</u> <u>K_d (ml/g)</u>
42.5	500	73	1.2×10^7
38.0	1500	21	3.0×10^6

Table 4.7. The amount of Cu adsorbed from solution by the particles in the Carnon mixing experiments. The calculated minimum values of K_d are also given.

Two desorption experiments were carried out, as discussed with respect to Zn, by resuspending particles in buffered water, which

had been filtered from 1500mg/L Carnon water suspensions (similar to that used to derive Figure 4.17) after 1h and 24h adsorption. The release of Cu from these aged samples was monitored over 96h and the profiles are illustrated in Figures 4.18 and 4.19. These samples desorbed in both cases of <5% of the observed adsorbed Cu which contrasts with Zn for which 20-25% was released. The sample aged for 1h quickly desorbed Cu to a maximum concentration of about 1.5µg/L (4% of the adsorbed) and after 2-3h readsorption was apparent until the 90h end of the experiment. For the sample aged for 24h the total Cu desorbed, 1.0µg/L (2% of the adsorbed), was about half that seen in the 1h experiment and this desorption was much slower. It is interesting to note that the amount of Cu desorbed was very small for both samples and that this amount is very similar to that desorbed by the untreated Tamar particles (see Figure 4.10). This demonstrates that a significant proportion of the Cu was lost irretrievably to the particulate phase as is supported by the high K_d values.

% Cu Desorbed

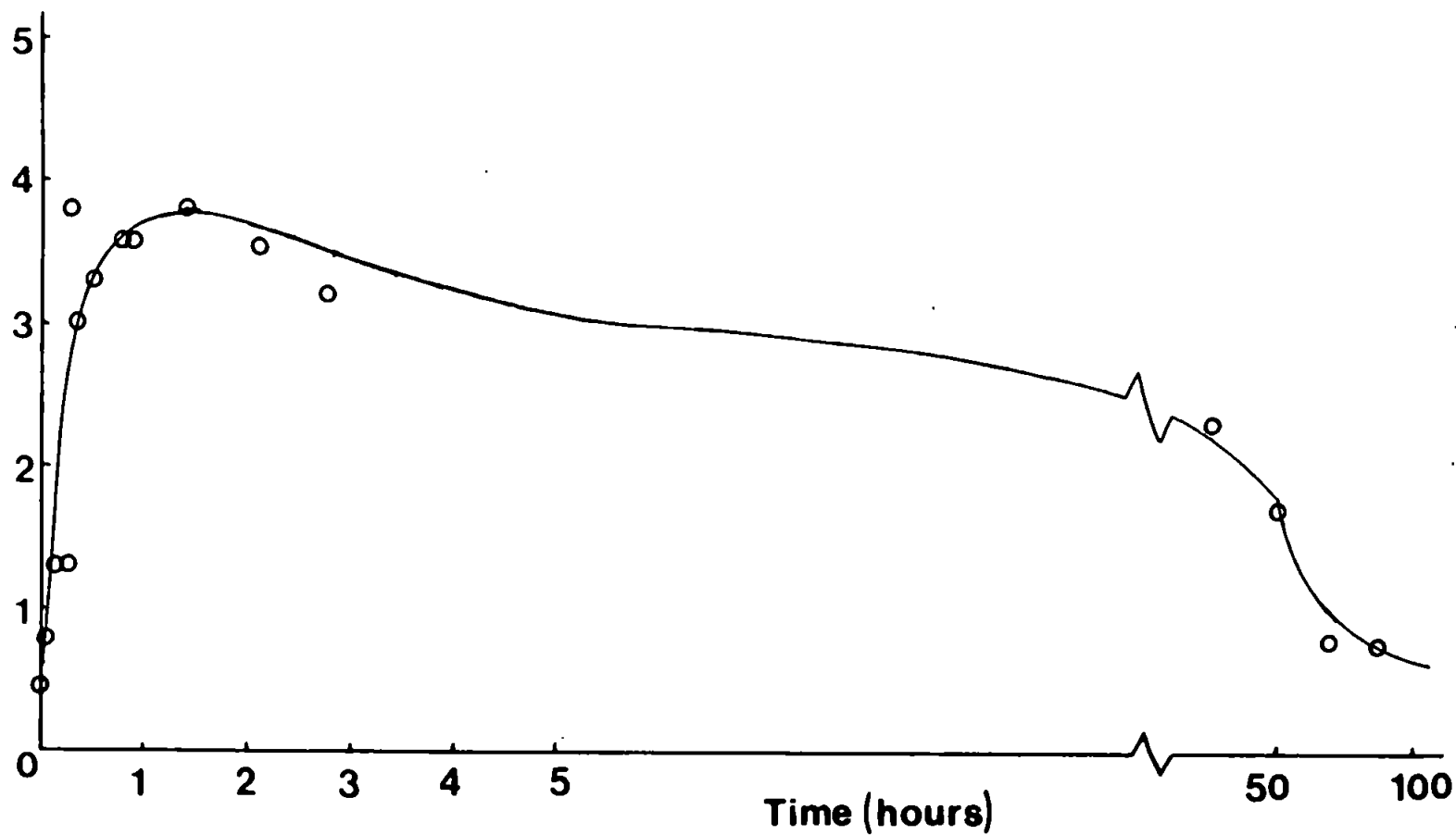


Figure 4.18. The percentage adsorbed Cu released to solution by particles aged for 1h in a suspension similar to that shown in Figure 4.17. The total Cu adsorbed during ageing was $46.5\mu\text{g/L}$, the pH = 6.5 and the turbidity = 1500 mg/L.

% Cu Desorbed

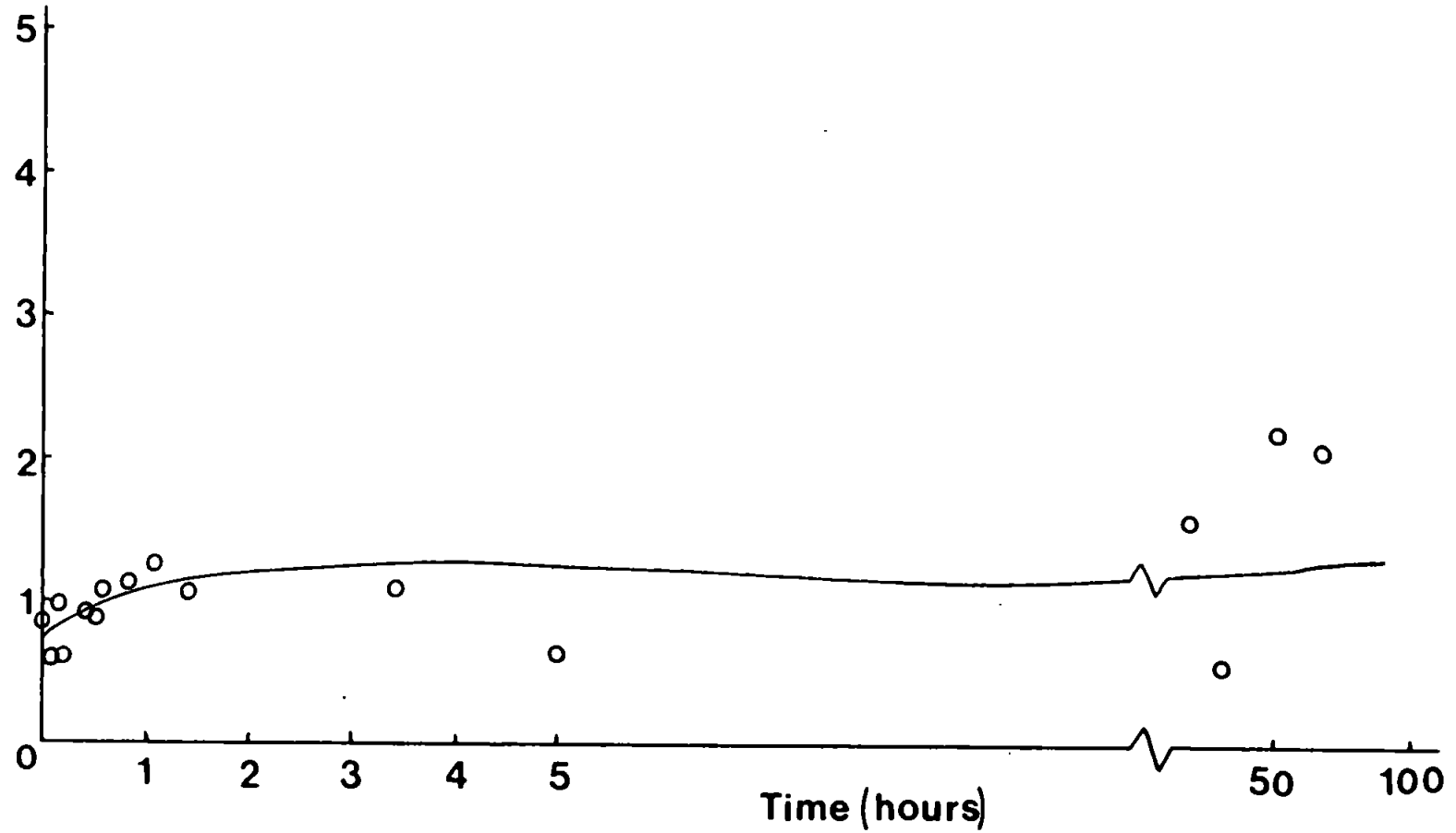


Figure 4.19. The percentage adsorbed Cu released to solution by particles aged for 24h in a suspension similar to that shown in Figure 4.17. The total Cu adsorbed during ageing was 67.0 μ g/L, the pH = 6.5 and the turbidity = 1500 mg/L.

4.4. Release from Carnon Sediment.

The desorption experiments carried out in the previous section suggest that suspended particles and sediments may contain trace metals trapped in the interior of the particles. Another way of observing this is to carry out time dependent desorption studies on natural particles. Tipping et al. (1986) have studied the release of trace metals from an iron oxide solid collected from a metalliferous mine stream. The sample desorbed between 50% and 75% of the final metal in solution in the first day after which there was a slow approach to equilibrium within about 21 days. It was shown that the desorption isotherms for Ca, Cd, Cu, Fe, Pb and Zn were not mirror images of adsorption isotherms (as has been seen in this work for Cu and Zn). This suggested that a solid state diffusion process was taking place.

Carnon sediments were suspended in various media to observe the desorption, if any, of the trace metals Fe, Mn, Cu and Zn. The particles were taken from the sediment surface in water which had a pH of 4.8-5.0 and trace metal concentrations similar to those given in Table 4.3. The suspensions were prepared in solutions of acidic Nanopure water (pH = 1.3-4.6) and NaHCO_3 buffered water (pH = 7).

The results for the amount of metal in solution after 4 days and 21 days are shown in Figures 4.20a and b, respectively. These showed a steadily increasing amount of Zn was released as the final pH in solution decreases from 4.5 to 1.5. A similar amount of Cu was released for each experiment from the samples with pH values between 3 and 4.5 below which the concentration increased. Mn had a sharp desorption edge between pH 3.2 and 3.9 and Fe had one between pH 2.4

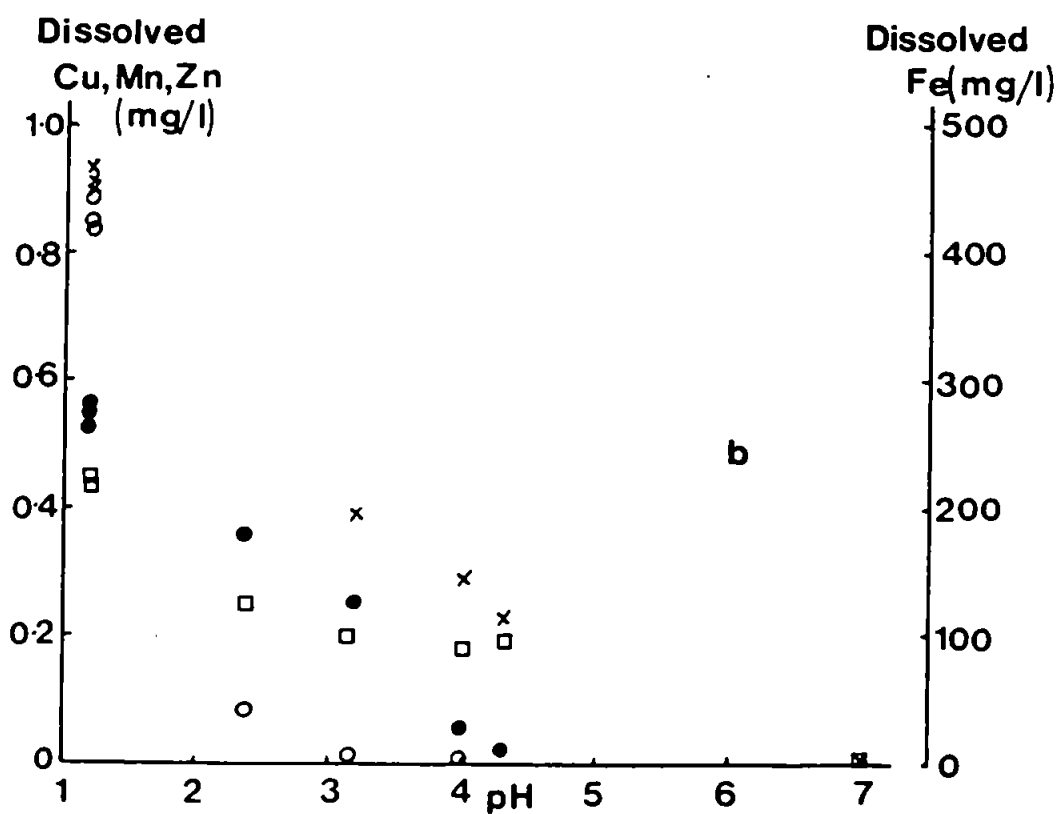
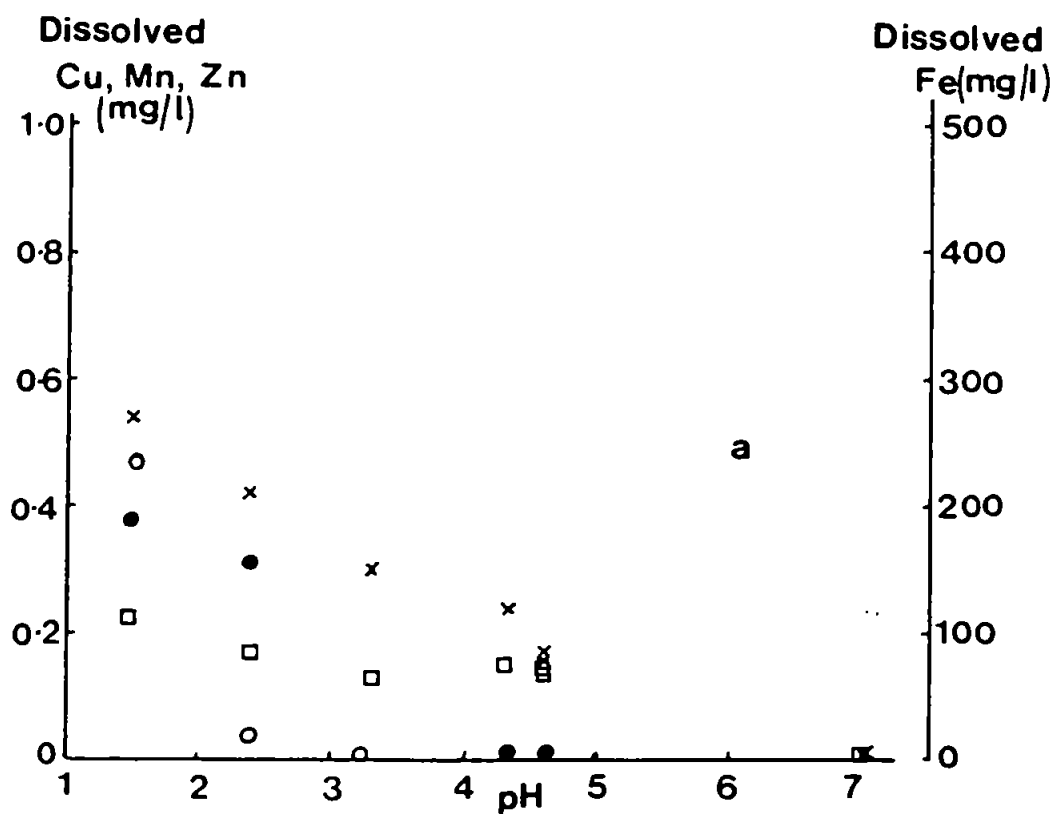


Figure 4.20. The concentration of Cu, Fe, Mn and Zn released from Carnon sediments after suspension for (a) 4 days and (b) 21 days at a range of pH values. ○ Fe ● Mn □ Cu × Zn.

and 1.5. Comparison between the two figures indicates that the increased time in suspension increased the amount of metal in solution. This could be due to (a) a gradual dissolution of the solid, compounded by the decreasing pH as the particles are left in suspension or (b) desorption of matrix held metal which would be slow due to diffusion from within the matrix of the particles. There does not appear to be an obvious correlation between the concentration of Mn or Fe released and that of Cu and Zn. This suggests that the release of Cu and Zn was due to a desorption mechanism rather than to dissolution of coprecipitates formed with Mn or Fe. Additionally, at pH values between 3 and 4.5, where there was no desorption of Fe, there was a greater release of Cu and Zn after 21 days than after 4 days. This concurs with the idea that a solid state diffusion process is taking place.

These results are in many respects consistent with those of Tipping et al. (1986) for different particle types. They observed a slow approach to equilibrium (21 days) and virtually no release of Fe from samples with a pH >3 while considerable amounts of Zn and Cu were transferred to the solution phase. They concluded that there was no evidence from their experiments to suggest that metals were held within coprecipitates. Rather they were adsorbed to sites within the porous structure of the particles and thus a considerable time was required before equilibration.

4.5. A Quantitative Summary.

Many aspects of the data throughout this chapter has strongly suggested that the interaction between natural particles and the trace metals Zn and Cu involves a two step sorption process. It is proposed that these two stages are (1) a rapid equilibration of the external surface of the particles with ambient dissolved metal and (2) a diffusion controlled movement of surface bound metal to or from adsorption sites within the matrix of the particles. This second process which is kinetically slow necessitates the re-equilibration of the particle surface with metal in solution and thus further slow uptake or release of dissolved metal.

The Zn adsorption results presented here concur with this mechanism and suggest that the surfaces of the particles were far from equilibrium on mixing with Tamar or Carnon River water. Therefore, there was a rapid initial (<2h) uptake of a significant proportion of the Zn in solution which was followed by a slow uptake for at least 90h. In brackish water both the apparent rate and extent of Zn adsorption was reduced presumably due to competition with seawater ions for active sorption sites. The observation that a similar amount of Zn was desorbed from the particles aged for 1 and 24h in Carnon water, despite the latter having adsorbed more Zn is also in agreement with a two step mechanism. It suggests that there was a similar amount of surface bound Zn while the residual Zn adsorbed over a longer time was held within the matrix.

The results for Cu can also be explained by the same two stage mechanism. The adsorption experiments suggest that the particles were at a quasi-equilibrium (i.e. the external particle

surface was at equilibrium) with a dissolved Cu concentration of 10µg/L, as only a slow steady removal from solution was observed. This quasi-equilibrium was disturbed by suspending the particles in Nanopure water to remove some of the loosely bound Cu from the surface before mixing with the river water and by suspending the particles in river water with a high Cu concentration. In both cases there was a rapid (<2h) re-establishment of the quasi-equilibrium followed by a slower uptake equivalent to that seen in the other Tamar adsorption experiments. In addition, there was a discrepancy in the percentage of adsorbed Cu desorbed in the Carnon experiments which suggested that during long term adsorption (24h) more Cu was lost to the matrix than in the short adsorption time (1h). In brackish water there was no apparent competition with major seawater ions although this could have been masked by flocculation of Cu complexed in organic material which increased the extent of Cu removal.

In Chapter 5 the rates of these interactions are quantified in order to develop an understanding of the importance of these heterogeneous processes to the bio-geochemistry of trace metals in estuaries.

CHAPTER FIVE

KINETIC ANALYSIS OF THE SORPTION DATA

This chapter provides a quantitative analysis of the data discussed in Chapter 4. Visual inspection of the adsorption profiles suggests that the time-dependent uptake is apparently exponential. However, such a superficial interpretation of the data conceals the complex reactions that can occur in the heterogeneous chemistry of natural suspensions. The basis of the analysis presented below is that the complex series of reactions which occur may be represented by an overall mechanism involving reversible sorption reactions at the particle surface and within the particle matrix.

5.1. Results from the Tamar Experiments.

5.1.1. Kinetic Analysis of Tamar Adsorption Data.

The adsorption profiles in Section 4.2 were tested against simple first and second order kinetics assuming the reaction mechanism was as follows:-



where M is the dissolved metal, S represents an active site on the particle, MS is the surface adsorbed metal and k the rate constant. None of these profiles fitted this simplistic mechanism. A viable alternative to this scheme is one involving a reversible first order reaction of the type:



In this case the rate of removal of M from solution is given by:

$$-\frac{d[M]}{dt} = k_1[M] - k_{-1}[MS] \quad (5.3)$$

where k_1 is now dependent on the turbidity which is constant in any given experiment. The integrated form of this rate equation (Swinbourne, 1971) is:

$$([M]_t - [M]_E) = ([M]_0 - [M]_E) \cdot \exp - (k_1 + k_{-1})t \quad (5.4)$$

where $[M]_t$ is the concentration of metal at time t , $[M]_E$ the concentration at equilibrium and $[M]_0$ the starting concentration.

Assuming that at equilibrium:

$$\frac{k_1}{k_{-1}} = \frac{[MS]_E}{[M]_E} \quad (5.5)$$

and using the mass balance:

$$[MS]_E = [M]_0 - [M]_E \quad (5.6)$$

then k_{-1} is defined by:

$$k_{-1} = \frac{k_1[M]_E}{[M]_0 - [M]_E} \quad (5.7)$$

Substituting Equation 5.7 into Equation 5.4 allows the integrated rate equation to be derived in terms of k_1 only:

$$k_1 t = \left(\frac{[M]_0 - [M]_E}{[M]_0} \right) \ln \left(\frac{[M]_0 - [M]_E}{[M]_t - [M]_E} \right) \quad (5.8)$$

Plotting values for the right hand side (designated as F for the purpose of the figures) of Equation 5.8 versus time allows the rate constant for the forward reaction, k_1 , to be calculated from the slope of the line.

This procedure was followed for the initial stages of both the Zn and Cu adsorption experiments from Sections 4.2.1 and 4.2.2 and the results of this are shown in Figures 5.1 and 5.2 for Zn and Cu, respectively. There is some variability in the analytical data, and

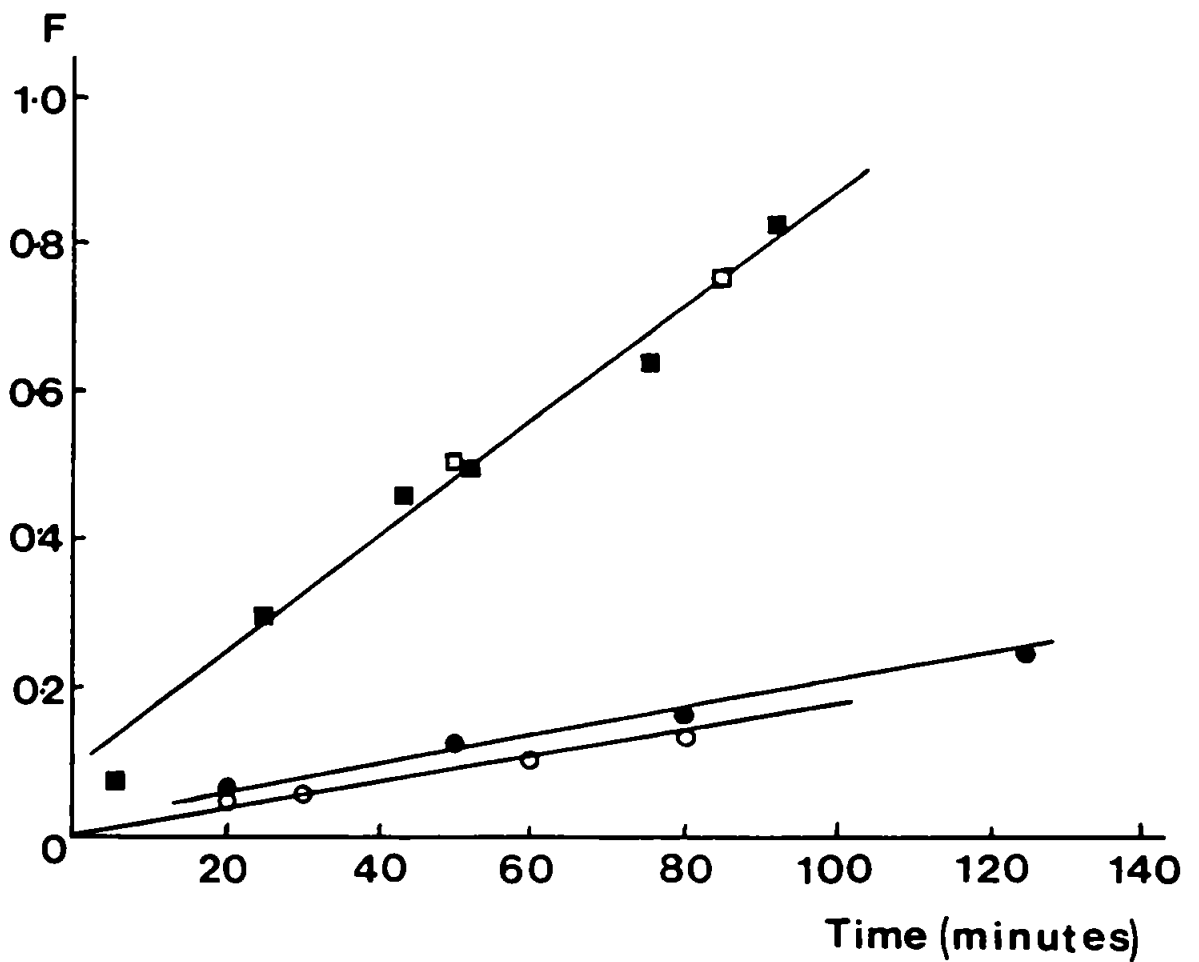


Figure 5.1. Kinetic analysis of Zn Tamar adsorption profiles using the Swinbourne (1971) method as discussed in the text.

Salinity = 0‰, turbidity = 200mg/L; data from Figure 4.4: □
 Salinity = 0‰, turbidity = 400mg/L; data from Figure 4.3: ■
 Salinity = 1‰, turbidity = 200mg/L; data from Figure 4.4: ○
 Salinity = 10‰, turbidity = 400mg/L; data from Figure 4.3: ●

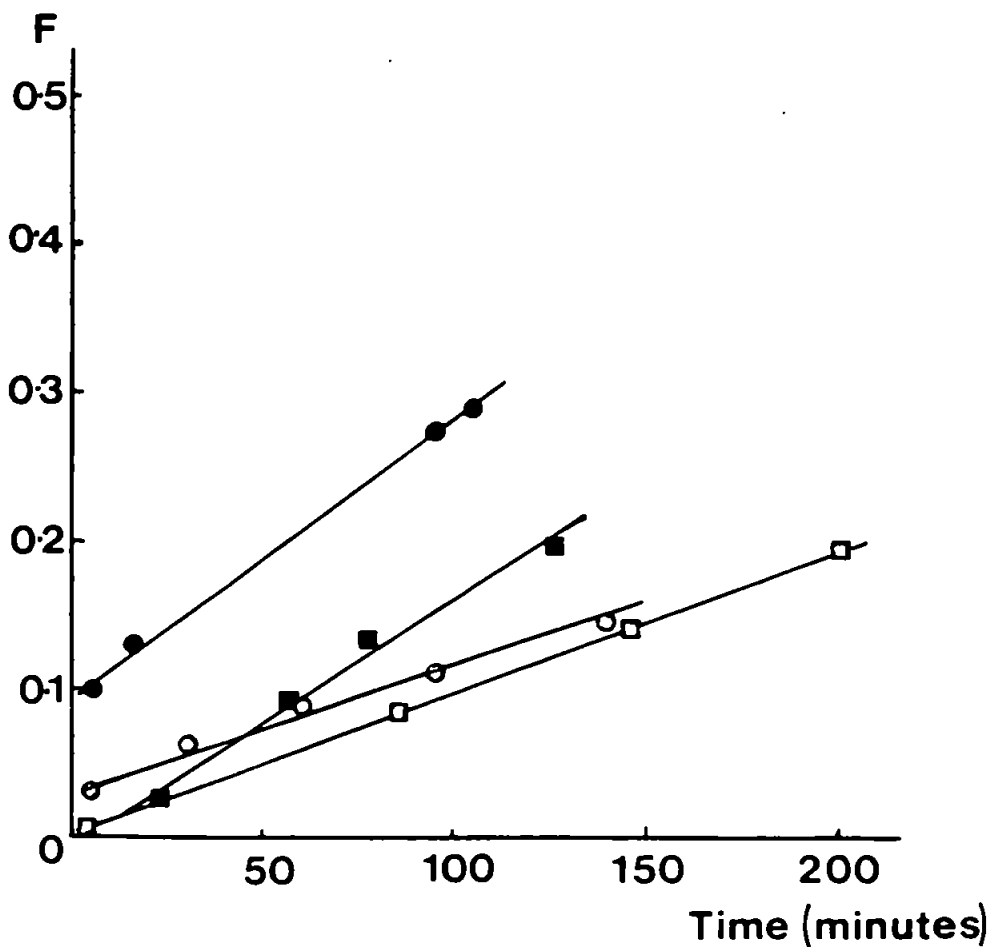


Figure 5.2. Kinetic analysis of Cu Tamar adsorption profiles using the Swinbourne (1971) method as discussed in th text.

Salinity = 0‰ , turbidity = 200mg/L; data from Figure 4.9: □
 Salinity = 0‰ , turbidity = 400mg/L; data from Figure 4.8: ■
 Salinity = 1‰ , turbidity = 200mg/L; data from Figure 4.9: ○
 Salinity = 10‰ , turbidity = 400mg/L; data from Figure 4.8: ●

so not all points are included in these graphs. One data set in particular had a high variability in the early stages of the reaction but the plots demonstrate linearity and have correlation coefficients at least to the 80% confidence level. The derived rate constants are given in Table 5.1. Since k_1 is turbidity dependent the value of the particle concentration, p , in kg/L is taken into account in k_1° , where $k_1^\circ = k_1/p$.

Salinity (‰)	Turbidity (mg/L)	Zn		Cu	
		$k_1 (h^{-1})$	$k_1^\circ (Ld^{-1}kg^{-1})$	$k_1 (h^{-1})$	$k_1^\circ (Ld^{-1}kg^{-1})$
0	200	4.6×10^{-1}	5.5×10^4	5.8×10^{-2}	6.9×10^3
0	400	4.6×10^{-1}	2.8×10^4	9.6×10^{-2}	5.8×10^3
1	200	9.6×10^{-2}	1.5×10^4	5.1×10^{-2}	6.1×10^3
10	400	9.6×10^{-2}	5.8×10^3	1.2×10^{-1}	7.2×10^3

Table 5.1. The forward rate constants as determined from Equation 5.8 for the Tamar adsorption experiments described in Section 4.2.

In the case of the Zn rate constants the range of k_1° is about 6×10^3 to 6×10^4 which compares well with the values of k_1° obtained by Nyffeler et al. (1984) for widely differing marine sedimentary material in seawater. They found $k_1^\circ = 60 Ld^{-1}kg^{-1}$ for Narrangansett Bay sediments and a maximum of $k_1^\circ = 1 \times 10^4 Ld^{-1}kg^{-1}$ for MANOP site H sediments. The data in Table 5.1 also show that the uptake rate was slower in brackish water than in

freshwater. This is possibly due to the competition for active adsorption sites on the particles with major seawater cations (Schindler, 1981). There will also be a tendency for Zn to complex with seawater ligands as the freshwater fraction decreases (Bourg, 1983). These two possibilities exist to explain the differences in k_1 but how it is achieved mechanistically is not known.

For Cu the values of k_1^0 lie in the range $6-7 \times 10^3$ $\text{Ld}^{-1}\text{kg}^{-1}$ and these represent the only values currently available.

The rate constants, k_1 , were susceptible to changes in turbidity but not to changes in salinity as indicated by the similarity of the constants in fresh and brackish waters of equal turbidity. Thus, the uptake rate of Cu in the estuarine mixing zone is likely to depend on the prevailing turbidity.

Approximate estimates of k_{-1} from Equation 5.7 show that for Zn it is about $2 \times 10^{-1} \text{ h}^{-1}$ and for Cu it is $3 \times 10^{-2} \text{ h}^{-1}$. These values may be overestimates because there is the possibility that an additional reaction will affect the concentration of MS. This problem is addressed later in this chapter.

5.1.2. Desorption of Metals from Tamar Particles.

The desorption of Zn from Tamar particles (at a particle concentration of 500mg/L) is shown in Figure 4.5. The rate constants derived for Zn (at a particle concentration of 400 mg/L) were thought to be suitable for predicting the appearance of dissolved Zn as a function of time. Equations 5.4 and 5.6 were then used to calculate the Zn desorption and a comparison of actual and two sets of calculated data is given in Figure 5.3. The observed data compares

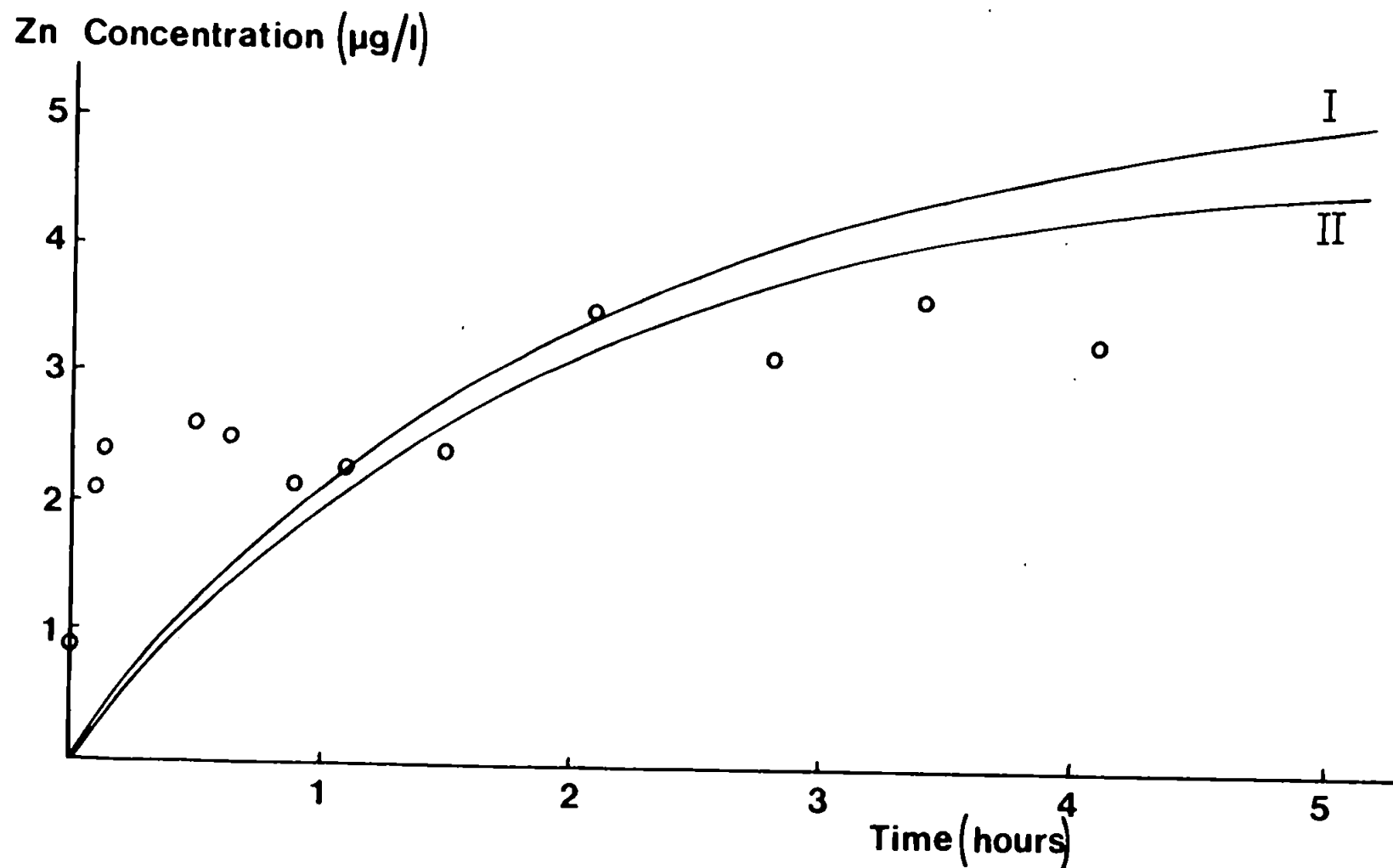


Figure 5.3. A comparison of actual Zn desorbed by Tamar particles with two sets of simulation results
 Case I - $k_1 = 0.46\text{h}^{-1}$; $k_{-1} = 0.20\text{h}^{-1}$; $[\text{MS}] = 15.0\mu\text{g/L}$.
 Case II - $k_1 = 0.46\text{h}^{-1}$; $k_{-1} = 0.06\text{h}^{-1}$; $[\text{MS}] = 42.5\mu\text{g/L}$.

reasonably well with the calculated data, given the analytical difficulty of estimating low concentrations in the early stages of the desorption reaction. In addition the calculated data begins to seriously over-estimate the amount of dissolved Zn when the time approaches about 5h which suggests that the solid state diffusion reaction is becoming operative. Inclusion of this in the mechanism would tend to reduce the over-estimate at long times.

Comparison of the two calculated profiles reveals an interesting feature. In Case I where k_1 and the estimated value of k_{-1} were used the best fit was only obtained if the value of desorbable Zn was reduced to 30% of the amount obtained by chemical leaching (i.e. 15 μ g particulate Zn/L compared to 42.5 μ g particulate Zn/L, see Table 4.2). This suggests that while chemical leaching techniques may well yield surface bound metal not all of this can participate in exchange reactions with the solution phase. For Case II the value of surface bound metal was 42.5 μ g particulate Zn/L and in order for the calculated data to match the observed the value of k_{-1} had to be reduced by a factor of 3. Although this test leaves some doubt as to the absolute magnitude of $[MS]_0$ and k_{-1} it does suggest that the values for k_1 and k_{-1} are reasonable and can be used with some confidence. A similar set of runs was carried out with the Cu desorption data (see Figure 4.10) with similar results. Thus, the values of k_1 and k_{-1} for both Zn and Cu can be used in direct comparison with the time constants for physical processes as shown in the next section.

5.1.3. Comparison of Rate Constants with Tamar Estuary Field

Observations.

The rate constants for the forward reaction of Equation 5.2 have been converted to half-lives via the equation:

$$t_{1/2} = 0.693/k_1 \quad (5.9)$$

and are listed in Table 5.2. The value of these is that the importance of the adsorption process relative to the hydrodynamic timescales can be assessed. This assessment can be best carried out by comparisons with the field observations of Ackroyd et al. (1986). Of particular relevance is a series of four summer (the 23rd, 27th and 31st of July and 31st of August, 1984) and four winter (the 31st of January and the 4th, 8th and 12th of February, 1985) axial surveys of dissolved Zn and Cu in the Tamar Estuary which each covered the full 30km of the estuary.

<u>Salinity</u> <u>(‰)</u>	<u>Turbidity</u> <u>(mg/L)</u>	<u>Zn half-life</u> <u>(h)</u>	<u>Cu half-life</u> <u>(h)</u>
0	200	1.5	12.0
0	400	1.5	7.2
1	200	7.2	14.0
10	400	7.2	5.8

Table 5.2. The half lives calculated from the forward rate constants for the Tamar adsorption experiments.

The four summer profiles showed a well developed turbidity maximum (maximum particle concentrations from 50-400mg/L) associated with low river flows (1.1 to 2.3m³/s). Each of the four profiles indicates removal of dissolved Zn in the turbidity maximum region of the freshwater above the salt wedge. In calculations of the flushing time of the Tamar Estuary, Uncles et al. (1983a) found that in the upper Tamar, when the river flow is 1.8m³/s, the flushing time is of the order 1-5h, which is comparable to the half-life of dissolved Zn in freshwater (1.5h). The implication of these results is that the combination of surface for adsorption ($P_{\max} = 400\text{mg/L}$ with a specific surface area of around 20m²/g) and residence time of the water in this zone is sufficient for adsorption reactions to proceed almost to completion (i.e. 4-6 half-lives). In contrast the winter surveys carried out by Ackroyd et al. (1986) were under conditions where the river flow varied between 25 and 53m³/s. These high river flows gave a very much reduced turbidity maximum (always <100mg/l) and there was little or no removal of dissolved Zn. The reason is that in addition to the considerably less active surface the residence time of the water is <1h and given the data in Table 5.2 the adsorption reactions tend to be far removed from equilibrium. Careful examination of data from other surveys by Ackroyd et al. (1986) carried out between October 1976 and February 1981 shows that in the cases where the river flow was <10 m³/s there were very low concentrations of dissolved Zn at the freshwater-brackish water interface. During the survey of 18/2/81 (river flow 13.4 m³/s), when there was a high turbidity of 600mg/L there was no discernible removal of dissolved Zn. The implication from these results is that

the timescale of adsorption in the Tamar Estuary is of utmost importance. At higher salinities the half-life for the removal increases (and the extent of removal decreases) which means that as the particle concentration declines away from the turbidity maximum, uptake onto particles becomes even slower. Even though the flushing time of down estuary segments increases it cannot compensate for the decline in the concentration of active surfaces and the increase in the adsorption half-life - thus the solution phase is preferred for Zn.

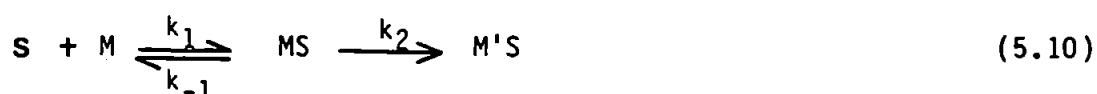
In the case of Cu the half-lives are turbidity dependent with the shortest half-life being associated with the highest turbidities. The 1984/5 data on dissolved Cu in the Tamar Estuary suggests that for the high turbidity summer surveys the dissolved Cu concentrations in the turbidity maximum were usually a factor of two lower than the low turbidity in winter surveys. This is also suggested by some of the October 1976 to February 1981 surveys but it is not as clear because these surveys do not cover the complete mixing zone.

5.2. Kinetic Analysis of the Carnon Data.

The adsorption and desorption profiles shown in Chapter 4 suggest that a two stage mechanism is operational over the period of several days. Interpretation of the profile over this sort of timescale requires a more sophisticated mechanism, with a consequent increase in the complexity of the integrated equations and their simultaneous solution, than was adopted in Section 5.1.1 for the short-term adsorption. The method adopted for the analysis of the Carnon desorption profiles is described below using the Zn results as an example. The Cu rate constants are discussed in Section 5.2.2.

5.2.1 Method for Analysis of Zn Desorption Profiles.

In this case the reaction mechanism shown in Equation 5.2 was expanded to include a reaction in which surface adsorbed metal undergoes migration into the pore space of the particles, viz:



where M'S is the metal adsorbed in the particle matrix. This assumes that the reverse solid state diffusion reaction, k_{-2} , is small enough to neglect (as it is likely to be at least in the initial stages of the reaction) and that the extra step is described also by first-order kinetics. The differential equations for each of the species in this type of reversible consecutive reaction are:

$$\frac{d[M]}{dt} = k_{-1}[MS] - k_1[M] \quad (5.11)$$

$$\frac{d[MS]}{dt} = k_1[M] - k_{-1}[MS] - k_2[MS] \quad (5.12)$$

$$\frac{d[M'S]}{dt} = k_2[MS] \quad (5.13)$$

The integrated forms of these coupled differential equations can be derived using Laplacian Transform techniques (Rodiguin and Rodiguina, 1964) and the solutions are as follows:

$$[M] = \frac{k_{-1}[MS]_0}{(R_2 - R_1)} \left(\exp(-R_1 t) - \exp(-R_2 t) \right) \quad (5.14)$$

$$[MS] = \frac{[MS]_0}{(R_2 - R_1)} \left((k_1 - R_1) \cdot \exp(-R_1 t) - (k_1 - R_2) \cdot \exp(-R_2 t) \right) \quad (5.15)$$

$$[M'S] = \frac{[MS]_0}{(R_2 - R_1)} \left(1 - \frac{k_2(k_1 - R_1)}{R_1} \cdot \exp(-R_1 t) + \frac{k_2(k_1 - R_2)}{R_2} \cdot \exp(-R_2 t) \right) \quad (5.16)$$

where $[MS]_0$ is the initial concentration of the surface bound metal and where R_1 and R_2 are the roots of the equation given by:

$$R_{1,2} = \frac{-b \pm \sqrt{b^2 - 4g}}{2} \quad (5.17)$$

$$\text{in which } b = k_1 + k_{-1} + k_2 \quad (5.18)$$

$$\text{and } g = k_1 \cdot k_2 \quad (5.19)$$

Equations 5.17, 5.18 and 5.19 are the products of the transform method adopted for the integration of the rate equations (Rodiguin and Rodiguina, 1964).

The approach taken here was to establish the values of the constants in Equation 5.14, which can be rewritten as:

$$[M] = A \left(\exp(-R_1 t) - \exp(-R_2 t) \right) \quad (5.20)$$

$$\text{by defining } A = \frac{k_1 [MS]_0}{R_2 - R_1} \quad (5.21)$$

A maximum likelihood estimation programme (Ross, 1980) with an iterative curve fitting routine (in Fortran-77) was used to fit the Zn desorption data (from Figure 4.13) to a double exponential equation of the form shown in Equation 5.20. The agreement between the fitted values and real data was good as shown in Table 5.3. Table 5.3 also lists the derived values of R_1 , R_2 and A which were then used to calculate k_1 and k_{-1} as discussed below.

If the values of A , R_1 , R_2 and the concentration of surface or loosely bound Zn are known then k_{-1} can be calculated. In these desorption experiments it was assumed that the quantity of Zn adsorbed in the 1h ageing could be used as this loosely bound quantity (2100µg particulate Zn/L) and thus k_{-1} for Zn was calculated to be 0.9 h^{-1} . The value of b was then estimated from the roots given in Equation 5.17 and it was found to be 4 h^{-1} . It is reasonable to assume that $k_1 + k_{-1} \gg k_2$ (Nyffeler et al., 1984) then using Equation 5.18 and $b = 4$ the value of k_1 is found to be 3.1 h^{-1} .

<u>Time (h)</u>	<u>Measured</u>	<u>Computed</u>	<u>Difference (µg/L)</u>
	<u>conc.(µg/L)</u>	<u>conc.(µg/L)</u>	
0.00	15.00	0.00	15.00
0.08	130.00	128.98	1.02
0.17	190.00	220.39	-30.39
0.33	355.00	330.85	24.15
0.42	385.00	363.10	21.90
0.75	405.00	420.23	-15.23
0.83	400.00	425.37	-25.37
1.42	435.00	432.72	2.28
2.08	450.00	427.16	22.84
2.75	435.00	420.53	14.47
25.00	200.00	247.80	-47.81
50.00	130.00	136.79	-6.79
70.00	100.00	85.03	-14.97
90.00	100.00	52.86	47.14

$$R_1 = 4.09 \text{ h}^{-1}$$

$$R_2 = 0.0237 \text{ h}^{-1}$$

$$A = - 449 \text{ µg/L}$$

Table 5.3. The actual and computed Zn concentrations from the maximum likelihood programme with the values of the constants for Equation 5.20.

Having thus derived k_1 and k_{-1} the question was how to derive a value for k_2 . It is not practical to obtain k_2 from Equation 5.16 because of the uncertainty in estimating M'S and so an alternative approach was adopted. This was a trial and error method in which the two known rate constants were inserted, with estimates of k_2 , into the set of coupled differential equations, Equations 5.11, 5.12 and 5.13. These were then integrated simultaneously using a modified Runge-Kutta technique (Treanor, 1966) in a Fortran-77 computer model with double precision numbers. The amount adsorbed in the 1h ageing period was used as the loosely bound fraction of the particulate Zn and the Zn concentration in solution was followed. The results of the initial modelled desorption, in which only k_1 and k_{-1} were included, are plotted with the actual data in Figure 5.4. This run shows good agreement for the first 2h after which the modelled data has reached a plateau, while the real data begin to decrease. To improve the fit of the long-term data, estimates of k_2 were included in the model to incorporate the solid state diffusion process. The optimum value of k_2 was found to be $4 \times 10^{-2} \text{h}^{-1}$ and this was used to generate the results plotted in Figure 5.5 where there is a good fit to the experimental data. The rate constants evaluated in this section are summarised in Table 5.4.

The value of k_1 obtained here is an order of magnitude higher than that given in Table 5.1. However, the desorption experiments were carried out with $p = 1500 \text{mg/L}$ and normalisation gives $k_1^0 = 4.9 \times 10^4 \text{Ld}^{-1} \text{kg}^{-1}$ which is in good agreement with the values in Table 5.1.

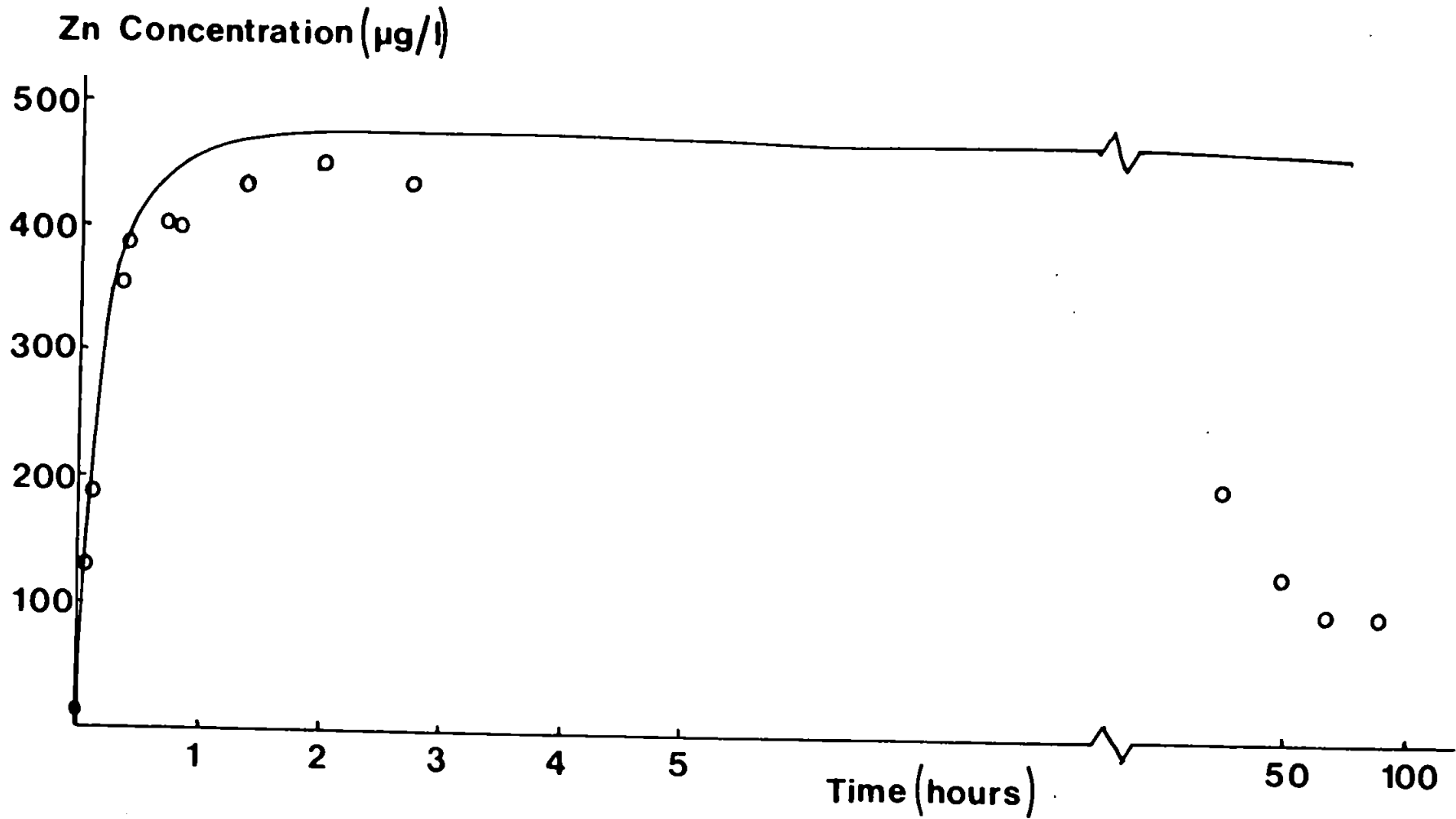


Figure 5.4. A comparison of the measured Zn desorption data (see Figure 4.14) with the results modelled by the integration routine using optimum values for k_1 and k_{-1} only.

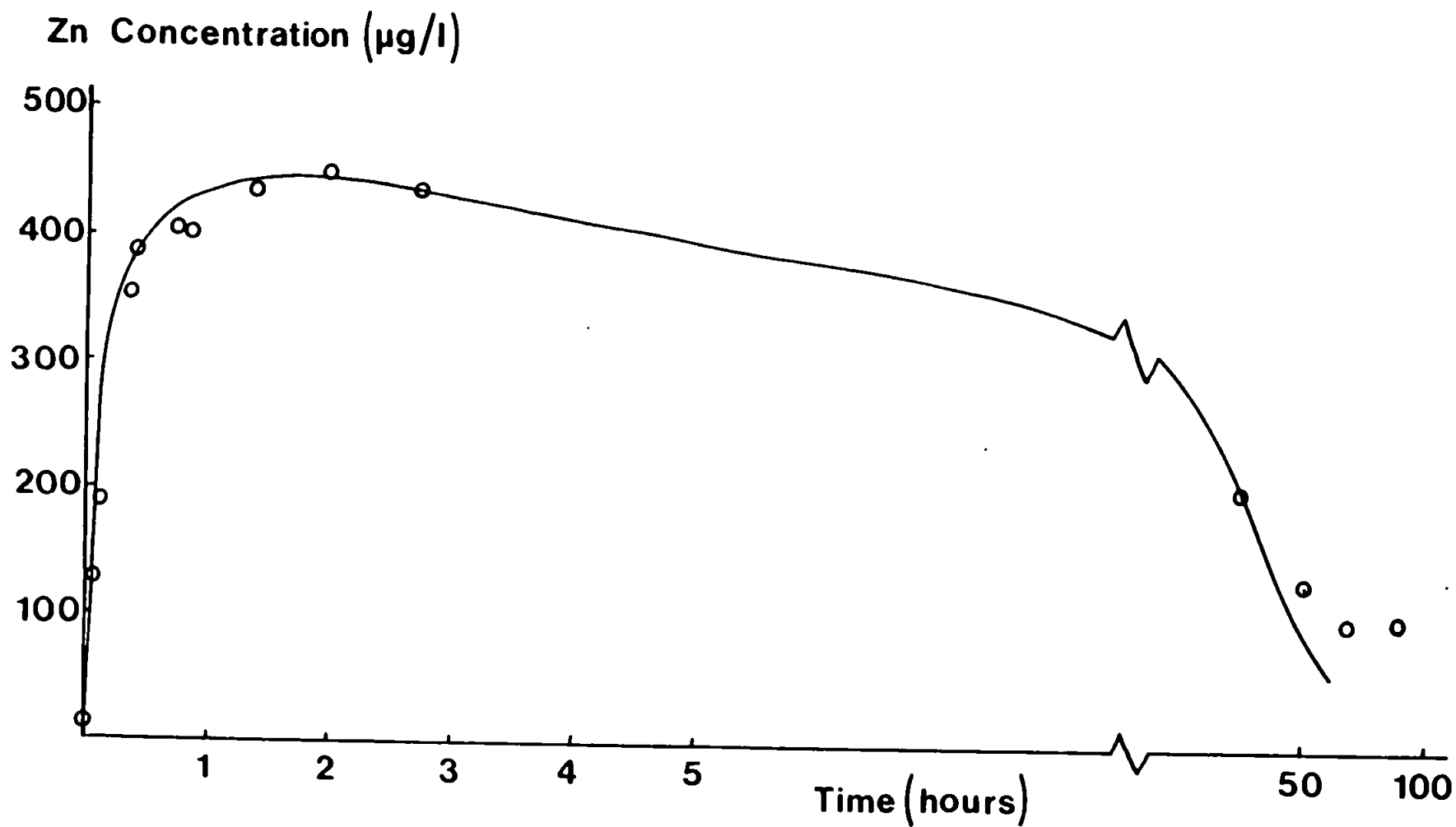


Figure 5.5. A comparison of the measured Zn desorption data (see Figure 4.14) with the results modelled by the integration routine using optimum values k_1 , k_{-1} and k_2 .

	k_1	k_{-1}	k_2
Optimum rate constant (h^{-1})	3.1	0.9	4.0×10^{-2}
Half life (h)	0.22	0.8	17

Table 5.4. The optimum rate constants for the desorption of Zn from the Tamar particles after ageing in contact with Carnon water for 1h at 10°C and pH = 7.

The half lives corresponding with each rate constant are listed in Table 5.4. The significance of this data relates to the injection of metal rich particles into the freshwaters of estuaries. Desorption of the metal from the particles occurs relatively quickly with a half life of about 1h. The solid state diffusion reaction has a half-life of about 1 day and this means that a considerable proportion of the metal will remain attached to the particles. In addition, the k_2 value suggests that in an estuary like the Tamar where the residence time may be approximately 10 days a considerable proportion of the metal may be removed to the matrix of the particles where it may not be available to the biota.

Additional runs with the integration routine were carried out to test the sensitivity of the reaction scheme to variations in the rate constants. The results in Table 5.5 show the percentage change of predicted Zn in solution after adjusting the values of the rate constants k_1 , k_{-1} and k_2 by 20% and of including a value for k_{-2} . These results identify that changing the values of k_1 and k_{-1} alters the solution concentration over the entire 50h period.

However altering the values of k_2 and k_{-2} has little effect on the data during the initial stages of mixing and only after some considerable time will these values become of importance. Nyffeler et al. (1986) suggested that k_{-2} would be less than $2.5 \times 10^{-4} \text{h}^{-1}$ and Table 5.5 shows this would have virtually no effect on these results within two days. The changes in the concentration of loosely bound metal appear to be reflected in the same proportion as the change.

<u>Variable</u>	<u>Optimum</u>	<u>Adjusted</u>	<u>% Change</u>	
<u>(a) Rate Constants (h^{-1})</u>			<u>1h</u>	<u>50h</u>
k_1	3.1	3.7	-13	-19
k_{-1}	0.9	1.1	+15	+23
k_2	0.04	0.05	-0.5	-27
k_{-2}	0	5×10^{-4}	0	+4
k_{-2}	0	5×10^{-3}	0	+31
<u>(b) Loosely Bound metal ($\mu\text{g/L}$)</u>				
[MS]	2100	2520	+20	+20
[MS]	2100	1680	-20	-20

Table 5.5. (a) The effect of individually changing the optimum rate constants k_1 , k_{-1} and k_2 by 20 %, and of adding a k_{-2} value, on the predicted solution concentration of Zn.

(b) The effect of changes in the concentration of loosely bound Zn on the predicted solution concentration of Zn.

5.2.2. Analysis of Cu Desorption.

The same procedure as discussed with respect to Zn was used to determine the rate constants k_1 , k_{-1} and k_2 for the Cu desorption data of Figure 4.17. In Table 5.6 the measured Cu data is shown with the data derived from the maximum likelihood curve fitting routine which was used to determine R_1 , R_2 and A . There was good agreement between the two sets of data and so the values for A , R_1 and R_2 were used with $[\text{CuS}]_0 = 45 \text{ } \mu\text{g particulate Cu/L}$ to calculate k_1 and k_{-1} . These two values were then included in the integrative model to give the profile shown in Figure 5.6. An estimate was then made for k_2 and adjusted to give the optimum fit as shown in Figure 5.7.

The optimum values for the three rate constants are given in Table 5.7. The k_1° calculated from this desorption experiment, $5.9 \times 10^4 \text{ Ld}^{-1} \text{ kg}^{-1}$, is an order of magnitude higher than those determined for the adsorption experiments. It is conceivable that this higher rate constant may be due to the absence of dissolved humic materials in the desorption experiments which, in the adsorption experiments would have been in competition with the particle surface for dissolved Cu. The half-lives for these reactions are also shown in Table 5.7. They suggest there would be very rapid removal to the adsorbed phase via k_1 while the significant desorption of labile Cu would only occur over many hours. However, simultaneously the labile metal will be removed to the matrix bound form over a period of a few days. Therefore it may be expected that on addition of Cu rich particles to an estuary a minimal desorption would be observed and after a few days a large percentage of the Cu would be bound in the

<u>Time (h)</u>	<u>Measured</u> <u>conc.(µg/L)</u>	<u>Computed</u> <u>conc.(µg/L)</u>	<u>Difference (µg/L)</u>
0.00	0.20	0.00	0.20
0.03	0.37	0.21	0.16
0.12	0.60	0.63	-0.03
0.18	0.60	0.88	-0.28
0.33	1.40	1.25	0.15
0.48	1.54	1.46	0.08
0.77	1.70	1.63	0.07
0.88	1.67	1.67	0.01
1.40	1.78	1.69	0.09
2.07	1.64	1.68	-0.04
2.73	1.48	1.66	-0.18
24.17	1.06	1.09	-0.03
50.00	0.79	0.66	0.18
68.33	0.35	0.46	-0.11
86.67	0.36	0.33	0.03

$$R_1 = 3.87 \text{ h}^{-1}$$

$$R_2 = 0.019 \text{ h}^{-1}$$

$$A = -1.746 \text{ µg/L}$$

Table 5.6. The actual and computed Cu concentrations from the maximum likelihood programme with the values of the constants for Equation 5.19.

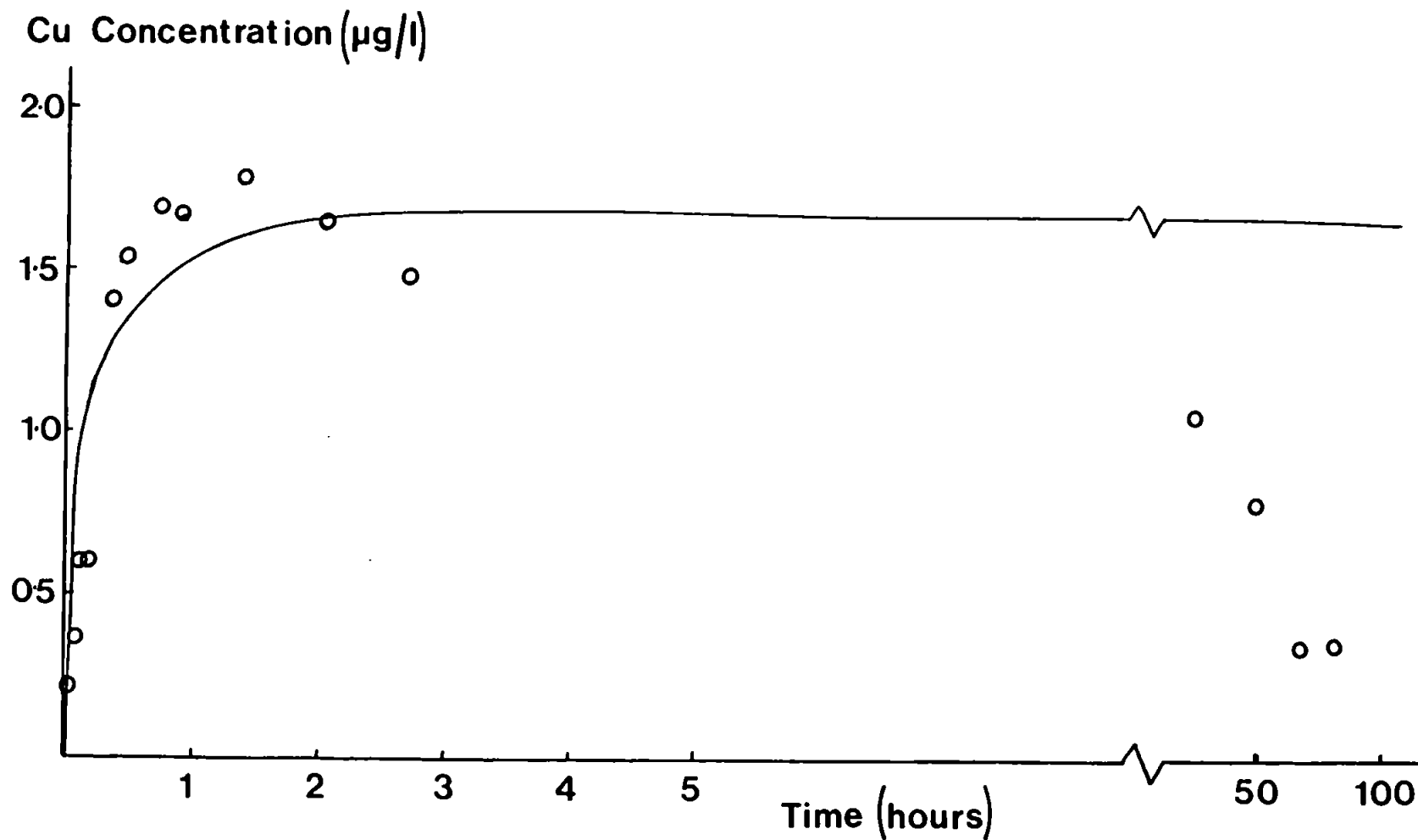


Figure 5.6. A comparison of the measured Cu desorption data (see Figure 4.18) with the results modelled by the integration routine using optimum values for k_1 and k_{-1} only.

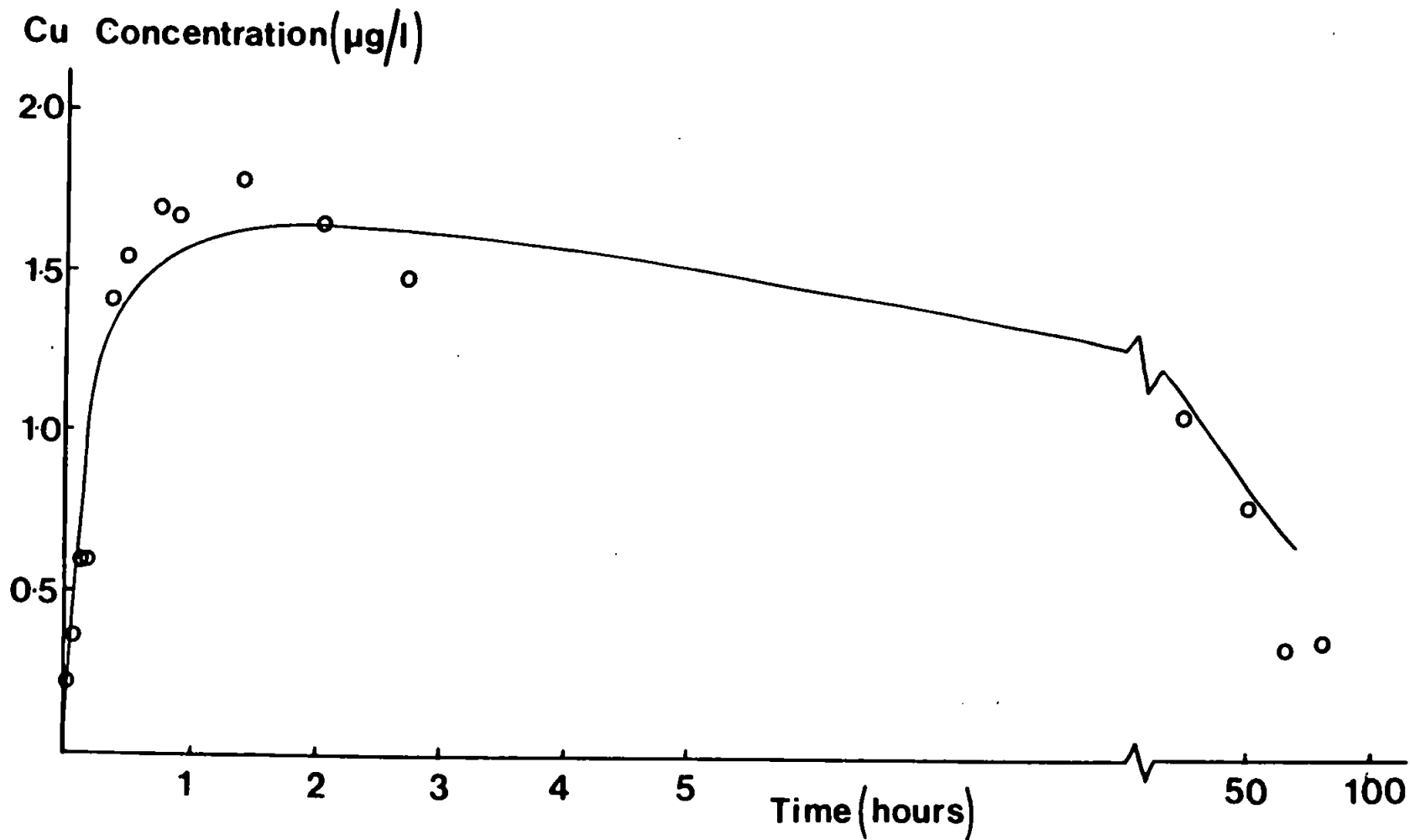


Figure 5.7. A comparison of the measured Cu desorption data (see Figure 4.18) with the results modelled by the integration routine using optimum values for k_1 , k_{-1} and k_2 .

particle matrix.

As in the case of Zn additional model runs were carried out to test the sensitivity of the rate constants, the results of which are listed in Table 5.8. These results are very similar to those for Zn and emphasise that a small change in the rate constants may have a considerable effect on the concentration of Cu in solution.

Variations in k_2 have little effect in the first few hours but become of importance in the later stages. Inclusion of a fairly large k_{-2} has very little effect in the first hour but over the longer term the diffusion out of the pore spaces could be important. A 20% alteration in the value for k_{-1} changes the observed concentration in solution by 20% at 1h and 50h.

	<u>k_1</u>	<u>k_{-1}</u>	<u>k_2</u>
Optimum rate constant (h^{-1})	3.66	0.14	1.5×10^{-2}
Half-life (h)	0.19	4.9	46

Table 5.7. The optimum rate constants and half-lives for the desorption of Cu from Tamar particles which were aged in Carnon water for 1h.

<u>Variable</u>	<u>Optimum</u>	<u>Adjusted</u>	<u>% Change</u>	
<u>(a) Rate Constants(h⁻¹)</u>			<u>1h</u>	<u>50h</u>
k ₁	3.66	4.39	-15	-17
k ₋₁	0.14	0.17	+19	+20
k ₂	0.015	0.018	0	-14
k ₋₂	0	5 x 10 ⁻³	0	+10
k ₋₂	0	5 x 10 ⁻²	0	+60
<u>(b) Loosely Bound metal (µg/L)</u>				
MS	45	54	+19	+20
MS	45	36	-19	-20

Table 5.8(a). The effect of individually changing the optimum rate constants k₁, k₋₁ and k₂ by 20% and of adding a k₋₂ value, on the predicted solution concentration of Cu. (b) The effect of changes in the concentration of loosely bound Cu on the predicted solution concentration of Cu.

5.2.3. Analysis of Carnon Adsorption Data.

The data (especially those for Cu) for these adsorption experiments (see Figures 4.12, 4.13, 4.16 and 4.17) produced the smoothest adsorption profiles in this work. An analysis as carried out for the Tamar adsorption experiments showed that none of these profiles followed simple first or second order kinetics. Using the procedure outlined in Section 5.1.1 the data was tested with the first order reversible reaction scheme but this was also unsuccessful even if only the initial (<2h) results were used. Finally, an attempt was

made to model the data using the two step reaction scheme in Equation 5.10 with the integration routine. The rate constants derived from the Carnon desorption experiments at the same turbidity and the initial dissolved metal concentrations were inserted in the programme with the leachable particulate metal concentration from Table 4.2. These results were not in absolute agreement with the measured data for Zn or Cu and while possible reasons are discussed below more work would be required to fully explain those observations.

For Zn either of these conditions predicted a massive adsorption from an initial concentration of 16000µg/L to around 800µg/L at 50h as opposed to the observed final concentration of 12000µg/L. A better fit to the data might have been expected, despite the system specificity of rate constants, when the agreement between the k_1^* constants derived from the Tamar adsorption and the Carnon desorption is contemplated. The discrepancy between the modelled and real data for Zn could be because, as suggested in Section 4.3.1, the particles are saturated with respect to Zn at a concentration of about 3000µg Zn/g particles. This restraint on further adsorption would not be mirrored in the modelled data.

In contrast, the results for the Cu adsorption analysed in the same way disagree with the observed values by only 50%, which considering the difference in solution conditions is acceptable. It is possible that the absence of competition for Cu from organic material in the desorption experiments carried out in synthetic buffered media, gave higher k_1^* values than would be observed in Carnon River water. Addition of a small amount of dissolved humic material has been shown to reduce the adsorption of Cu to hydrous

ferric oxide (Laxen, 1985) and kaolin (Gupta and Harrison, 1983).

In the concluding chapter to this thesis the relationship between the results of these sorption studies and natural particle morphologies will be examined. The implications of this work on our knowledge of trace metal cycling in the estuarine environment will also be discussed.

CHAPTER SIX

CONCLUSIONS

6.1. The Relationship Between Particle Microstructure and Trace Metal Sorption Processes.

This study has produced the only systematic description of the microstructure of estuarine particulate material. Despite the experimental problems of sample preparation, details of this kind are urgently required in order that a more complete understanding of particle sorption processes is gained. It could be argued that site bonding models of the type produced by Davis and Leckie (1978a) will never be fully developed unless the morphological dimension is included.

Natural particles from the Tamar Estuary were shown to be composed of a complex mixture of quartz, kaolinite, muscovite, illite and chlorite with surface coatings of organic matter and hydrous Fe and Mn oxides. An examination of estuarine particulate material found the BET nitrogen adsorption surface areas to be in the range 8-22m²/g and revealed that these were in general higher for suspended material than sediment material and that the highest surface areas were for suspended particle populations taken from the low salinity turbidity maximum region. No correlation between the leachable Fe (range 6-10mg Fe/g particles) or Mn (range 0.3-0.7 mg Mn/g particles) or the carbon contents (range 4-7%) and the surface areas of suspended samples collected during axial traverses of the estuary was observed. However, there was a greater carbon content for the low surface area

sedimentary material and an increase in surface area was indicated for all samples on removal of surface carbon (by hydrogen peroxide digestion). For samples from an axial survey of the Tamar Estuary, the surface areas all increased after digestion to $25\text{m}^2/\text{g}$. After removal of surface Fe and Mn hydrous oxides (by acetic acid hydroxylamine hydrochloride or EDTA leaching) there was an assimilation of surface area values to a constant low level for each of two axial surveys ($10.2\text{m}^2/\text{g}$ and $16.3\text{m}^2/\text{g}$). This work is corroborated by the comparable observations of Martin et al. (1986) in two French estuaries.

No correlation between particle size and surface area was found. Nitrogen adsorption desorption hysteresis established that the untreated suspended Tamar particles contained slit shaped pores in the size range $<2\text{-}50\text{nm}$ with a mesopore volume of about $1.6 \times 10^{-2} \text{cm}^3/\text{g}$. The leached particles had similar pore characteristics but the digested samples showed evidence of pores in the size range $<2\text{-}200\text{nm}$ and had a mesopore volume of $2.3 \times 10^{-2} \text{cm}^3/\text{g}$. Analysis of suspended material from the Restronguet Creek, which has a high Fe concentration, indicated that it had a high surface area of $125\text{m}^2/\text{g}$, pores in the size range $2\text{-}200\text{nm}$ and a mesopore volume of $3.7 \times 10^{-2} \text{cm}^3/\text{g}$. This study demonstrated that a large proportion of the surface area of these natural samples was within the porous matrix of the particulate material. The only method currently available from which information on these characteristics is readily accessible is gas adsorption on the dried solid.

A review of the literature indicated the enormous difficulty involved in attempting to relate sorption processes

observed in experiments using synthetic media or adsorbents (or both) to the conditions encountered within natural estuarine suspensions. This identified the need to carry out sorption studies with estuarine particles under natural conditions with the natural dissolved metal speciations and concentrations in order that the study would be applicable to the estuarine situation. There are great difficulties associated with the analysis of dissolved trace metals at ambient concentrations in natural waters. The speed of sampling required for a kinetic analysis applicable to estuarine systems is an additional constraint in this type of study. Therefore, a multichannel micro-chelex preconcentration method was designed which enabled the accurate determination of the trace metals Zn and Cu in small samples of natural suspensions extracted from a reaction vessel on a timescale suitable for kinetic analysis.

Adsorption profiles were analysed in this way after addition of well-characterised particles from the turbidity maximum region of the Tamar Estuary to river waters. On mixing the particles with filtered river water, dissolved Zn was removed from solution. In freshwater, the removal was initially rapid followed by a long term adsorption which approached completion after 96h. In brackish water the adsorption process was slower presumably due to competition from major seawater ions. The Cu concentrations in Tamar water appeared to be at a quasi-equilibrium with the particles on mixing. There was a slow adsorption from solution observed for 96h. This quasi-equilibrium could be disturbed by either removing some of the surface bound Cu from the particles or by suspending the particles in Carnon water which has a higher Cu concentration. Under either of these

conditions there was a rapid initial uptake, similar to that seen for Zn, followed by the slower removal. A similar apparently two step adsorption process has been reported in work on the adsorption of phosphate to iron oxides (Madrid and De Arambarri, 1985) and trace metals to marine sediment particles (Nyffeler et al., 1984).

The mechanism proposed to explain these observations was a two step reversible reaction involving equilibration of dissolved metal with the external surface followed by a diffusion controlled tunnelling and equilibration of the internal matrix of the particles as shown in Equation 6.1.



The Tamar suspended particles were shown to have pores in the size range <2-50nm and this is sufficiently large to permit the diffusion of Zn and Cu ions into the matrix. Once the metal is adsorbed it is possible that it could become irreversibly adsorbed across narrow slits or plates and not be available to chemical or biological remobilisation. However observing this is difficult as tracing the metal ions migrating to and from the particle is not experimentally possible and there is much doubt about the specificity of sequential extraction methods.

Kinetic analysis of the trace metal adsorption profiles involving both Tamar particles and water omitted the solid state diffusion step and considered only the reversible surface sorption process. The results for Zn gave k_1° values, for the forward reactions, in the range 6×10^3 - 6×10^4 Ld⁻¹kg⁻¹ which agree

well as shown in Table 6.1, with the values obtained by Nyffeler et al. (1984) for marine sedimentary material in seawater. The analyses in this work indicated a decrease in the Zn adsorption rate constants on increasing the salinity. The data for Cu gave k_1^0 rate constants in the range $5.8 \times 10^3 - 7.2 \times 10^3 \text{ Ld}^{-1}\text{kg}^{-1}$ which were not dependent on salinity.

From the k_1 rate constants the half lives of the dissolved species, with respect to the adsorption processes were calculated. These showed the removal of Zn would occur quickly, with a half life of 1.5h, in freshwater but more slowly in seawater in which the half life was 7h. Dissolved Cu showed slower removal overall with the higher turbidity experiments (400mg/L) giving a half life of 5-7h while in the lower turbidity samples (200mg/L) it had a half life of 12-14h. These results compared extremely well with the field observations of Zn and Cu distributions in the Tamar Estuary by Ackroyd et al. (1986). This comparison provides unequivocal evidence of the coupling of the physical and chemical timescales which occurs in estuaries. The importance of this observation is discussed in more detail in the next section.

The desorption profiles for particles doped by suspension in Carnon River water provided actual evidence for the second step of the proposed two step reaction in Equation 6.1. These identified a discrepancy in the maximum amount of Zn and Cu desorbed by the particles, depending on the time for which they were doped, and the profiles indicated readsorption in the later stages of these experiments. The rate constants from the kinetic analysis of the Zn data are listed in Table 5.1 with the particle characteristics. The

Sample	Rate Constants			Chemical Characteristics			
	k_1^* (Ld ⁻¹ kg ⁻¹)	k_{-1} (d ⁻¹)	k_2 (d ⁻¹)	Surface Area (m ² /g)	Carbon (%)	Fe (mg/g)	Mn (mg/g)
Tamar Suspended Solids ^a	55,000 -5,760	<4.8	- -	14.0	5.1	6.8	0.39
Tamar Suspended Solids ^b	49,600	21.6	0.96	13.1	5.2	7.0	0.38
Narrangansett Bay Sediment ^c	390	0.32	- -	12.9	2.0	2.9	0.04
San Clemente Basin Sediment ^c	660	0.6	- -	10.0	2.0	3.9	0.09
MANOP site H Sediments ^c	10,000	0.07	0.04	110	1.0	- -	3.5

Table 6.1. Comparison of rate constants for Zn uptake onto particles via a two-stage reaction and the associated characteristics of the particles. ^a This work with the rate constants from adsorption experiments; ^b This work with rate constants from desorption experiments; ^c Nyffeler et al. (1984).

k_1^0 constants for Zn compare well with those derived from the Tamar adsorption experiments. The values of Nyffeler et al. (1984) for Zn indicate that k_1^0 is highest for the Manop H site sample which had the largest surface area ($110\text{m}^2/\text{g}$). While this value is still not as high as those observed here it must be remembered that rate constants are system specific and those of Nyffeler et al. (1984) were for the behaviour of added radioisotopes and in a low turbidity seawater suspension. The k_1^0 value for Cu desorption is an order of magnitude higher ($5.9 \times 10^4 \text{Ld}^{-1}\text{kg}^{-1}$) than observed in the adsorption experiments which again identifies the system specificity of rate constants.

Conversion of the k_2 rate constants to half lives indicates that within the flushing time of the Tamar Estuary (7-10 days; Uncles et al., 1983a) a considerable proportion of both Zn (k_2 half life = 17h) and Cu (k_2 half life = 46h) will be adsorbed within the particle matrix. Although it was not possible to calculate k_{-2} , due to experimental restrictions, this work did indicate that desorption from the matrix would be a very slow process and is therefore not likely to be of importance in estuaries, like the Tamar, with relatively short flushing times.

While this study has been unable to identify quantitative relationships between the sorption processes and surface morphology of natural particles it has provided useful techniques for further investigation of these relationships. It may be that the rate of the initial sorption process (i.e. the first step of the reaction scheme) is related to the surface area of the particles while the second slower step is related to the porosity of the particles as Madrid and

De Arambarri (1985) have described with respect to the sorption behaviour of phosphate with synthetic iron oxides. Information such as this, on the parameters which dictate the sorption behaviour of trace metals is essential if any true comprehension of the pathways of trace metals in estuaries is to be attained.

6.2. The Refinement of Hydrodynamic Models of Estuarine Systems.

The long-term aim of studies of heterogeneous chemical reactivity is to enable the pathways of trace metals in the estuarine environment to be accurately predicted. Non-conservative trace metal distributions in estuaries are controlled by both physical and chemical processes and a knowledge of the timescales of these processes will be an essential component of any predictive model.

This work has discovered the strong relationship that exists between the chemical and physical timescales. The results suggested that the short adsorption half life of Zn in freshwater, in the presence of sufficient turbidity, would cause under conditions of low river flow, and relatively long flushing times in the upper segments of the Tamar Estuary, considerable removal of dissolved Zn to the particulate phase. This was directly reflected in the axial distribution profiles of dissolved Zn carried out by Ackroyd et al. (1986). Less removal of dissolved Zn from solution was observed, as would be predicted by the half lives, during conditions of high river flow with a corresponding short flushing time.

The modelling of physical processes in estuaries is reasonably well advanced (Uncles et al., 1985) and hydrodynamic models can be used to predict the distribution of salinity and turbidity with some confidence. Uncles (Personal Communication, 1984) has developed a computer based mathematical model for the Tamar Estuary which is based on a knowledge of the dimensions of the estuary, the river flow, tidal conditions and sediment flux data for various hydrodynamic conditions (Bale et al., 1985). This model was used to predict the conditions prevailing on 30-10-80 which correspond to a survey by

Ackroyd et al. (1986). On this occasion the river flow was $29.0\text{m}^3/\text{s}$ and the tidal range 3m, being two days before neaps. The results of the simulation are compared in Figure 6.1 to the actual results obtained during the survey. The agreement between the calculated and observed profiles is good. This hydrodynamic model can also be used to predict the dispersion of a dissolved constituent in the Tamar Estuary from a point source (i.e. either a pore water infusion or inputs from the banks) assuming conservative mixing and a constant influx to and outflow from the estuary. Thus, conservative mixing is coupled to the hydrodynamics of the estuary. A model calculation was carried out for a point source injection of Zn and is compared in Figure 6.2 to the measured data of dissolved Zn on the 30-10-80 from Ackroyd et al. (1986). While the location of this peak is reasonable (due to the appropriate choice of position for the point source input) this conservative model does not describe the shape of the peak well. This is to be expected as in many cases dissolved Zn is known to behave non-conservatively. A considerably worse comparison would be predicted if the day chosen for comparison of real and simulated values were one on which the river flow was low and thus the Zn removal in the freshwater large.

In order that these non-conservative aspects of trace metal behaviour can be simulated it is necessary to incorporate suitable chemical rate constants in the hydrodynamic model. The particular complexity of this problem lies in the variability of these rate constants which can be mediated (as has been shown in this study) by the prevailing physico-chemical conditions in the estuary. This is a

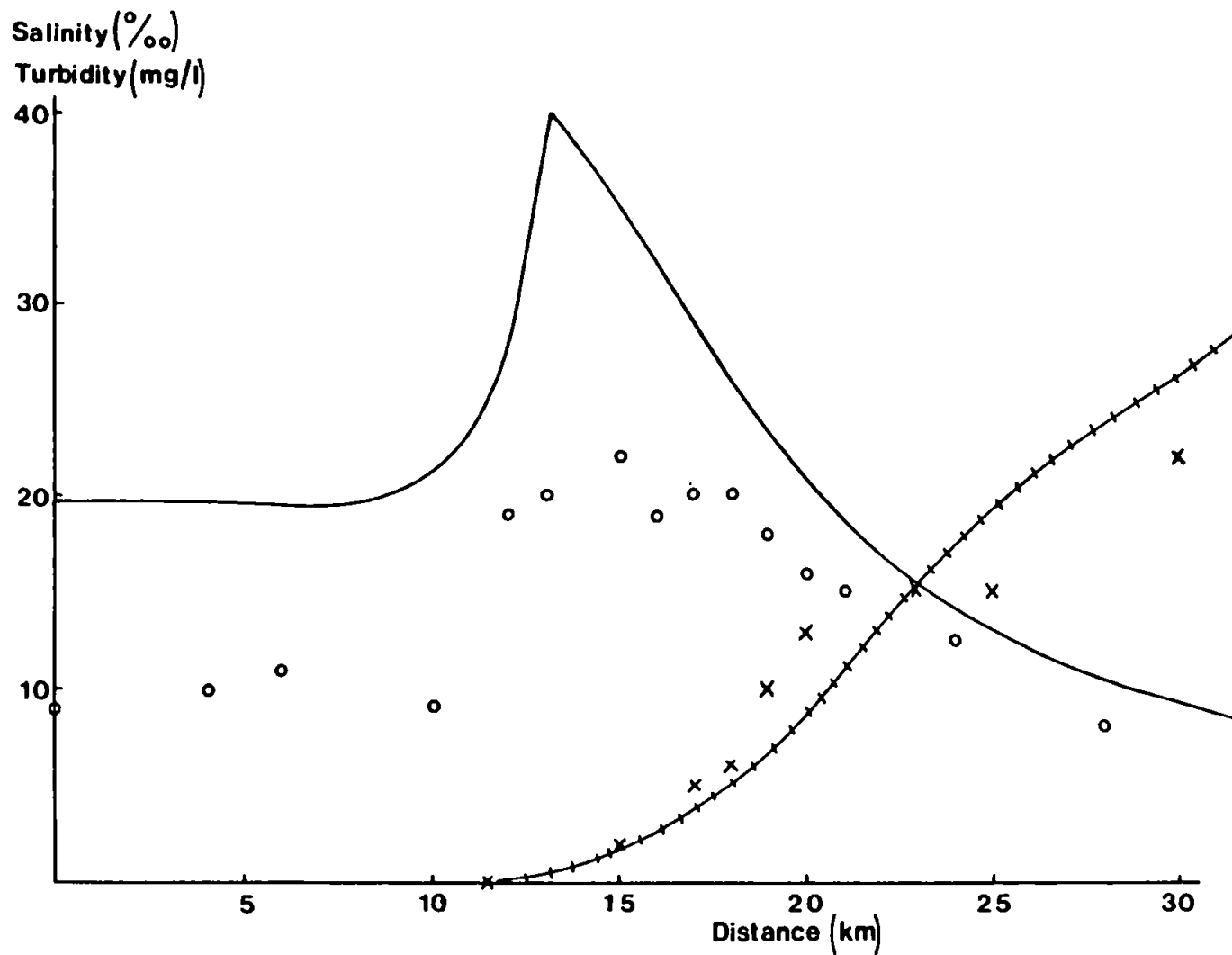


Figure 6.1. A comparison of computed salinity (crossed line) with measured salinity (x) and computed turbidity (full line) with measured turbidity (o) for 30-10-80. Measured data from Ackroyd et al. (1986).

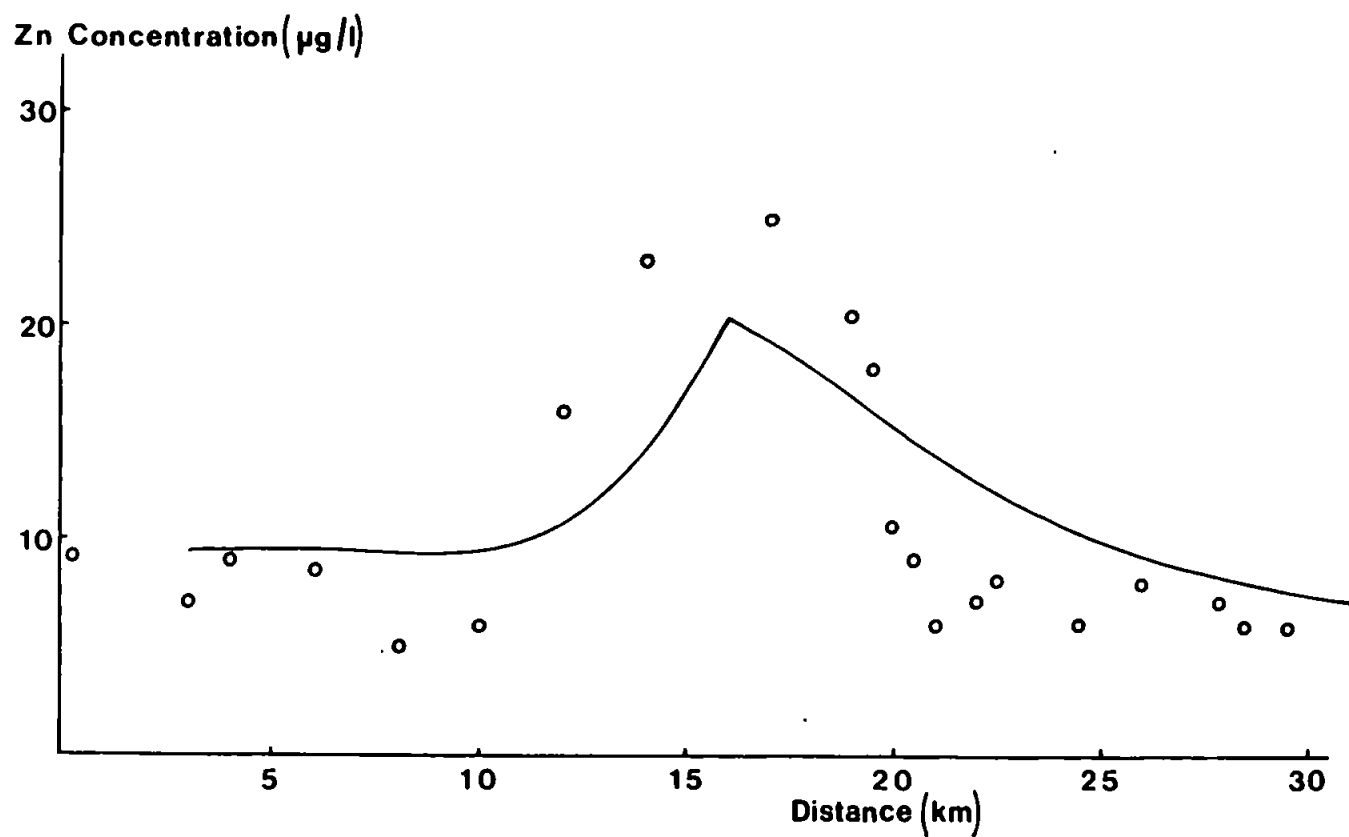


Figure 6.2. A comparison of the computed dissolved Zn concentrations (full line) with measured dissolved concentrations (o) from Ackroyd et al. (1986) for 30-10-80.

problem for both chemists and mathematicians. First the rate constants and their variability must be identified and then these parameters must be mathematically incorporated in the hydrodynamic expressions. This appears to be a daunting task but these difficulties must be overcome if accurate prediction of pollution dispersion in estuaries is to be achieved.

6.3. Recommendations for Future Work.

This study suggests that future work in heterogeneous chemical reactivity should be directed toward the following points:

1. Further investigation of the controls on the surface areas of natural particulate materials. This study has partially identified the influence of organic material and oxides of Fe and Mn on surface morphology. However, the specific role of coatings has to be fully evaluated, (particularly with respect to the interplay between Fe and Mn content) if the microstructures of particles from different estuaries (such as the Loire and Gironde, Martin et al., 1986) are to be compared. It is suggested that in particular the interplay between Fe and Mn content is investigated and that modelling experiments involving the coating of pure clay particles will aid the development of this knowledge.

2. The development of a theoretical basis for determining the microstructures of particles in situ. As yet there is no theoretical nor indeed satisfactory practical method for achieving this as Everett (1982) has pointed out. A knowledge of the in situ surface characteristics would enable a comprehensive study of the actual pore shapes and sizes to be carried out. The value of this would be that the sorption behaviour of trace constituents could be truly related to the particle microstructure as Madrid and De Arambarri (1985) have suggested. The work here is the first of its type using natural estuarine particles and suggests that microstructure is an important component of the sorption process.

3. Further intensive kinetic analyses must be carried out to identify the variability of rate constants with respect to the physico-chemical parameters (importantly salinity, turbidity, pH and temperature) in estuaries. Of particular interest to this work would be to determine whether varying the surface characteristics of the particulate phase would have an identifiable effect on the rate constants. This work is essential if those rate constants are to be used in the refinement of hydrodynamic models of estuaries which can then be used to predict the dispersion of non-conservative materials.

4. The kinetic analysis of the sorption profiles suggests that there are two forms of particulate trace metal; one of which is surface bound the other being matrix bound. The precise location of trace metals in both cases needs to be evaluated in order to determine the bioavailability of adsorbed metals and to assess whether they can be released by estuarine chemical processes.

5. This work has shown that there is pronounced coupling between the chemical and physical time constants at low salinity. The development of predictive mathematical models which must now be of prime importance has to include well-founded chemical time constants.

REFERENCES

- Aarons, A.B. and Stommel, H. (1951). A Mixing-length Theory of Tidal Flushing. *Trans. Amer. Geophys. Union.* 32, 419-421.
- Ackroyd, D.R. (1983). The Removal and Remobilisation of Heavy Metals during Estuarine Mixing. Ph.D. Thesis, Plymouth Polytechnic. 222 pp.
- Ackroyd, D.R., Bale, A.J., Howland, R.J.M., Knox, S., Millward, G.E. and Morris, A.W. (1986). Distributions and Behaviour of Dissolved Cu, Zn and Mn in the Tamar Estuary. *Estuar. Coastal Shelf Sci.* 23, 621-640.
- Adamson, A.W. (1982). *Physical Chemistry of Surfaces*. John Wiley, New York. 664 pp.
- Aggett, J. and Roberts, L.S. (1986). Insight into the Mechanism of Accumulation of Arsenate and Phosphate in Hydro Lake Sediments by Measuring the Rate of Dissolution with Ethylene Diamine Tetra-acetic Acid. *Environ. Sci. Technol.* 20, 183-186.
- Allen, G.P., Salomon, J.C., Bassoullet, P., Du Penhoat, Y. and De Grandpré, C. (1980). Effects of Tides on Mixing and Suspended Sediment Transport in Macrotidal Estuaries. *Sediment Geol.* 26, 69-90.
- Anderson, M.A. and Malotky, D.J. (1979). The Adsorption of Protolysable Anions on Hydrous Oxides at the Isoelectric pH. *J. Colloid Interface Sci.* 72, 413-427.
- Anderson, M.A., Palm-Gennen, M.H., Renard, P.N., Defosse, C. and Rouxhet, P.G. (1984). Chemical and XPS Study of the Adsorption of Iron(III) onto Porous Silica. *J. Colloid Interface Sci.* 102, 328-336.
- Anderson, P.R., Benjamin, M.M. and Ferguson, J.F. (1985). Bulk and Surface Properties of Mixed Al/Fe Hydrous Oxides. *American Chemical Society Symposium Series, Division of Environmental Chemistry.* 25, 312-315.
- D'Anglejan, B.F. and Ingram, R.G. (1984). Near Bottom Variations of Turbidity in the St Lawrence Estuary. *Estuar. Coastal Shelf Sci.* 19, 655-672.
- D'Anglejan, B.F. and Smith, E.C. (1973). Distribution, Transport and Composition of Suspended Matter in the St. Lawrence Estuary. *Can. J. Earth Sci.* 10, 1380-1396.
- Aston, S.R. and Chester, R. (1973). The Influence of Suspended Particles on the Precipitation of Iron in Natural Waters. *Estuar. Coastal Mar. Sci.* 1, 225-231.
- Aston, S.R. and Chester, R. (1976). Estuarine Sedimentary Processes. In "Estuarine Chemistry", (Eds Burton, J.D. and Liss, P.S.) 37-54. Academic Press, London.

- Aston, S.R. and Duursma, E.K. (1973). Concentration Effects on ^{137}Cs , ^{65}Zn , ^{60}Co and ^{106}Ru Sorption by Marine Sediments with Geochemical Implications. *Neth. J. Sea Res.* 6, 225-240.
- Avotins, P.V. (1975). Adsorption and Coprecipitation Studies of Mercury on Hydrous Iron Oxides. Ph.D. Thesis, Stanford University, California. 134 pp.
- Bale, A.J. (1987). The Characteristics and Heterogeneous Chemical Reactivity of Estuarine Suspended Particles. Ph.D. Thesis, Plymouth Polytechnic. 216 pp.
- Bale, A.J., Morris, A.W. and Howland, R.J.M. (1984). Size Distribution of Suspended Material in the Surface Waters of an Estuary as Measured by Laser Fraunhofer Diffraction. In "Transfer Processes in Cohesive Sediment System", (Eds Parker, W.R. and Kinsman, D.J.J.) 75-85. Plenum Press, London.
- Bale, A.J. and Morris, A.W. (1981). Laboratory Simulation of Chemical Processes Induced by Estuarine Mixing: The Behaviour of Iron and Phosphate in Estuaries. *Estuar. Coastal Shelf Sci.* 13, 1-10.
- Bale, A.J., Morris, A.W. and Howland, R.J.M. (1985). Seasonal Sediment Movement in the Tamar Estuary. *Oceanol. Acta.* 8, 1-6.
- Balistrieri, L.S. and Murray, J.W. (1982). The Adsorption of Cu, Pb, Zn and Cd on Goethite from Major Ion Seawater. *Geochim. Cosmochim. Acta.* 46, 1253-1265.
- Barby, D. (1976). Silicas. In "Characterisation of Powder Surfaces", (Eds Parfitt, G.D. and Sing, K.S.W.) 353-425. Academic Press, London.
- Barrow, N.J. (1983). A Mechanistic Model for Describing the Sorption and Desorption of Phosphate by Soil. *J. Soil Sci.* 34, 733-750.
- Benjamin, M.M. and Leckie, J.O. (1981). Competitive Adsorption of Cd, Cu, Zn and Pb on Amorphous Iron Oxyhydroxide, *J. Colloid Interface Sci.* 83, 410-419.
- Van den Berg, C.M.G., Merks, A.G.A. and Duursma, E.K. (1987). Organic Complexation and its Control of Dissolved Concentrations of Copper and Zinc in the Scheldt Estuary. *Estuar. Coastal Shelf Sci.* 24, 785-797.
- Bland, S., Ackroyd, D.R., Marsh, J.G. and Millward, G.E. (1982). Heavy Metal Content of Oysters from the Lynher Estuary UK. *Sci.Total Environ.* 22, 235-241.

- De Boer, J.H., Lippens, B.C., Linsen, B.G., Broekhoff, J.C.P., Van den Heuvel, A. and Osinga, Th.J. (1966). The t-curve of Multimolecular N₂-adsorption. *J. Colloid Interface Sci.* 21, 405-414.
- Bolan, N.S., Barrow, N.J. and Posner, A.M. (1985). Describing the Effect of Time on Sorption of Phosphate by Iron and Aluminium Hydroxides. *J. Soil Sci.* 36, 187-197.
- Borggaard, K. (1983). Effect of Surface Area and Mineralogy of Iron Oxides on their Surface Charge and Anion-Adsorption Properties. *Clays Clay Min.* 31, 230-232.
- Bourg, A.C.M. (1983). Role of Fresh Water/Sea Water Mixing. In "Trace Metals in Sea Water", (Eds Wong, C.S., Boyle, E., Bruland, K.W., Burton, J.D. and Goldberg, E.D.) 195-209. NATO Conf. Series IV-9, Plenum Press, New York.
- Bowden, K.F. (1980). Physical Factors: Salinity, Temperature, Circulation and Mixing Processes. In "Chemistry and Biogeochemistry of Estuaries", (Eds Olausson, E. and Cato, I.) 33-71. John Wiley, Chichester.
- Boyle, E., Collier, R., Dengler, A.T., Edmond, J.M., Ng, A.C. and Stallard, R.F. (1974). On the Chemical Mass Balance in Estuaries. *Geochim. Cosmochim. Acta.* 38, 1719-1728.
- Boyle, E.A., Edmond, J.M. and Sholkovitz, E.R. (1977). The Mechanism of Iron Removal in Estuaries. *Geochim. Cosmochim. Acta.* 41, 1313-1324.
- Boyle, E.A., Huested, S.S. and Grant, B. (1982). The Chemical Mass Balance of the Amazon Plume - II, Copper, Nickel and Cadmium. *Deep Sea Res.* 29, 1355-1364.
- Breen, C., Adams, J.M. and Riekell, C. (1985). Review of the Diffusion of Water and Pyridine in the Interlayer Space of Montmorillonite: Relevance to Kinetics of Catalytic Reactions in Clays. *Clays Clay Min.* 33, 275-284.
- Brezonik, P.L., Brauer, P.A. and Stumm, W. (1976). Trace Metal Analysis by Anodic Stripping Voltammetry: Effect of Sorption by Natural and Model Organic Compounds. *Water Res.* 10, 605-612.
- Brunauer, S., Emmet, P.H. and Teller, E. (1938). Adsorption of Gases in Multimolecular Layers. *J. Amer. Chem. Soc.* 60, 309-319.
- Buckley, J.A., Yoshida, G.A., Wells, N.A. and Aquino, R.T. (1985). Toxicities of Total and Chelex-labile Cadmium to Salmon in Solutions of Natural Water and Diluted Sewage with Potentially Different Cadmium Complexing Capacities. *Water Res.* 19, 1549-1554.

- Burford, J.R., Deshpande, T.L., Greenland, D.J. and Quirk, J.P. (1964). Influence of Organic Materials on the Determination of Specific Surface Areas of Soils. *J. Soil Sci.* 15, 192-201.
- Burton, J.D. (1976). Basic Properties and Processes in Estuarine Chemistry. In "Estuarine Chemistry", (Eds Burton, J.D. and Liss, P.S.) 1-36. Academic Press, London.
- Bye, G.C. and Sing, K.S.W. (1972). Ageing of Flocculated Hydrous Oxides. In "Particle Growth in Suspensions", Monograph 38, 129-145. Soc. Chem. Ind.
- Cabrera, F., De Arambarri, P., Madrid, L. and Toca, C.G. (1981). Desorption of Phosphates from Iron Oxides in Relation to Equilibrium pH and Porosity. *Geoderma*. 26, 203-216.
- Campbell, J.A., Gardner, M.J. and Gunn, A.M. (1985). Short Term Stability of Trace Metals in Estuarine Water Samples. *Anal. Chim. Acta*. 176, 193-200.
- Carter, M.A. (1983). Carbon and Coke Reactivity in Zinc-Lead Blast Furnace Practice. Ph.D. Thesis, Plymouth Polytechnic. 365pp.
- Chau, Y.K. and Lum-Shue-Chan, K. (1974). Determination of Labile and Strongly Bound Metals in Lake Water. *Water Res.* 8, 383-388.
- Chester, R. and Hughes, M.J. (1967). A Chemical Technique for the Speciation of Ferromanganese Minerals, Carbonate Minerals and Adsorbed Trace Elements from Pelagic Sediments. *Chem. Geol.* 2, 249-262.
- Clark, B.D. (1983). The Aims and Objectives of Environmental Impact Assessments. In "Environmental Impact Assessment", (Eds PADC Environmental Impact Assessment and Planning Unit) 3-12. Martinus Nijhoff, Netherlands.
- Clark, R.B. (1986). *Marine Pollution*, Oxford University Press, Oxford. 215 pp.
- Cohen, A.L. (1974). Critical Point Drying. In "Principles and Techniques of Scanning Electron Microscopy", Vol. 1 (Ed. Hayat, S.A.) 44-105. Van Nostrand Reinhold, New York.
- Cranston, R.W. and Inkley, F.A. (1957). Determination of Pore Structures from Nitrogen Adsorption Isotherms. *Advan. Catal.* 9, 143-154.
- Crosby, S.A. (1982). The Interaction of Phosphate with Iron Oxyhydroxides in Simulated Estuarine Conditions. Ph.D. Thesis, Plymouth Polytechnic. 281 pp.

- Crosby, S.A., Glasson, D.R., Cuttler, A.H., Butler, I., Turner, D.R., Whitfield, M. and Millward, G.E. (1983). Surface Areas and Porosities of Fe(III)- and Fe(II)-derived Oxyhydroxides. *Environ. Sci. Technol.* 17, 709-713.
- Crosby, S.A., Millward, G.E., Butler, E.I., Turner, D.R. and Whitfield, M. (1984). Kinetics of Phosphate Adsorption by Iron Oxyhydroxides in Aqueous Systems. *Estuar. Coast. Shelf Sci.* 19, 257-270.
- Danielsson, L-G., Magnusson, B., Westerlund, S. and Zhang, K. (1983). Trace Metals in the Gota River Estuary. *Estuar. Coastal Shelf Sci.* 17, 73-85.
- Davies-Colley, R.J., Nelson, P.O. and Williamson, K.J. (1984). Copper and Cadmium Uptake by Estuarine Sedimentary Phases. *Environ. Sci. Technol.* 18, 491-499.
- Davis, J.A. (1982). Adsorption of Natural Dissolved Organic Matter at the Oxide/Water Interface. *Geochim. Cosmochim. Acta.* 46, 2381-2393.
- Davis, J.A. (1984). Complexation of Trace Metals by Adsorbed Natural Organic Matter. *Geochim. Cosmochim. Acta.* 48, 679-691.
- Davis, J.A. and Leckie, J.O. (1978a). Surface Ionisation and Complexation at the Oxide/Water Interface. *J. Colloid Interface Sci.* 67, 90-107.
- Davis, J.A. Leckie, J.O. (1978b). Effect of Adsorbed Complexing Ligands on Trace Metal Uptake by Hydrous Oxides. *Environ. Sci. Technol.* 12, 1309-1315.
- Dryssen, D. and Wedborg, M. (1980). Major and Minor Elements; Chemical Speciation in Estuarine Waters. In "Chemistry and Biogeochemistry of Estuaries", (Eds Olausson, E. and Cato, I.) 71-121. John Wiley, Chichester.
- Duinker, J.C. (1980). Suspended Matter in Estuaries: Adsorption and Desorption Processes. In "Chemistry and Biogeochemistry of Estuaries", (Eds Olausson, E. and Cato, I.) 121-153. John Wiley, Chichester.
- Duinker, J.C., Van Eck, G.T.M. and Nolting, R.F. (1974). On the Behaviour of Copper, Zinc, Iron and Manganese, and Evidence of Mobilization Processes in the Dutch Wadden Sea. *Neth. J. Sea Res.* 8, 214-239.
- Duinker, J.C., Hillebrand, M.T.J., Nolting, R.F. and Wellershaus, S. (1982a). The River Elbe: Processes Affecting the Behaviour of Metals and Organochlorines during Estuarine Mixing. *Neth. J. Sea Res.* 15, 141-169.

- Duinker, J.C., Hillebrand, M.T.J., Nolting, R.F. and Wellershaus, S. (1982b). The River Weser: Processes Affecting the Behaviour of Metals and Organochlorines During Estuarine Mixing. *Neth. J. Sea Res.* 15, 170-195.
- Duinker, J.C., Hillebrand, M.T.J., Nolting, R.F., Wellershaus, S. and Jacobsen, N.K. (1980). The River Varde Å: Processes Affecting the Behaviour of Metals and Organochlorines during Estuarine Mixing. *Neth. J. Sea Res.* 14, 237-267.
- Duinker, J.C. and Nolting, R.F. (1976). Distribution Model for Particulate Trace Metals in the Rhine Estuary, Southern Bight and Dutch Wadden Sea. *Neth. J. Sea Res.* 10, 71-102.
- Duinker, J.C. and Nolting, R.F. (1977). Dissolved and Particulate Trace Metals in the Rhine Estuary and Southern Bight. *Mar. Poll. Bull.* 8, 65-71.
- Duinker, J.C. and Nolting, R.F. (1978). Mixing, Removal and Remobilisation of Trace Metals in the Rhine Estuary. *Neth. J. Sea Res.* 12, 205-223.
- Duinker, J.C., Wollast, R. and Billen, G. (1979). Behaviour of Manganese in the Rhine and Scheldt Estuaries II, Geochemical Cycling. *Estuar. Coastal Mar. Sci.* 9, 727-738.
- Dutta, R. and Gupta, V.K. (1974). Surface area of Indian Clay Minerals. *J. Indian Chem. Soc.* 51, 972.
- Dyer, K.R. (1972). Sedimentation in Estuaries. In "The Estuarine Environment", (Eds. Barnes, R.S.K. and Green, J.) 10-32. Applied Science, London.
- Dyer, K.R. (1973). *Estuaries: A Physical Introduction*. John Wiley, London. 140 pp.
- Dyer, K.R. (1979). Estuaries and Estuarine Sedimentation. In "Estuarine Hydrography and Sedimentation", (Ed. Dyer, K.R.) 4-18. Cambridge University Press, Cambridge.
- Eastman, K.W. and Church, T.M. (1984). Behaviour of Iron, Manganese, Phosphate and Humic Acid During Mixing in a Delaware Salt Marsh Creek. *Estuar. Coastal Shelf Sci.* 18, 447-458.
- Eisma, D (1986). Flocculation and Deflocculation of Suspended Matter in Estuaries. *Neth. J. Sea. Res.* 20, 183-199.
- Eisma, D., Boon, J., Groenewegen, R., Ittekkoot, V., Kalf, J. and Mook, M.G. (1983). Observations on Macro-aggregates, Particle Size and Organic Composition of Suspended Matter in the Ems Estuary. *Mitt. Geol. Palaont. Inst. Univ. Hamburg.* 55, 295-314.
- Eisma, D., Van der Gaast, S.J., Martin, J.M. and Thomas, A.J. (1978). Suspended Matter and Bottom Deposits of the Orinoco Delta: Turbidity, Mineralogy and Elementary Composition. *Neth. J. Sea Res.* 12, 224-251.

- Egashira, K. and Aomine, S. (1974). Effects of Drying and Heating on the Surface Area of Allophane and Imogolite. *Clay Sci.* 4, 231-242.
- Elderfield, H. and Hepworth, A. (1975). Diagenesis, Metals and Pollution in Estuaries. *Mar. Poll. Bull.* 6, 85-87.
- Elderfield, H., Hepworth, A., Edwards, P.N. and Holliday, L.M. (1979). Zinc in the Conwy River and Estuary. *Estuar. Coastal Mar. Sci.* 9, 403-422.
- Evans, D.W. and Cutshall, N.H. (1973). Effects of Ocean Water on the Soluble Suspended Distribution of Columbia River Radionuclides. *Proceedings on Radioactive Contamination of the Marine Environment*, Seattle. 125-140. IAEA, Vienna.
- Everett, D.H. (1982). Adsorption from Solution and Gas Adsorption. In "Adsorption at the Gas-solid and Liquid-solid Interface", (Eds. Roquerol, J. and Sing, K.S.W.) 1-20. Elsevier, London.
- Fairbridge, R.W. (1980). The Estuary: its Definition and Geodynamic Cycle. In "Chemistry and Biogeochemistry of Estuaries", (Eds. Olausson, E. and Cato, I.) 1-37. John Wiley, Chichester.
- Faisst, W.K. (1980). Characterisation of Particles in Digested Sewage Sludge. In "Particulates in Water: Characterisation, Effects and Removal", (Eds. Kavanaugh, M.C. and Leckie, J.O.) 259-282. Amer. Chem. Soc., Washington.
- Festa, J.F. and Hansen, D.V. (1978). Turbidity Maxima in Partially Mixed Estuaries: A Two Dimensional Numerical Model. *Estuar. Coastal Mar. Sci.* 7, 347-359.
- Florence, T.M. (1977). Trace Metal Species in Fresh Waters. *Water Res.* 11, 681-687.
- Folk, R.L. (1966). A Review of Grainsize Parameters. *Sedimentology* 6, 73-93.
- Förstner, U. (1980). Inorganic Pollutants, Particularly Heavy Metals in Estuaries. In "Chemistry and Biogeochemistry of Estuaries", (Eds. Olausson, E. and Cato, I.) 307-348. John Wiley, Chichester.
- Fox, L.E. and Wofsy, S.C. (1983). Kinetics of Removal of Iron Colloids from Estuaries. *Geochim. Cosmochim. Acta.* 47, 211-216.
- Freely, R.A., Massoth, G.J., Baker, E.T., Gendron, J.F., Paulson, A.J. and Crecelius, E.A. (1986). Seasonal and Vertical Variations in the Elemental Composition of Suspended and Settling Particulate Matter in Puget Sound, Washington. *Estuar. Coastal Shelf Sci.* 22, 215-239.

- Garcia-Miragaya, J., Cardenas, R. and Page, A.L. (1986). Surface Loading Effect on Cd and Zn Sorption by Kaolinite and Montmorillonite from Low Concentration Solutions. *Water Air Soil Poll.* 27, 181-190.
- Gardiner, J. and Stiff, M.J. (1975). The Determination of Cadmium, Lead, Copper and Zinc in Ground Water, Estuarine Water, Sewage and Sewage Effluent by Anodic Stripping Voltammetry. *Water Res.* 9, 517-523.
- Van Der Geissen, A.A. (1966). The Structure of Fe(III) Oxide Hydrated Gels. *J. Inorganic Nuclear Chem.* 28, 2155-2159.
- Gerlach, S.A. (1981). *Marine Pollution*. Springer-Verlag, Berlin. 218pp.
- GESAMP (1976). IMCO/FAO/UNESCO/WMO/IAEA/UN. Joint Group of Experts on the Scientific Aspects of Marine Pollution; Review of Harmful Substances Rep. Stud. GESAMP2, 80 pp.
- Gibbs, R.J. (1973). Mechanisms of Trace Metal Transport in Rivers. *Science.* 180, 71-73.
- Gibbs, R.J. (1974). Principles of Studying Suspended Materials in Water. In "Suspended Solids in Water", (Ed. Gibbs, R.J.) 3-15. Plenum Press, London.
- Gibbs, R.J. (1986). Segregation of Metals by Coagulation in Estuaries. *Mar. Chem.* 18, 149-159.
- Giles, C.H., Harward, D.C., McMillan, W., Smith, T. and Wilson, R. (1979). A Comparison of Mercury Prosimetry, Gas Adsorption and Dye Adsorption Data on a Series of Mesoporous Silica Gel Materials. In "Characterisation of Porous Solids", (Eds. Gregg, S.J., Sing, K.S.W. and Stoeckli, H.F.) 267-284. Chem. Soc. Ind., London.
- Glasson, D.R. and Linstead-Smith, D.E.B. (1973). Vacuum Balance Studies of the Formation and Reactivity of some Synthetic and Natural Phosphates. In "Progress in Vacuum Microbalance Techniques", Volume 2, (Eds. Bevan, S.C., Gregg, S.J. and Parkyns, N.D.) 209-214. Heyden, London.
- Glegg, G.A., Titley, J.G., Glasson, D.R., Millward, G.E. and Morris, A.W. (1987). The Microstructures of Estuarine Particles. In "Particle Size Analysis - 1985", (Ed. Lloyd, J.P.) 591-597. John Wiley, Chichester.
- Gregg, S.J. and Sing, K.S.W. (1982). *Adsorption, Surface Area and Porosity*. 2nd Edition. Academic Press, London. 303 pp.
- Greenland, D.J. and Quirk, J.P. (1962). Surface Area of Soil Colloids. *Trans. Comm. IV and V Int. Soc. Soil Sci.* New Zealand. 79-87.

- De Groot, A.J., Salomons, W. and Allersma, E. (1976). Processes Affecting Heavy Metals in Estuarine Sediments. In "Estuarine Chemistry", (Eds. Burton, J.D. and Liss, P.J.) 131-159. Academic Press, London.
- Gupta, G.C. and Harrison, F.L. (1982). Effect of Humic Acid on Copper Adsorption by Kaolin. *Water Air Soil Poll.* 17, 357-360.
- Guy, R.D., Chakrabarti, C.L. and McBain, D.C. (1978). An Evaluation of Extraction Techniques for the Fractionation of Copper and Lead in Model Sediment Systems. *Water Res.* 12, 21-24.
- Haas, C.N. and Horowitz, N.D. (1986). Adsorption of Cadmium to Kaolinite in the Presence of Organic Material. *Water Air Soil Poll.* 27, 131-140.
- Hansen, D.V. and Ratray, J.M. (1966). New Dimensions in Estuary Classification. *Limnol. Oceanogr.* 11, 319-326.
- Hansmann, D.D., Hackley, V.A. and Anderson, M.A. (1985). Aggregation and Adsorption Interdependence in Heterogeneous Systems. American Chemical Society Symposium, Division of Environmental Chemistry. 25, 412-413.
- Harris, J.R.W., Bale, A.J., Bayne, B.L., Mantoura, R.F.C., Morris, A.W., Nelson, L.A., Radford, P.J., Uncles, R.J., Weston, S.A. and Widdows, S.J. (1983/4). A Preliminary Model of the Dispersal and Biological Effect of Toxins in the Tamar Estuary, England. *Ecol. Model.* 22, 253-284.
- Holliday, L.M. and Liss, P.S. (1976). The Behaviour of Dissolved Iron, Manganese and Zinc in the Beaulieu Estuary, S. England. *Estuar. Coastal Mar. Sci.* 4, 349-353.
- Van Den Hul, H.J. and Lyklema, J. (1968). Determination of Specific Surface Areas of Dispersed Materials: Comparison of the Negative Adsorption Method with some Other Methods. *J. Amer. Chem. Soc.* 90, 3010-3015.
- Hunter, K.A. (1980). Microelectrophoretic Properties of Natural Surface-active Organic Matter in Coastal Seawater. *Limnol. Oceanogr.* 25, 807-822.
- Hunter, K.A. and Liss, P.S. (1979). The Surface Charge of Suspended Particles in Estuarine and Coastal Rivers. *Nature.* 282, 823-825.
- Hunter, K.A. and Liss, P.S. (1982). Organic Matter and the Surface Charge of Suspended Particles in Estuarine Waters. *Limnol. Oceanogr.* 27, 322-335.
- Jackson, M.L. (1958). *Soil Chemical Analysis*. Constable and Co., London. 485 pp.

- James, A.E. (1987). Rheology and Floc Structure. Paper presented at NERC Geocolloids Group Meeting "Particle Aggregation Processes in the Natural Environment", University of Lancaster.
- Johnson, C.A. (1986). The Regulation of Trace Element Concentrations in River and Estuarine Waters Contaminated with Acid Mine Drainage: The Adsorption of Cu and Zn on Amorphous Fe Oxyhydroxides. *Geochim. Cosmochim. Acta.* 50, 2433-2438.
- Keeney-Kennicutt, W.L. and Presley, B.J. (1986). The Geochemistry of Trace Metals in the Brazos River Estuary. *Estuar. Coastal Shelf Sci.* 22, 459-477.
- Ketchum, B.H. (1951). The Flushing of Tidal Estuaries. *Sewage Ind. Wastes.* 23, 198-209.
- Kinniburgh, D.G. (1985). ISOTHERM-A Computer Programme for Analysing Adsorption Data. Report WD/ST/85/02; British Geological Survey. Wallingford.
- Kinniburgh, D.G. and Jackson, M.L. (1982). Concentration and pH Dependence of Calcium and Zinc Adsorption by Iron Hydrous Oxide Gel. *Soil Sci. Soc. Amer. J.* 46, 56-61.
- Kinniburgh, D.G., Jackson, M.L. and Syers, J.K. (1976). Adsorption of Alkaline Earth, Transition and Heavy Metal Cations by Hydrous Oxide Gels of Iron and Aluminium. *Soil Sci. Soc. Amer. J.* 40, 796-799.
- Knox, S., Turner, D.R., Dickson, A.G., Liddicoat, M.I., Whitfield, M. and Butler, E.I. (1981). Statistical Analysis of Estuarine Profiles; Applications to Mn and NH₄ in the Tamar Estuary. *Estuar. Coastal Shelf Sci.* 13, 357-371.
- Kolthoff, I.M. and Bowers, R.C. (1954). Studies on Ageing and Coprecipitation- XLIV. Aging of Silver Bromide in the Colloidal State. *J. Amer. Chem. Soc.* 76, 1503-1515.
- Kranck, K. (1981). Particle Matter Grain-size Characteristics and Flocculation in a Partially Mixed Estuary. *Sedimentology.* 28, 107-114.
- Krom, M.D. and Sholkovitz, E.R. (1978). The Association of Iron and Manganese with Organic Matter in Anoxic Pore Waters. *Geochim. Cosmochim. Acta.* 42, 607-611.
- Laxen, D.P.H. (1985). Trace Metal Adsorption/Coprecipitation on Hydrous Ferris Oxide Under Realistic Conditions. *Water Res.* 19, 1229-1236.
- Li, Y-H., Burkhardt, L., Buchholtz, M., O'Hara, P. and Santschi, P.H. (1984a). Partition of Radiotracers between Suspended Particles and Seawater. *Geochim. Cosmochim. Acta.* 48, 2011-2019.

- Li, Y-H., Burkhardt, L. and Teraoka, H. (1984b). Desorption and Coagulation of Trace Elements during Estuarine Mixing. *Geochim. Cosmochim. Acta.* 48, 1877-1884.
- Lijklema, L. (1980). Interaction of Orthophosphate with Iron (III) and Aluminium Hydroxides. *Environ. Sci. Technol.* 14, 537-541.
- Liss, P.S. (1976). Conservative and Non-conservative Behaviour of Dissolved Constituents during Estuarine Mixing. In "Estuarine Chemistry", (Eds. Burton, J.D. and Liss, P.S.) 93-127. Academic Press, London.
- Lion, L.W., Altmann, R.S. and Leckie, J.O. (1982). Trace Metal Adsorption Characteristics of Estuarine Particulate Matter: Evaluation of Contributions of Fe/Mn Oxide and Organic Surface Coatings. *Environ. Sci. Technol.* 16, 660-666.
- Lippens, B.C., Linsen, B.G. and De Boer, J.H. (1964). Studies on Pore Systems in Catalysts 1. The Adsorption of Nitrogen; Apparatus and Calculation, *J. Catalysis.* 3, 32-37.
- Lockwood, S.J. (1986). Fisheries Interests in Relation to the Management of Estuaries. Presented to the European Intensive Course "Evaluation of Criteria for the Management of Estuarine Systems", The University, Southampton.
- Loring, D.H. (1981). Potential Bioavailability of Metals in Eastern Canadian Estuarine and Coastal Sediments. *Rapp. P.-V. Réun. Cons. (Perm) Int. Explor. Mer.* 181, 93-101.
- Loring, D.H. (1982). Geochemical Factors Controlling the Accumulation and Dispersal of Heavy Metals in the Bay of Fundy Sediments. *Can. J. Earth Sci.* 19, 930-944.
- Loring, D.H., Rantala, R.T.T., Morris, A.W., Bale, A.J. and Howland, R.J.M. (1983). Chemical Composition of Suspended Particles in an Estuarine Turbidity Maximum Zone. *Can. J. Fish. Aquat. Sci.* 40, (supplement no. 1) 201-206.
- Luoma, S.N. and Bryan, G.W. (1981). A Statistical Assessment of the Form of Trace Metals in Oxidised Estuarine Sediments Employing Chemical Extractants. *Sci. Tot. Environ.* 17, 165-196.
- Lyman, J. and Fleming, R.H. (1940). Composition of Seawater. *J. Mar. Res.* 3, 134-146.
- Madrid, L. and De Arambarri, P. (1985). Adsorption of Phosphate by Two Iron Oxides in Relation to their Porosity. *J. Soil. Sci.* 36, 523-530.
- Mantoura, R.F.C., Dickson, A. and Riley, J.P. (1978). The Complexation of Metals with Humic Materials in Natural Waters. *Estuar. Coastal Mar. Sci.* 6, 387-408.

- Mantoura, R.F.C. and Morris, A.W. (1983). Measurement of Chemical Distributions and Processes. In "Practical Procedures for Estuarine Studies", (Ed. Morris, A.W.) 55-100. NERC, Swindon.
- Marsh, J.G., Crosby, S.A., Glasson, D.R. and Millward, G.E. (1984). BET Nitrogen Adsorption Studies of Iron Oxides from Natural and Synthetic Sources. *Thermochimica Acta.* 82, 221-229.
- Martin, J.M. and Letolle, R. (1979). Oxygen-18 in Estuaries. *Nature.* 282, 292-294.
- Martin, J.M. and Meybeck, M. (1979). Elemental Mass Balance of Material Carried by Major World Rivers. *Mar. Chem.* 7, 173-206.
- Martin, J.M., Mouchel, J.M. and Nirel, P. (1986). Some Recent Developments in the Characterisation of Estuarine Particles. *Water Sci. Technol.* 18, 83-93
- Martin, J.M. and Whitfield, M. (1983). The Significance of the River Input of Chemical Elements to the Oceans. In "Trace Metals in Seawater", (Eds. Wong, C.S., Boyle, E., Bruland, K.W., Burton, J.D. and Goldberg, E.D.) 265-296. Plenum Press, New York.
- Mayer, L.M. (1982). Aggregation of Colloidal Iron during Estuarine Mixing: Kinetics, Mechanisms and Seasonality. *Geochim. Cosmochim. Acta.* 46, 2527-2535.
- Mikhail, R.Sh., Guindy, N.M. and Hanafi, S. (1979). Vapour Adsorption on Expanding and Non-expanding Clay Minerals. *J. Colloid Interface Sci.* 70, 282-292.
- Millero, F.J. (1969). The Partial Molal Volumes of Ions in Seawater. *Limnol. Oceanogr.* 14, 376-385.
- Millward, G.E. and Burton, J.D. (1975). Association of Mercuric Ions and Humic Acid in Sodium Chloride Solution. *Mar. Sci. Comm.* 1, 15-26.
- Millward, G.E., Glegg, G.A., Glasson, D.R., Morris, A.W. and Bale, A.J. (1985). The Microstructures of Estuarine Particles and their Role in Heterogeneous Chemical Reactivity. American Chemical Society Symposium Series, Division of Environmental Chemistry. 25, 418-420.
- Millward, G.E. and Marsh, J.G. (1986). Dissolved Arsenic Behaviour in Estuaries Receiving Acid Mine Wastes. In "Chemicals in the Environment", (Eds. Lester, J.N., Perry, R. and Sterritt, R.M.) 470-477. Selper, London.
- Millward, G.E. and Moore, R.M. (1982). The Adsorption of Cu, Mn and Zn by Iron Oxyhydroxides in Model Estuarine Solutions. *Water Res.* 16, 981-985.

- Millward, G.E. and Titley, J.T. (1985). The Microstructures of Estuarine Particles. An Interim Report for NERC Research Grant GR3/5712. 22 pp.
- Moore, R.M., Burton, J.D., Williams, P.J. Le B. and Young, M.L. (1979). The Behaviour of Dissolved Organic Material, Iron and Manganese in Estuarine Mixing. *Geochim. Cosmochim. Acta.* 43, 919-926.
- Moore, R.M. and Millward, G.E. (1987). The Kinetics of Reversible Th Reactions with Marine Particles. *Geochim. Cosmochim. Acta.* Submitted for Publication.
- Morris, A.W. (1983). Strategy for Practical Estuarine Studies. In "Practical Procedures for Estuarine Studies", (Ed. Morris, A.W.) 1-18. NERC, Swindon.
- Morris, A.W. (1986). Removal of Trace Metals in the Very Low Salinity Region of the Tamar Estuary, England. *Sci. Tot. Environ.* 49, 297-304.
- Morris, A.W. and Bale, A.J. (1979). Effects of Rapid Precipitation of Dissolved Manganese in River Water on Estuarine Manganese Distributions. *Nature.* 279, 318-319.
- Morris, A.W., Bale, A.J. and Howland, R.J.M. (1981). The Dynamics of Estuarine Manganese Cycling. *Estuar. Coastal Mar. Sci.* 14, 175-192.
- Morris, A.W., Bale, A.J. and Howland, R.J.M. (1982a). Chemical Variability in the Tamar Estuary. *Estuar. Coastal Shelf Sci.* 14, 649-661.
- Morris, A.W., Bale, A.J., Howland, R.J.M., Millward, G.E., Ackroyd, D.R., Loring, D.H. and Rantala, R.T.T. (1986). Sediment Mobility and its Contribution to Trace Metal Cycling and Retention in a Macrotidal Estuary. *Water Sci. Technol.* 18, 111-119.
- Morris, A.W., Loring, D.H., Bale, A.J., Howland, R.J.M., Mantoura, R.F.C. and Woodward, E.M.S. (1982b). Particle Dynamics, Particulate Carbon and the Oxygen Minimum in an Estuary. *Oceanol. Acta.* 5, 349-353.
- Morris, A.W., Mantoura, R.F.C., Bale, A.J. and Howland, R.J.M. (1978). Very Low Salinity Regions of Estuaries: Important Sites for Chemical and Biological Reactions. *Nature.* 274, 678-680.
- Mouvet, C. and Bourg, A.C.M. (1983). Speciation (Including Adsorbed Species) of Copper, Lead, Nickel and Zinc in the Meuse River. *Water Res.* 17, 641-649.
- Murray, J.W. (1979). Iron Oxides. In "Marine Minerals", Volume 6, (Ed. Burns, R.G.) 47-98. Amer. Min. Soc. Short Course Notes.

- McKay, D.W. (1986). The Clyde: A Management Success Story. Presented to the European Intensive Course "Evaluation of Criteria for the Management of Estuarine Systems", The University, Southampton.
- McLusky, D.S. (1981). The Estuarine Ecosystem. Blackie, London. 150pp.
- Neihof, R.A. and Loeb, G.I. (1972). The Surface Charge of Particulate Matter in Seawater. *Limnol. Oceanogr.* 17, 7-16.
- Nelson, A. and Donkin, P. (1985). Processes of Bioaccumulation: The Importance of Chemical Speciation. *Mar. Poll. Bull.* 16, 164-169.
- Nelson, A. and Mantoura, R.F.C. (1984a). Anodic Stripping Voltammetry of Copper in Estuarine Media. In "Complexation of Trace Metals in Natural Waters", (Eds. Kramer, C.J.M. and Duinker, J.C.) 119-130. Martinus Nijhoff/Dr W.Junk Publishers, Netherlands.
- Nelson, A. and Mantoura, R.F.C. (1984b). Voltammetry of Copper Species in Estuarine Waters III. *J. Electroanal. Chem.* 164, 265-272.
- Nyffeler, U.P., Li, Y-H. and Santschi, P.H. (1984). A Kinetic Approach to Describe Trace-Element Distribution between Particles and Solution in Natural Aquatic Systems. *Geochim. Cosmochim. Acta.* 48, 1513-1522.
- Olsen, S., Pessenda, L.C.R., Růžicka, J. and Hansen, E.H. (1983). Combination of Flow Injection Analysis with Flame Atomic Absorption Spectrophotometry: Determination of Trace Amounts of Heavy Metals in Polluted Seawater. *Analyst.* 108, 905-917.
- Officer, C.B. (1980). Discussion of the Turbidity Maximum in Partially Mixed Estuaries. *Estuar. Coastal Mar. Sci.* 10, 239-246.
- Olausson, E. and Cato, I. (1980). (Eds.) Chemistry and Biogeochemistry of Estuaries. John Wiley, Chichester. 452pp.
- Van Olphen, H. (1976). Clays, In "Characterisation of Powder Surfaces", (Eds. Parfitt, G.D. and Sing, K.S.W.) 428-455. Academic Press, London.
- Parfitt, G.D. and Sing, K.S.W. (1976). (Eds.) Characterisation of Powder Surfaces. Academic Press, London. 464 pp.
- Perdue, E.M., Beck, K.C. and Reuter, J.H. (1976). Organic Complexes of Iron and Aluminium in Natural Waters. *Nature.* 260, 418-420.

- Ponec, V., Knor, Z. and Cerny, S. (1974). Adsorption onto Solids. Butterworths, London. 693 pp.
- Pritchard, D.W. (1967). What is an Estuary: a Physical Viewpoint. In "Estuaries", (Ed. Lauff, G.H.) 3-6. Amer. Assoc. Adv. Sc. Washington.
- Quirk, J.P. (1978). Some Physico-Chemical Aspects of Soil Structure - A Review. In "Modification of Soil Structure", (Eds. Emerson, W.W., Bond, R.D. and Dexter, A.R.) 3-16. John Wiley, Chichester.
- Rainbow, P.S. (1985). Accumulation of Zn, Cu and Cd by Crabs and Barnacles. *Estuar. Coastal Shelf Sci.* 21, 669-686.
- Reid, J.D. and McDuffie, B. (1981). Sorption of Trace Cadmium on Clay Minerals and River Sediments: Effects of pH and Cd(II) Concentrations in a Synthetic River Water Medium. *Water Air Soil Poll.* 15, 375-386.
- Rhodes, M. (1985). An Investigation into the Variability over a Spring to Neap Tidal Cycle of the Organic and Total Carbon Content and Size of Suspended Particles in the Turbidity Maximum Zone of the Tamar Estuary. Project Report, Plymouth Polytechnic. 49 pp.
- Riley, J.P. (1975). Analytical Chemistry of Seawater. In "Chemical Oceanography", Volume 3, (Eds. Riley, J.P. and Skirrow, G.) 193-477. Academic Press, London.
- Rimmer, D.L. (1987). Flocculation Plus: Aggregation of Soil Particles. Paper presented at NERC Geocolloids Group Meeting "Particle Aggregation Processes in the Natural Environment". University of Lancaster.
- Rodiguin, N.M. and Rodiguina, E.N. (1964). Consecutive Chemical Reactions: Mathematical Analysis and Development. Van Nostrand, London. 136 pp.
- Roebens, E. (1980). Physical Adsorption Studies. In "Micro-weighing in Vacuum and Controlled Environments". (Eds. Czandema, A.W. and Wolsky, S.P.) 151-172. Elsevier, Amsterdam.
- Rosental, R., Eagle, G.A. and Orren, M.J. (1986). Trace Metal Distribution in Different Chemical Fractions of Nearshore Marine Sediments. *Estuar. Coastal Shelf Sci.* 22, 303-324.
- Ross, G.J.S. (1980). Maximum Likelihood Program. Statistics Department, Rothampsted Experimental Station, Harpenden.
- Rouqu  rol, J., Rouqu  rol, F., P  r  s, C., Grillet, Y. and Boudellal, M. (1979). Calorimetric Study of Nitrogen and Argon Adsorption on Porous Silicas. In "Characterisation of Porous Solids" (Eds. Gregg, S.J., Sing, K.S.W. and Stoeckli, H.F.) 107-116. Soc. Chem. Ind., Luton.

- Royal Commission on Environmental Pollution (1972). Third Report: Pollution in some British Estuaries and Coastal Waters. HMSO, London. 128 pp.
- Royal Commission on Environmental Pollution (1984). Tenth Report: Tackling Pollution - Experience and Prospects. HMSO, London. 231 pp.
- Saleh, A.M. and Jones, A.A. (1984). The Crystallinity and Surface Characteristics of Synthetic Ferrihydrite and its Relationship to Kaolinite Surfaces. *Clay Min.* 19, 745-755.
- Schindler, P.W. (1981). Surface Complexes at Oxide Water Interfaces. In "Adsorption of Inorganics at Solid Liquid Interfaces", (Eds. Anderson, M.A. and Rubin, A.J.) 1-50. Ann Arbor, Michigan.
- Schwertmann, U., Cambier, P. and Murad, E. (1985). Properties of Goethites of Varying Crystallinity. *Clays Clay. Min.* 33, 369-378.
- Schwertmann, U. and Fischer, W.R. (1973). Natural "Amorphous" Ferric Hydroxide. *Geoderma*. 10, 237-247.
- Shaw, D.J. (1970). Introduction to Colloid and Surface Chemistry. 2nd Edition. Butterworths, London. 236 pp.
- Sholkovitz, E.R. (1976). Flocculation of Dissolved Organic and Inorganic Matter during Mixing of River Water and Seawater. *Geochim. Cosmochim. Acta*. 40, 831-845.
- Sholkovitz, E.R. (1979). Chemical and Physical Processes Controlling the Chemical Composition of Suspended Material in the River Tay. *Estuar. Coastal Mar. Sci.* 8, 523-545.
- Sholkovitz, E.R., Boyle, E.A. and Price, N.B. (1978). The Removal of Dissolved Humic Acids and Iron during Estuarine Mixing. *Earth Planet. Sci. Lett.* 40, 130-136.
- Sholkovitz, E.R. and Copland, D. (1981). The Coagulation, Solubility and Adsorption Properties of Fe, Mn, Cu, Ni, Cd, Co and Humic Acids in a River Water. *Geochim. Cosmochim. Acta*. 45, 181-189.
- Sholkovitz, E.R. and Price, N.B. (1980). The Major Element Chemistry of Suspended Matter in the Amazon Estuary. *Geochim. Cosmochim. Acta*. 44, 163-171.
- Sigleo, A.C. and Helz, G.R. (1981). Composition of Estuarine Colloidal Materials: Major and Trace Elements. *Geochim. Cosmochim. Acta*. 45, 2501-2509.
- Sing, K.S.W. (1976). Surface Characterisation: Physical. In "Characterisation of Powder Surfaces", (Eds. Parfitt, G.D. and Sing, K.S.W.) 1-56. Academic Press, London.

- Sing, K.S.W. (1982). Reporting Physisorption Data for Gas/Solid Systems. *Pure and Appl. Chem.* 54, 2201-2218.
- So, C.L. (1978). Environmental Pollution of Estuaries - a Problem of Hazards. *Environ. Conserv.* 5, 205-211.
- Spellerburg, I. (1986). Impact Assessment in Estuaries. Paper Presented to the European Intensive Course "Evaluation of Criteria for the Management of Estuarine Systems". The University, Southampton.
- Study of Critical Environmental Problems (SCEP). (1970). *Mans Impact on the Global Environment, Assessment and Recommendations for Action*. MIT Press, London. 319 pp.
- Stumm, W. and Morgan, J.J. (1981). *Aquatic Chemistry - An Introduction Emphasizing Chemical Equilibria in Natural Waters*. John Wiley, London. 780 pp.
- Sundby, B., Silverberg, N. and Cheeselet, R. (1981). Pathways of Manganese in an Open Estuarine System. *Geochim. Cosmochim. Acta.* 45, 293-307.
- Sung, W. and Morgan, J.J. (1980). Kinetics and Products of Ferrous Iron Oxidation in Aqueous Systems. *Environ. Sci. Technol.* 14, 561-568.
- Sunila, I. and Lindstrom, R. (1985). Survival, Growth and Shell Deformities of Copper- and Cadmium-Exposed Mussels (*Mytilus edulis* L.) in Brackish Water. *Estuar. Coastal Shelf Sci.* 21, 555-565.
- Swallow, K.C., Hume, D.N. and Morel, F.M.M. (1980). Sorption of Copper and Lead by Hydrous Ferric Oxide. *Environ. Sci. Technol.* 14, 1326-1331.
- Swinbourne, E.S. (1971). *Analysis of Kinetic Data*. Thomas Nelson, London. 126 pp.
- Tessier, A., Campbell, P.G.C. and Bisson, M. (1980). Trace Metal Speciation in Yamaska and St Francois Rivers (Quebec). *Can. J. Earth Sci.* 17, 90-105.
- Tessier, A., Rapin, F. and Carnigan, R. (1985). Trace Metals in Oxidic Lake Sediments: Possible Adsorption onto Iron Oxyhydroxides. *Geochim. Cosmochim. Acta.* 49, 183-194.
- Theis, T.L. and Kaul, L.W. (1985). Rates of Sorption at the Goethite-Water Interface. American Chemical Society Symposium Series, Division of Environmental Chemistry. 25, 418-420.
- Thomas, D.J. and Grill, E.V. (1977). The Effect of Exchange Reactions between Fraser River Sediment and Seawater on Dissolved Cu and Zn Concentrations in the Strait of Georgia. *Estuar. Coastal Mar. Sci.* 5, 421-427.

- Tipping, E. and Cooke, D. (1982). The Effects of Adsorbed Humic Substances on the Surface Charge of Goethite (α -FeOOH) in Freshwaters. *Geochim. Cosmochim. Acta.* 46, 75-80.
- Tipping, E., Thompson, D.W., Ohnsted, M.Z. and Hetherington, N.B. (1986). Effects of pH on the Release of Metals from Naturally Occurring Oxides of Mn and Fe. *Environ. Technol. Lett.* 7, 109-114.
- Titley, J.G., Glegg, G.A., Glasson, D.R. and Millward, G.E. (1987). Surface Areas and Porosities of Particulate Matter in Turbid Estuaries. *Continental Shelf Res.* In Press.
- Torres-Sanchez, R.M., Palm-Gennen, M.H., Stone, W.E.E., Herbillon, A.J. and Rouxhet, P.G. (1985). Retention of Iron(III) by Kaolinite and Silica: Adsorption and Induced Precipitation. *American Chemical Society Symposium Series, Division of Environmental Chemistry.* 25, 326-329.
- Treanor, C.E. (1966). A Method for the Numerical Integration of Coupled First-order Differential Equations with Greatly Differing Time-constants. *Math. Comput.* 20, 39-45.
- Turekian, K.K. (1969). The Oceans, Streams and Atmosphere In "Handbook of Geochemistry", Volume 1, (Ed. Wedepohl, K.H.) 297-320. Springer-Verlag, Berlin.
- Turekian, K.K. (1971). Rivers, Tributaries and Estuaries. In "Impingement of Man on the Oceans", (Ed. Hood, D.W.) 9-73. Wiley-Interscience, New York.
- Turner, D.R., Whitfield, M. and Dickson, A.G. (1981). The Equilibrium Speciation of Dissolved Components in Freshwater and Seawater at 25° and 1 atm Pressure. *Geochim. Cosmochim. Acta.* 45, 855-881.
- Uncles, R.J., Bale, A.J., Howland, R.J.M., Morris, A.W. and Elliott, R.C.A. (1983a). Salinity of Surface Water in a Partially Mixed Estuary, and its Dispersion at Low Run-off. *Oceanol. Acta.* 6, 289-295.
- Uncles, R.J., Jordan, M.B. and Elliott, R.C.A. (1983b). Sampling and Analysis of Physical Features. In "Practical Procedures for Estuarine Studies", (Ed. Morris, A.W.) 19-54. NERC, Swindon.
- Uncles, R.J., Elliott, R.C.A. and Weston, S.A. (1985). Observed Fluxes of Water, Salt and Suspended Sediment in a Partly Mixed Estuary. *Estuar. Coastal Shelf Sci.* 20, 147-167.
- Vranken, G. and Heip, C. (1986). Toxicity of Copper, Mercury and Lead to a Marine Nematode. *Mar. Poll. Bull.* 17, 453-457.

- Van der Weijen, C.H., Arnoldus, M.J.H.L. and Meurs, C.J. (1977). Desorption of Metals from Suspended Material in the Rhine Estuary. *Neth. J. Sea Res.* 11, 130-145.
- Williams, D.J.A. and James, A.E. (1978). Rheology of Suspensions. NERC Grant F60/B4/02, Report 5. University College of Swansea.
- Yasunaga, T. and Ikeda, T. (1985). Intercalation Dynamics at the Layered Compound/Aqueous Solution Interface Studied by the Chemical Relaxation Method. *American Chemical Society Symposium Series, Division of Environmental Chemistry.* 25, 391-394.

APPENDIX 1
Published Work

THE MICROSTRUCTURES OF ESTUARINE PARTICLES

G.A. Glegg, J.G. Tittley, D.R. Glasson, G.E. Millward*
and A.W. Morrist†

Departments of Marine and Environmental Science,
Plymouth Polytechnic, Plymouth. PL4 8AA, U.K.

†Institute for Marine Environmental Research,
Prospect Place, the Hoe, Plymouth. PL1 3DH, U.K.

ABSTRACT

Samples of bed sediment have been collected from the Tamar Estuary and the surface areas and porosities of the dried materials were determined using a vacuum microbalance technique. The surface areas, calculated from the BET plots, were in the range 4 - 19 m²/g and the hysteresis loops showed that the particles had slit-shaped mesopores. The organic carbon contents of the particles varied between 1 and 10%. Careful removal of the surface organic coating lead to a systematic increase in the surface areas, suggesting that adsorbed organic matter affects the porosity of lithogenic particles. These results are of relevance to the sorption behaviour of natural particles in estuarine systems.

INTRODUCTION

The surface characteristics of estuarine particles are important in the partitioning of trace constituents between the dissolved and solid phases (Stumm and Morgan, 1981; Li *et al.*, 1984). Estuarine bed sediments, which can be resuspended by tidal stirring (Bale *et al.* 1985) are a complex mixture of quartz grains, aluminosilicates, Fe/Mn oxyhydroxides, organic detritus and biogenic materials all of which are implicated in scavenging processes. However, the amount of systematic information on natural particle microstructures is limited to some surface area studies, especially on iron oxides (Davis and Leckie (1978); Crosby *et al.*, 1983; Marsh, *et al.*, 1984).

It is surprising that this lack of knowledge in estuarine chemistry exists given the existing quantitative basis for evaluating particle microstructure (e.g. Greg and Sing, 1982) and it is a fact that little of this theory has been applied to natural particles. The reason is probably because ideally surface characterisation studies should be carried out *in situ*, with the surface area being determined by the uptake of some dissolved constituent. This presents a problem because one has to assume a non-porous surface, as is the case with negative adsorption (Hul and Lyklema, 1968). The major advantages of the BET gas adsorption method using the dried solid are that estimates of porosity and assessments of the control of particle morphology by surface coatings can be made. Comparable experiments are very difficult to perform *in situ*. Thus,

the objectives of this work were to determine the surface areas and porosities of bed sediments and to evaluate the role of adsorbed organic materials in the modification of particle microstructure.

METHODS

Sample Collection. The samples were collected from the Tamar Estuary, which is located in South West England. The samples were retrieved from the low salinity regions of the estuary. The bed sediments were obtained either by a surface scrape of mobile material (0 - 2 cm) or by a gravity cover from a survey vessel. In the laboratory the samples were washed in distilled water and filtered. This was followed by freeze drying using a vacuum freeze drier (Edwards High Vacuum Ltd.).

Experimental Techniques. A gravimetric BET nitrogen adsorption technique (Crosby *et al.*, 1983) was used to determine the surface areas and porosities of the samples. Approximately 0.2 g portions of the dried samples were used which usually resulted in the adsorption of 1 mg of nitrogen or more. The microbalance was evacuated and the sample retained under vacuum at 77 K using liquid nitrogen. The sample was dosed repeatedly with nitrogen gas and up to 0.5 h was allowed for equilibration during the adsorption stage and up to 2 h in the desorption stage. In some cases the particles were gently heated with 6% v/v hydrogen peroxide, prior to microstructural analysis, in an attempt to assess the effect of organic coatings. Particle size analyses were carried out using a Malvern Instruments 2200 particle sizes system (Bale *et al.*, 1984). Small aliquots of the samples were kept in suspension in a sample cell by stirring. Each sample was scanned 100 times using a lens of focal length 100 mm and the output from the detectors was transferred to a microcomputer which calculated particle diameters in the range 1.9 - 188 μm . Standard beads of 5 μm diameter were used to calibrate the instrument. The organic carbon analyses were carried out using a combustimetric technique (Carlo Erba Elemental Analyser).

RESULTS AND DISCUSSION

Two difficulties arise when carrying out microstructural studies on natural particles. Firstly it is essential to use a consistent preparative method since one is interested in relative surface areas (Greg and Sing, 1982). In this work freeze drying was preferred over air drying since the former has been used effectively for iron oxides (Davis and Leckie, 1978) and structural changes have been observed in the air drying method (Egashira and Aomine, 1974). Linked to this is the problem of the variability in the composition of portions of material taken for analysis from the bulk sample. To establish the variability in the samples and the drying method, the surface areas of ten portions of a Tamar sediment sample were obtained. These analysis gave a surface area of $12.66 \pm 1.19 \text{ m}^2/\text{g}$ (coefficient of variation 9.4%) and a similar number of organic carbon analyses on the same sample gave $4.53 \pm 0.12\%$ organic carbon (coefficient of variation 3%). These results suggest that the

samples were reasonably homogeneous and that realistic comparisons between samples could be made. The second problem concerns the ageing of the material by water vapour uptake after drying (Egashira and Aomine, 1974). This phenomena was observed in this study and dried materials left open to the atmosphere lost 30% of their original surface area after 30 days. Thus, samples were analysed as soon as possible after collection and were stored in a dessicator under vacuum.

Laser particle size analyses were carried on the sediment samples and a typical analysis is shown in Fig. 1. The particle diameters fall in the range 1 to 100 μm with a mean grain size of 13.6 μm .

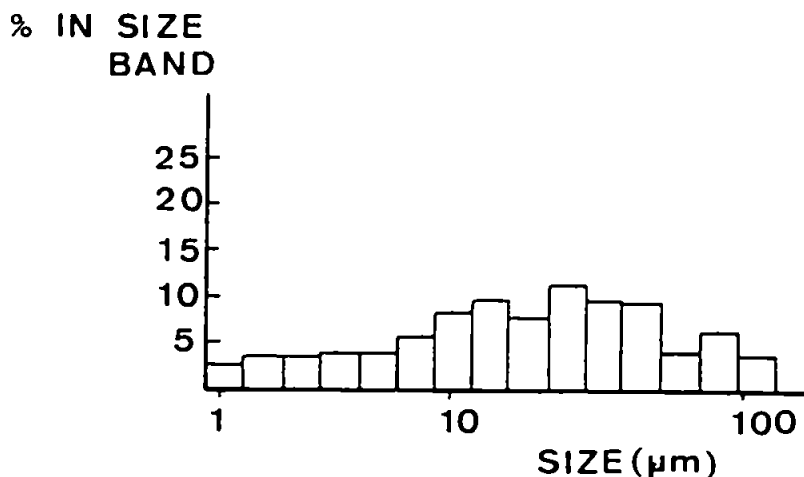


Fig. 1. Laser particle size analysis for a surface sediment from the Tamar Estuary.

In all the cases studied the range for the mean grain size was 8 - 15 μm . These particle diameters give a specific surface area of the order 0.2 m^2/g (assuming a sediment density of 3000 kg/m^3). This surface area is two orders of magnitude less than the BET nitrogen adsorption value of 12.66 m^2/g which demonstrates the considerable quantity of internal surface in natural particles, which is available to adsorbates in the water column. Additional samples, including a sediment core, were taken in the Tamar Estuary. A surface sediment sample was particle fractionated using a 45 μm sieve and a complete isotherm was obtained for each fraction. Fig. 2 shows the hysteresis loop for the coarse fractions (> 45 μm) which had a surface area of 19.0 m^2/g . The fine fraction (< 45 μm) had a surface area of 14.1 m^2/g and showed a similar hysteresis loop. The classification of the hysteresis loops suggests that

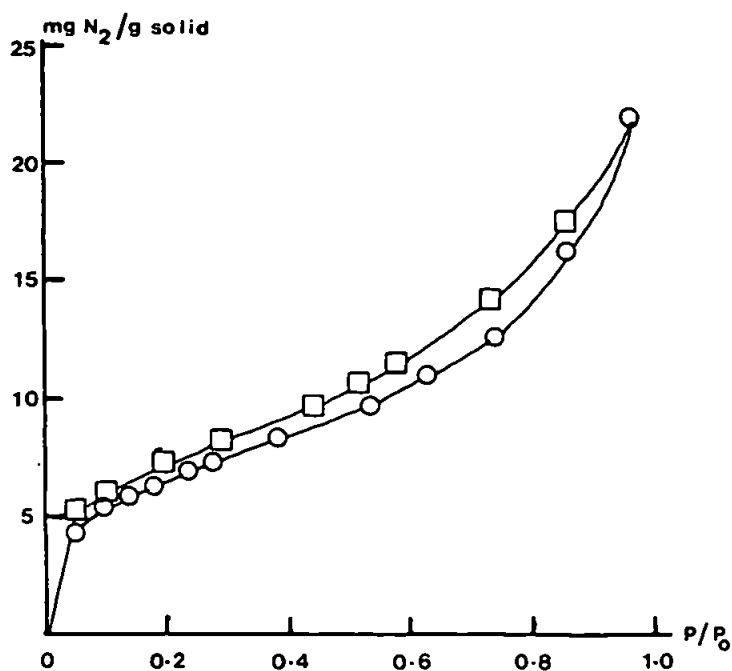


Fig. 2. The adsorption isotherm and hysteresis loop for a surface sediment sample. \circ - Adsorption; \square - Desorption.

the particles have slit-shaped pores with pore radii in the range 2 - 20 nm and pore volumes of the order $20 \times 10^{-3} \text{ m}^3/\text{g}$. The results of the analysis of sections of the core (which had been separated by a 45 μm sieve) are shown in Table 1. In general

TABLE 1. Surface areas and organic carbon contents of a sediment core from the Tamar Estuary.

Depth in core, cm	Grain size $\% < 45 \mu\text{m}$	Fraction $> 45 \mu\text{m}$		Fraction $< 45 \mu\text{m}$	
		Surface Area, m^2/g	% Carbon	Surface Area, m^2/g	% Carbon
0-2	76	10.74	5.40	10.34	3.20
6-8	77	9.50	9.70	10.48	3.16
11-13	76	8.40	5.70	10.20	2.45
17-19	84	6.12	10.0	10.31	2.65

the fine fraction had a constant surface area through the column. These surface areas compare reasonably well with a pure kaolinite sample (laser particle diameter 5 μm) which gave a value of 12.9 m^2/g . They are, however, consistently lower than an amorphous manganese dioxide, 470 m^2/g and amorphous iron oxides, 160 - 230 m^2/g (Crosby *et.al.*, 1983). Thus, it appears unlikely that ferromanganese coatings play a significant role in determining the surface areas of these particles since one might have anticipated higher values for the surface areas. Alternatively, organic carbon may be involved in the surface coating. In the fine fraction the organic carbon decreased by about 15% between the top and bottom of the column suggesting that some carbon could have been mineralised in the deeper anoxic zone (i.e. below about 4 cm). Although the loss of this amount of carbon from the particle appeared to have little effect on the surface area. In contrast the coarse fraction (> 45 μm) showed a consistent decrease in surface area but this was not always accompanied by a systematic change in the organic carbon content. However, closer inspection of the material at the bottom of the core showed evidence of remanant organic detritus, such as small pieces of terrestrial vegetation, which may have contributed to the low surface area. To investigate the role of the surface bound carbon a series of experiments were carried out in which a sediment sample was digested with 6% H_2O_2 for various times, see Table 2. These results

TABLE 2. The surface areas and organic carbon contents of a sediment digested with H_2O_2 for different times.

Digestion Time, h	Surface ^a Area, m^2/g	Z Carbon ^a
Untreated	12.66 ^b	4.53 ^b
0.5	11.22	4.00
2.5	15.14	2.46
4.5	17.57	1.21
24	22.99	0.71

^a

The average of 4 determinations.

^b

The average of 10 determinations.

show that the selective removal of surficial organic carbon leads to an increase in surface area. This suggests that the loss is in internal surface because the organic material adsorbed from the water column occupies a significant portion of the pore space in lithogenic materials.

In conclusion, this work is one of the first attempts to provide urgently needed microstructural information on estuarine particles.

It has demonstrated that the wide variety of the solid phases in a sample can contribute to differences in surface areas. In particular, the incorporation of significant quantities of organic detritus can lead to a lowering of the surface area. Furthermore, in the case of lithogenic particles the adsorption of organic molecules leads to an occupation of pore space and a consequent loss of surface area. However, more work needs to be done on assessing the microstructural changes induced by the adsorption of organic and ferromanganese coatings onto natural particles. It is only with this kind of information that interfacial sorption phenomena involving natural particles will be fully understood.

ACKNOWLEDGMENTS

C.A. Glegg is funded by an NERC (CASE) research studentship and J.C. Tiley is an NERC research assistant funded under Contract Number GR3/5712.

REFERENCES

- Bale, A.J., Morris, A.W. and Howland, R.J.M. (1984). Size distributions of suspended material in the surface waters of an estuary as measured by laser Fraunhofer diffraction, in *Transfer Processes in Cohesive Sediment Systems*. (Eds. Parker and Kinsman), pp 75-85. Plenum Publishing Corp., New York.
- Bale, A.J., Morris, A.W. and Howland, R.J.M. (1985). Seasonal sediment movement in the Tamar Estuary. *Oceanologica Acta*, 8, 1-6.
- Crosby, S.A., Classon, D.R., Cutler, A.H., Butler, I., Turner, D.R., Whitfield, M. and Millward, G.E. (1983). Surface areas and porosities of Fe (III) - and Fe (II) - derived oxyhydroxides. *Environmental Science and Technology*, 17, 709-713.
- Davis, J.A. and Leckie, J.O. (1978). Surface ionisation and complexation at the oxide/water interface. *Journal of Colloid and Interface Science*, 67, 90-107.
- Egashira, K. and Aomine, S. (1974). Effects of drying and heating on the surface area of allophane and imogolite. *Clay Science*, 4, 231-242.
- Greg, S.J. and Sing, K.S.W. (1982). Adsorption, Surface Area and Porosity. 303 pp. Academic Press, London.
- Hulvanden, H.J. and Lyklema, J. (1968). Determination of specific surface areas of dispersed materials. Comparison of the negative adsorption method with some other methods. *Journal of the American Chemical Society*, 90, 3010-3015.
- Li, Y-H., Burkhardt, L. and Teraoka, H. (1984). Desorption and coagulation of trace elements during estuarine mixing. *Geochimica et Cosmochimica Acta*, 48, 1879-1884.
- Marsh, J.G., Crosby, S.A., Classon, D.R. and Millward, G.E. (1984). BET nitrogen adsorption studies of iron oxides from natural and synthetic sources. *Thermochimica Acta*, 82, 221-229.
- Stumm, W. and Morgan, J.J. (1981). *Aquatic Chemistry: An Introduction Emphasising Chemical Equilibria in Natural Waters*. 780 pp. Wiley Interscience, New York.

DISCUSSION

Dr. Wanogho, University of Strathclyde, asked: 1. Could you explain why you used two different percentages of hydrogen peroxide? Could the different times and percentages give different results?

Mr. Titley replied: The experiments carried out with the 6% hydrogen peroxide solution were designed to remove the surface carbon gradually over a period of several hours. We wished to demonstrate that carbonaceous coatings on particles tend to reduce the surface area. Having shown this we then used the 30% solution of hydrogen peroxide to effect the oxidation in a shorter time, even so the oxidation of all forms of organic matter was not complete. In almost all cases there was a resistant fraction which was not oxidised. Some of this may be organic detritus, such as fragments of vegetation, but we need to carry out further work on the contribution this makes to the overall surface area of the sample.

Mr. Kiff, Hydraulics Research Limited, asked: You quote an organic carbon figure of about 4% for one of your sediments. This corresponds to a volume percentage of organic matter of about 20%. Did you do any size gradings of sediment before and after the destruction of the organic matter to see if the organics are attached to the surface of the particle or entirely or partially absorbed with the particles.

Mr. Titley replied: The grading of sediment before and after an experiment has not yet been carried out. As we have already pointed out a natural sediment sample contains organic matter in three forms 1) as organic molecules adsorbed to particle surfaces; 2) as organic detritus, mainly land-derived and 3) as biogenic materials. It is not yet possible to assess the contribution made by each of these forms to the overall surface area of the particles. We are currently working on this problem, in the first instance looking at the contribution made by biogenic materials. It is through further experimentation of this kind that we intend to unravel the role that the organic mentioned has in determining the overall surface area.

"PREPRINT EXTENDED ABSTRACT"

Presented Before the Division of Environmental Chemistry
American Chemical Society
Chicago, Illinois September 1985

THE MICROSTRUCTURES OF ESTUARINE PARTICLES
AND THEIR ROLE IN HETEROGENEOUS CHEMICAL REACTIVITY

G.E. Millward, G.A. Clegg, D.R. Glasson, A.W. Morris* & A.J. Bale*

Department of Marine Science, Plymouth Polytechnic, Plymouth.
PL4 8AA U.K.

*Institute for Marine Environmental Research, Prospect Place,
The Hoe, Plymouth. PL1 3DH U.K.

The surface characteristics of estuarine particles are important in the partitioning of trace constituents between the dissolved and solid phases. There is an urgent need to determine the range of surface areas and porosities (microstructures) of the solid phases found in estuarine systems as a step in the development of a precise understanding of natural heterogeneous chemical reactivity. This work is concerned with the determination of the particle microstructures of suspended material and sediments from two estuaries, as well as natural and synthetic precipitates of iron oxyhydroxides. The results of this study are discussed in the context of the behaviour of the estuarine trace constituents, phosphate and zinc.

Samples of suspended solids and associated sediments were collected during axial surveys of the Tamar Estuary, with a particular emphasis on the turbidity maximum zone. Additional samples were collected from the contaminated, iron-rich environment of Restronguet Creek, Cornwall, South-West England. All the samples were washed with distilled water and outgassed at room temperature. The surface areas of the dried solids were determined using a gravimetric B.E.T. nitrogen adsorption technique on a C.I. Mark 2B vacuum microbalance. Nitrogen desorption experiments were also carried out and estimates of pore shape and size obtained from the hysteresis loops. The organic carbon content of the samples was obtained using a commercial combustometric technique (Carlo Erba Analyser). Complimentary particle size analyses were undertaken using a Malvern laser diffraction particle sizer. Liquid phase adsorption studies involving the uptake of either phosphate or zinc were carried out under carefully controlled conditions.

The mean particle diameters of the suspended solids and sediments in the Tamar Estuary were in the range 10 - 100 μm for which specific surface areas of 0.2 to 0.02 m^2/g can be calculated. In contrast, the surface areas obtained from the nitrogen adsorption studies were in the range 19 - 22 m^2/g for suspended solids and 9 - 16 m^2/g for the sediments, see Table 1.

Sample Turbidity mg/l	Suspended Solids		Sediments	
	Surface Area, m ² /g	Organic Carbon, %	Surface Area, m ² /g	Organic Content, %
65	19.4	4.0	13.1	6.2
190	22.1	3.6	16.2	4.0
260	20.4	2.6	12.4	4.6
270	22.5	3.2	14.8	3.8
690	22.7	3.8	9.1	4.7

Table 1: Surface areas and organic contents of suspended solids and sediments from the Tamar Estuary.

These data show the importance of the internal surfaces of the particles which is not revealed by the laser particle sizing method. Analysis of the hysteresis loops showed that the estuarine particles had slit-shaped mesopores of size 2 to 20 nm. A coefficient of variation of $\pm 10\%$ was obtained from replicate analyses (5) of separate aliquots of a sample of suspended particles with a mean surface area of 17 m²/g. Similar analyses of a sediment with a surface area of 8.6 m²/g gave a coefficient of variation of $\pm 11\%$. This analytical precision confirms that the suspended particles have consistently higher surface areas than those in the sediments. This is due to the fact that the suspended matter is associated with finer particles, which are selectively mobilised within the turbidity maximum zone. The samples had carbon contents varying from 2 to 4% and the higher carbon contents were systematically associated with lower surface areas. The role of the organic matter was further examined by digesting the particles with hydrogen peroxide (see Table 2).

Sample Site	Suspended Solids		Sediments	
	Surface Area, m ² /g	Organic Carbon, %	Surface Area, m ² /g	Organic Carbon, %
Tamar Estuary (Undigested)	19.4	4.0	13.1	6.2
Tamar Estuary (Digested)	31.5	0.5	15.4	1.0
Restronguet Creek (Undigested)	125.5	2.8	35.5	1.7
Restronguet Creek (Digested)	184.7	0.1	60.9	0.0

Table 2: Surface areas and organic contents of particles prior to and following digestion with hydrogen peroxide.

These results suggest that adsorbed organic carbon occupies a fraction of the pore space with a consequent reduction in surface area.

Similar studies were carried out on iron-rich particles which showed suspended solids with much larger surface areas upto $125 \text{ m}^2/\text{g}$ and sediments upto $35 \text{ m}^2/\text{g}$. These results were compared to several fresh and aged iron oxyhydroxides which had surface areas in the range 100 to $240 \text{ m}^2/\text{g}$. The iron-coated estuarine particles and the precipitates showed both microporosity (pore size 1 - 5 nm) and mesoporosity (pore size 2 - 20 nm). The pores were mainly of the narrow-necked, widebodied type which restrict the desorption of adsorbed species, and which provide an explanation for the irreversible uptake of trace constituents.

These results demonstrate the variety of surface areas and porosities available in an estuarine system and they identify the role played by physical particle selection processes and the chemical adsorption of organic matter. These processes lead to changes in the surface activity which directly affects the rate and extent of the uptake of trace constituents. The results are used to evaluate the behaviour of phosphate and zinc at particle surfaces and predictions are made on the potential transport in the particulate phase.